LA-13730-PR
Progress Report

Approved for public release; distribution is unlimited.

1999

LDRD

Laboratory Directed Research and Development

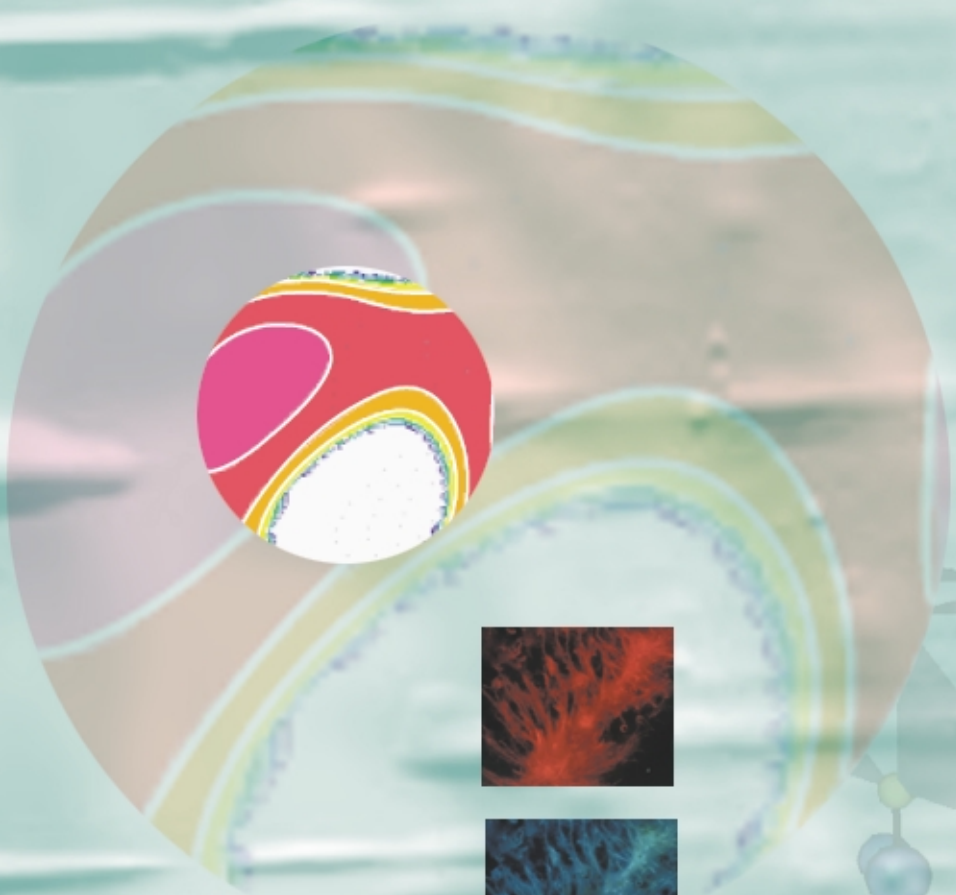

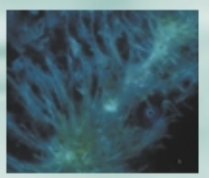

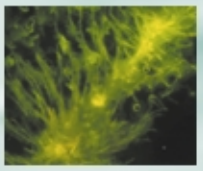

Los Alamos
NATIONAL LABORATORY

Los Alamos National Laboratory is operated by the University of California for the United States Department of Energy under contract W-7405-ENG-36.

Abstract

This is the FY 1999 Progress Report for the Laboratory Directed Research and Development (LDRD) Program at Los Alamos National Laboratory. It gives an overview of the LDRD Program, summarizes work done on individual research projects, relates the projects to major Laboratory program sponsors, and provides an index to the principal investigators. Project summaries are grouped by their LDRD component: Competency Development, Program Development, and Individual Projects. Within each component, they are further grouped into nine technical categories: (1) materials science, (2) chemistry, (3) mathematics and computational science, (4) atomic, molecular, optical, and plasma physics, fluids, and particle beams, (5) engineering science, (6) instrumentation and diagnostics, (7) geoscience, space science, and astrophysics, (8) nuclear and particle physics, and (9) bioscience.

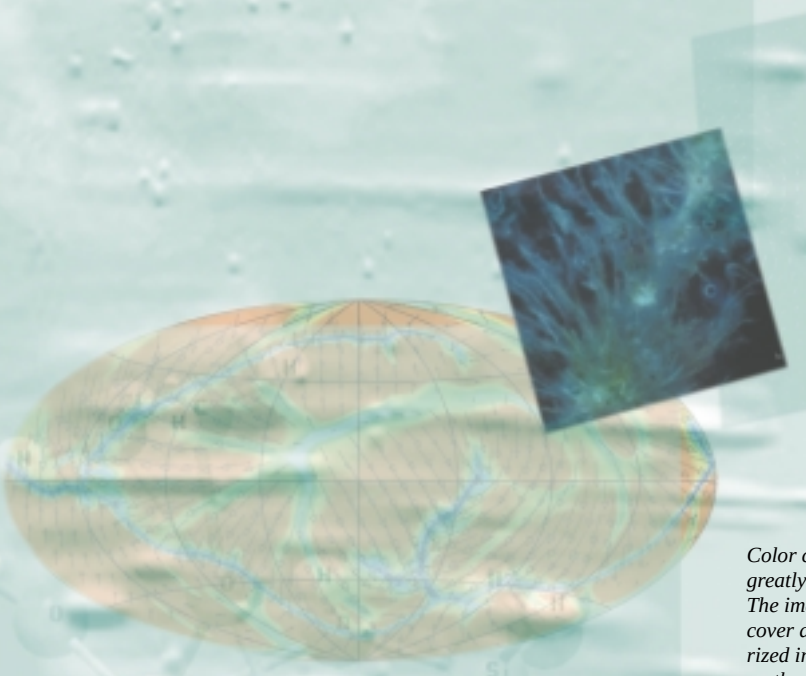

Color computer simulations greatly aid many LDRD projects. The images on the front and back cover are from projects summarized in this report; the images on the section dividers are from projects described in the respective sections.

LA-13730-PR
Progress Report

Issued: June 2000

1999 LDRD

Laboratory Directed Research and Development

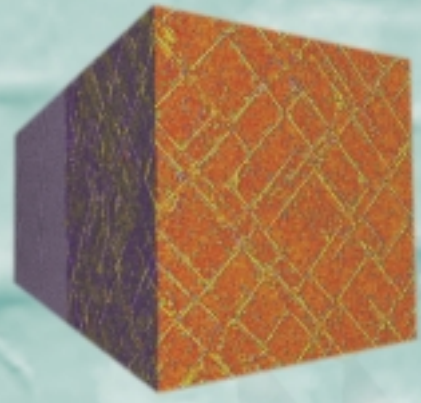

FY1999 Progress Report

Compiled and Edited by
Rita Spencer and Kyle Wheeler

Published by Los Alamos National Laboratory

Laboratory Director: **John C. Browne**

Director for Science and Technology Base Program: **Allen Hartford**

Program Manager for Laboratory Directed Research and Development: **David E. Watkins**

Scientific Editors: **Rita Spencer and Rey Morales**

LDRD Office Team: **Diana Baker, Victoria DeVargas, Betty Gunther, and Leonard Salazar**

Managing Editors: **Kyle Wheeler and Eileen Patterson (CIC-1)**

Editors: **Marty DeLanoy, Earlene Hammock, Faith Harp, Nikki Goldman, Sheila Molony, Cynthia Phillips, Judy Prono, Denise Sessions, Karen Sharkey, and Marv Wetovsky (CIC-1)**

Designer: **Susan Carlson (CIC-1)**

Layout, Composition, and Production: **Wendy Burditt (CIC-1)**

Printing Coordination: **CIC-9 Imaging Services**

The previous reports in this unclassified series are LA-13278-PR, LA-13433-PR, and LA-13595-PR.

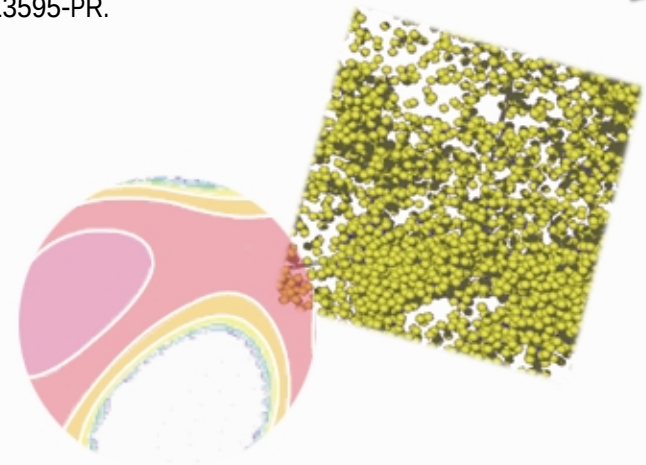

Contents

Directed Research Projects

Materials Science

Chemistry

Directed Research Projects (cont.)

Mathematics and Computational Science

Atomic, Molecular, Optical, and Plasma Physics, Fluids, and Beams

Engineering Science

Instrumentation and Diagnostics

Directed Research Projects (cont.)

Geoscience, Space Science, and Astrophysics

Nuclear and Particle Physics

Bioscience

Exploratory Research Projects

Materials Science

Chemistry

Exploratory Research Projects (cont.)

Mathematics and Computational Science

Atomic, Molecular, Optical, and Plasma Physics, Fluids, and Beams

Exploratory Research Projects (cont.)

Engineering Science

Instrumentation and Diagnostics

Exploratory Research Projects (cont.)

Geoscience, Space Science, and Astrophysics

Nuclear and Particle Physics

Exploratory Research Projects (cont.)

Nuclear and Particle Physics

Bioscience

Overview

LDRD Program Overview—FY 1999

David Watkins and Rita Spencer

The Laboratory Directed Research and Development (LDRD) Program is authorized by Congress as a means for the Laboratory to maintain its scientific and technological vitality. Through the LDRD Program, the Laboratory invests in innovative research and development projects commensurate with our mission and in support of the nation's scientific needs.

Sustained excellence in mission execution requires that our capabilities be continually reinvigorated. Scientific institutions must have means to allow their best researchers to pursue innovative ideas that are too embryonic for programmatic focus. The ability to direct resources to such work is often the difference between institutional excellence and mediocrity. The LDRD Program is the engine that drives the creation of powerful scientific and technological capabilities that are applied to national problems for which science can provide a solution. It is key to ensuring a high return on the nation's investment in the Laboratory.

The LDRD budget consists of both operating and capital equipment funds that are generated through the application of a uniform assessment to all programs at the Laboratory that receive direct funding either from Department of Energy (DOE) programs or reimbursable "Work for Others" (WFO). LDRD annual funding is authorized by Congress to a maximum of 6% of the Laboratory's operating budget.

A breakdown of the LDRD Program's actual and projected costs from FY99 through FY05 is shown in the accompanying table. In FY99 the DOE-approved assessment rate was 6%, and the actual Laboratory operating costs were $1,258 million. The projected costs are based on Laboratory assessments of how much money will be allocated to LDRD. A breakdown of the Laboratory's FY99 funding by major program sponsor is shown in the first figure; a table of LDRD projects as they relate to these sponsors is provided at the end of this report.

The LDRD Program is subject to congressional authorization language, applicable DOE regulations and orders (primarily DOE Order 413.2), and the prime contract between the University of California and DOE. The Institutional Management Team of DOE's Albuquerque Operations Office oversees the LDRD Program. LDRD financial activities are conducted in accordance with generally accepted accounting principles and cost accounting standards.

LDRD Program Structure

The LDRD Program structure consists of two components with distinct institutional objectives: Exploratory Research (ER) and Directed Research (DR). In FY99 LDRD funded 214 projects for a total expenditure of $71 million. The funding distribution between the two components (ER and DR) was approximately one-third and two-thirds, respectively, as shown in the second figure. All LDRD projects are selected through competitive processes involving scientific review by management and/or peers. There are three ways in which the LDRD Program extends Laboratory science and technology capabilities. First, it may explore new ways of tackling

Projected Funding for Laboratory Directed Research and Development ($M)

	Actual Cost	Projected Cost[1]						
Funding Area	**FY99**	**FY00**	**FY01**	**FY02**	**FY03**	**FY04**	**FY05**	**FY06**
Operating	71.1	45.5[2]	75.0	75.0	75.0	75.0	75.0	75.0
Capital Equipment	2.9	2.5	2.5	2.5	2.5	2.5	2.5	2.5
Total	73.0	48.0	77.5	77.5	77.5	77.5	77.5	77.5

[1]Projected amounts for FY00 and beyond are subject to approval in accordance with DOE Order 413.2.
[2]Projected cost for FY00 includes congressional reduction of assessment rate to 4% for that year.

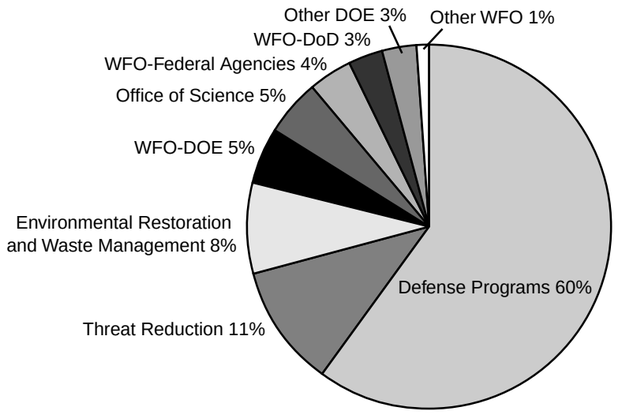

Funding for major programs at Los Alamos National Laboratory during FY 1999.

mission problems, thereby identifying opportunities to execute mission objectives in a cheaper, faster, or better way. Second, it may develop new capabilities in areas of expertise needed to fulfill the missions, perhaps adding new techniques for solving problems or using new, multidisciplinary approaches that provide added insight. Third, it may broaden the fundamental science and technology base in areas that underpin the Laboratory's ability to execute its missions.

Exploratory Research Projects

The Exploratory Research (ER) component of the LDRD Program funds smaller projects involving from one scientist to a few scientists. These projects are clearly at the forefront of science and technology in disciplines that underpin the Laboratory mission. The ER component is used to fund fundamental and far-reaching science and technology. One-third of the overall LDRD budget is typically allocated to this component. Project support is available in nine technical categories:

Atomic, Molecular, Optical, and Plasma Physics, Fluids, and Beams
Bioscience.
Chemistry
Engineering Science
Geoscience, Space Science, and Astrophysics
Instrumentation and Diagnostics
Materials Science
Mathematics and Computational Science
Nuclear and Particle Physics

Directed Research Projects

The Directed Research (DR) component of LDRD is intended to be most guided by the longer-term Laboratory strategy and most influenced by the Laboratory's scientific management. The projects in this component are, by nature, strategic scientific thrusts: strategic thrusts are meant to be conscious and deliberate investments with the intent of achieving defined institutional objectives. The strategic thrusts are generally somewhat larger, coherent investments averaging about a million dollars, with a single, unifying strategic goal. However, the thrust may comprise a number of distinct and complementary tasks. The DR component of the LDRD Program is funded at a level equal to about two-thirds of the total program.

The Director has decided that the formulation of the science and technology strategies for the Laboratory is to be led and monitored by the Deputy Laboratory Director for Science, Technology, and Programs (DLDSTP), who works in close coordination with the three Associate Laboratory Directors (ALDs). The DLDSTP is also responsible for oversight and strategic management of the LDRD Program. This makes it easier to align investment of the LDRD resources with the goals and needs outlined in the Laboratory's Strategic Plan.

Selection of LDRD Projects

The LDRD Program is led by the Laboratory Director through a formal management process to impose accountability in the selection, execution, and documentation of projects. All projects are selected through competitive review by peers and/or scientific management. Innovation and scientific excellence are key selection criteria, and all projects must be in science and technology areas that support the Laboratory's mission. Decisions on project funding are ultimately the responsibility of the Director.

The annual LDRD proposal cycle begins in January with a formal call for new proposals for LDRD projects. Detailed guidance is provided in the calls for both LDRD components. The guidance includes estimates of component funding for planning purposes and background on the research and development areas that will be supported. Successful proposals must provide an annual statement of work.

New ER proposals are reviewed by one of the LDRD technical category teams. Proposals are evaluated and ranked based on scientific and technical merit, creativity and originality of proposed effort, and capability of the team to succeed within the budgetary constraints. Continuing ER proposals are subject to scientific management review and annual review by the relevant ER technical category team. Funding is extended into a subsequent fiscal year if the projects were previously approved for multi-year funding and if adequate progress was made toward stated objectives.

The DR component solicits proposals in two phases. The first phase consists of a broad call for brief pre-proposals identifying strategic LDRD investment opportunities that support the Laboratory's Strategic Plan. The pre-proposals are assessed by a strategy team chaired by the DLDSTP. Based on the information submitted in the pre-proposals, the strategy team recommends science and technology thrusts to the DLDSTP and the three ALDs for a directed call for full proposals. The DLDSTP and the ALDs make the final decision on the directed call for full proposals and issue it. This call is targeted at specific authors and specific scientific thrusts, and includes a budget estimate. The sum of the budgets for the full proposals in the call exceeds the funding available by about a factor of 2. Once the full proposals are received, they are reviewed by the strategy team and ranked on the basis of scientific and strategic merit. The DLDSTP and ALDs use this ranking to determine the portfolio of proposals to be funded as projects.

The Success of LDRD

Los Alamos National Laboratory's core mission is to enhance global security by ensuring safety and confidence in the U.S. nuclear weapons stockpile, developing technical solutions to reduce the threat of weapons of mass destruction, and improving the environmental and nuclear materials legacies of the cold war. LDRD is a vital tool supporting this mission.

The quality of LDRD-supported research and development is demonstrated by a significant number of related awards, scientific publications, and patents. In 1999, following the tradition of previous years, LDRD-supported scientists garnered national and international recognition for their work. Recognition included the American Physical Society's Pipkin Prize, the Australian National University Medal, a Packard Foundation Award, the Otto Hahn Medal for Young Scientists from the Max Planck Society of Germany, the Marie Curie Award from the Radiation Research Society (the award was for outstanding radiation-related research by a young investigator in the areas of biology, medicine, chemistry, or physics). Further recognition included the Non-tenured Scientist Award from the International Congress on Radiation Research, the Margaret O. Dayhoff Award from the Biophysical Society, and citation for one of the top ten breakthroughs of 1998 by the journal *Science* (also in the top achievements cited by the American Physical Society). In addition, an LDRD-supported scientist was elected to the American Academy of Arts and Sciences, another was elected as a foreign member to the Royal Swedish Academy of Science, and yet another was elected to the National Academy of Engineering.

The number of publications stemming from LDRD research continues to be substantial. More than 410 publications had been logged by the end of the year, and many more publications resulting from the year's work are in progress. Over the past several years, more than 30% of the patents awarded to LANL had their roots in LDRD work, and more than 60% of the R&D 100 awards were the result of LDRD investments. These achievements attest to the far-reaching and groundbreaking nature of LDRD research. In addition, the LDRD Program provides a valuable tool for attracting new talent to the Laboratory. In FY99, 195 postdoctoral staff members participated in LDRD projects. Of these, about one-fourth are expected to become permanent Laboratory employees, rejuvenating our work force and contributing to our central mission.

Four LDRD projects are mentioned below to illustrate just a few of the significant contributions these projects can make to fundamental science and technology in a range of national security areas:

Electrons in High Magnetic Fields

Project 97611, *Electrons in High Magnetic Fields* (see page 10), aimed for a determination of the electronic structure of the various allotropes of plutonium and its application to the equation of state of the material. Among the specific questions to be answered by this project were the following: Are the six structural phases of plutonium a consequence or a correlate of electronic many-body effects? To what extent can electronic structure calculations be applied to understanding plutonium's equation of state? Does plutonium's notorious autocatalytic reaction with hydrogen have anything to do with the quantum-mechanical specifics of its *5f* electrons? What else about the chemistry of elemental plutonium is understandable in these terms? What insights into the metallurgical properties of the actinides become possible with first-principles understanding of their electronic structure and dynamics? Based on electronic properties, can simple and inexpensive experiments be devised that will interrogate aging effects in nuclear materials? This study provides

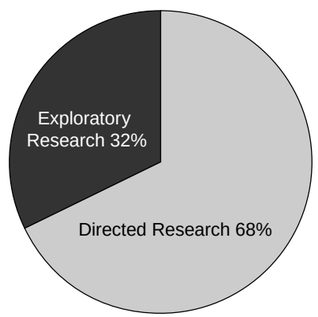

Distribution of FY1999 funding among the two program components.

valuable leading insights in support of the stockpile stewardship mission.

Optical Biosensor

The research performed in the *Optical Biosensor* project (99506), see page 88, is providing an in-depth understanding of the underlying science of optical sensors based on protein-receptor binding, cell membrane mimics, and receptor aggregation that is triggered by protein-receptor recognition. The development of a biosensor platform that can be used for the detection of protein toxins has primary application to environmental work. However, there is potential to enhance our threat reduction capabilities by adapting this sensor approach to other applications including early diagnosis of infection and exposure.

Ultracold Neutron (UCN) Science

The *Ultracold Neutron Science* project (98606), summarized on page 80, used a UCN rotor source as a test bed for developing techniques for carrying out an exciting research program using UCNs. Simultaneously, the researchers have been developing advanced UCN source concepts. The source work has concentrated on using cryogenic deuterium as a UCN converter. Fundamental physics that can be performed using UCNs includes determination of neutron lifetime and decay parameters that can provide sensitive tests of the standard model of electro-weak interactions.

Bioremediation Science to Meet National Challenges

Because of its ability to remediate dilute, diffuse, and inaccessible contaminants cost effectively, in situ bioremediation offers the potential of solving the most difficult of environmental legacies of the cold war—the remediation of contaminated aquifers. The persistence of many contaminants in the environment is evidence that microorganisms are not naturally adapted to degrade these contaminants at either the rates required or to the extent required. The objective of this project is to develop and apply capabilities in Bioremediation Science by gaining understanding of and improving enzyme catalysis, gene expression, and microbe survival to enable the application of in situ bioremediation to meet regulations for contaminant destruction. The project (99500) is described in more detail on page 85.

1999
LDRD

Directed Research Projects

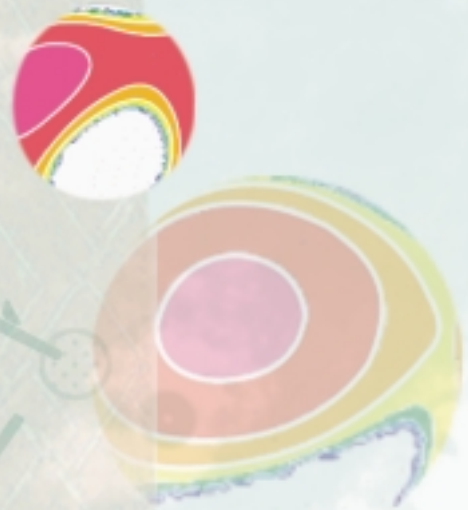

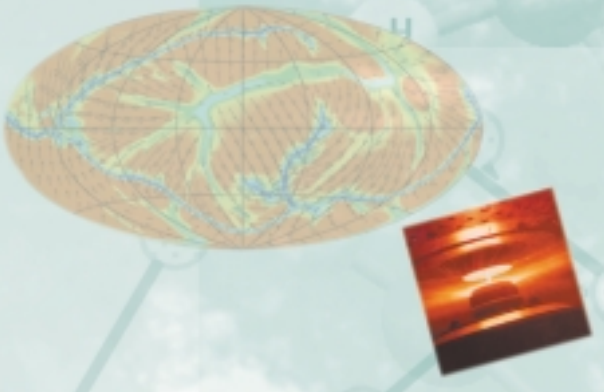

Materials Science

Neutron and Accelerator-Based Science

99519

Daniel Strottman

One objective of this project is to research and develop novel methods for inelastic neutron scattering spectroscopy on pulsed spallation sources. The implementation of the innovative technology will allow us to achieve 30 times higher data rates than at the best comparable facility in the world. This will permit dramatic new advances in the study of dissipative processes in complex systems and in the hierarchy of length and time scales.

Another objective is to construct a unique gamma-ray detector to measure (n,g) reactions on highly radioactive nuclei. With this detector and our unique capabilities to produce highly radioactive targets, we will have an unequaled ability to address problems in nucleosynthesis.

This year we made significant progress in each of the thrust areas of the proposal.

We began initial design work for the inelastic scattering instrument. Pre-engineering design plans for the neutron guide/shield insert and for an integrated beam line package for flight paths 11, 12, and 13 at the Los Alamos Neutron Science Center are nearly complete. This integrated beam package is required because of the extreme closeness of the four beam lines that will emerge through the bulk shielding.

Work on the detector for neutron capture experiments (DANCE) has progressed rapidly. For the proposed array, very extensive simulations of the background resulting from neutron scattering off the shielding and frame are complete. These simulations required a new design using larger crystals than originally envisaged. We completed the design of the frame with the larger crystals and put out for bid the fabrication of the frame. We also purchased prototype BaF_2 crystals and tested them for signal response and timing. Discussions with potential suppliers of the crystals are ongoing. We tested and ordered prototype photomultiplier tubes. Design of the shielding on the new flight path is complete, and we ordered prototypes for suitability testing. During the summer, we installed a shutter on flight path 14, paving the way for testing during the coming year.

We also developed an analysis technique that allows the determination of phonon dispersion relations from powder diffraction data. This technique relies on a sophisticated modeling of the lattice dynamics. We have extended our previous work, which was restricted to one-phonon processes only, to include all multiphonon processes in the quasiharmonic approximation. We investigated in detail, the role of powder averaging with the surprising result that the common assumption of Gaussian peaks in a pair density function is wrong.

Publications

Louca, D., and H. Röder, "Phonons from Neutron Powder Diffraction," *Phys. Rev. B* **60**, 6204 (1999).

Rundberg, R., et al., "Neutron Capture Cross Section Measurements and the Analysis of the S Process" (Am. Chem. Soc. semi-annual meeting, New Orleans, LA, August 1999).

Ullman, J., et al., "Neutron Capture Measurements on Unstable Nuclei at LANSCE" (Denton Accelerator Conference, Denton, TX, December 1998).

Wilhelmy, J., et al., "Neutron Capture on Radioactive Targets: Probing the S Process" (Conference on Fission and Neutron-Rich Nuclei, St. Andrews, Scotland, July 1999).

Electrons in High Magnetic Fields

97611

Aloysius J. Arko

This project's goal is to determine the electronic structure of 5f-based conducting materials, specifically plutonium and its compounds. This year we applied the capabilities of the National High Magnetic Field Laboratory to the solution of fundamental unsolved problems in the many-body physics of condensed matter. In focusing on 4f- and 5f-based conducting materials that exhibit many-body correlations in their electronic properties, we studied two complementary areas: the electronic structure of plutonium and related actinide intermetallics, and the femtosecond dynamics of many-body phenomena. The first activity focuses on the more traditional Fermiology (Fermi surface topology, effective masses, metamagnetic transitions) of 5f metals and compounds. By contrast, the second activity focuses on microscopic mechanisms of electron-electron correlations (e.g., polarons) that cause the electronic structure to deviate from what is expected from band calculations.

We interpreted data from our ultrafast optical pump probe measurements on the defined materials in terms of photo-induced demagnetization and its subsequent remagnetization due to the exchange of energy and equilibration with lattice. We used optical-pump/terahertz-probe spectroscopy to study transient conductivities in yttrium-barium-copper oxide (YBCO). For optimally doped YBCO, the temperature dependence is as predicted by earlier Bardeen-Cooper-Schrieffer (BCS)-based models. For underdoped YBCO, temperature dependence is consistent with a pseudogap.

We developed terahertz reflectivity to measure the conductivity of bulk materials (thin films were not always available). A new, redesigned source yields tunable narrow-band terahertz radiation with frequencies as low as 10 GHz. We used a powerful new technique to calculate various polaron dynamics, and we calculated minimum energy electron structure and mapped Fermi surfaces of Pu(3)Ga, PuGa, and PuGa(3). New calculations on δ-Pu agree more finely with photoemission data. We also calculated the band structure of NpAs and UAs for comparison to photoemission.

We also determined the de Hass-van-Aalpen (dHvA) effect in $ThBe_{13}$ and $CeRhIn_5$ as a function of angle. We obtained good agreement with band calculations in $ThBe_{13}$. Band calculations do not explain transition in UGa_3.

We obtained specific heat measurements in magnetic fields up to 60 T for UBe_{13}, $Ce_3Bi_4Pt_4$, $La_{2x}Sr_xCuO_4$, and UCd_{11} and observed the magnetocaloric effect in UCd_{11} during pulse. We performed the first-ever measurement of α-Pu magnetization in a pulsed field up to 50 T. To search for flaws in the dHvA technique, we used a polycrystalline sample.

Publications

Averitt, R.D., et al., "Conductivity Artifacts in Optical-Pump, THz-Probe Measurements of YBa(2)Cu(3)O(7)," *J. Opt. Soc. Am. B* **17**, 327 (2000).

Bonca, J., et al., "Holstein Polaron," *Phys. Rev. B* **60**, 1633 (1999).

Cornelius, A.L., et al., "de Haas-van Alphen Effect, Magnetic Transitions and Specific Heat in the Heavy Fermion System UCd(11)," *Phys. Rev. B* **59**, 13542 (1999).

Cornelius, A.L., et al., "Electronic Properties of UX(3) (X=Ga, Al, Sn) Compounds in High Magnetic Fields: Transport, Specific Heat, Magnetization and Quantum Oscillations," *Phys. Rev B* **59**, 14473 (1999).

Jaime, M., et al., "Heat Capacity Measurements in Pulsed Magnetic Fields," in *Proceedings of the PPHMF-III Conference, Z.* Fisk, L. Gor'kov, and R. Schrieffer, Eds. (World Scientific, Singapore, 1999), p. 148.

Jaime, M., et al., "Heat Capacity Measurements Up to 60 Tesla in $Ce_3Bi_4Pt_3$ Kondo Insulator" (to be published in *Physica B*).

Lobad, A.I., et al., "Laser-Induced Dynamics Spectral Weight Transfer in La(0.7)Ca(0.3)MnO(3)" (to be published in *Chem. Phys.*).

Modler, R., et al., "Magnetization of a Kondo Insulator $Ce_3Bi_4Pt_3$ and a Metal $CeRh_2Si_2$ in Pulsed Fields," in *Proceedings of the PPHMF-III Conference, Z.* Fisk, L. Gor'kov, and R. Schrieffer, Eds. (World Scientific, Singapore, 1999).

Mustre de Leon, J., et al., "Isotopic Shifts in a Polaronic System," *J. Superconductivity* **12**, 37 (1999).

Mustre de Leon, J., et al., "Isotopic Substitution in a Model Polaronic System," *Phys. Rev. B* **59**, 8359 (1999).

Park, S.-G., et al., "High-Power, Narrowband THz Radiation Using Large Aperture Photoconductors," *IEEE J. Quantum Electron.* **35**, 1257 (1999).

Siders, C.W., et al., "Generation and Characterization of Terahertz Pulse Trains from Biased, Large-Aperture Photoconductors," *Opt. Lett.* **24**, 241 (1999).

Siders, J.L.W., et al., "Nonequilibrium Superconductivity and Quasiparticle Dynamics in YBa(2)Cu(3)O(7)," in *Ultrafast Phenomena XI* (Springer-Verlag, Berlin, 1998), p. 365.

Trugman, S.A., and J. Bonca, "The Polaron: Ground State, Excited States, and Far From Equilibrium," *J. Superconductivity* **12**, 221 (1999).

Organizing Principles of Materials near a Quantum-Critical Point

99528

Alan Bishop

Our objective in this one-year project was to begin the exploration of unifying principles in so-called strongly correlated electronic materials. We used an integrated synthesis-experimental-theoretical approach to study the novel phases of matter near critical points occurring at very low temperature, referred to as "quantum critical points." The classes of materials we studied were f-electron "heavy fermion" compounds, such as $CeRh_2Si_2$, and transition metal oxides, especially nickelates and cuprates.

We focused on three key scientific issues: (1) How does the balance among competing interactions, and associated length and energy scales, change as a quantum-critical point is approached? (2) How does extrinsic disorder influence physical properties near the quantum-critical point, as it competes with intrinsic inhomogeneity that arises from coupled spin, charge, and lattice degrees of freedom? (3) Does the nature of the broken symmetry transition change near the quantum-critical point as the system explores other broken symmetries?

From this research, we established theoretically and experimentally that local structural inhomogeneity produces a distribution of coupling strengths among spin and charge degrees of freedom. This intrinsic effect, arising from spin-charge-lattice coupling, controls macroscopic transitions between broken symmetry ground states in classes of correlated electron materials near a quantum-critical point and leads to striking non-Fermi-liquid behavior.

Highlights of our work included research focused on probing the competition and coupling among spin, charge, and lattice degrees of freedom in $CeRh_2Si_2$ as its ground state was tuned toward a quantum-critical point by pressure and the controlled introduction of extrinsic disorder. We used neutron scattering to discover subtle changes in the local structure of $CeCu_2Si_2$ and high magnetic fields to establish for the first time a common field-temperature phase diagram for $CeRh_2Si_2$ and $CeCu_2Si_2$.

In transition metal oxides, we found that spin-charge separation into intrinsically fine-scale (mesoscopic stripe) patterns can be driven by hole doping into broken-symmetry backgrounds (spin-density, charge-density, Jahn-Teller). We showed that a competition between short-range (lattice scale) and long-range (Coulomb, elastic) fields plays a fundamental role in determining the landscape of inhomogeneous ground states and metastable mesoscopic patterns.

Publications

Bonca, J., et al., "Holstein Polaron," *Phys. Rev. B* **60**, 1633 (1999).

Bonca, J., et al., "Mobile Bipolaron" (submitted to *Phys. Rev. Lett.*).

Chernyshev, A., et al., "Metallic Stripe in 2-Dimensions: Stability and Spin-Charge Separation" (submitted to *Phys. Rev. Lett.*).

Erloes, J., et al., "Inhomogeneity-Induced Superconductivity" (submitted to *Nature*).

Liu, C.-Y., et al., "Disorder-Driven Non-Fermi-Liquid Behavior in $CeRhRuSi_2$," *Phys. Rev. B* **61**, 432 (2000).

Louca, D., et al., "The Local Atomic Structure and Phonons in $Ba_{.5}Sr_{.5}TiO_3$" (to be published in *J. Phys. Chem. Solids*).

Modler, R., et al., "Magnetization of a Kondo Insulator $Ce_3Bi_4Pt_3$ and Metal $CeRh_2Si_2$ in Pulsed Fields," in *Physical Phenomena at High Magnetic Fields-III*, Z. Fisk et al., Eds. (World Scientific, Singapore, 1999), p. 154.

Mustre de Leon, J., et al., "Isotopic Shifts in a Polaronic System," *J. Supercond.* **12**, 37 (1999).

Mustre de Leon, J., et al., "Isotopic Substitution in a Model Polaronic System," *Phys. Rev. B* **59**, 8359 (1999).

Schmeltzer, D., and A. Bishop, "Theoretical Investigation of the Phases of the Organic Insulator $(TMTSF)_2PF_6$," *Phys. Rev. B* **59**, 4541 (1999).

Stojkovic, B., et al., "Charge Ordering and Long-Range Interactions in Layered Transition Metal Oxides," *Phys. Rev. Lett.* **82**, 4679 (1999).

Thompson, J.D., et al., "Competing Ground States in Heavy-Fermion Materials" (to be published in *J. Alloys Compd.*).

Trugman, S.A., and J. Bonca, "The Polaron: Ground State, Excited States, and Far From Equilibrium," *J. Supercond.* **12**, 221 (1999).

Yi, Y., et al., "Spin-Peierls Ground State in an Electron-Lattice Periodic Anderson Model," *J. Phys.: Condens. Matter* **11**, 3547 (1999).

Science of Polymer-Based Materials Aging

97614

Edward M. Kober

Our goal is to develop experimental and modeling techniques that can help us understand the complex aging phenomena of polymer-based materials. Such materials are used in nuclear weapons systems, and the ability to predict how their properties change with age is an area of intense interest for science-based stockpile stewardship. We are focusing on two polymeric systems, Estane 5703 and a silica-filled polydimethylsiloxane, that are relevant to Laboratory-designed weapons systems. Related materials are used in a variety of commercial and other defense applications, so this project helps integrate competencies in those areas. The experimental aspects of our project have promoted the development of novel instrumentation and analyses, resulting in measurements and characterizations not previously achieved.

We have shown that the primary structures of the original and aged polymers can be determined from two-dimensional nuclear magnetic resonance measurements. We characterized the vibrational spectra of these materials through a combination of isotopic labeling and quantum chemical calculations. This characterization quantifies the intermolecular interactions that determine the physical properties of the materials.

We characterized the mechanical properties of the aged systems at a variety of temperatures and at low, moderate, and high strain rates. We designed an experiment to measure the tensile failure of these materials at high strain rates. We found that all of these mechanical properties undergo significant changes as a function of aging, and these observations are of substantial interest to the weapons programs.

We demonstrated vibrational spectroscopy (infrared and Raman) as an excellent means for characterizing the temperature-dependent and long-time (>1 min.) relaxation properties of the materials and for quantifying the effect of aging on these properties. These results could be related to mechanical property changes and provide an auxiliary method for kinetics and material characterization. We have also shown that Electron Paramagnetic Resonance (EPR) and luminescence techniques can be used to characterize radiation damage and relaxation processes for the polymers.

With small-angle neutron scattering (SANS), we measured changes in the domain structure of these materials in response to temperature, long-time relaxation, and aging effects, where this structure determines the mechanical properties of the materials. We used a Bond Fluctuation Model (BFM) code to model the domain formation in these materials and how these domains evolve with time and chemical aging. We quantified these results by comparing them with the SANS and vibrational spectra.

We developed a mesoscale analytic model that can relate the static and dynamical mechanical properties of domain-based polymeric systems to the fundamental properties derived from the SANS spectra and the BFM modeling. Based on these observations, we derived the framework for a continuum model that represents the observed mechanical properties and how they evolve with aging.

Publications

Chitanvis, S.M., "Mesoscopic Theory of the Viscoelasticity of Polymers," *Phys. Rev. E* **60**, 3432 (1999).

Cooke, D.W., et al., "Luminescence, Optical Absorption and Electron Spin Resonance of an X-Irradiated Poly(esterurethane)," *Rad. Phys. Chem.* **55**, 1 (1999).

Cooke, D.W., et al., "Optical and Magnetic Resonance Measurements of a Segmented Poly(esterurethane)," *Nucl. Instrum. Methods* **B151**, 186 (1999).

Cooke, D.W., et al., "X-Ray-Induced Thermally Stimulated Luminescence and Electronic Processes in a Segmented Poly(esterurethane)" (submitted to *Rad. Phys. Chem.*).

Graff, D.K., et al., "Static and Dynamic FT-IR Linear Dichroism Studies of Plasticization Effects in a Polyurethane Elastomer" (submitted to *Macromolecules*).

Johnson, J.N., and J.J. Dick, "Spallation Studies in Estane" (The 1999 APS Shock Compression of Condensed Matter meeting, Snowbird, Utah, June 27–July 2, 1999).

Kober, E.M., "Accelerated Aging Studies on Estane" (The International Conference on Aging and Lifetime Extension of Materials, Oxford, UK, July 12–14, 1999).

Menikoff, R.S., and E.M. Kober, "Equation of State and Hugoniot Locus for Porous Materials: P-alpha Model Revisited" (The 1999 APS Shock Compression of Condensed Matter meeting, Snowbird, Utah, June 27–July 2, 1999).

Palade, L.-I., et al., "Complex Dielectric Relaxation Behavior of Highly Crosslinked PDMS Networks in the Glass Transition Region: An Experimental Study" (submitted to *Polymer*).

Palade, L.-I., et al., "Linear Thermo-viscoelastic Behavior of Highly Crosslinked Silica Reinforced Poly(dimethyl-siloxane) Elastomers" (submitted to *J. Mater. Res*.).

Patterson, C.W., et al., "Conformational Analysis of the Crystal Structure for MDI/BDO Hard Segments of Polyurethane Elastomers," *J. Polym. Sci. B: Polym. Phys.* **37**, 2303 (1999).

Ponomarev, A.L., et al., "Adsorption of a Flexible Polymer onto a Strongly Attracting Surface" (to be published in *Macromolecules*).

Ponomarev, A.L., et al., "Surface Diffusion and Relaxation of Partially Adsorbed Polymers" (to be published in *J. Polym. Sci., Polym. Phys.*).

Wang, H., et al., "Static and Dynamic Infrared Linear Dichroic Study of a Polyester/Polyurethane Copolymer Using Step-Scan FT-IR and a Photoelastic Modulator," *Appl. Spectrosc.* **53** (6), 29 (1999).

Self-Assembling Organic Electronic Materials

99503

Alan Bishop

A central scientific endeavor of this century will be understanding the physical principles that govern the relationships between (1) molecular level (microscopic) interactions and self-assembly into mesoscopic structures, and (2) mesoscopic structure and (macroscopic) electronic functionality in organic electronic and biomolecular materials. These relationships are important for many physical systems, and understanding their governing principles will have important implications in many areas of science and technology.

The goal of our project is to elucidate, control, and exploit these relationships for complex organic materials by understanding (1) the self-assembling processes in macromolecular organic structures and the relationship between mesoscopic structure and electronic functionality, and (2) using this understanding, along with an application of novel molecular synthesis and mesoscale fabrication techniques, to design and build new organic electronic materials. Our project focuses on three critical cross-cutting scientific issues: the fundamental mechanisms of organic self-assembly, the electronic structure and transport properties of organic interfaces, and the dipole alignment in multilayer organic films.

In this first year we have made progress toward each of our research targets. We have integrated synthesis-characterization modeling teams around classes of organic self-assembling materials, focusing on (a) controlling two- and three-dimensional self-assembly, (b) understanding and using the electronic structure and transport properties of organic heterojunctions, and (c) self-assembly and characterization of photoactive multilayered polar organic superlattices.

Publications

Campbell, I.H., and D.L. Smith, "Physics of Polymer Light-Emitting Diodes" (to be published as a chapter in *Semiconducting Polymer—Chemistry, Physics and Engineering,* VCH Wiley, NY).

Campbell, I.H., and D.L. Smith, "Schottky Energy Barriers and Charge Injection in Metal/Alq/Metal Structures," *Appl. Phys. Lett.* **74**, 561 (1999).

Campbell, I.H., et al., "Charge Transport in Polymer Light-Emitting Diodes at High Current Density," *Appl. Phys. Lett.* **75**, 841 (1999).

Campbell, I.H., et al., "Consistent Time-of-Flight Mobility Measurements and Polymer Light-Emitting Diode Current-Voltage Characteristics," *Appl. Phys. Lett.* **74**, 2809 (1999).

Chen, L., et al., "Highly-Sensitive Biological and Chemical Sensors Based on Reversible Flourescence Quenching in a Conjugated Polymer" (to be published in *Proc. Nat. Acad. Sci.*).

Crone, B.K., et al., "Device Physics of Single Layer Organic Light-Emitting Diodes" (submitted to *J. Appl. Phys*).

Eberhardt, A.S., et al., "Defects in Microcontact-Printed and Solution-Grown Self-Assembled Monolayers," *Langmuir* **15**, 1595 (1999).

Gao, J., et al., "Direct Observation of Junction Formation in Polymer Light-Emitting Electrochemical Cells" (to be published in *Phys. Rev. B. Rapid Comm.* **59**).

Johal, M.S., et al., "Second-Harmonic and Sum-Frequency Generation Studies of Spontaneously Self-Assembled Polar H-Bond Asymmetric Multilayers" (to be published in *Chem. Mater*.).

Johal, M.S., et al., "Study of the Conformational Structure and Cluster Formation in a Langmuir-Blodgett Film Using Second Harmonic Generation, Second Harmonic Microscopy, and FTIR Spectroscopy," *Langmuir* **15**, 1275 (1999).

Kirova, N., et al., "A Systematic Theory for Optical Properties of Phenylene-Based Polymers," *Synth. Met.* **100**, 29 (1999).

Kozhevnikov, M., et al., "Effect of Electron Scattering on Second Derivative Ballistic Electron Emission Spectroscopy in Au/GaAs/AlGaAs Heterostructures," *Phys. Rev. Lett.* **82**, 3677 (1999).

Kozhevnikov, M., et al., "Ordering-Induced Band Structure Effects in $GaInP_2$ Studied by Ballistic Electron Emission Spectroscopy" (submitted to *Appl. Phys. Lett.).*

Kraabel, B., et al., "Ultrafast Spectroscopic Holography in Conjugated Polymers," *Synth. Met.* **101**, 281 (1999).

Li, D., et al., "Transport Properties of Metal/Organic Monolayers/ Semiconductor Heterostructures" (to be published in *Appl. Phys. Lett.*).

Mashl, R.J., et al., “Theoretical and Experimental Adsorption Studies of Polyelectrolytes on an Oppositely Charged Surface,” *J. Chem. Phys.* **110**, 2219 (1999).

McBranch, D.W., et al., “Ultrafast Energy Transfer and Holography in Molecularly-Engineered Thin Films” (to be published in *SPIE Proceedings, Third-Order Nonlinear Optical Materials*).

Parikh, A.N., et al., “Characterization of Sandwiched Chain Molecular Assemblies in Long-Chain Layered Silver Thiolates,” *J. Phys. Chem.* **103**, 2850 (1999).

Parikh, A.N., et al., “Preparation and Characterization of Hybrid Bilayer Membranes at Oxide Surfaces,” *Langmuir* **15**, 5369 (1999).

Parikh, A.N., et al., “A Structural Comparison between Long-Chain Silver Thiolates and Single Monolayers of Alkanethiols on Ag” (submitted to *J. Phys. Chem.*).

Saxena, A., et al., “Dynamics and Role of Nonadiabatic Effects on Nonlinear Optical Response of Conjugated Polymers,” *Synth. Met.* **101**, 257 (1999).

Saxena, A., et al., “Stability of Bipolarons in Conjugated Polymers,” *Synth. Met.* **101**, 325 (1999).

Wang, H.-L., et al., “Controlled Unidirectional Energy Transfer in Luminescent Self-Assembled Conjugated Polymer Superlattices” (to be published in *Chem. Phys. Lett.*).

Wang, R., et al., “Non-Equilibrium Pattern Formation in Langmuir-Phase Assisted Assembly of Silane Monolayers” (to be published in *J. Phys. Chem.*).

Wang, W.Z., et al., “Effect of Nonadiabaticity on Nonlinear Optical Response in a Holstein-Hubbard Model,” *Phys. Rev. B* **59**, 1697 (1999).

Yu, Z.G., et al., “Dynamics of Electronic Transmission in Metal/Organic/Metal Structures,” *Synth. Met.* **102**, 1057 (1999).

Yu, Z.G., et al., “Dynamics of Electronic Tunneling in Metal/Oligomer/Metal Structures,” *J. Phys.: Condens. Matter* **11**, L7 (1999).

Yu, Z.G., et al., “Green Function Approach to Dynamical Transport in Organic Devices,” *Phys. Rev. B* **59**, 16001 (1999).

Coordinated Synthesis, Characterization, and Modeling of Materials

99507

Don M. Parkin

This project develops both existing and new competencies in materials science through a collaboration between Laboratory staff and external materials scientists to explore new techniques in a variety of areas related to the synthesis, characterization, and modeling of materials. Each task selected is built on a strength within the Laboratory community that can be significantly further developed with a new direction or next step in that technical area. New applications and development of materials synthesis and characterization techniques form the basis for increasing our broad technical capabilities to perform on programmatic activities.

We successfully developed and tested two-dimensional magnetometers designed for de Haas–van Alphen measurements in pulsed magnetic fields. Collaborators at the University of New South Wales, Australia, fabricated 80-turn magnetometers using high-precision electron-beam writing techniques. Measurements on a CeB_6 sample at 450 mK in a 50-T pulsed magnet resulted in extremely high-quality data.

To investigate the fundamental processes governing the retention and release of helium-3 in films, we explored ion-beam materials analysis techniques. The experimental approach addresses the effects of the addition of dopant atoms at the few-percent level (<5%) on the helium-3 behavior. Zirconium-doped erbium films have been prepared for helium ion implantation. Experiments to study the helium migration as a function of temperature are under way.

Research on ductile spallation fracture to understand the mechanisms of microvoid nucleation, growth, and coalescence under shock-loading conditions focused on modeling. We developed a model for ductile spallation fracture and for the mechanics of void growth and coalescence under shock-loading conditions, using the Ortiz and Molinari growth model as the basis. Our model gives good agreement with the Los Alamos spallation tests on tantalum.

We ran simulations and experiments on copper single crystals under laser-driven miniflyer spallation conditions. Calculations showed that the spall strengths of oriented single crystals are significantly higher than for polycrystalline copper. In the experimental micrographs, the spall damage indicates that the voids nucleate homogeneously in pure copper.

Publications

Eriksson, O., et al., “Novel Electronic Configuration in Delta Pu,” *J. Alloys Compd.* **287**, 1 (1999).

Grechnev, G.E., et al., Magnetovolume Effect in UGa_3,” *Phys. Rev. B* **59**, 1776 (1999).

A Scalable Silicon-Based Nuclear Spin Quantum Computer

99531

P. Chris Hammel

For certain problems in which quantum superposition can result in massive parallelism, a quantum computer (QC) would be much more powerful than any conventional computer. One researcher recently presented a well-thought-out and realistic proposal for a silicon-based QC with a highly scalable architecture. This project is the first phase of a multidisciplinary research program to test that proposal by building a two-qubit QC. We are collaborating with the Semiconductor Nanofabrication Facility at the University of New South Wales (UNSW), Caltech, and the University of Maryland on a number of different, complementary approaches to fabrication and single-spin control of the prototype device. As a world leader in computation, Los Alamos is well positioned to lead this revolutionary new approach to computation. Our early results represent important steps in developing state-of-the-art fabrication and spin readout techniques necessary for constructing a solid-state QC.

In collaboration with UNSW, we have fully tested an Ultrahigh Vacuum Variable Temperature Scanning Tunneling Microscope system, prepared and imaged a clean Si(100) 2×1 structure and the monohydride passivation resist layer, and carried out initial hydrogen removal lithography experiments. We constructed and tested a magnetic resonance force microscope (MRFM) operating at 4 K that employs a cantilever detector with an integral magnetic probe (~100–200 nm tip radius). The MRFM operates both as a scanning atomic force microscope (AMF) and a scanning nuclear magnetic resonance (NMR) microscope.

The figures show a topographic image of an array of 3-μm-diam. cobalt disks obtained with the microscope in AFM mode and the NMR spectrum obtained in the central dot. This spectrum agrees with those from conventional NMR techniques. We began an analysis of the decoherence mechanisms relevant to the operation of the solid-state QC. We completed a theoretical/numerical study of the dynamics of spin measurements and are working on related questions (fundamental limitations of the technique and tomographic techniques for image recovery) with the MRFM. Other, ongoing efforts include the study of the effects of isotopic impurities and a fluorescent readout method.

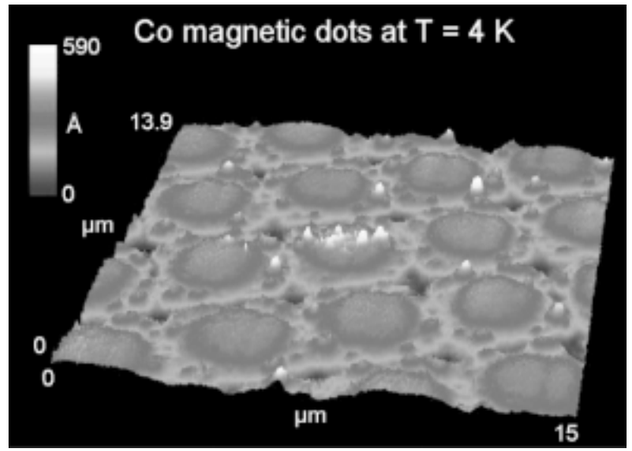

(a) A topographic image of a cobalt dot sample obtained with the microscope in AFM mode. (b) The NMR spectrum from a particular location in the center cobalt dot. The inset shows the time dependence of the cantilever oscillation for RF excitation at 226.2 MHz.

Publications

Berman, G.P., et al., “Dynamics of Nuclear Spin Measurement in a Mesoscopic Solid-state Quantum Computer” (submitted to *Phys. Rev. B*).

Competing Interactions in Complex Materials—Bridging Hard, Soft, and Biological Matter

99526

David G. Whitten

Entire classes of hard, soft, or biological materials are characterized by large-scale sensitivity and extreme nonlinear behavior in response to small perturbations of variables such as temperature, pressure, or composition. Examples include colossal magnetoresistance materials; magnetic glasses; organic-inorganic hybrid materials; self-assembling organics; inorganic, organic, and hydrogels; colloidal nanoparticles; and biomembranes. Our purpose in this one-year project was to develop research activities that would ultimately provide a set of organizing principles for a cross-disciplinary approach to describing structure, properties, and dynamics in such complex materials. Results in several areas follow.

Spin Dynamics in Doped $LaMnO_3$ Compounds. We used muon-spin relaxation and neutron-spin echo spectroscopy to study spin dynamics in calcium-doped $LaMnO_3$. Potential applications of this class of materials include use as magnetic sensors. We observed multiple-time-scale dynamics that could be associated with segregation of doped holes in the material. Such segregation likely arises from a competition between long- and short-range interactions, which is also the underlying reason for the appearance of spatially modulated structures in two- and three-dimensional soft materials.

Wetting-Instability-Induced Pattern Formation in Monolayers at an Air/Water Interface. Research showed that dewetting instabilities in amphiphilic molecules lead to the formation of spatially modulated architectures in monolayers of long-chain trifunctional silanes at an air/water interface. These structures result from the competition between short-range attractive interactions of the aliphatic chains and the long-range repulsive interactions of the polar head groups.

Nonequilibrium Pattern Formation in Monolayers on Oxide Surfaces. Our work showed that structural reconstructions in organic monolayers upon transfer to a substrate from an air/water interface produce self-patterned surfaces. We described the results in terms of competing interactions and reaction-diffusion models and developed a strategy that will afford a wide range of control over the generation of patterned organic films. Possible applications include thin-film biological and chemical sensor development.

Thermal Phase Behavior of Three-Dimensional Spatially Modulated Architectures in Mixed Organic-Inorganic Crystals. We used temperature-dependent infrared spectroscopy to probe the molecular-level structural dynamics associated with phase transitions in a layered inorganic-organic silver dodecylthiolate, $AgS(CH_2)_{12}CH_3$. The results help address melting issues in organic phases within the constrained environment of organic-inorganic network solids, a class of materials with increasingly important applications in sensing, separation science, and catalysis.

Publications

Bardeau, J.F., et al., "Phase Behavior of a Structurally Constrained Organic-Inorganic Crystal: Temperature Dependent Infrared Spectroscopy of Silver *n*-dodecanethiolate," *J. Phys. Chem. B.* **104**, 627 (2000).

Geiger, C., et al., "Organogels Resulting from Competing Self-Assembly Units in the Gelator: Structure, Dynamics, and Photophysical Behavior of Gels Formed from Cholesterol-Stilbene and Cholesterol-Squaraine Gelators," *Langmuir* **15**, 2241 (1999).

Heffner, R.H., et al., "Evidence for a Distributed Ferromagnetic Transition in (La,Ca)MnO_3" (to be published in *Physica B.*).

Heffner, R.H., et al., "Observation of Two Time Scales in the Ferromagnetic Manganite $La_{(1-x)}Ca_xMnO_3$, $x \approx 0.3$" (submitted to *Phys. Rev. Lett.*).

Parikh, A.N., et al., "Characterization of Chain Molecular Assemblies in Long-Chain, Layered Silver Thiolates: A Joint infrared Spectroscopy and X-Ray Diffraction Study," *J. Phys. Chem. B.* **103**, 2850 (1999).

Wang, R., et al., "Nonequilibrium Pattern Formation in Langmuir-Phase Assisted Assembly of Alkylsiloxane Monolayers," *J. Phys. Chem. B.* **103**, 10149 (1999).

Advanced Research Capabilities for Neutron Scattering

98610

Robert A. Robinson

This project covers a range of new technologies that can potentially improve the performance of neutron spectrometers at the Los Alamos Neutron Science Center (LANSCE) and elsewhere. The project covers four major areas: (1) novel position-sensitive detectors, (2) time-resolved cold-neutron radiography, (3) beam optics for neutron-scattering applications, and (4) Monte Carlo simulation tools. The specific remaining goal in the beam optics area is to bring out the most intense polarized-neutron beam to date, anywhere in the world, at a spallation neutron source. In the Monte Carlo simulations, we plan to include provision for polarized-neutron beams and backgrounds. These activities have the potential for long-term benefit by impacting instrument design and providing polarized-neutron beams to all applications of the neutron-scattering method.

In the beam optics area, we performed Monte Carlo simulations on the problem of bringing two neutron guides out of the same beam hole, while maintaining a good vacuum and alignment capability. Two 6.5- by 12-cm^2 guides will work. We have fabricated and tested the polarizer components. Their design uses a material that does not need an applied magnetic field to saturate them. The flipping ratios (degree of neutron polarization) are good. We have also studied the problems of how to engineer the thimble that holds the guides within the bulk shield and how to build external beam shutters and shield them properly.

One of the results of the Monte Carlo simulations of neutron-scattering instruments is an easy-to-use Web interface, MC Web. The latest improvements include parsers for expert users, automatic generation of drift spaces, automatic generation of geometry visualization, and on-line help. We have modeled four of the LANSCE instruments and done some benchmarking against real performance. Variance reduction techniques have been added, as have various spectrometer components, particularly Fermi choppers, crystals in Bragg and Laue geometries, new moderators, and inelastic scattering kernels. Finally, we have developed the methodology for low-probability background events.

Other project achievements this year include the allowance of a U.S. patent on a novel, cheap neutron guide technology; mechanical design of a neutron "wobbulator"; tomographic reconstruction of a rock-core sample, using our source; and Monte Carlo simulation of time-resolved radiography data. In addition, our pad detector was transferred to the proton radiography program at Los Alamos and used for image plates for fast-neutron radiography.

Publications

Claytor, T.N., et al., "Thermal and Cold Neutron Imaging at the Los Alamos Neutron Scattering Center Using an a-Si Detector Array," *Nucl. Instrum. Methods Phys. Res., Sect. A* **424**, 84 (1999).

Daemen, L.L., et al., "Monte Carlo Tool for Neutron Optics and Neutron Scattering Instrument Design," *Proc. SPIE Int. Soc. Opt. Eng.* **3771**, 80 (1999).

Daemen, L.L., et al., "A Monte Carlo Tool for Simulations of Neutron Scattering Instruments," *AIP Conf. Proc.* **479**, 41 (1999).

McDonald, T.E., Jr., et al., "Time-Gated Energy-Selected Cold Neutron Radiography," *Nucl. Instrum. Methods Phys. Res., Sect. A* **424**, 235 (1999).

Fundamental Studies of Radiation Damage in Two-Phase Oxide Composites

97801

Kurt E. Sickafus

Our goal is to understand radiation-induced damage in multiphase ceramic oxide materials, whose component phases have different radiation tolerances and mechanical properties. We hope to learn about damage evolution in two-phase ceramic composites. Such composites could be used (1) to form rocklike wasteforms to immobilize plutonium and other high-level radioactive wastes, or (2) to form rocklike nuclear fuelforms to destroy plutonium and higher actinides by burning the nuclear fuel in a conventional nuclear reactor.

We developed a new ceramic-ceramic composite consisting of the mineral geikielite ($MgTiO_3$) as a matrix phase and the mineral pyrochlore ($Er_2Ti_2O_7$) as a minor, second phase. We are investigating this composite's potential to immobilize and store surplus actinides or high-level radioactive wastes.

We performed radiation-damage experiments by implanting composite $MgTiO_3$–$Er_2Ti_2O_7$ samples (at a temperature of about 120 K) with 350-keV xenon^{++} ions to ion fluences ranging from 10^{14} to 10^{16} cm^{-2}. We analyzed these irradiated samples using transmission electron microscopy (TEM) and nanoindentation techniques (in the latter case, we measured the Young's modulus and the hardness of the implanted samples). Nanoindentation measurements indicate that these composites experience a dramatic loss of modulus and hardness at moderate ion doses, but that they recover these properties somewhat at higher ion doses. TEM observations indicate that the pyrochlore phase (intended as an actinide-host phase for waste applications) amorphizes at a lower dose than the geikielite matrix phase. This behavior is similar to the radiation response behavior of the pure compounds.

Under light microscope we observed that the irradiated composite samples experience microcracking upon amorphization of the second-phase pyrochlore precipitates. This cracking is caused by the volume change that accompanies amorphization. Unless we can mitigate this problem, radiation-induced microcracking will limit the amount of actinide dopants (or other radioactive species) that we can introduce into the pyrochlore phase in $MgTiO_3$–$Er_2Ti_2O_7$ composite wasteforms.

Development of Semiconducting Polymeric Films with High Concentrations of Boron

99509

DeQuan Li

Current neutron detection mechanisms rely primarily on neutron-absorbing gas-filled detectors, such as the helium-3 gas detectors used at the Los Alamos Neutron Science Center (LANSCE). Other neutron detection technologies include scintillators (ZnS) and pyroelectric detectors [$Pb(Zr,Ti)O_3$]. The drawbacks of these technologies are their slow response time, sensitivity to gamma-radiation, and the high cost of fabricating large area detectors. This program is aimed at developing a new class of neutron detectors based on organic, conductive polymeric films doped with boron compounds. Upon interacting with neutrons, energetic lithium-7 and alpha particles are created from boron-10 and yield an induced current under the application of a bias, which is our primary signal for neutron detection.

This year we succeeded in preparing composite films with two essential components: a conductive polymer, polythiolphene, and a boron-containing compound, m-carborane (1,7-$C_2B_{10}H_{12}$). We have fabricated freestanding, high-quality homogenous films as well as films on supporting substrates. Ultraviolet-visible and Fourier transform infrared spectroscopy showed that the interactions between polythiophene and carborane are miscible at the molecular level even at high concentrations of boron. An area of concern was the loss of carborane from the films, which we observed through kinetic infrared studies of carborane-doped films. Spin casting a protective layer of polyvinyl alcohol on top of the boron-doped polythiolphene films solved this problem.

When we measure the current-voltage characteristics of these boron-doped polymeric devices, we observe that they behave like a diode. Exposure to neutrons induces a change in the devices' electric properties. The response of the electrical property change depends on the level and degree of interactions between the conductive polymers and carborane in the absence of neutrons.

To be efficient in detecting neutrons, we need to fabricate boron-doped films with thicknesses of 100–200 μm in order to have good neutron efficiency while using boron compounds with natural abundance. Our freestanding present film has a typical thickness of about 10 μm, and a stack of 10–20 layers of these films should yield the desired total thickness.

Critical Current Mechanisms in High-Temperature Superconducting Films

99530

Martin Maley

The recent dramatic advance in development of a high-temperature superconducting (HTS) tape with superior properties at liquid-nitrogen temperature has improved prospects for near-term commercialization of HTS technology. The advance has been achieved by understanding the physical, chemical, and microstructural mechanisms that determine the performance of HTS materials. This understanding has directed our efforts toward controlling such factors as grain alignment, interfaces, and flux pinning that are critical for the improvement of performance.

The object of this project is to understand the relation between the dependence of critical current density of $YBa_2Cu_3O_7$ (YBCO) films on temperature, field, and field orientation and the microstructural defects that are responsible. We hope to identify optimum defect structures for improving the performance of these films and to explore processing strategies to control them. We will explore new chemical means of introducing strong pinning nanoscale defects by substitutions for the rare-earth site.

We have experimentally studied the relationship between the film thickness and the critical current of YBCO-coated conductors. Our successful experiment was carried out by repeatedly etching the top of a thick YBCO film. We measured the critical current carried by the remaining part of the film after each etching. Experimental results show that the top region of the thick YBCO films (above 2 μm) carries almost no current. The change of microstructure with film thickness seems to play a big role in determining the current-carrying capability of coated conductors.

Next, we investigated the effect of surface roughness on the structural and superconducting properties of the YBCO films. We also investigated the influence of surface roughness on the crystallinity of the ion-beam-assisted deposition (IBAD) MgO buffer layers. The YBCO films on rough substrates show reduced critical transition temperature and current density. The crystallographic misalignment, both out-of-plane and in-plane, for the films on rough substrates increases compared with the films on very smooth substrates. To achieve the highest in-plane texture of IBAD MgO buffer layers, smooth substrate finish is necessary. YBCO films grown on these MgO-buffered smooth substrates now exhibit megaampere-per-square-centimeter current densities.

In addition, we have developed our own processing conditions to deposit superconducting Sm123 and Nd123 films with smoother surface morphology. By using YBCO as a buffer, we have routinely fabricated Sm123 films with critical current density above 10^6 A/cm^2 at 75 K. We have also deposited high-quality Nd123 films with a critical current density of 6.4×10^6 A/cm^2 at 75 K.

Thus, we have successfully demonstrated that a multilayer approach can be used to enhance the total current-carrying capability of thick YBCO films both on single crystal and polycrystal metal substrates.

Publications

Cho, J.H., et al., "Effects of Unidirectional and Isotropic Columnar Defects in $Bi_2Sr_2CaCu_2O_8$ Single Crystals," *Physica C* **302**, 113 (1998).

Coulter, J.Y., et al., "Magnetic Field Anisotropy of High-Critical-Current YBCO Coated Conductors," *IEEE Trans. Appl. Supercond.* **9**, 1487 (1999).

Foltyn, S.R., et al., "Relationship Between Film Thickness and the Critical Current of $YBa_2Cu_3O_7$ Coated Conductors" (submitted to *Appl. Phys. Lett.*).

Kwon, C., et al., "Fabrication and Characterization of $REBa_2Cu_3O_7$ (RE = Y, Er, Sm, and Nd) Films," *IEEE Trans. Appl. Supercond.* **9**, 1575 (1999).

Kwon, C., et al., "Improved Superconducting Properties of $SmBa_2Cu_3O_7$ Films Using $YBa_2Cu_3O_7$ Buffer Layer" (to be published in *Phil. Mag. B*).

Mazilu, A., et al., "Vortex Dynamics of Heavy-Ion-Irradiated $YBa_2Cu_3O_{7-d}$: Experimental Evidence for a Reduced Vortex Mobility at the Matching Field," *Phys. Rev. B* **58**, R8909 (1998).

Comparative Investigation of Spin, Charge, and Lattice Degrees of Freedom in Colossal Magnetoresistive Materials

98817

Robert Heffner

The ground states of transition metal oxides (TMOs) are extraordinarily interesting, encompassing superconducting, magnetic, insulating, and metallic behavior. We are studying TMOs exhibiting colossal magnetoresistance (CMR)—a large decrease of electrical resistance on application of an external magnetic field—for two principal reasons. First, the materials are of fundamental scientific interest because conventional theories of magnetic ordering and charge transport do not apply to these materials, which have unusually strong coupling between their lattice, spin, and charge degrees of freedom. Second, a predictive understanding of these systems may enable us to use these materials for applications like magnetic field sensors and data storage. We are also studying related TMOs such as the pyrochlore structures $Re_2A_2O_7$ (Re = rare earth, A = transition metal).

Our goal is to understand the microscopic mechanisms responsible for such macroscopic phenomena as CMR. Our approach is first to synthesize the highest-quality materials and then to study their lattice and spin properties using (primarily) two microscopic probes: neutron scattering and muon-spin relaxation (μSR). Finally, we employ theoretical modeling to understand and stimulate our measurement program.

We synthesized single crystals of bilayer CMR materials (which allow us to study the effects of reduced dimensionality on magnetic and structural properties), polycrystals of the three-dimensional CMR perovskites, and polycrystals of a pyrochlore frustrated-spin system. We performed neutron, μSR, x-ray, Raman, and electron-spin-resonance experiments.

We subjected one bilayer CMR material—a ferromagnet—to extensive studies. Using neutron scattering we found (1) that the unpaired spin density resides primarily on the manganese and not on the oxygen sites and (2) that charge transfer to specific manganese d-spin orbitals accompanies ferromagnetic ordering. We also carried out a neutron spin echo (NSE) experiment showing inhomogeneous spin freezing in the frustrated pyrochlore spin system. A complete analysis of these experiments is still in progress.

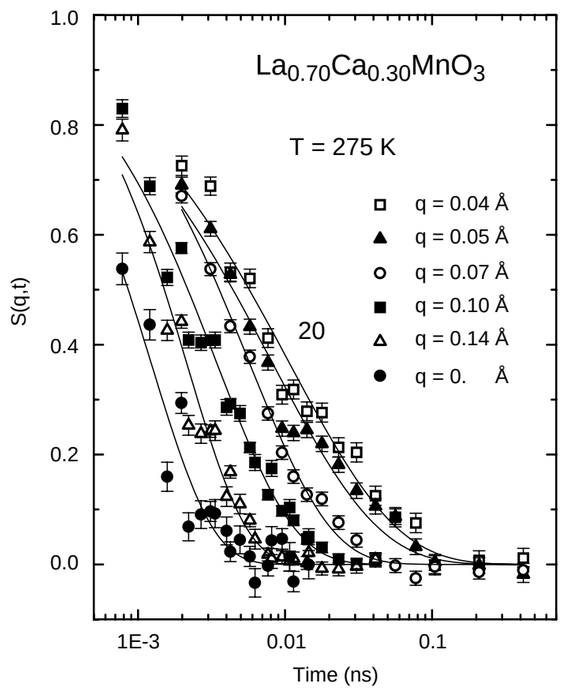

Spin-spin correlation function S(q,t) measured by NSE spectroscopy just above the ferromagnetic transition temperature T_C. The solid lines are fits to the sum of two exponential relaxation functions, corresponding to "fast" and "slow" manganese-ion correlation times, τ_F and τ_S, respectively.

We completed two additional experiments. (1) From measurements of thermal diffuse scattering, manganese-oxygen bond lengths, and displacement (Debye-Waller) factors in the bilayer CMR material, we showed that the bond-length distribution narrows below the insulator-to-metal transition because of carrier delocalization. (2) Through a comparative mSR and NSE study of the spin dynamics in ferromagnetic perovskites, we demonstrated that there are at least two intrinsic time scales above and below the ferromagnetic critical temperature (see the figures). The presence of two distinct relaxation times reflects the intrinsic inhomogeneity in the spin fluctuation spectrum of these systems.

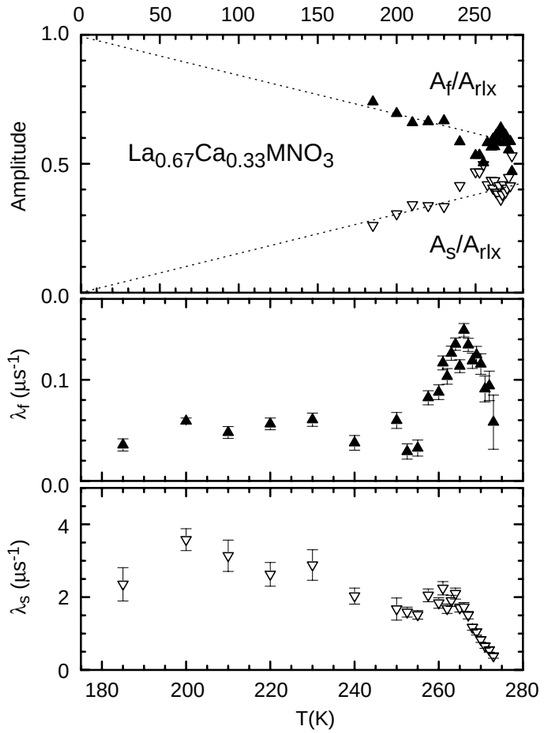

Temperature dependence of the amplitudes (top) of the fast (A_f/A_{rlx}) and slow (A_s/A_{rlx}) mSR rates $\lambda_f \propto \tau_F$ (middle) and $\lambda_s \propto \tau_S$ (bottom) in this ferromagnetic CMR material. The data were fit to a two-exponential form analogous to the NSE S(q,t) in the first figure. Note that the λ_f rate peaks at T_C, and its amplitude increases below T_C, indicating that this component of the spin fluctuation spectrum grows in volume fraction as the temperature is lowered. The rates measured with μSR are consistent with the NSE experiments.

Publications

Argyriou, D.N., et al., "Lattice Displacements above T_C in the Layered Manganite $La_{1.2}Sr_{1.8}Mn_2O_7$" (submitted to *Phys. Rev. B.*).

Argyriou, D.N., et al., "Lattice Effects and Magnetic Structure in the Layered Colossal Magnetoresistance Manganite," *Phys. Rev. B.* **59**, 8695 (1999).

Billinge, S.J.L., et al., "Evidence for Charge Localization in the Ferromagnetic Phase of $La_{1-x}Ca_xMnO_3$ from High Real-Space-Resolution X-Ray Diffraction" (to be published in *Phys. Rev. B.*).

Gardner, J.S., et al., "Glassy Statics and Dynamics in the Chemically Ordered Pyrochlore Antiferromagnet $Y_2Mo_2O_7$," *Phys. Rev. Lett.* **83**, 211 (1999).

Heffner, R.H., et al., "Observation of Two Time Scales in the Ferromagnetic Manganite (La, Ca)MnO_3" (submitted to *Phys. Rev. Lett.*).

Moreno, N.O., et al., "Extrinsic and Intrinsic Features above T_C in Layered Manganite: $La_{1.2}Sr_{1.8}Mn_2O_7$" (submitted to *Phys. Rev. B.*).

Atomic Resolution Probes of Materials

98801

Carl J. Maggiore

The purpose of this project is to enhance capabilities for the atomic scale measurement and analysis of materials at the Electron Microscope Facility (EMF) and the Ion Beam Materials Laboratory (IBML).

For the electron microscopes, we are developing image processing and computational methods to realize the true atomic-scale resolution of the field-emission scanning transmission and the high-resolution microscopes. This work emphasizes the very high vacuum capabilities of the instruments and uses the Z contrast methods of imaging atomic planes in materials such as superconductors. We continue to conduct many research projects using optical microscopy, scanning electron microscopy, orientation imaging microscopy, analytical electron microscopy, high-resolution electron microscopy, and scanning transmission electron microscopy. Notable projects include the study of modulated structures in silicides, oxygen ion implantation of SiC, cross-sections of complex superconducting tapes, texture in a wide variety of metallic materials, and, in collaboration with the University of California at Riverside, the chemistry of nano-inclusions in metamorphic diamonds. New in situ straining holders for the AEM allow us to perform deformations studies of copper at cryogenic temperatures and steels at elevated temperatures.

The IBML has been used for many research projects requiring the extended development of ion beam analytical methods. Deep multilayer analysis using micro RBS (Rutherford backscattering with a microbeam) has been extended to higher energies for deeper subsurface analysis. A new method for determining the porosity of alumina membranes has been developed using resonant backscattering, and the method has been generalized to materials containing at least one element with a sufficiently narrow backscattering resonance. The facility has been used extensively to study the oxidation and corrosion of sensitive materials and steels in extremely hostile environments. The in situ measurements of polymeric breakdown products caused by radiation damage have continued, and the method has been extended to time-dependent experiments. Developing optimized methods for studying the oxidation of ceramics, salts, and subsurface metallized layers has continued to be an important part of the work at the facility.

Publications

Chu, F., et al., "Elastic and Mechanical Properties of $Nb(Cr,V)_2$ C**15** Laves Phases" (to be published in *J. Mater. Sci.)*.

Gahagan, K.T., et al., "Fabrication and Characterization of High-Speed Integrated Electro-Optic Lens and Scanner Devices," Proceedings SPIE, 3620, 374 (1999).

Gahagan, K.T., et al., "Integrated Electro-Optic Lens/Scanner in a $LiTaO_3$ Single Crystal," *Appl. Opt.* **38**, 1186 (1999).

Gopalan, V., et al., "In-Situ Video Measurement of 180 Domain Mobility in Congruent $LiTaO_3$ Using Electro-Optic Imaging Microscopy," *J. Appl. Phys.* **86**, 1638 (1999).

Gopalan, V., and T.E. Mitchell, "In-Situ Video Observation of 180 Degree Domain Switching in $LiTaO_3$ by Electro-Optic Imaging," *J. Appl. Phys.* **85**, 2304 (1999).

Gopalan, V., et al., "Switching Kinetics of 180 Domains in Congruent $LiNbO_3$ and $LiTaO_3$ Crystals," *Solid State Commun.* **109**, 111 (1999).

Keast, V.J., et al., "Compositional Mapping of Nanoscale Metallic Multilayers: A Comparison of Techniques" (to be published in EMAG 99, Institute of Physics).

Koike, J., et al., "Relationship between High-Strain-Rate Superplasticity and Interface Microstructure in Aluminum Alloy Composites," *Microscopy and Microanalysis* **5**, Suppl.2, 772 (1999).

Lu, Y.-C., et al., "Deposition of Cu/Ni Multilayers on Cu Single Crystals by e-Beam Evaporation" (submitted to *J. Mater. Res.*).

Maloy, S.A., et al., "Dislocations and Mechanical Properties of Single Crystal $NbSi_2$" (to be published in *J. Am. Ceram. Soc.*).

Misra, A., et al., "Defect Structures in Semiconducting $ReSi_{2-x}$ Thin Films," *Microscopy and Microanalysis* **5**, Suppl. 2, 726 (1999).

Misra, A., et al., "Electrical Resistivity of Sputtered Cu/Cr Thin Films," *J. Appl. Phys*. **85**, 302 (1999).

Misra, A., et al., "Incommensuration and Other Structural Anomalies in Rhenium Disilicide," *Philos. Mag. A* **79**, 1411 (1999).

Misra, A., et al., "Microstructures and Mechanical Properties of a Mo_3Si-Mo_5Si_3 Composite," *Scripta Mater.* **40**, 191 (1999).

Misra, A., et al., "Rapid Solution Hardening at Elevated Temperatures by Substitutional Re Alloying in $MoSi_2$" (to be published in *Acta Metall. Mater*.).

Misra, A., et al., "Residual Stresses and Ion Implantation Effects in Cr Thin Films," *Nucl. Instrum. Methods Phys. Res., Sect. B* **148**, 211 (1999).

Misra, A., and T.E. Mitchell, "Twinning in Incommensurate and Commensurate Structures of $ReSi_{2-x}$ Alloys," in *Advances in Twinning*, S. Ankem and C.S. Pande, Eds. (The Minerals, Metals and Materials Society, Warrendale, PA, 1999), p. 253.

Mitchell, T.E., and A. Misra, Structure and Mechanical Properties of (Mo, Re)Si_2 Alloys, *Mater. Sci. Eng., A* **261**, 106 (1999).

Mitchell, T.E., et al., "Unusual Incommensurate, Modulated and Disordered Structures in Refractory Metal Disilicides" (to be published in EMAG 99, Institute of Physics).

Peralta, P., et al., "Effects of Small Aluminum Additions on Mechanical, Elastic and Structural Properties of Monocrystalline C11b $MoSi_2$" (to be published in *Proceedings of the Conference on Computer Aided Design of High Temperature Materials*).

Peralta, P., et al., "Fatigue Crack Nucleation in Metallic Materials, in Small Fatigue Cracks" (to be published in *Mechanics and Mechanisms*, Engineering Foundation Conference Proceedings).

Peralta, P.D., et al., "Fatigue Fracture of Bicrystal Interfaces: Fractography," *Mater. Sci. Eng., A* **264**, 215 (1999).

Peralta, P., et al., "Residual Thermal Stresses in $MoSi_2$-Mo_5Si_3 In-Situ Composites," *Mater. Sci. Eng., A* **261**, 261 (1999).

Wetteland, C.J., et al., "Radiation Damage Effects in Ferroelectric $LiTaO_3$ Single Crystals in Atomic Mechanisms in Beam Synthesis and Irradiation of Materials," *Mater. Res. Soc. Symp. Proc.* **504**, 159 (1999).

Materials with Complex Electronic/Atomic Structures

97619

Don M. Parkin

The challenge for the next millennium is to understand, design, and exploit complexity in materials. Our research focuses on topics in complex materials to understand how complexity leads to materials behavior and function. The first topic addresses the theoretical strength of solids, which can be described by reference to the bonding forces. Our objectives are two-fold: The basic science aspect deals with the study of the mechanisms of attaining ultra materials both by thermal mechanical sequences and by novel phase transitions. In addition, attention is being given to developing methodologies for the production of ultrahigh strength materials and rationalizing of these materials in engineering design. The second topic addresses the design and synthesis of new molecules with novel self-assembling properties and reactivity as supramolecular assemblies (organogels in particular). These might be used to develop novel and efficient photoredox reactions of organic and inorganic molecules based on single electron transfer processes.

Using the Taylor wire synthesis technique, we encapsulated cold-drawn rods of copper-l6 at.% silver in tubes of 7740 borosillicate glass that had a softening temperature of 821°C and working temperature of 1252°C. The assembly was heated to a temperature between the softening and working temperatures of the glass and drawn vertically. The glass-coated wires cooled in air at rates estimated to be in the range of $l0^2$ °C /s to 10^5 °C/s, depending on the diameter of the drawn wire. We obtained nanograins when the wire diameter was about l0 μm with a cooling rate of about10^5 °C/s. When the diameter of the wire was larger than 20 μm, we found proeutectic copper and eutectic copper-silver.

This year we also studied the structures of organogels by a variety of techniques including neutron scattering and x-ray scattering techniques, various forms of imaging, and spectroscopic and calorimetric investigations. Although we learned much about the structure and properties of these organogels, many questions remain. Some of these include the relationship between gelator structure in the gel and the crystal structure of pure gelator, the specific interaction between the solvent and gelator, the state or states of the solvent, and the factors that determine what solvents a given gelator will gel and how the material properties of the gel on a macroscopic scale will be influenced by the nano- and mesostructures of the gel.

Publications

Chen, L., et al., "Super Quenching Behavior between a Conjugated Polymer and Molecular Quenchers and Its Application in Biological/Chemical Sensors," *Proc. SPIE–Int. Soc. Opt. Eng.* **3858**, 32 (1999).

Han, K., et al., "The Fabrication, Properties and Microstructure of Cu-Ag and Cu-Nb Composite Conductors," *Mater. Sci. Eng., A* **267**, 99 (1999).

Multiscale Phenomena in Materials

97802

Alan Bishop

We are developing and supporting a technology base in nonequilibrium phenomena that underpins fundamental issues in condensed matter and materials science, and we are applying this technology to selected problems. The increasingly sophisticated synthesis and characterization of complex electronic and structural materials provide a test bed for nonlinear science, while nonlinear and nonequilibrium techniques advance our understanding of the scientific principles underlying the control and evolution of material microstructures and textures.

We extended our large-scale molecular dynamics simulation studies and associated nonlinear analysis of deforming materials to include stress distribution in stacked quantum-dot systems (silicon and germanium). We also studied friction dynamics in the presence of thin lubricant films, three-dimensional dislocation interactions in solids, and crack propagation in amorphous and hierarchical solids (see accompanying figure).

We made substantial progress in understanding and modeling energy localization and transduction in deformable (hard and soft) media, in both classical and quantum systems. In particular, we demonstrated the essential interplay of discreteness and nonlinearity in the existence and stability of intrinsically localized modes, including a demonstration of novel local, soft-mode mechanisms for (1) their transport; (2) their long-lived nonthermal distributions and slow (multi-time-scale) decay channels; (3) their competition with disorder in classical discrete nonlinear systems; (4) their quantum and nonadiabatic manifestations in strongly correlated electronic materials, including both electronic ground state and photoexcited state signatures; and (5) their possible role in energy focusing in biological molecules, such as myoglobin.

We used numerical and analytical methods to study key features of mesoscale pattern formation and dynamics in multiscale models and systems, including identification of the surprising "mesoscopic statistical mechanics" behavior of coherent nonlinear modes (vortices, spirals, etc.) in a frustrated spin model, a complex Ginzberg-Landau description of spiral surface growth, and flux ordering and flow in superconductors.

We also performed an experimental/theoretical study of soap films and a Ginzburg-Landau modeling of elasticity at solid-solid phase transformations. The latter yielded systematic statistical descriptions of fine-scale materials structure (hierarchical twinning, tweed, etc.) and explicit thermodynamic and structural signatures (for comparison with ongoing resonant ultrasound, neutron, and x-ray scattering and thermal expansion experiments).

We identified competitions between short- and long-range interactions and entropy as basic mechanisms associated with multi-time-scale dynamics in hard, soft, and biomimetic materials. We developed numerical tools and physical insights to handle these competitions, which we applied to charge ordering in complex transition metal oxides (e.g., layered cuprate oxides), electrostatic interactions in polyelectrolytes and biological macromolecules studied for adhesion and aggregation, and organic gelation phenomena.

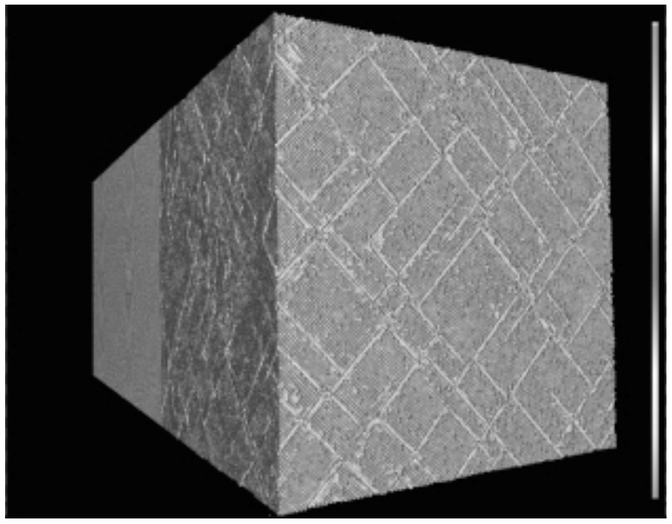

Large-scale molecular dynamics simulation of materials deformation. A perfect face-centered cubic crystal has been collided with an infinitely massive piston with a velocity such that pairs of partial dislocations are emitted along slip planes. The rearward-moving partials are visible, viewed from the piston end. The stacking faults are the manifestation of the emitted partial dislocations (forward and rearward) on the four available slip systems. [B.L. Holian and P.S. Lomdahl, Science **280**, 2085 (1998); copyright owned by DOE.].

Publications

Aranson, I., and I. Mitkov, "Helicoidal Instability of a Scroll Vortex in Three-Dimensional Reaction-Diffusion Systems," *Phys. Rev. E* **58**, 4556 (1998).

Ashurst, W.T., and B.L. Holian, "Droplet Formation by Rapid Expansion of a Liquid," *Phys. Rev. E* **59**, 6742 (1999).

Ashurst, W.T., and B.L. Holian, "Droplet Size Dependence Upon Volume Expansion Rate" (submitted to *J. Chem. Phys.*).

Beardmore, K.M., and N. Gronbech-Jensen, "Direct Simulation of Ion Beam Induced Stressing and Amorphization of Silicon" in *Proceedings of the Fifth International Symposium on Process Physics and Modeling in Semiconductor Technology* (Electrochemical Society, New Jersey, 1999), p. 96.

Beardmore, K.M., and N. Gronbech-Jensen, "Direct Simulation of Ion Beam Induced Stress and Amorphization of Silicon" (to be published in *Phys. Rev. B*).

Beardmore, K.M., and N. Gronbech-Jensen, "An Efficient Molecular Dynamics Scheme for Predicting Dopant Implant Profiles in Semiconductors," *Nucl. Inst. Meth. Phys. Res. B* **153**, 391 (1999).

Beardmore, K.M., and N. Gronbech-Jensen, "Predicting Low-Energy Dopant Implant Profiles in Semiconductors Using Molecular Dynamics" (195th Semiannual Meeting of the Electrochemical Society, Seattle, WA, May 1999).

Braun, O., et al., "Multistep Locked-to-Sliding Transition in a Thin Lubricant Film," *Phys. Rev. Lett.* **82**, 3097 (1999).

Cai, D., et al., "A Perturbed Toda Lattice Model for Low-Loss Nonlinear Transmission Lines," *Physica D* **123**, 291 (1998).

Carmelo, J.M.P., and N.M.R. Peres, "Anomalous Transport Behavior in 1-D Multicomponent Integrable Systems with Umklapp Scattering" (submitted to *Phys. Rev. Lett.*).

Carmelo, J.M.P., et al., "Finite-Energy Correlation Functions of 1-D Integrable Many-Electron Quantum Liquids" (submitted to *Phys. Rev. B*).

Cirillo, M.V., et al., "Analysis of Linear Branches in the I-V Characteristics of Josephson Junctions" (IEEE Proceedings from Applied Superconductivity, Palm Springs, CA, September 1998).

Cirillo, M.V., et al., "Fiske Modes and Eck Steps in Long Josephson Junctions: Theory and Experiments," *Phys. Rev. B* **58**, 12377 (1998).

Daruka, I., et al., "Molecular Dynamics Simulations of the Surface Stress Distribution in Stacked Quantum Dot Systems," *Phys. Rev. B* **60**, R2150 (1999).

Egolf, D.A., "Equilibrium Regained: From Nonequilibrium Chaos to Statistical Mechanics" (submitted to *Science*).

Gaididei, Y., et al., "Noise-Induced Switching Between Vortex States with Different Polarization in 2-Dimensional Easy-Plane Classical Magnets," *Phys. Rev. B* **59**, 7010 (1999).

Germann, T.C., et al., "Orientation Dependence in Molecular Dynamics Simulations of Shocked Single Crystals" (submitted to *Phys. Rev. Lett.*).

Germann, T.C., et al., "Plastic Deformation in Shock Waves via Molecular-Dynamics Simulations" (APS 1999 Topical Conference on Shock Compression of Condensed Matter, Snowbird, UT, June 28–July 2, 1999).

Gronbech-Jensen, N., "Summation of Logarithmic Interactions in Nonrectangular Periodic Media," *Comput. Phys. Comm.* **119**, 115 (1999).

Gronbech-Jensen, N., et al., "Interactions Between Charged Spheres in Divalent Courterion Solution," *Physica A* **261**, 74 (1998).

Hammerberg, J.E., et al., "Molecular Dynamics Studies of Dry Friction Under High Compression and Velocity" (submitted to *Phys. Rev. B*).

Hirth, J.P., et al., "Shock Relaxation by a Strain Induced Martensitic Phase Transformation" (submitted to *Acta Metall.*).

Holian, B.L., et al., "The Birth of Dislocations in Shock Waves and High-Speed Friction," *J. Comput. Aided Mater. Des.* **5**, 207 (1998).

Holian, B.L., et al., "Shock Waves and Their Aftermath: A View from the Atomic Scale" (APS 1999 Topical Conference on Shock Compression of Condensed Matter, Snowbird, UT, June 28–July 2, 1999).

Kamppeter, T., et al., "Finite Temperature Dynamics of Vortices in the Two-Dimensional Anisotropic Heisenberg Model," *Eur. Phys. J. B* **7**, 607 (1999).

Kamppeter, T., et al., "Stochastic Vortex Dynamics in 2-Dimensional Easy-Plane Ferromagnets: Multiplicative Versus Additive Noise" (to be published in *Phys. Rev. B*).

Kawabata, C., et al., "Critical Temperature and Current of 3-D Anisotropic Josephson Junction Arrays" (submitted to *J. Phys. Soc. Jpn.*).

Kirova, N., et al., "A Systematic Theory for Optical Properties of Phenyleve-Based Polymers," *Synth. Met.* **100**, 29 (1999).

Kladko, K., et al., "Intrinsic Localized Modes in the Charge-Transfer Solid PTCL" (submitted to *J. Phys.: Condens. Matter*).

Mashl, R.J., et al., "Theoretical and Experimental Absorption Studies of Polyelectrolytes on an Oppositely Charged Surface," *J. Chem. Phys.* **110**, 2219 (1999).

Mertens, F.G., and A.R. Bishop, “Dynamics of Latices in 2-Dimensional Magnets,” in *Nonlinear Science at the Dawn of the 21st Century*, P. Christiansen and M. Soerenser, Eds. (Springer-Verlag, New York, in press).

Mikulla, R.P., et al., “Dislocation Nucleation and Dynamics at Sliding Interfaces,” in *Proceedings of Materials Research Society* (Materials Research Society, Pittsburgh, PA, 1998), Vol. 522, p. 385.

Mitkov, I., “One- and Two-Dimensional Wave Fronts in Diffusive Systems with Discrete Sets of Nonlinear Sources” (to be published in *Physica D*).

Mitkov, I., et al., “Dynamics of Wetting Fronts in Porous Media,” *Phys. Rev. E* **58**, R5245 (1998).

Mitkov, I., et al., “Localized Structures in Nonlinear Lattices with Diffusive Coupling and External Driving” (submitted to *Phys. Rev. Lett.*).

Mitkov, I., et al., “Tunable Pinning of Burst-Waves in Extended Systems with Discrete Sources,” *Phys. Rev. Lett*. **81**, 5453 (1998).

Mustre de Leon, J., et al., “Isotopic Substitution in a Model Polaronic System,” *Phys. Rev. B* **59**, 8359 (1999).

Pellegrini, M., et al., “A New Constrained Langevin Method: Application to Protein Crystallographic Refinement,” *Physica A* **261**, 224 (1998).

Prosen, T., and D.K. Campbell, “Momentum Conservation Implies Anomalous Energy Transport in ID Classical lattices” (submitted to *Phys. Rev. Lett*.).

Raghavan, S., et al., “Quantum Versus Semiclassical Description of Self-Trapping” (to be published in *Phys. Rev. B*.).

Rasmussen, K.O., and A. Bishop, “Multiple States of Intrinsic Localized Modes,” *Phys. Rev. B* **58**, 5423 (1998).

Rasmussen, K.O., et al., “Discrete Nonlinear Schrödinger Breathers in a Phonon Bath” (to be published in *Eur. Phys. J. B*).

Rasmussen, K.O., et al., “Higher-Order Effects on Shapiro Steps in Josephson Junctions,” *Phys. Rev. B* **59**, 58 (1999).

Rasmussen, K.O., et al., “Localization in a Nonlinear Disordered System” (to be published in *Europhys. Lett.*).

Rasmussen, K.O., et al., “Soliton Motion in a Parametrically AC-Driven Damped Toda Lattice,” *Phys. Rev. E* **58**, 6695 (1998).

Rightley, P.M., et al., “Friction in High-Speed Impact Experiments” (APS 1999 Topical Conference on Shock Compression of Condensed Matter, Snowbird, UT, June 27–July 2, 1999).

Roeder, J., et al., “Simplified Model for Energy Transport Away from a Sliding Interface” (submitted to *Physica D*).

Sandvik, A.W., “Spin-Peierls Transition In the Heisenbert Chain with Finite-Frequency Phonons” (submitted to *Phys. Rev. Lett*.).

Sandvik, A.W., “Stochastic Series Expansion Method with Operator-Loop Update” (submitted to *Phys. Rev. B*).

Schmeltzer, D., and A.R. Bishop, “Theoretical Investigation of the Phases of the Organic Insulator $(TMTTF)_2PF_6$,” *Phys. Rev. B* **59**, 4541 (1999).

Stojkovic, B.P., et al., “Charge Ordering and Long-Range Interactions in Layered Transition Metal Oxides,” *Phys. Rev. Lett*. **82**, 4679 (1999).

Tartakovsky, D.M., and I. Mitkov, “Some Aspects of Head-Variance Evaluation,” *Comp. Geosci*. **3** (1), 89 (1999).

Tsironis, G., et al., “Dependence of Thermal Conductivity on Discrete Breathers in Lattices,” *Phys. Rev. E* **60**, 6610 (1999).

Vorobeiff, P., and R.E. Ecke, “Cylinder Wakes in Flowing Soap Films” (submitted to *Phys. Rev. Lett.*).

Zou, L.J., and D.K. Campbell, “Spin Dynamics and Diffusion in Double Exchange Ferromagnets” (submitted to *Phys. Rev. Lett.*).

Chemistry

Energy Transfer in Molecular Solids

97807

Juergen Eckert

The goal of our research is to advance our understanding of energy transfer processes and vibrational dynamics in molecular crystals of two important classes: those closely related to high explosives (HEs) and biological model systems containing peptide hydrogen bond chains. We are using inelastic neutron scattering (INS) vibrational spectroscopy in combination with theoretical modeling of the INS spectra since these can be related to molecular interactions or force fields in a much more direct way than other spectroscopic techniques.

In HEs, mechanical energy from a shock wave is transferred to chemical energy in individual molecules. Understanding how this happens requires detailed knowledge of the molecular interactions for the derivation of vibrational densities of state and energy transfer rates.

We made electronic structure calculations to understand the nature of hydrogen bonding in molecules such as the high explosive TATB using the GAMESS parallel electronic structure code and the ASCI Blue supercomputer at Lawrence Livermore National Laboratory. To assess the role of intermolecular interactions, we studied dimers of nitrobenzene, nitroaniline, and TATB rather than isolated molecules. We also made large calculations on a cluster of seven TATB molecules with a minimal basis set at the Hartree-Fock level of theory.

The agreement between the cluster calculation and the INS spectra was particularly striking for TATB and clearly demonstrates the importance of intermolecular interactions.

In the case of biomolecules, the mechanism of long-range energy transport is still unresolved despite its importance in the function of proteins. It was recently suggested that proton transfer along the chemically asymmetric peptide H-bond may be responsible for this process and may account for the vibrational anomalies in these systems. We have carried out extensive INS, IR, and Raman spectroscopy; neutron diffraction; ^{13}C nuclear magnetic resonance; and theoretical studies of various simple systems with such hydrogen bonds as formamide, N-methylacetamide, acetanilide, L-alanine, and uracil. Our results rule out a number of proposed explanations for the vibrational anomalies, and have conclusively shown that proton transfer does not occur in the condensed phase. Instead we favor energy-transfer models based on polarons, in accord with a currently emerging consensus that charge transfer in DNA may also involve polaronic states.

Publications

Barthes, M., et al., “Dynamics of Crystalline N-methylacetamide: Temperature Dependence of Infrared and Inelastic Neutron Scattering Spectra,” *J. Phys. Chem.* **102**, 6177 (1998).

Bordallo, H.N., et al., “Vibrational Dynamics of Crystalline L-alanine,” *Physica B* **241**, 1138 (1998).

Eckert, J., et al., “No Evidence for Proton Transfer along the N-H...O Hydrogen Bond in N-methylacetamide: Neutron Single Crystal Structure at 250 and 276K” (submitted to *J. Phys. Chem.*).

Catalysis Science and Technology

97603

Kevin C. Ott

Our objective was to discover new catalytic chemistry and understand the structure of catalysts that transform organic substrates into molecules having greater complexity. Our studies have used a unique combination of capabilities from across the Laboratory in materials synthesis, organometallic chemistry, theoretical chemistry, neutron scattering, reaction chemistry, and nuclear magnetic resonance spectroscopy. We used these capabilities to answer key questions about catalyst structure and reactivity.

Progress this year included the exploration of the structure of site-isolated oxidation catalysts. We focused on theoretical chemistry studies of the structure of cobalt ions in inorganic frameworks and the interaction of dioxygen with the cobalt using density functional theory (DFT) techniques. We benchmarked these studies against x-ray absorption fine structure (EXAFS) data and known molecular analogs of Co-O_2 complexes. We conducted a series of cluster DFT calculations on models of the zeolite TS-1 in order to understand the steps involved in the selective oxidation of hydrocarbons at the titanium center. We determined the transition states and activation barriers for various reaction pathways for the epoxidation of ethylene, as shown in the first figure. We also carried out semiempirical calculations on very large cluster models of TS-1 to attempt to understand the preferential siting of titanium atoms at specific sites in the zeolite, as previously measured at Los Alamos using neutron diffraction. We examined the possibility of a correlation between either substitution energies of titanium for silicon at the 12 crystallographically distinct sites or the interactions of cationic templates with Ti-OH anionic defect sites with the observed preference. However, we found no correlation for either supposition.

To better understand the chemistry and structure of site-isolated catalysts such as TS-1 and the iron analog, we undertook the synthesis of soluble, molecular analogs of ferrisilicates, another class of potentially interesting catalysts. We were able to synthesize for the first time two iron silsesquioxane derivatives, the framework structures of which are shown in the second figure. Manipulation of the chemistry of these two compounds to uncover any potential catalytic activity is under way.

Additional activities in the area of site-isolated catalysts focused on using solid state xenon-129 nuclear magnetic resonance to study small metal clusters in zeolites. The results indicated relative preferences for xenon interactions with the walls of the zeolite vs. metal clusters of differing sizes within the constrained microporous environment.

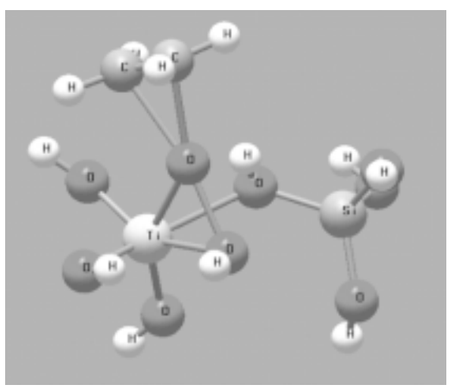

Calculated transition state for one reaction pathway of the oxidation of ethylene to ethylene oxide at the Ti site in the zeolite catalyst titanium silicalite.

As part of our effort to develop methods for characterizing site-isolated catalysts, we carried out neutron diffraction studies to assess the utility of pair-distribution function (PDF) analysis of diffraction data for this purpose. While an experiment designed to locate metal clusters in zeolite NaY was unsuccessful because of their very low concentration, we have been able to obtain local structural information on the location of adsorbed chloroform by means of a differential PDF between normal and deuterated adsorbed chloroform in NaY. This hydrogen PDF clearly shows peaks from the C-H···O(framework) hydrogen bond (2.2Å) as well as the H to Si(Al) at approximately 3.3Å.

We studied homogeneous catalysis in supercritical-CO_2 (hydroboration, hydrogenation, hydroformylation) using partially fluorinated phosphines as ligands for Rh(I) catalysts. This is the first demonstration of hydroboration in sc-CO_2 and we were able to get good to excellent regiocontrol using styrene derivatives as substrates.

We synthesized a variety of new metallophosphenium complexes of rhodium, platinum, and ruthenium, and then showed that careful design of the NR_2 substituents on phosphorus leads to control of the steric and electronic nature of the phosphenium ligand. This ligand may manifest itself as control over the electrophilic nature of the metal complex via interactions indicated in the last figure. We also determined the x-ray structure of a single crystal of one such complex.

Publications

Baker, R.T., and W. Tumas, "Homogeneous Catalysis: Toward Greener Chemistry," *Science* **284**, 1477 (1999).

Cameron, T.M., et al., "Metal-Catalyzed Multiple Boration of Ketimines," *Chem. Comm*. **21**, 2395 (1998).

Hay, P.J., et al., "Theoretical Studies of Pentene Cracking on Zeolites: C-C beta-Scission Processes," *Catalysis Today* **50**, 517 (1999).

Henson, N.J., et al., "Computational Studies of Cobalt Substituted Aluminophosphates" (submitted to *J. Phys. Chem*.).

Henson, N.J., et al., "Density Functional Theory Studies of the Binding of Molecular Oxygen with Schiff's Base Complexes of Cobalt," *Inorganic Chemistry* **38**, 1618 (1999).

Henson, N.J., et al., "Theoretical Studies of the Structure and Properties of Cobalt-Substituted Aluminophosphates," in *Proceedings of the 12th International Zeolite Conference, Vol. I* (Materials Research Society, Warrendale, PA, 1999), p. 379.

Labouriau, A., et al., "Probing the Structure of Metal Substituted Molecular Sieves by Solid State NMR," in *Proceedings of the 12th International Zeolite Conference, Vol. IV* (Materials Research Society, Warrendale, PA, 1999), p. 2489.

Labouriau, A., et al., "Probing Zeolite Internal Structures Using Very Low Temperature ^{129}Xe NMR," in *Proceedings of the 12th International Zeolite Conference, Vol. IV* (Materials Research Society, Warrendale, PA, 1999), p. 2265.

Labouriau, A., et al., "Temperature Dependence of Nuclear Magnetic Resonance Chemical Shifts of ^{129}Xe in the a-cages of NaY Zeolite," *J. Phys. Chem. B* **103**, 4323 (1999).

Labouriau, A., et al., "^{129}Xe NMR Spectroscopy of Metal Carbonyl Clusters and Metal Clusters in Zeolite NaY" (to be published in *J. Am. Chem. Soc.*).

Morita, D., et al., "Recent Advances in Chemistry and Chemical Processing in Supercritical Carbon Dioxide," in *Benign Synthesis*, Anastas and Williamson, Eds. (Oxford Press, Oxford, 1998).

Pesiri, D.R., et al., "Vanadium-Catalyzed Epoxidation of Olefinic Alcohols in Liquid Carbon Dioxide" (to be published in *Organometallics*).

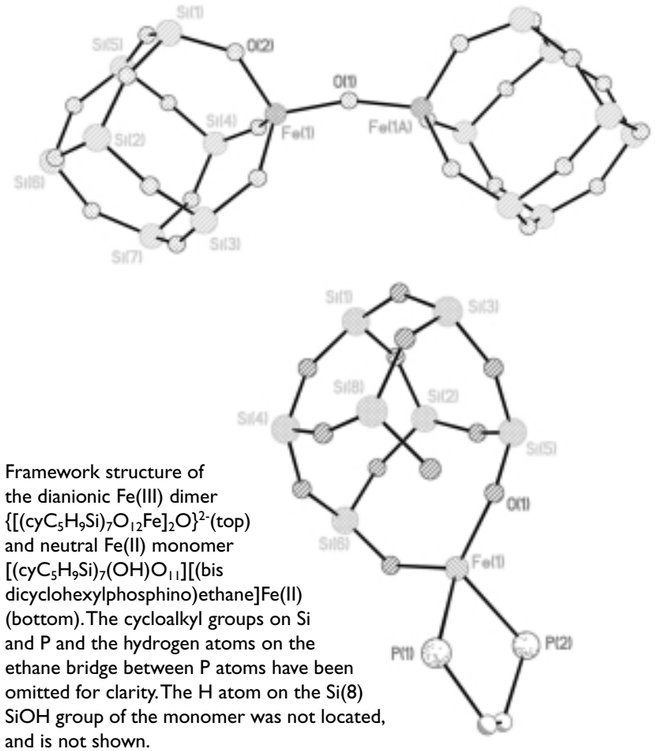

Framework structure of the dianionic Fe(III) dimer $\{[(cyC_5H_9Si)_7O_{12}Fe]_2O\}^{2-}$(top) and neutral Fe(II) monomer $[(cyC_5H_9Si)_7(OH)O_{11}][$(bis dicyclohexylphosphino)ethane]Fe(II) (bottom). The cycloalkyl groups on Si and P and the hydrogen atoms on the ethane bridge between P atoms have been omitted for clarity. The H atom on the Si(8) SiOH group of the monomer was not located, and is not shown.

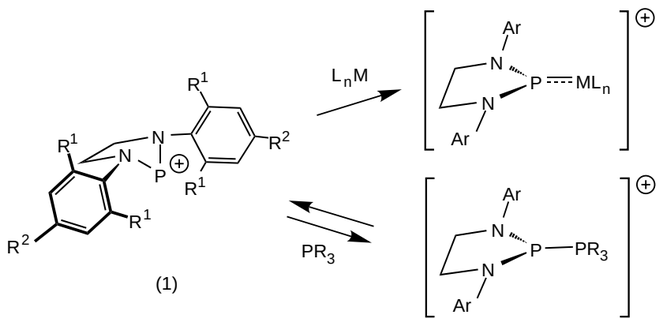

(1)

Proper choice of the aryl substituents R^1 and R^2 influence the steric and electronic nature of the interaction of phosphenium cations with neutral metal complexes and Lewis bases such as phosphines.

Condensed Phase Kinetics and Reduced Reaction Mechanisms of Energetic Materials

98603

Steven Son

High explosives (HE) science and modeling lie at the heart of the Laboratory's responsibilities in nuclear weapons applications. The HE component of a nuclear weapon furnishes the initial conditions for all other processes and, without HE, there would be relatively little concern for weapon safety. However, our current models of HE contain the least fundamental modeling of any component in a weapon.

The objective of our project is to become competent in predicting reaction processes in energetic materials, particularly octahydro-1,3,5.7-tetranitro-1,3,5.7-tetrazocine (HMX), using detailed and reduced chemical kinetics schemes. We will perform detailed chemistry experiments and calculations to contribute to the ultimate aim of developing simple, yet rigorous, models.

This year we studied selected chemical kinetic pathways. We explored reduction methods, applying for the first time the intrinsic low-dimensional manifold (ILDM) method to HMX chemistry. Our results show significant computational savings.

We developed further a novel nonlinear optical technique to study the kinetics of a solid-solid phase transition that occurs in heated HMX. We applied this second harmonic generation (SHG) technique also to triaminotrinitrobenzene (insensitive HE) (TATB), and we observed that, similar to HMX, SHG efficiency increases significantly upon heating TATB. This efficiency probably does not indicate a new phase (based on x-ray diffraction results) of TATB, but does indicate a crystalline change. We measured the kinetics of this process and showed that they correspond to the initial decomposition step, analogous to HMX. We investigated the effect of the HMX phase change in "cook-off" scenarios and began work on the effect of the structure of TATB on detonation behavior.

This year we performed laser ignition (see first figure) and deflagration (burn rate) experiments (see second figure) and obtained unique data sets for various explosives. We also performed novel experiments on the combustion in "cracks." Gaps were machined in PBX 9501, and the combustion dynamics were observed using high-speed photography and IR imaging. At lower pressure, oscillatory burning was observed. This behavior has been proposed, but never observed directly before.

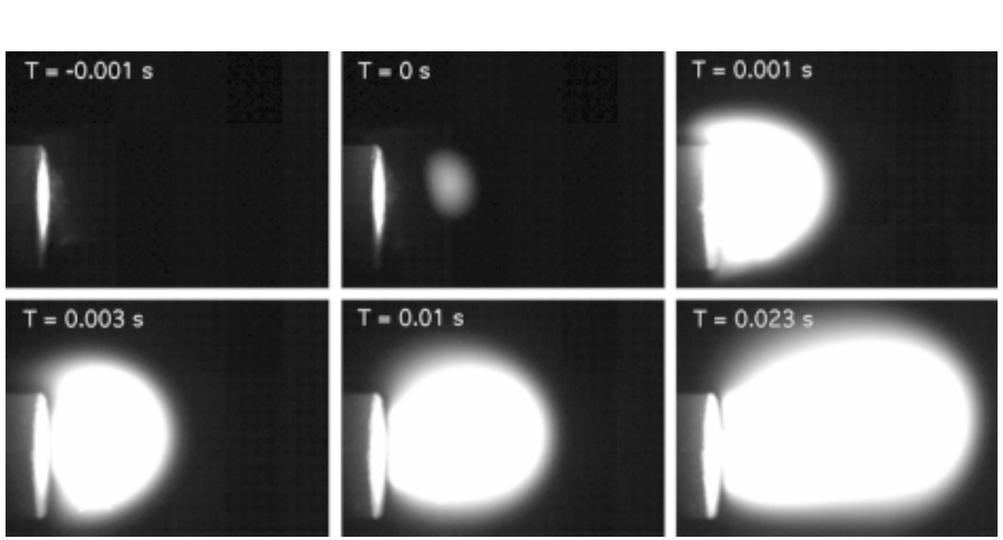

High-speed video images of the ignition of HMX at ambient conditions. These images capture the ignition dynamics, which include the initial gases evolving from the surface, ignition first occurring in the gas phase, propagation of the gas flame to the surface ("snap-back"), and blow-off of the gas phase flame ("bounce").

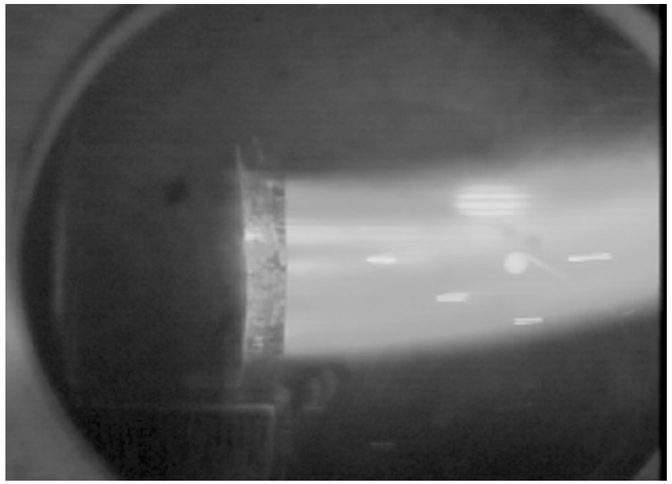

Image of PBX 9501 (HMX-based explosive) burning at 20 atm in our new combustion vessel. Burning proceeds right to left.

Publications

Ali, A.N., et al., "Ignition Dynamics of High Explosives," in *Proceedings of the 37th Aerospace Sciences Meeting & Exhibit* (Reno, Nevada, in press).

Asay, B.W., et al., "Dynamic Observation of Polymorph Changes in HMX by Second Harmonic Generation," *Proceedings of the 1998 JANNAF Propulsion Systems Hazards Subcommittee Meeting* (Tucson, Arizona, in press).

Berghout, H.L., et al., "Measurement of Convective Burn Rates in Gaps of PBX 9501," in *Proceedings of the 1999 APS Topical Conference on Shock Compression of Condensed Matter* (Snowbird, Utah, in press).

Henson, B.F., et al.,"Dynamic Measurement of the HMX—Phase Transition by Second Harmonic Generation," *Phys. Rev. Lett.* **82**, 1213 (1999).

Kennedy, J.E., et al., "Second Harmonic Generation and the Shock Sensitivity of TATB," in *Proceedings of the 1999 APS Topical Conference on Shock Compression of Condensed Matter* (Snowbird, Utah, in press).

Liau, Y-C., and J.L. Lyman, "Modeling Laser-Induced Ignition of Nitramine Propellants with Condensed and Gas-Phase Absorption," AIAA-99-0863, AIAA Aerospace Sciences Conference (Reno, Nevada, in press).

Liau, Y-C., et al., "Analysis of ADN Combustion with Detailed Chemistry," in *Proceedings of the 1998 JANNAF Propulsion Systems Hazards Subcommittee Meeting* (Tucson, Arizona, in press).

Liau, Y-C., et al., "Analysis of RDX/GAP Pseudopropellant Combustion with Detailed Chemistry," in *Proceedings of the 1998 JANNAF Propulsion Systems Hazards Subcommittee Meeting* (Tucson, Arizona, in press).

Liau, Y-C., et al., "Numerical Simulation of RDX/GAP Pseudo-Propellant Combustion" (to be published in *AIAA Journal of Propulsion and Power*).

Louwers, J., et al., "A Model for Steady-State HNF Combustion" (to be published in *AIAA Journal of Propulsion and Power*).

Powers, J.M., and S. Singh, "Modeling Gas Phase Reactions of RDX using Intrinsic Low Dimensional Manifolds," in *Proceedings—International Colloquium on Dynamics of Explosions and Reactive Systems* (Heidelberg, Germany, 1999).

Son, S.F., et al., "Dynamic Observation of a Thermally Activated Crystalline Change in 1,3,5-Triamino-2,4,6-trinitrobenzene," *J. Phys. Chem. B* **103**, 5434 (1999).

Son, S.F., et al., "Observation of a Thermally Activated Crystalline Change in TATB by Second Harmonic Generation," in *Proceedings of the 1998 JANNAF Propulsion Systems Hazards Subcommittee Meeting* (Tucson, Arizona, in press).

Ward, M.J., et al., "Simplified Combustion Modeling of Double Base Propellant: Gas Phase Chain Reaction vs. Thermal Decomposition" (to be published in *Combustion Science and Technology*).

Zerkle, D.K., "Phase Segregation Effects on the Calculation of ODTX in HMX Spheres," *Combustion and Flame* **117**, 657 (1999).

A New Paradigm in Separations: Molecular Recognition Membranes

98602

Gordon D. Jarvinen

Our project objectives are to understand the molecular-level mechanisms that govern transport of ions and molecules through a semi-permeable membrane and to develop a new class of robust molecular-recognition membranes. The approach uses recent advances in nano-technology to fabricate thin-membrane assemblies with specific receptors for molecular recognition incorporated into the pore structure. The membrane separation systems emerging from this effort may be attractive in nuclear processing applications because of the combination of selectivity, high throughput, stability, and efficiency of such systems. A wide variety of industrial separation problems could also benefit from advanced membrane technology.

This year we studied the transport of various metal cations through modified and unmodified Anodisc alumina membranes. These membranes contain straight nonintersecting pores with an average pore diameter of 20 or 100 nm (see the unmodified membrane in the first figure). After developing membrane characterization methods, we performed both molecular-level and macroscopic modeling to elucidate the experimental transport results.

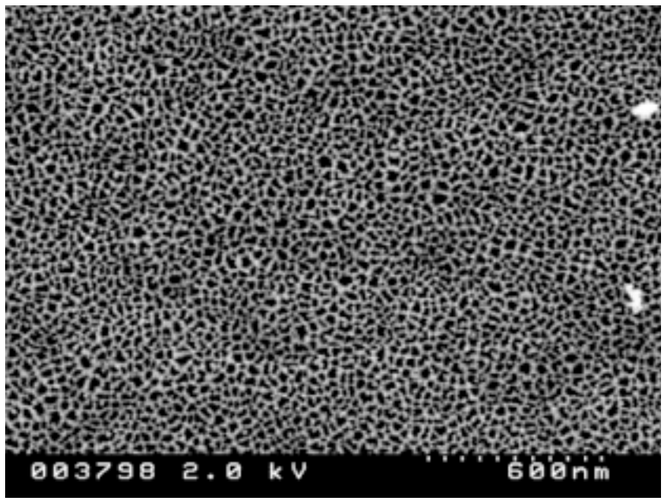

Scanning electron micrograph of the unmodified active surface of Anodisc alumina membrane with nominally 20-nm-diameter pores (the light-colored features on the right are gold-coated dust or other imperfections on the surface).

Our studies of the rate diffusion of divalent and monovalent cations through the alumina membranes as a function of pore diameter, ionic strength, and pH produced the interesting result that interactions with the charged membrane surface substantially retard diffusion through these relatively large pores. Even more curious is the observed order-of-magnitude increase in the transport rate of Ca^{2+} and Sr^{2+} when Na^{+} or Cs^{+} are co-transported.

To modify the membrane function, we applied thin gold coatings to the membranes followed by thiols to create a hydrophobic barrier (see the second figure). This hydrophobic barrier is key to achieving highly specific transport of the species of interest between aqueous feed and receive phases. We achieved quantitative transport of uranyl nitrate or 2,4,6-trichlorophenol with very high fluxes, indicating an active layer that is very thin (500–1000 Å). The uranium transport required the presence of the complexing agent tributyl phosphate in the membrane. The phenol diffused through the hydrophobic thiol coating that had been treated with dodecane to seal "holes" in the barrier layer.

We explored using Rutherford backscattering to determine gold-film thickness, depth of gold infiltration in the pores, and porosity. Liquid/liquid porosimetry capabilities are under development to determine the modified-membrane pore sizes and the pore-size distribution.

In addition, we developed a theoretical treatment based on the quasi-chemical theory of solutions to study alkali-metal hydration. The predicted most-probable number of directly bonded water molecules for the Li^{+} and Na^{+} ions in aqueous solution is four. Our molecular-dynamics calculations confirmed the instability of the commonly accepted six-water inner-sphere complex.

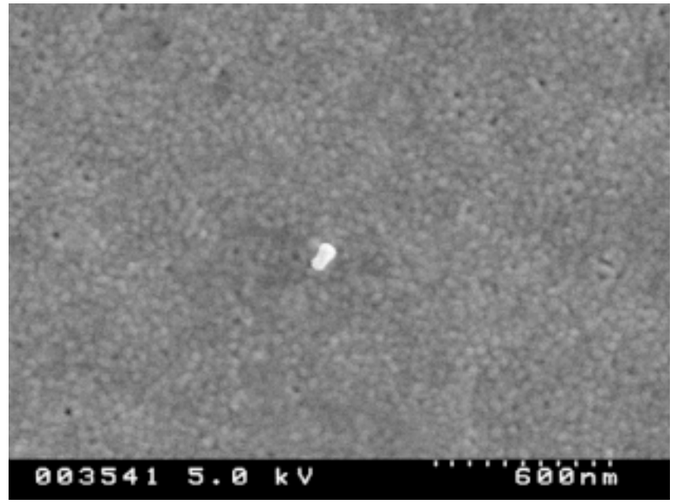

Scanning electron micrograph of Anodisc alumina membrane coated with 70 nm of gold (at the center is another imperfection). Spacing between the gold particles is the limiting factor for mass transport across the membrane. Thiols are attached to the gold surface to create a hydrophobic barrier that can be modified to provide selective transport of metal ions between aqueous feed and receive phases.

Publications

Bluhm, E.A., et al., "Surface Effects on Cation Transport across Porous Alumina Membranes," *Langmuir* **15**, 8668 (1999).

Jarvinen, G.D., "Technology Needs for Actinide and Technetium Separations Based on Solvent Extraction, Ion Exchange, and Other Processes." in *Chemical Separation Technologies and Related Methods of Nuclear Waste Management: Applications, Problems and Research Needs*, G.R. Choppin and M.Kh. Khankhasayev, Eds. (Kluwer, Boston, 1999), p. 53.

Pratt, L.R., and S.B. Rempe, "Quasi-Chemical Theories and Implicit Solvent Models for Simulations," *AIP Conf. Proc.* **492**, 172 (1999).

Pratt, L.R., et al., "Theories of Hydrophobic Effects and the Description of Free Volume in Complex Liquids," in *New Approaches to Problems in Liquid State Theory*, C. Caccamo, et al., Eds. (Kluwer, Dordrecht, 1999), p. 407.

Rempe, S.B., et al., "The Hydration Number of Li^{+} in Liquid Water," *J. Amer. Chem. Soc*. **122**, 966 (2000).

Cradle-to-Grave Carbon Management

99523

Hans-Joachim Ziock

Our project addresses the key issues involved in achieving fossil fuel use with zero CO_2 emissions, including truly zero emission coal. Our thrusts are twofold: separation of the energy from the carbon and permanent disposal of the resulting CO_2. The major areas of research in this project are shown in the first figure.

To generate hydrogen from the carbon found in the cleanest fossil fuel, natural gas (methane), we constructed a short-contact-time reactor. Using the nonequilibrium conditions found in the rapidly quenched reaction zone of the short-contact-time reactor, we hope to achieve extremely high-efficiency hydrogen production via steam reforming of methane by partial oxidation. To separate the high-temperature hydrogen and CO_2 generated in the reactor, we are developing high-temperature hydrogen separation membranes. We prepared two-phase ceramic mixture membrane materials that are proton and electron conductors and that are stable to 2900°F. Other performance evaluations of these ceramic mixtures are just starting.

We compared these data to theoretical models of these materials that we have developed, such as the model of $SrZrO_3$ shown in the second figure, with both protonic defects and oxygen vacancies. Subsequent theoretical models are used to predict the performance of new candidate membrane materials.

For dirty fuels, such as coal, we have devised extremely high efficiency routes for transforming the energy available from the fuels into electricity by means of a clean hydrogen intermediary. We use CaO to drive the conversion of water and carbon from the fossil fuel into hydrogen and $CaCO_3$, thereby simultaneously capturing the produced CO_2. Subsequent $CaCO_3$ calcination generates pure high-pressure CO_2 ready for disposal. For disposing of the CO_2, we are investigating the formation of carbonates from readily available minerals, thereby achieving permanent CO_2 disposal. Focus areas for in situ carbonation of minerals (by injection of liquid/super-critical CO_2 into Mg/Ca-silicate-bearing strata) include natural analogs, experimental/theoretical investigation of carbonation, and assessment of injection phenomena from past hot-dry-rock experiments. In a complementary investigation we are determining the kinetics of direct carbonation of serpentine as a way of achieving CO_2 sequestration in an industrial process.

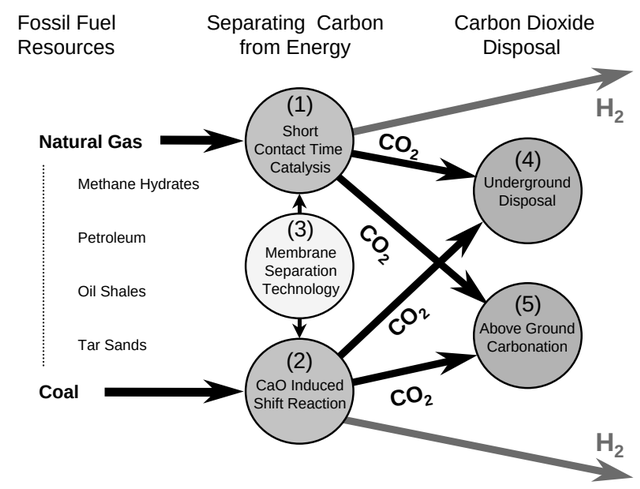

The key elements of our LDRD project. The two hydrogen production mechanisms span the range of fossil fuels. In addition, work on hydrogen separation membranes applicable to both mechanisms is being pursued. The mineral disposal work also spans the two extremes and offers a way of permanently dealing with the possible CO_2 emissions from all the world's carbon reserves. The close coupling of all these elements is key to the success of the overall project.

Publications

Goff, F., and G. Guthrie, "Field Trip Guide to Serpentinite, Silica-Carbonate Alteration, and Related Hydrothermal Activity in the Clear Water Region, California," Los Alamos National Laboratory report LA-13607-MS (June 1999).

Ziock, H.-J., et al., "The Need and Options Available for Permanent CO_2 Disposal," in *Reaction Engineering for Pollution Prevention* (Elsevier Science Publishing, New York, NY, in press).

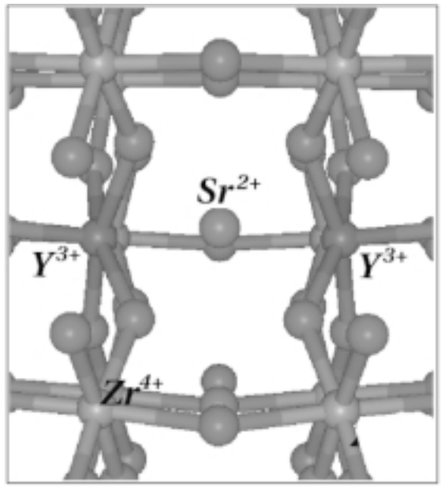

The calculated structure of an oxygen vacancy and associated Y^{3+} substitutional defect in $SrZrO_3$.

Actinide Molecular Science

97609

David L. Clark

The technical basis for process and separation chemistry and metallurgy related to the Los Alamos weapons mission is the chemistry and physics of the actinide elements. Our project goal is the integration of actinide chemical synthesis, characterization, spectroscopy, and theory to increase our understanding of the relative roles of 5f/6d electrons in chemical bonding, of the relative roles of ionic and covalent behaviors, and of polar and nonpolar solvents in controlling chemical reactivity.

We examined high-oxidation-state compounds with a linear bond in polar (aqueous) and nonpolar (nonaqueous) solution with similar supporting ligands. Structural, spectroscopic, and theoretical studies revealed fundamental differences between aqueous/nonaqueous chemistry and uranium/transuranium chemistry. We found that strong donor ligands weaken and lengthen the An=O bond (An = U, Np, Pu) and increase the electron density at the oxygen atom. Polar media stabilize this negative charge through weak solvent interactions. Nonpolar media cannot stabilize this charge, and promote redistribution and aggregate formation reactions. Our relativistic density functional theory calculations successfully predict this weakening effect on the bond and agree remarkably with both An=O bond lengths and vibrational frequencies that were determined experimentally.

Our studies reveal striking fundamental differences in chemical reactivity between uranium and transuranium elements. Light actinides form stable tetravalent, pentavalent, and hexavalent complexes for neptunium and plutonium, but the pentavalent state of uranium is chemically unstable. Hence, the difference in the reactivity of the light actinides.

Publications

Avens, L.R., et al., "Mon(pentamethylcyclopentadienyl)uranium(III) Complexes: Synthesis, Properties, and X-Ray Structures of $(\eta\text{-}C_5Me_5)UI_2(THF)_3$, $(\eta\text{-}C_5Me_5)UI_2(py)_3$, and $(\eta\text{-}C_5Me_5)U[N(SiMe_3)_2]_2$" (submitted to *Organometallics*).

Berg, J.M., et al., "Speciation Model Selection by Monte Carlo Analysis of Optical Absorption Spectra: Plutonium (IV) Nitrate Complexes" (submitted to *Appl. Spectrosc.*).

Duff, M.C., et al., "Spectroscopic Characterization of Uranium in Evaporation Basin Sediments" (submitted to *Geochim. Cosmochim. Acta*).

Reeder, R.J., et al., "U6+ Incorporation into Aragonite and Calcite" (submitted to *Science*).

Runde, W., et al., "X-Ray Absorption Spectra of Americium in Different Oxidation States" (submitted to *Radiochim. Acta*).

Schreckenbach, G., et al., "Density Functional Calculations on Actinide Compounds. Survey of Recent Progress and Application to $[UO_2X_4]^{2-}$ (X = F, Cl, OH) and AnF_6 (An = U, Np, Pu)," *J. Comput. Chem.* **20**, 70 (1999).

Wilkerson, M.P., et al., "The Basicity of the Uranyl Ion under Electron-Donor Coordination Environments" (submitted to *J. Am. Chem. Soc.*).

Mathematics and Computational Science

Discrete Simulation of Nonlinear Systems

98805

Shi-Yi Chen

We are developing discrete numerical methods for modeling multiscale physics in nonlinear systems. The methods include the kinetic lattice-Boltzmann method, dissipative particle dynamics, and molecular dynamics. In particular, complex fluids and soft condensed matter (granular materials, vesicles, colloids, and nano-tribology), as well as multiphase fluid flows in porous media, will be studied using the discrete methods. The simulation results will be compared with theoretical predictions from cycle expansions and renormalized perturbation schemes. The toolbox developed in this proposal will increase our simulation capabilities and provide detailed insight into physics at all scales from microscopic to macroscopic.

We established an active program this year in discrete simulation of nonlinear systems. In the simulation of granular materials, we have carried out molecular dynamics simulation to study granular physics in a vibrated monolayer. We observed the complicated phase transition from gas-like state to cluster-gas mixing state and showed that the probability density function (PDF) of velocity changes from Gaussian to non-Gaussian as the vibrated strength decreases.

This year we have also studied several physical arguments about contributions to hydrophobic hydration of inert gases. We have constructed default models and tested them using information theories. The models are consistent with information theory predictions and with moment information provided by simulations of liquid water. The tested physical features include packing effects, the role of attractive forces that lower the solvent pressure, and the roughly tetrahedral coordination of water molecules in liquid water.

We developed a lattice Boltzmann scheme to simulate single phase and multiphase Kelvin-Helmholtz instabilities, two-dimensional (2-D) and three-dimensional (3-D) fluid turbulence, and 2-D and 3-D Rayleigh-Taylor turbulent mixing.

We also explored the utility of the recently proposed alpha equations in providing a subgrid model for fluid turbulence. Our principal results are comparisons of direct numerical simulations of fluid turbulence using several values of the parameter alpha, including the limiting case in which the Navier-Stokes equations are recovered. Our studies show that the large-scale features, including statistics and structures, are preserved by the alpha models, even at coarser resolutions in which the fine scales are not fully resolved. We also described the differences that appear in simulations. We provided a summary of the principal features of the alpha equations and offered an explanation of the effectiveness of these equations as a subgrid model for 3-D fluid turbulence.

Publications

Ghosal, S., “Mathematical and Physical Constraints on LES” (The 29th AIAA Fluid Dynamics Conference, Albuquerque, NM, June 15–19, 1998).

He, G., et al., “Statistics of Dissipation and Enstrophy Induced by Loralized Vortices” (submitted to *Phys. Rev. Lett.*).

Marsden, J. E., “Discrete Euler-Poincare and Lie-Poisson Equations” (submitted to *Commun. Math. Phys.*).

Nadiga, B.T., and S. Shkoller, “A Conservative Numerical Model for Vortex Merger” (submitted to *J. Fluid Mech*.).

Nelkin, M., and S. Chen, “Intermittency Corrections to the Mean Square Particle Acceleration in High Reynolds Number Turbulence” (submitted to *Phys. Fluids*).

Nie, X., et al., “Lattice Boltzmann Simulation of the Two-Dimensional Rayleigh-Taylor Instability” (submitted to *Phys. Rev. E*).

Zoldi, S.M., “Escape Time Weighting of Unstable Stationary Solutions of Spatiotemporal Chaos” (submitted to *Phys. Rev. E*).

Multiscale Science for Science-Based Stockpile Stewardship

97601

Len Margolin

The physical processes that contribute to the performance of a nuclear weapon encompass a wide range of length scales. The smaller scales cannot be resolved in numerical simulation because of the size and speed limitations of today's computers; yet the effects of these small-scale processes cannot be ignored. The goal of this project is to develop and apply the methods of multiscale science to create models for these important small-scale processes; models that can be used to improve the predictability of the design and assessment codes now used in the nuclear weapons program.

Our research has concentrated on three general areas: (1) the evolution of fluid instabilities at material interfaces and the resulting large-scale mixing of materials, (2) the growth of microscopic cracks and pores leading to large-scale fracture and fragmentation, and (3) the prediction of alteration of solid material properties as a result of the presence of microstructure. In each case, our strategy is to study the physical process using analysis and numerical simulation and then to develop a coarse graining of the description, leading to a model suitable for implementation into a large-scale code.

Specific results from this year's research include a new model for Rayleigh-Taylor mixing based on two-phase flow. Parameters for this model are derived from microscopic conditions that ensure physical realizability and correct asymptotic behavior. We have made detailed comparisons with experimental data to validate this model.

We have developed microscale codes to study the dynamical properties of mixtures at a quantum level, a model to study the formation of ejecta at shocked solid surfaces, and two continuum codes with explicit front tracking to study fluid and solid instabilities. In addition, we have implemented new physics models into the Los Alamos Applied Physics Division's design and assessment codes, including a model for sliding friction coefficient with velocity dependence, a particle model to simulate the transport of ejecta in a turbulent fluid, and a hybrid mix model that couples turbulence and multiphase flow.

Publications

Ashurst, W.T., and B.L. Holian, "Droplet Formation by Rapid Expansion of a Liquid," *Phys. Rev. E* **59**, 6742 (1999).

Ashurst, W.T., and B.L. Holian, "Droplet Size Dependence upon Volume E Rate" (to be published in *J. Chem. Phys.*).

Bickham, S., et al., "Quantum Molecular Dynamics Simulations: An Overview," *Contrib. Plasma Phys.* **39**, p. 147 (1999).

Chen, T.T., et al., "Direct Numerical Simulations of the Navier-Stokes Alpha Model" (to be published in *Physica D*).

Clark, T.T., "Two-Point Closures and Statistical Equilibrium—Implications for Engineering Turbulence," in *Modeling Complex Turbulent Flows*, M. Salas et al., Eds. (Kluwer Academic Publishing, Norwell, Mass., 1999), p. 183.

Clark, T.T., et al., "Testing a Random Phase Approximation for Bounded Turbulent Flow," *Phys. Rev. E* **59**, 5511 (1999).

Clark, T.T., et al., "Two-Point Description of Two-Fluid Turbulent Mixing—I Model Formulation," *Int. J. Multiphase Flow* **25**, 599 (1999).

Clark, T.T., et al., "Two-Point Description of Two-Fluid Turbulent Mixing—II Numerical Solutions and Comparisons to Experiment," *Int. J. Multiphase Flow* **25**, 639 (1999).

Collins, L.A., et al., "Materials under Extreme Conditions" (to be published in *High Pressure Research*).

Glimm, J., and D.H. Sharp, "Stochastic Partial Differential Equations," in *Stochastic Partial Equations: Six Perspectives*, R. Carmona and B. Rozovskii, Eds. (American Mathematical Society, Providence, Rhode Island, 1999), p. 3.

Glimm, J., et al., "Two-Phase Modeling of a Fluid Mixing Layer," *J. Fluid Mech.* **378**, 119 (1999).

Hammerberg, J.E., et al., "Molecular Dynamics Studies of Dry Friction under High Compression and Velocity" (to be published in *Phys. Rev. B*).

Hirth, J.P., et al., "Shock Relaxation by a Strain Induced Martensitic Phase Transformation" (to be published in *Acta Mater.*).

Lenosky, T.J., et al., "Simulations of Fluid Hydrogen," *Phys. Rev. E* **60**, 1665 (1999).

Margolin, L.G., et al., "A Discrete Operator Calculus for Finite Difference Approximations" (to be published in *Comput. Meth. Appl. Mech. Eng.*).

Margolin, L.G., et al., "Large Eddy Simulations of Convective Boundary Layers Using Nonoscillatory Differencing" (to be published in *Physica D*).

Wilson, P., et al., "Spectral Nonequilibrium in a Turbulent Mixing Layer" (to be published in *Phys. Fluids*).

Advancing X-Ray Hydrodynamic Radiography

97604

Daniel Prono

The objective of advanced x-ray radiography is to produce high-resolution images of imploding mock-ups of primary weapon assemblies that can record the weapon's internal components as they undergo compression. Certifying the operational integrity of stockpiled nuclear weapons depends on our ability to validate the hydrocodes that are used to infer nuclear criticality and weapon performance. In the absence of underground testing, the only current way to validate these codes is with x-ray radiography measurement.

Our radiography measurements must now be able to resolve ~0.2-mm features and must be made several times during the implosion (so that mass flow and the evolution of three-dimensional features can be distinguished). Prior x-ray radiography measurements were limited to making only one image and resolving ~1- to 2-mm features. The progress we made this year in the five research areas of our project will help us achieve the requisite higher-resolution x-ray radiographs and make sequential images over the ~2-μs time frame associated with peak nuclear criticality.

Advanced Cathodes. For high-resolution radiographs, the x-rays must be emitted from a very small spot size (in effect, the x-ray spot must be a "point" source). Since the x-rays are generated by impinging a high-energy electron beam onto a bremsstrahlung converter target, the x-ray spot size is directly governed by how tightly we can focus the electron beam. If the cathode that emits the electron beam causes the beam to have high emittance (a beam property that determines how quickly the beam diverges), small, focused spot sizes cannot be attained. This year we developed fabrication techniques for large-area photocathodes that have abnormally high quantum efficiency (~2%) and low work functions. These properties were measured and tested to determine cathode surface lifetimes and durability under different vacuum conditions, and the results confirmed that our advanced cathodes will be suitable for creating very small, focused electron-beam spot sizes.

Analysis of Beam Dynamics. Between the cathode and the bremsstrahlung converter target, the electron beam must be transported through an accelerator structure to gain energy. During transport, there are physical processes that can cause the beam's radial profile to broaden and develop diffuse edges (referred to as "wings" or "halos"), which will blur a focused spot size. Numerical simulation codes were developed to analyze this phenomenon, and we are beginning to understand how to mitigate halo growth by properly adjusting the magnetic transport lattice to maintain laminar flow (i.e., to prevent individual beam electrons from crossing through the beam axis and extending into regions where the restoring forces are nonlinear).

Measurements of Beam/Target Interactions. When a highly focused electron beam impinges on the bremsstrahlung converter target, it quickly ionizes the target material. The resulting target plasma interacts with the electron beam in a manner that dilates the beam spot. The target plasma also expands and then interacts with the later sequence of incoming electron beams needed to make multiple x-ray radiographs over the 2-μs interval of interest (peak compression). This year we measured the target plasma's density and expansion velocity and now have the data needed to analyze design concepts for generating multiple-pulse, small-spot x-ray sources.

Three-Dimensional Reconstruction Techniques. Through analysis and many test simulations, we determined that more than ten different views will be needed to reconstruct objects with asymmetric anomalies in their geometry. Through extensive simulations involving synthetic radiographs, we also determined that there is no benefit in locating these views on other than a single equator surrounding the object to be radiographed. Both determinations help define the requirements for future radiographic facilities.

Fast-Framing Detector Data Recorder. To be able to sense and record x-ray radiographic images several times over a 2-μs duration, we must develop an electronic data recorder capable of ~10-MHz speeds. We have completed the system architecture for such a data recorder and have fabricated an electronic chip that can sense the photons produced when x-rays strike a scintillator material. It converts the photons into an electrical pulse and can then raster and electronically store the pulses in semiconductor junctions at a rate >10 MHz.

Publications

Carlsten, B.E., "Long-Term, Correlated Emittance Decrease in Intense, High-Brightness Induction Linacs," *Phys. Plasmas* **6**, 3615 (1999).

Carlsten, B.E., "Thermalization of an Intense, Space-Charge-Dominated Electron Beam in a Long Focusing Channel," *Phys. Rev. E* **60**, 2280 (1999).

Carlsten, B.E., "Using the Induced Axial Magnetic Field to Measure the Root Mean Square Beam Size and Beam Density Uniformity of an Electron Beam in an Induction Linac," *Rev. Sci. Instrum.* **70**, 3308 (1999).

Taking the Next Step with Intelligent Monte Carlo

99502

Thomas E. Booth

For many scientific calculations, the Monte Carlo method is either the method of choice or the only practical method available. Unfortunately, standard Monte Carlo methods have a very slow convergence rate $(1/\sqrt{T})$ with computing time T. For instance, if a Monte Carlo calculation has a 10% error after one week of computing, then it will take nearly two years to obtain a 1% error. We have shown, both numerically and theoretically, that the convergence rate can be increased dramatically if the Monte Carlo algorithm is allowed to adapt based on what it has learned from previous samples; this convergence has been demonstrated on increasingly realistic and complex problems. As long as the learning continues, the computational efficiency increases, often geometrically fast. This project builds on our recent successes in particle transport, statistics, and statistical physics by extending adaptive methods to complex real problems.

The particle transport work concentrated on achieving geometric convergence (GC). The reduced source method achieved GC on a two-region problem by iteratively using the interface leakage from one region as a source into the other region. We also achieved GC for energy-independent transport in a rectangular box, although a (removable) approximation limited the GC to the first few iterations. Adaptive importance sampling achieved GC on energy-dependent problems with rapidly varying cross section and importance functions by allowing the Monte Carlo algorithm to learn better basis functions.

The statistical work produced promising initial results on adaptive learning algorithms for problems involving airborne migration of particles, with potential applications to pollution modeling and chemical/biological warfare. Using a standard Lagrangian model for homogeneous turbulence, we obtained an order-of-magnitude improvement in estimation of plume spread. We provided theoretical proof of geometric convergence for continuous state space problems. We also completed a theoretical proof of variance reduction regarding the use of transition dynamics relative to the standard Metropolis analysis for statistical physics problems.

The statistical physics work focused on applying extensions of recently developed algorithms to a variety of physical problems. We applied a bivariate version of the multicanonical method to the three-dimensional Ising glass. At low temperatures, we found its ground state to be consistent with the droplet picture. At higher temperatures, but still below the glass transition temperature, we found the ground state to be consistent with the ultrametric picture. We improved algorithms for quantum scattering and eigenvalue problems and applied them to parity violation in low-energy scattering in nuclear physics. We also developed a new adaptive approach to the construction of trial wave functions for diffusion Monte Carlo methods and applied it to the problem of D_3O^+ in an aqueous solution. An improved estimate of the excited state energy resulted.

Publications

Baggerly, K., et al., "Exponential Convergence of Adaptive Importance Sampling for Markov Chains" (to be published in *Journal of Applied Probability*).

Booth, T.E., "Monte Carlo Estimates of Transport Solutions to the Isotropic Slab Problem," *Nucl. Sci. Eng.* **130**, 374 (1998).

Booth, T.E., "Simultaneous Monte Carlo Zero-Variance Estimates of Several Correlated Means," *Nucl. Sci. Eng.* **129**, 199 (1998).

Carlson, J., "Quantum Monte Carlo in Few Body Systems," *Few Body Systems Supplement* **10**, 1 (1999).

Carlson, J., "Quantum Monte Carlo Methods in Nuclear Physics," in *Quantum Monte Carlo Methods in Physics and Chemistry*," M.P. Nightingale and C.J. Umrigar, Eds. (Kluwer, Dordrecht, 1999), p. 287.

Favorite, J.A., and H. Lichtenstein, "Exponential Monte Carlo Convergence of a Three-Dimensional Discrete Ordinates Solution," *Trans. Am. Nucl. Soc.* **81**, 147 (1999).

Fitzgerald, M., et al., "Adaptive Monte Carlo in Generalized Ensembles," in *Condensed Matter Theories*, Vol. 14, D. Ernst et al., Eds. (Nova Science Publishers, Commack, New York, in press).

Fitzgerald, M., et al., "Canonical Transition Probabilities for Adaptive Metropolis Simulation," *Europhys. Lett.* **46**, 282 (1999).

Fitzgerald, M., et al., "Monte Carlo Transition Dynamics and Variance Reduction" (to be published in *J. Stat. Phys.*).

Gomez, M.A., and L.R. Pratt, "Construction of Simulation Wave Functions for Aqueous Species," *J. Chem. Phys.* **109**, 8783 (1999).

Gomez, M.A. et al., "Molecular Realism in Default Models for Information Theories of Hydrophobic Effects," *J. Phys. Chem.* **103**, 3520 (1999).

Gubernatis, J.E., and N. Hatano, "The Multi-Canonical Method" (to be published in *Computers in Science and Engineering*).

Hatano, N., and J.E. Gubernatis, "A Bi-Variate Multicanonical Monte Carlo Method for the Three-Dimensional J Ising Model," in *Computer Simulations Studies in Condensed Matter Physics XII*, D. Landau, Ed. (Springer-Verlag, Heidelberg, in press).

Kollman, C., et al., "Adaptive Importance Sampling on Discrete Markov Chains," *Annals of Applied Probability* **9**, 391 (1999).

Lichtenstein, H., "Exponential Convergence Rates for Reduced-Source Monte Carlo Transport in [x, mu] Geometry," *Nucl. Sci. Eng.* **133**, 258 (1999).

Evolutionary Computation

97621

Chris Barrett

Simulation-based analysis of sociotechnical systems (those possessing physical, technological, and human components) is often characterized by a lack of detailed theoretical knowledge of the systems being studied. This is especially so when compared with the principles and concepts that guide modeling and computation in purely physical sciences. It is crucial that the representational tools themselves are well understood and theoretically grounded. Thus, we have developed a theoretical framework for computer simulations that is based on a new class of dynamical systems: sequential dynamical systems (SDS).

Our research goal is to understand how the dynamical properties of a simulation depend on underlying rules, the structural and logical constraints of these rules, and, in particular, the ordering of these rules. We related symmetry properties of these underlying dependencies to symmetry properties of a corresponding simulation. The analysis breaks into two basic approaches: one is a purely combinatorial study of the dependency structure without specific reference to the particular local mappings; the other focuses on phase-space properties of particular local mappings in certain classes of dependency graphs.

We found that the structure of a certain sequence-structure mapping is of central importance in the search for the "right" order in which a simulation has to be updated. This sequence-structure map turned out to be closely related to a map arising in the context of folding molecular sequences into their corresponding spatial structures. This relation establishes an interesting link between mathematical biology and our framework, and has led to a series of studies on random subgraphs of *n*-cubes, random subgraphs of Cayley graphs, acyclic orientations of random graphs, and neutrality in fitness landscapes.

Additionally, SDS have decomposition properties that are mathematically very closely related to Cartier-Foata's Normal Form, arising in the context of partially commutative monoids in connection with parallel compilation of computer programs.

Our SDS results pertaining to representation, validation, and parallelization of a simulated system include the following: an upper bound on the number of "dynamically different" simulations generated from a fixed object library; general phase space properties of SDS over arbitrary graphs induced by certain local Boolean functions; characterization of invertible SDS; and analysis of fixed points of SDS.

We have begun to apply the SDS setup to various difficult engineering problems, including detailed analysis of large packet-switched communication systems and analysis of interdependencies among critical national network infrastructures.

Publications

Barrett, C.L., and C.M. Reidys, "Theoretical Issues on Computer Simulations" (Artificial Life and Robotics, AROB IV, Japan, January 1999).

Barrett, C.L., et al., "Elements of a Theory of Simulation {II}: Sequential Dynamical Systems," *Appl. Math. Comp*. **107**, 121 (2000).

Barrett, C.L., et al., "Elements of a Theory of Simulation {III}: Sequential Dynamical Systems" (to be published in *Appl. Math. Comp.*).

Mortveit, H. and C.M. Reidys, "Discrete, Sequential Dynamical Systems" (to be published in *Discrete Math.*).

Reidys, C.M., "Acyclic Orientations and Sequential Dynamical Systems" (submitted to *Adv. Appl. Math.*).

Reidys, C.M., "Random Graphs and Sequence to Structure Maps" (to be published in *Combinatorics Prob. Comp.*).

Reidys, C.M., "Random Structures" (to be published in *Ann. Combinatorics*).

Reidys, C.M., "Random Subgraphs of Cayley Graphs Over p-Groups" (to be published in *Europ. J. Comb.*).

Reidys, C.M., and P.F. Stadler, "Neutrality in Fitness Landscapes" (to be published in *Appl. Math. Comp.*).

Reidys, C.M., et al., "Replication and Mutation on Neutral Networks of {RNA} Secondary Structures," *Bull. Math. Biol.* **59** (2) (1998).

Nonlinear Complex Phenomena

99508

Hans Frauenfelder

Within the past few decades, the study of complex systems has become an important field, with applications from ocean dynamics to medicine. We are investigating complex systems experimentally, theoretically, and computationally, and have organized our project into four subtasks: (1) nonlinear and stochastic dynamics; (2) non-equilibrium statistical physics; (3) energy landscapes, dynamics, and function of proteins; and (4) multiscale phenomena in electronic and structural materials. Project goals are to establish interactions among the subtasks, to strengthen the connections between the physical and the biological sciences, and to foster links to other parts of the Laboratory by organizing collaborations and workshops. Recent work in two of the subtasks is described below.

Nonlinear and stochastic dynamics: We have continued our research into simulating turbulence. This effort has included the generalization of our earlier models in which a crucial length parameter (alpha) becomes a tensor that evolves under its own governing equations. This generalization allows representing non-isotropy and heterogeneity in the turbulent flow, as well as a more realistic treatment of the boundary conditions at walls. We have completed direct numerical simulation of the equations in which the length parameter is constant throughout space and have compared the result to those obtained by using the Navier-Stokes equation. The comparison confirms the ability of our equations to represent the large scales of turbulence without the need to resolve the small scales of motion. We have also discovered an intriguing relationship between our equations and the equations of the numerical model.

Non-equilibrium statistical physics: We have studied a two-dimensional soap film flow past a cylinder. We show that three different regions can be accurately characterized in the wake: the near wake, a transition zone, and a turbulent far wake. In the near-wake region, we have settled a 30-year controversy on the mechanism of the wake transition. We show that the shear of the flow creates a secondary, Kelvin-Helmholtz instability. We have demonstrated, computationally, that the state of spiral-defect chaos in convection is an extensively chaotic system. Unlike other calculations, this work is directly applicable to experiments and shows that the system has a relatively small number of degrees-of-freedom. For low-dimensional systems, we have shown that chaotic synchronization can happen up to scale factors. This demonstrates that the most studied dynamical model, the Lorenz system, will synchronize for a larger class of couplings than was previously thought possible.

Publications

Boettcher, S., and A.G. Percus, "External Optimization: Methods Derived from Co-Evolution" (The Genetic and Evolutionary Computing Conference, Orlando, FL, July 13–17, 1999).

Frauenfelder, H., et al., "Biological Physics" (submitted to *Rev. Mod. Phys.*).

Ghosal, S., and L. Vervisch, "Asymptotic Theory of Triple Flames" (submitted to *J. Fluid Mechanics*).

Herron, I.H., "Exchange of Stabilities in Rayleigh-Benard Convection with Heat Sources and Variable Gravity" (submitted to *Math. Meth. Appl. Sci.*).

Herron, I.H., "Onset of Convection in a Porous Medium with Internal Heat Source and Variable Gravity" (submitted to *Int. J. Eng. Sci.*).

Herron, I.H., "Onset of Instability in Poiseuille Flow between Rapidly Rotating Coaxial Pipes" (submitted to *J. Appl. Math. Phys.*).

Herron, I.H., and A.D. Clark, "Instabilities in the Gortler Model for Wall Bounded Flows" (submitted to *Appl. Math. Lett.*).

Li, Y.A., "The Mechanism of the Polarizational Mode Instability in Birefringent Fiber Optics" (submitted to *SIAM J. Math. Anal.*).

L'Vov, V.S., et al., "Anisotropic Spectra of Acoustic Turbulence" (submitted to *Phys. Rev. E*).

Marsden, J.E., et al., "The Geometry and Analysis of the Averaged Euler Equations with Normal Boundary Conditions" (submitted to *Geometric Functional Anal.*).

McMahon, B.H., et al., "Density Functional Theory Calculation of Barrier to Ligand Binding in Myoglobin" (submitted to *J. Chem. Phys.*).

Sasik, R., "Replica Theory of the Random Spherical Manifold" (submitted to *Phys. Rev. B*).

Vorobieff, P., and R.E. Ecke, "Growth of Disordered Features in a Two-Dimensional Cylinder Wake" (5th Experimental Chaos Conference, Orlando, FL, June 27–July 1, 1999).

Vorobieff, P., and R.E. Ecke, "Wakes in Soap Films" (5th Experimental Chaos Conference, Orlando, Fl, June 27–July 1, 1999).

Vorobieff, P., et al., "Deterministic and Stochastic Features in Shock-Driven Transition to Turbulence" (18th Annual Workshop on Chaos and Nonlinear Dynamics, Dynamics Days '99, Atlanta, GA, January 4–8, 1999).

Vorobieff, P., et al., "Shock-Driven Mixing Transition: Quantitative Analysis" (23rd International Symposium on Shock Waves, Imperial College, London, U.K., July 18–23, 1999).

Vorobieff, P., et al., "Soap Film Flows Statistics of 2D Turbulence" (submitted to *Phys. Fluids*).

Wang, L.-P., et al., "Examination of Hypotheses in the Kolmogorov Refined Turbulence Theory through High-Resolution Simulations, Part 2. Passive Scalar Field" (submitted to *J. Fluid Mech.*).

Zoldi, S.M., et al., "Stabilizing Unstable Periodic Orbits in Reaction Diffusion Systems by Global Time-Delayed Feedback Control" (submitted to EQYADUFF 99, Berlin, Germany, August 1–7, 1999).

Zoldi, S.M., et al., "Stationarity and Redundancy of Multichannel EEG Data Recorded During Generalized Tonic-Clonic Seizures" (submitted to *Brain Topography*).

Management of Nuclear Warhead and Infrastructure Reduction

99513

James E. Doyle

The goal of this project is to provide a scientific basis for next-generation technologies and approaches for monitoring deep reductions in numbers of nuclear weapons and for assessing the impact of these reductions on national security issues.

In one component of the project, we are using modern computer technology with massive data quantities to generate models of nuclear weapon complexes and materials flow. Such models provide rapidly accessible information about weapon stocks and associated materials and can be applied to concerns about force reconstitution capabilities and preparation of draft treaty protocols. This work supports development of a variety of computer-based analytical tools for assessing the Russian nuclear infrastructure. We completed several such tools this past year.

We are also conducting strategic dynamics assessments, for example, force stability analyses. During the past year this work has supported development of a multipolar nuclear-exchange model capable of assessing the stability of nuclear forces at much lower levels, taking into account the possibility of multilateral conflict with other nuclear powers such as China or India. This work has led to new Laboratory collaborations with the U.S. Strategic Command

Our transparency and verification technology work focuses on nuclear archaeology and on warhead transparency and monitoring measurements. We are focusing our efforts on providing off-the-shelf systems applicable to arms-reduction verification or transparency measures. This year we developed a prototype integrated facility monitoring system that provides chain-of-custody monitoring during nuclear-warhead dismantlement and a magazine transparency system that monitors weapons in storage. These systems are practical yet innovative applications of the most current work in image processing, change-detection software, monitored seals, and computer science.

Publications

Bodenstein, Y., et al., "Comprehensive Review of Nuclear Materials of the Former Soviet Union, Including Illicit Diversions" (The 40th Annual Meeting of the Institute of Nuclear Materials Management, Phoenix, AZ, July 25–29, 1999).

Voss, S., et al., "An Overview of Minatom's Ten Closed Nuclear Cities" (The 40th Annual Meeting of the Institute of Nuclear Materials Management, Phoenix, AZ, July 25–29, 1999).

Quantifying and Reducing Uncertainty in Predictions of Complex Phenomena

99512

David H. Sharp

This project is developing a fundamental set of tools for quantifying and reducing uncertainty in the assessment of nuclear weapons performance.

The work is organized around two principal objectives. The first is to develop probabilistic and statistical methods for quantifying uncertainty of sufficient power for Science-Based Stockpile Stewardship (SBSS) needs. The second is to illustrate the application of existing and new methods for quantifying uncertainty to five specific problems. These five problems have been selected to represent the breadth of topics encountered in SBSS performance analysis of actual weapons systems. Our goal is to demonstrate that quantifying uncertainty is an essential tool in maintaining confidence in the certification process. A second project goal is to determine where existing techniques are sufficient, and where better methods are needed. The underlying point is that no method for quantifying uncertainty can be regarded as established until it has been used successfully on a complex problem.

We have made progress in five areas. (1) The procedure for nuclear test analysis has been analyzed and many sources of uncertainty identified. A Bayesian framework for quantifying uncertainty in nuclear weapons is being developed, and its relation to the usual nuclear weapon certification uncertainty bounds is being determined. Useful results have been obtained at each stage of partial analysis. (2) We are developing predictive codes for analyzing problems in structural engineering. The focus is to generate precise models of test units (metal marine floats) and test them against large deformation crushing experiments. This year a database of crush behavior was generated and an idealized computational model was developed. A cross-divisional collaboration among thrust participants was established to characterize the constitutive behavior of the units. (3) We are evaluating the effect of uncertainties in shear moduli, yield strength, and heat capacity on the dynamic behavior of shocks in metals. We are also investigating the inverse problem: how experimental data can reduce uncertainties in these quantities. We are assembling all available stress-strain and thermodynamic data on U-Nb alloys with the aim of determining probability distributions of the key material properties. (4) We have modeled the static case radiograph for PHERMEX shot 3578. We have used a variety of models, of increasing complexity, for the scatter background and bremsstrahlung spectrum, which are two systematic effects felt to introduce the greatest uncertainties in data interpretation. We hope that this analysis can be used to characterize the uncertainty in our estimates of density and interface locations derived from the dynamic case radiograph. (5) We successfully demonstrated the use of variance-based importance measures to identify important inputs. The methodology was demonstrated on an in-use Applied Physics Division code.

Publications

Doebling, S., et al., "Validation of Probabilistic Finite Element Buckling Predictions for Spherical Shells" (submitted to *Proceedings of the Third Biennial Tri-Laboratory Engineering Conference on Modeling and Simulation*).

Doebling, S.W., et al., "Validation of Probabilistic Finite Element Buckling Predictions for Spherical Shells" (submitted to *IMAC XVIII: A Conference & Exposition on Structural Dynamics*).

Dolin, R.M., et al., "As-Builts/As-Is Assessment of Geometric and Material Properties for One-Hundred Manufactured Products" (submitted to *Proceedings of the Third Biennial Tri-Laboratory Engineering Conference on Modeling and Simulation*).

French S., et al., "Critique of and Limitations on the Use of Expert Judgements in Accident Consequence Uncertainty Analysis" (to be published in *Radiation Protection Dosimetry*).

Glimm, J., and D.H. Sharp, "Prediction and the Quantification of Uncertainty," in *Proceedings of the 18th Annual International CNLS Conference*, S. Chen, et al., Eds. (North Holland, Amsterdam, in press)

Glimm, J., and D.H. Sharp, "Stochastic Methods for the Prediction of Complex Multiscale Phenomena," *Q. Appl. Math.* **LVI**, 741 (1998).

McKay, M., et al., "Sample Size Effects When Using R2 to Measure Model Input Importance" (submitted to *Proceedings of the International Conference on Safety and Reliability*).

Treml, C.A., and A.S. Heger, "Using Bayesian Belief Networks for Quantifying and Reducing Uncertainty in Prediction of Buckling Characteristics of Marine Floats" (submitted to *Proceedings of the Third Biennial Tri-Laboratory Conference on Modeling and Simulation*).

Treml, C.A., et al., "Reducing Uncertainty in Buckling Analysis Using Bayesian Belief Networks and an As-Built Philosophy" (submitted to *Proceedings of the Eighth ASCE EMD/SEI/GI/AD Joint Specialty Conference on Probabilistic Mechanics and Structural Reliability*).

Strategic Computing Applications

99515

Andrew White

Our project has three components linked by the need to effectively employ parallel processing supercomputers for computationally intense applications. Each component represents a significant scientific challenge, explores the capabilities of terascale computing, and addresses an area of intense societal concern. The lessons learned will benefit future terascale computing applications.

The first component, Global Climate Modeling: The Role of the Thermohaline Circulation in Climate, seeks to compare simulations to determine the dependence of the global thermohaline circulation (THC) system on key physical processes. Using the flux coupler at the National Center for Atmospheric Research, we coupled several models. One model showed coupled variability modes representing El Niño, the North Atlantic Oscillation, and a 30-year mode in the strength of the meridional overturning. Its simulated intermediate and abyssal currents, critical to the THC, compared favorably with three-dimensional hydrographic observations. We are now tracking the "ventilation time" (the time since the water was last in contact with the ocean surface) and other deep water water-mass properties with Lagrangian tracers transported by model currents. We are developing a novel statistical technique for setting values of physical process parameters in coarse-resolution models with output from fine-resolution models.

The goal of the second component, Epidemiology Modeling: Molecular Causes to Macroscopic Consequences, is to illuminate the fundamental mechanisms of disease and to provide insight into protection against nonnatural pathogens. Initial work indicated the HIV epidemic originated in the years between 1921 and 1943. We applied the robustness of phylogenetic methods to real data to better understand the causes of errors in phylogeny reconstruction and the robustness of different popular methods. We simulated the immune response to influenza vaccine and replicated the virus with this model; our results show that although vaccination would improve the response to live virus, under some circumstances having repeat vaccination is worse than having a single vaccination. We are combining global data from the HIV sequence and molecular databases to estimate the variation in known immunogenic domains relative to candidate vaccine strains. In epidemiology, we tracked HIV variants around the world and plan to apply these tracking techniques to influenza. We searched statistics in U.S. Mortality and Morbidity Weekly Reports for the incidence of stereotyped influenza viruses throughout the flu season and prepared summary reports for the years 1985–1998. With an agent-based model of epidemic dynamics, we described the spread of transmissible disease such as influenza using software "agents" to represent humans following realistic "traffic patterns" such as airline routes. We implemented a relational database to host preliminary influenza epidemiology data and have connected to the Centers for Disease Control databanks.

With the third component, Critical Infrastructure Modeling, we aim to research and develop a high-quality, flexible, and extensible software framework to model, simulate, and analyze interdependent infrastructures such as the national electrical power grid. This year we obtained a well-established computer code for AC power flow and modified it to run in our environments. We supplemented its Newton-Raphson performance with a DC-approximation and Gauss-Seidel preprocessors. We developed market abstractions for two cases: the actual California market and a model continuous market. Our major achievement was a continuous market prototype demonstration with power flow ensuring that electrical congestion limits are observed as individual end-users load the system with competitive purchases.

Publications

Cook, D., et al., "Combinatorial Problems Arising in Deregulated Electrical Power Industry: Survey and Future Directions," in *Proc. Approximation and Complexity in Numerical Optimization: Continuous and Discrete Problems*, P.M. Pardalos, Ed. (Kluwer Academic Publishers, Norwell, MA, in press).

Dowell, L.J., "Estimation of the Service Areas of Electricity-Power Substations by Cellular Automata" (Advanced Simulation Technologies Conference of the Society for Computer Simulation International, San Diego, CA, April 11–15, 1999).

Dowell, L.J., and D.B. Henderson, "A Comprehensive, Detailed Simulation of the Electric-Power Industry: Harnessing the Los Alamos National Laboratory HPC Infrastructure" (Advanced Simulation Technologies Conference of the Society for Computer Simulation International, San Diego, CA, April 11–15, 1999).

Kopp, S, et al., "Sequential Dynamical Systems and Simulation" (Genetic and Evolutionary Computation Conference [GECCO], Orlando, FL, July 13–17, 1999).

Korber, B., et al., "Epidemiological and Immunological Implications of the Global Variability of HIV-1" in *Retroviral Immunology*, B. Walker and G. Pantaleo, Eds. (Humana Press, Totowa, NJ, in press).

Krumke, S.O., et al., “Improving Spanning Trees by Upgrading Nodes,” *Theoretical Computer Science*, **221**, 139 (1999).

Krumke, S.O., et al., “Upgrading Bottleneck Constrained Forests” (to be published in *Discrete Applied Mathematics*).

Kuiken, C.R., et al., “Genetic Analysis Reveals Epidemiological Patterns in the Spread of HIV” (submitted *to American Journal of Epidemiology*).

Lapedes, A., and R. Farber, “The Geometry of Immunological Shape Space: Application to Influenza” (submitted to *Proc. Natl. Acad. Sci. USA*).

Maheshwari, S., and L.J. Dowell, “Integrated Modeling of Earthquake Impacts to the Electric-Power Infrastructure of an Elysian Park Scenario in the Los Angeles Metropolitan Area” (Urban and Regional Information Systems Association 1999 Annual Conference, Chicago, IL, August 21–25, 1999).

Smith, D.J., et al., “Variable Efficacy of Repeated Annual Vaccinations against Influenza,” *Proc. Natl. Acad. Sci. USA* **96**, 14001 (1999).

Probabilistic Combinatorial Analysis for Biological Systems

98806

David C. Torney

We are undertaking several types of combinatorial analysis motivated by new molecular-biological data. To further the mathematical statistical analysis of biological sequences and systems, we are continuing to study the characterization of collections of numbers that are potentially the cumulants of a probability distribution. To make inroads into the analysis of evolution, we continue to pursue enumeration of evolutionary trees. We continue to study the existence and construction of Hadamard matrices and projective planes, issues central to the design of large-scale biological experiments and to the analysis of sequence data.

Finally, we continue to undertake a detailed combinatorial and probabilistic modeling of mutation and selection of HIV strains in humans.

We investigated the general issue of the existence of Hadamard matrices of order 4^n. We discovered a family of linear Diophantine equations that have a solution in non-negative integers if and only if a Hadamard matrix of the corresponding order exists. The analysis of these systems was facilitated by their transformation to Smith Normal Form, but further investigation of the transforming matrices is required to resolve the issue of their solubility.

On the topic of probability distributions on sequences, we focused on moment representations. In particular, we developed a theory for those distributions on binary n-sequences whose “higher” moments vanish. For example, when all moments of three or more positions vanish, the domain of admissible moments is a polytope, which is dual to the corresponding cut polytope. This enables Bayesian classification of sequences, given examples of sequences from each of the classes.

We also continued to model the mutation and selection of HIV strains in humans, focusing on heterogeneity of the processes.

Publications

Bruno, W.J., et al., “Probability Set Functions” (to be published in *Annals of Combinatorics*).

Novel Fundamentals in Strategic Computing

99517

Adolfy Hoisie

Software, hardware, and algorithms are continually increasing in size and/or complexity, resulting in large, compositional systems. They are engineered by systematically combining smaller, well-understood components. Despite this trend, the techniques for building such systems are poorly understood. Our project adds insight into compositional software, hardware, and algorithms.

This year we developed a high-level design and implemented a prototype of a component architecture for high-performance scientific applications. This concrete implementation will allow us to experiment and empirically evaluate techniques and abstractions, as well as provide a vehicle for building actual multicomponent applications. In collaboration with scientists from academia and other national laboratories, we made significant progress in formulating an interoperability standard for high-performance computing component architectures: the Common Component Architecture.

We carried out extensive research on existing memory models of computation. From a theoretical/practical standpoint we have identified the models of Alpern et al. and Vitter et al. as suitable for future exploration. We also studied different memory-efficient algorithms for linear-relaxation-type problems that have been proposed in the literature. As a step toward building a robust complexity theory for memory-centric computation, we have begun identifying generic algebraic specifications that can be used to represent large classes of seemingly unrelated problems in the same framework. We have also begun to identify necessary characteristics of transformations (reductions) that can be used to establish equivalence classes of problems under a given computational model.

We initiated a performance evaluation of commodity processor architectures with the intention of studying their performance on ASCI and “driver” (multimedia, web, and data-mining) applications. We then created a preliminary set of multimedia benchmark codes, which cover a variety of mass-market applications. We have developed a novel hardware-counter-based instruction-level analysis technique that is suited for characterizing multimedia and other commercial applications. We also proposed a methodology for performance modeling and prediction of large-scale scientific applications, which we then used to characterize one major ASCI application.

Publications

Armstrong, R., et al., “Toward a Common Component Architecture for High Performance Scientific Computing,” in *Proc. 8th IEEE International Symposium on High Performance Distributed Computing* (August 1999).

Barrett, C., et al., “Formal Language Constrained Path Problems” (to be published in *SIAM J. Computing*).

Cameron, K.W., and Y. Luo, “Instruction-Level Microprocessor Modeling of Scientific Applications,” in *Lecture Notes in Computer Science* **1615** (Springer-Verlag, Berlin, 1999), p. 29.

Carr, R., et al., “On the Red-Blue Set Cover Problem” (submitted to 11th ACM-SIAM Symposium on Discrete Algorithms [SODA], July 1999).

Doddi S., et al., “Point Set Labeling with Specified Positions” (submitted to 11th ACM-SIAM Symposium on Discrete Algorithms [SODA], July 1999).

Hoisie, A., et al., “Performance Analysis of Large-Scale Applications Based on Wavefront Algorithms,” in *Proceedings of the NASA HPCCP/CAS Workshop* (January 1999), p. 15.

Hoisie, A., et al., “Performance Analysis of Wavefront Algorithms on Very-Large Scale Distributed Systems,” in *Lecture Notes in Control and Information Sciences* **249** (Springer-Verlag, Berlin, 1999), p. 171.

Hoisie, A., et al., “Scalability Analysis of Multidimensional Wavefront Algorithms on Large-Scale SMP Clusters,” in *Proceedings of the 7th Symposium on the Frontiers of Massively Parallel Computations* (February 1999), p. 5.

Hunt, H.B. III, et al., “On the Efficient Approximability of ‘HARD’ Problems: A Survey,” in *Proceedings of Approximation and Complexity in Numerical Optimization: Continuous and Discrete Problems*, P.M. Pardalos, Ed. (Kluwer Academic Publishers, Norwell, MA, 1999).

Hunt, H.B. III, et al., “Parallel Approximation Schemes for a Class of Planar and Near Planar Combinatorial Problems” (to be published in *Information and Computation*).

Joubert, W., et al., “Domination Problem with Edge Covering Constraints” (11th ACM-SIAM Symposium on Discrete Algorithms [SODA], July 1999).

Krumke, S.O., et al., “Improving Spanning Trees by Upgrading Nodes” (to be published in *Theoretical Computer Science*).

Krumke, S.O., et al., “Upgrading Bottleneck Constrained Forests” (to be published in *Discrete Applied Mathematics*).

Luo, Y., and K.W. Cameron, "Instruction-Level Characterization of Scientific Computing Applications Using Hardware Performance Counters," in *Workload Characterization: Methodology and Case Studies* (IEEE-CS Press, 1999), p. 90.

Sun, X.H., et al., "A Factorial Performance Evaluation for Hierarchical Memory Systems," in *Proceedings of IPPS'99* (San Juan, Puerto Rico, April 1999), p. 70.

Atomic, Molecular, Optical, and Plasma Physics, Fluids, and Beams

Strongly and Moderately Coupled Plasma Physics in Inhomogeneous Matter

99525

Michael S. Murillo

The focus of this project is on understanding the properties of materials under extreme conditions, especially hot, dense matter that cannot be described in terms of solid, liquid, or dense gas physics. Such matter, termed a "strongly coupled plasma," is a disordered state of matter that is characterized by long-range strong repulsive interactions. Although statistical properties of strongly coupled plasmas are fairly well known, much less is known about dynamical properties. Our main interest is in understanding how dynamical strong coupling effects modify the transport of charged particles, the dynamical screening of fusion reactions in dense plasmas, and the hydrodynamics at short length and fast time scales.

We have developed a generalized hydrodynamic theory of strongly coupled plasmas by combining basic plasma theory with strongly interacting liquid theory. From basic plasma theory we know that the mean field plays an essential role in screening long-ranged Coulomb interactions, and we take this as our starting point in defining a dynamical response function. Our full theory is thus guaranteed to reduce to standard plasma theory, in contrast to some other approaches based on quasi-lattice models. An interpolative ansatz is then made for the excess response beyond the mean field that is due to strong coupling effects. The ansatz is constrained by enforcing sum rules for the exact response function that result from analytic properties of causal responses. We find that this approach matches the viscoelastic hydrodynamic limit and gives a prescription for the nonlocal compressibility. A clear separation of low-frequency and high-frequency structure results in terms of a generalized viscoelastic relaxation time.

This model has been applied to the Yukawa system, which provides an approximate description for dusty plasmas, since it is easy to both create a strongly coupled dusty plasma and to drive waves into them. Moreover, by applying the theory to collective modes of a strongly coupled dusty plasma, we provide a critical test of the viscoelastic separation of time scales, since the dispersion of dust collective modes is acoustic-like, meaning the mode exists for vanishingly small frequencies and rises linearly to high frequencies at large wavevectors. We are also comparing these results with molecular dynamics simulations. This theory can easily be generalized to the recently produced ultra-cold plasmas, which are strongly coupled as a result of their extremely low temperatures.

Publications

Murillo, M.S., "Collective Modes in Strongly Coupled Dusty Plasmas," in *Non-Neutral Plasma Physics III*, J.J. Bollinger et al., Eds., AIP **498**, 376 (1999).

Murillo, M.S., "Dynamical and Structural Properties of Strongly Coupled Dusty Plasmas," in *Frontiers in Dusty Plasmas*, Y. Nakamura et al., Eds. (Elsevier Science, Amsterdam, in press).

Murillo, M.S., "Longitudinal Collective Modes of Strongly Coupled Dusty Plasmas at Finite Frequencies and Wavevectors," *Phys. Plasmas* **7**, 33 (2000).

Murillo, M.S., "Static Local Field Correction of Acoustic Waves in Strongly Coupled Dusty Plasmas," *Phys. Plasmas* **5**, 3116 (1998).

Next-Generation Sophistication in Defense and High-Energy-Density Physics Exploratory Research

99524

Carter Munson

Our major goal in this project is to develop advanced experimental measurement capabilities and associated theoretical and computational designs to maximize the proposed Atlas pulsed-power facility's physics return. We will develop capabilities for conducting strongly coupled plasma (SCP) hydrodynamics experiments and characterizing surface phase transitions in the dynamic Atlas environment.

This year we established experimental facilities to produce SCPs for equation-of-state (EOS) measurements using shock compression of a plasma jet produced by a tamped exploding wire (see first figure), and we are currently testing an x-ray microscope required for shock velocity and density measurements. We completed designs for testing target plasma-formation characteristics for Atlas SCP hydrodynamics experiments and are configuring the Los Alamos COLT pulsed-power facility for plasma-formation studies during FY 2000.

We also completed a conceptual design and system-performance analysis for a possible neutron resonance spectroscopy (NRS) temperature measurement of Atlas SCP experiments (see second figure) and are assembling a transportable, intense, pulsed ion beam for beam-target production of neutrons required by an NRS measurement. We conducted numerical design studies using both one- and two-dimensional codes to provide guidance for more complete Atlas SCP experimental designs. Tests of the pressure system for the Laboratory's isobaric expansion facility, which was to be used as a test bed for dynamic melt diagnostics, are complete.

We performed experimental measurements examining the broad-band reflectivity and nonlinear optical response of materials under perturbed conditions (using an intense laser to produce shock heating, melting, and structural disorder). These experiments have demonstrated changes in both the complex dielectric constant $\varepsilon(\omega)$—caused by modification of the material band structure—and in the nonlinear optical response, which reveals changes in material crystal symmetry and temperature. The third figure shows the dynamic behavior of the complex dielectric constant for aluminum as it undergoes a solid-to-liquid transition. We also examined possible melt diagnostics using x-ray and x-ray ultraviolet scattering and are currently evaluating preliminary experimental results. In addition, we are evaluating photoelectron and resonant fluorescence spectroscopic techniques to probe valence electron structure for studying solid-state phase transitions in materials under extreme temperatures and pressures.

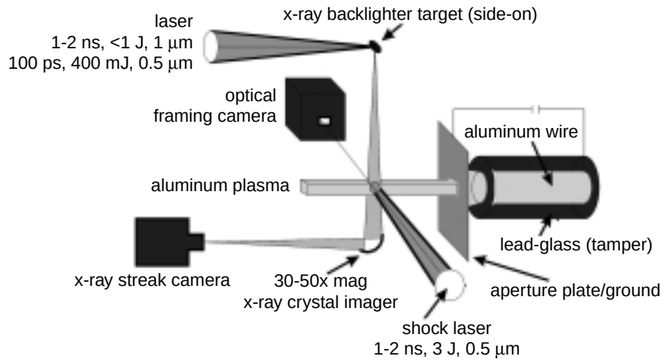

Schematic layout of the SCP EOS experiment. The initial target plasma is formed by ohmically exploding a tamped aluminum wire. A jet of this plasma is shocked into the strongly coupled regime by the shock laser, and shock propagation characteristics are then measured.

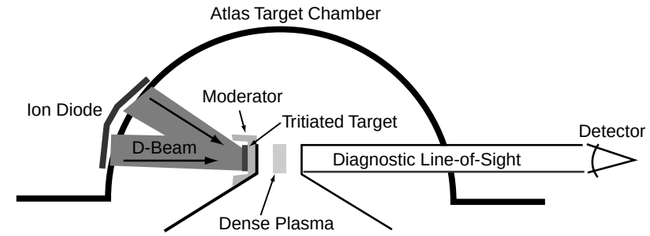

A schematic layout of a possible NRS temperature diagnostic for the Atlas configuration. Shown are the intense ion beam, tritiated target for neutron production, neutron moderator, the dense target plasma, and the line of sight for observation of the neutron time of flight.

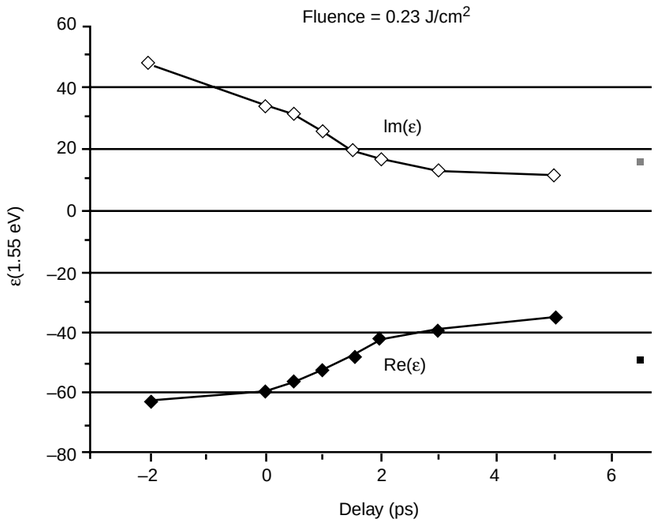

Aluminum undergoes a solid-to-liquid transition when laser radiation depletes the conduction electrons (~280%). The time history of the real (solid diamonds) and imaginary (open diamonds) components of the complex dielectric constant is shown for an incident laser fluence of 0.23 J/cm^2. The points (solid squares) on the far right are from the Drude model.

Publications

Bartlett, R.J., "X-Ray Absorption Spectroscopy: Diagnostic Tool for Probing Material Properties on Dynamic Experiments" (12th IEEE Pulsed Power Conference, Monterey, CA, June 27–30, 1999).

Guo, C., and A.J. Taylor, "Structural Phase Transition of Aluminum Induced by Electronic Excitation" (submitted to *Phys. Rev. Lett.*).

Taylor, A.J., et al., "Diagnostic Development for the Atlas Pulsed Power Facility" (12th IEEE Pulsed Power Conference, Monterey, CA, June 27–30, 1999).

Wood, B.P., et al., "Shock Compression Experimental Capabilities of the Atlas Facility" (American Physical Society Conference on Shock Compression of Condensed Matter, Snowbird, UT, June 27–July 2, 1999).

Workman, J., et al., "One-Dimensional X-Ray Microscope for Shock Measurements in High-Density Aluminum Plasmas," *Rev. Sci. Instr.* **70**, 613 (1999).

High-Power Microwave Science and Technology

99522

Michael V. Fazio

This multidimensional project emphasizes (1) expanding and applying high-power microwave (HPM) R&D capabilities to develop systems suitable for defense applications, (2) developing threat reduction approaches to defend against foreign or terrorist HPM threats, and (3) enhancing the understanding of how the use of HPM devices would affect systems.

The goal of this project is to produce a field-tested HPM source driven by a compact pulsed-power system. This year we focused on the tasks in support of the annular-beam klystron (ABK) HPM source effort. One of the most challenging problems for the ABK microwave source is producing the high-current, thermionic, annular-beam electron gun. This gun will be an order of magnitude beyond the state of the art and a factor of 5 higher in current than the thermionic gun at the Dual-Axis Radiographic Hydrodynamics Testing facility. Our gun must produce an electron beam of sufficient quality and intensity to be efficiently converted to microwave energy. The gun voltage and current design specifications are 800 kV and 5 kA.

The key tasks addressed this year were the electron-gun electrical and mechanical design, initiation of fabrication, and beginning the theoretical research on annular-beam physics issues. We chose the magnetron injection gun configuration over the more standard Pierce gun geometry after comparing properties that included emission current density, thermal loading, beam stability, mechanical stability, and mechanical fit into the available physical envelope.

With the design tradeoffs achieved, electron-gun fabrication is under way at DOE's Stanford Linear Accelerator Center klystron production facility, which is the world's most advanced facility for this type of work. Key hardware elements put in place in order to test the ABK tube included modifications to the Banshee pulsed-power modulator for a 5-Hz pulse repetition rate, so that the ABK can be radio-frequency high-voltage conditioned over about 5 million pulses to achieve full design performance, and the 10-kG direct-current magnet (with power supplies, water cooling, and interlocks) on the Banshee modulator beam line, which is required for transporting the intense electron beam through the ABK in repetitively pulsed ABK operation.

Numerical Modeling and Diagnostic Methods for Magnetized Target Fusion

99527

Richard Siemon

We are preparing a magnetized target fusion (MTF) experiment in which a preheated magnetized plasma will be compressed to fusion conditions by a pulsed-power-driven imploding liner. MTF represents a new approach to developing controlled fusion energy that promises low-cost development and use of relatively low-technology drivers. One of the three critical areas that MTF needs to address in preparation for a proof-of-principle demonstration is the preparation of a target plasma suitable for compression. We intend to use two benchmarked magnetohydrodynamic (MHD) codes to explore target plasma configurations with an internal magnetic field suitable for translation from a formation region into an already-demonstrated liner and compression.

We have imported the Eulerian MHD computer simulation code Moqui from the University of Washington and a PC version of the Mach-2 MHD code from Numerex. Moqui is specialized to the simulation of the dynamic formation and translation of field-reversed configurations (FRCs), and Mach-2 can follow the dynamic compression of complex plasmas. Together, these two codes form the necessary computational capability to completely simulate an MTF proof-of-principle experiment. Because we are currently designing the equipment for FRC formation, we have begun using Moqui to study design parameter variations; the code will also be used later to provide diagnostic predictions and to design translation experiments.

Publications

Intrator, T.P., et al., "Experimental Measurements of Solid Liner Implosion onto Vacuum for Magnetized Target Fusion Applications" (APS-DPP meeting, Seattle, WA, November 1999).

Applications of Quantum Technologies

99505

David J. Vieira

The main goal of our project is to apply the latest technologies in laser and trapping to control and manipulate the quantum states of atomic systems. Of particular interest are experiments related to the development of a quantum computer. Quantum computation would undermine the security of public key-encryption systems used throughout the world; therefore, understanding the feasibility of quantum computation is important to national security interests. Our project is also allowing us to advance our abilities to concentrate, confine, manipulate, and detect selected radioactive (and stable) atoms using optical and magnetic traps. This work has important applications for (1) understanding fundamental electroweak interactions, (2) investigating ultracold atoms, and (3) detecting trace amounts of nuclear proliferants relevant to treaty verification and environmental concerns.

This year we have demonstrated quantum cryptography over atmospheric paths at record setting distances of 0.5 km in daylight and 1.6 km at night. From these results we believe that re-keying of satellites with quantum cryptography will be possible. We have demonstrated quantum control of decoherence in an all-optical setting and invented an ultrabright, tunable source of polarization-entangled photon pairs for which we have submitted a patent. We have completed an all-solid-state light source at 397 nm and used it to laser-cool and image trapped calcium ions for the quantum computing part of this project. We have also started a new experiment to study coherent multi-atomic quantum processes with trapped strontium ions. The laser system and ion trap for this experiment have been constructed.

Using a magneto-optical trap (MOT) coupled to a mass separator, we have been able to trap and detect five different radioactive species (rubidium-82, -83, -84 plus cesium-135, -137), with up to six million rubidium-82 atoms trapped and as few as 100 atoms being detected in a secondary low-background measurement MOT. This technology is being applied in three different areas: (1) the high-precision, parity violation measurement of the beta-decay asymmetry of polarized rubidium-82; (2) the study of cold fermionic rubidium-84 atoms that have been sympathetically cooled by a rubidium-87 Bose-Einstein condensate; and (3) the use of magneto-optical traps for ultrasensitive detection. Although all these projects are in a formative stage of development, we have made good progress in (1) the trapping of rubidium atoms in a time-orbiting-potential (TOP) magnetic trap for the beta-asymmetry experiment; (2) the first reported measurement of the atomic D_1 line in rubidium-82 and the remeasurement of the D_2 line with higher precision (important in polarizing rubidium-82); (3) the simultaneous trapping of cold rubidium-84 and rubidium-87 atoms as an initial step in the sympathetic cooling experiment; and (4) the first reported isotopic ratio measurement for radioactive atoms (cesium-135/cesium-137) in a magneto-optical trap.

Publications

Aerts, S., et al., "Two-Photon Franson-Type Experiments and Local Realism" (to be published in *Phys. Rev. Lett.*).

Berkeland, D.J., "Cooperative Effects in Trapped Strontium Ions" (to be published in *Proceedings of the International Conference on Laser Spectroscopy*).

Berkeland, D.J., et al., "High-Resolution, High-Accuracy Spectroscopy of Trapped Ions," in *Atomic Physics* **16**, 29, W.E. Baylis and G.W.F. Drake, Eds. (The American Institute of Physics, Woodbury, NY, 1999).

Buttler, W.T., et al., "Practical Free-Space Quantum Key Distribution Over 1 km," *Phys. Rev. Lett.* **81**, 3283 (1998).

Hughes, R.J., "Quantum Computation," in *Feynman and Computation*, A.J.G. Hey, Ed. (Perseus, Reading, MA, 1999), p. 191.

Hughes, R.J., "Quantum Computation" (to be published in the *Encyclopedia of Computer Science*).

Hughes, R.J., "Quantum Computing with Trapped Ions," Proc. SPIE **3270**, 120 (1998).

Hughes, R.J., and D.F.V. James, "Prospects for Quantum Computation with Trapped Ions," *Fortschr. Phys.* **46**, 759 (1998).

Hughes, R.J., and J.E. Nordholt, "Quantum Cryptography Takes to the Air," *Physics World*, 31 (1999).

Hughes, R.J., et al., "Practical Free-Space Quantum Key Distribution," in *Springer-Verlag Lecture Notes in Computer Science* **1509**, C.P. Williams, Ed., ISBN 3-540-65514-X (1999).

Hughes, R.J., et al., "Quantum Cryptography for Secure Free-Space Communications," Proc. SPIE **3615**, 98 (1999).

Kwiat, P.G., and L. Hardy, "The Mystery of the Quantum Cakes" (to be published in *Am. J. Phys.*).

Kwiat, P.G., and H. Weinfurter, "Embedded Bell-State Analysis," *Phys. Rev. A* **58**, R2623 (1998).

Kwiat, P.G., et al., "All-Optical Implementation of Grover's Search Algorithm" (to be published in special issue of *J. Mod. Opt.*).

Kwiat, P.G., et al., “High-Efficiency Interaction-Free Measurements” (submitted to *Phys. Rev. Lett.*).

Kwiat, P.G., et al., “Optical Implementation of Grover’s Algorithm: It’s All Done with Mirrors,” in *Proceedings of the 4th International Conference on Quantum Communication, Measurement and Computing* (Evanston, IL, 1998).

Kwiat, P.G., et al., “Ultrabright Source of Polarization-Entangled Photons” (to be published as Rapid Communications in *Phys. Rev. A.*).

Kwiat, P.G., et al., “What Does a Quantum Eraser Really Erase?,” in *Mysteries, Puzzles, and Paradoxes in Quantum Mechanics*, R. Bonifacio, Ed. AIP Conf. Proc. **461**, (AIP Publishing, New York, 1999), p. 69.

Schwindt, P.D.D., et al., “Quantitative Wave-Particle Duality and Non-Erasing Quantum Erasure” (to be published in *Phys. Rev. A.*).

Vieira, D.J., et al., “Trapping ^{82}Rb for Beta-Decay Parity Violation Measurements,” *International Conference on Trapped Charged Particles and Fundamental Physics*, AIP Conf. Proc. **457**, 143 (1998).

White, A.G., et al., “Non-Maximally Entangled States: Production, Characterization, and Utilization” (submitted to *Phys. Rev. Lett.*).

Zhao, X., et al., “Developing Optical Traps for Ultra-Sensitive Detection,” SPIE Proc. **3270**, 70 (1998).

Zhao, X., et al., “Hyperfine Structure and Isotope Shift of ^{82}Rb D_1 and D_2 Transitions,” *Phys. Rev. A* **60**, 4730 (1999).

Engineering Science

Manipulation of Residual Stresses to Control Material Properties

97809

Mark Bourke

This project takes an innovative approach to controlling material properties by manipulating residual stress generated during phase transformations. Because most ceramics exhibit a low fracture toughness, one approach to overcome this limitation is to temper them (much like the tempering of glass). We have attempted to do so using a volume change associated with a reduction reaction. Although the focus is on the reduction reaction, the capabilities and methodology will be applicable to other transformation mechanisms. Our initial approach studied the residual stresses generated from the volume shrinkage that occurs when a ceramic oxide is reduced to a metal/ceramic composite.

In the demonstration phase of this research, questions were raised concerning the kinetics and relaxation processes associated with the reduction. To explore the real-time behavior of the reduction, we used neutron diffraction. Neutrons provide a tool to monitor the reduction process by offering real-time in situ measurements at temperature in the reducing atmosphere. Our objectives were to track the evolution of the reduction and to monitor its effects on a single-phase spinel specimen. By understanding the kinetics we hoped to identify an optimal processing route for tempering.

We heated a series of spinel samples to the reduction temperature (in excess of 1250°C) under nitrogen. By recording diffraction data during heating (including a measurement at the reduction temperature), we determined the coefficient of thermal expansion and spinel lattice constant before the start of the reaction. The reduction was initiated by introducing a carbon monoxide/dioxide mixture, diluted with nitrogen, which established a reducing atmosphere with oxygen partial pressures of 10^{-12} to 10^{-14}. Spectra, recorded every 0.5 hour, were analyzed by Rietveld refinement. The observed 4:1 ratio of the alumina and nickel volume fractions agreed with the expected stoichiometry. However, the strain evolution as determined from lattice parameter changes of the spinel proved to be counterintuitive and smaller than expected.

To explore the strain effect, we performed finite element method (FEM) simulations incorporating plastic flow by power-law creep and characterized changes in spinel order and disorder using Rietveld refinement. The neutron data proved to be consistent with the FEM models that assume that creep relaxes the strain at high temperatures. This relaxation suggests why the measured strains were smaller than expected and is leading us to explore (1) alternate processing routes that will mitigate the creep relaxation and (2) alternate reactions, such as martensitic, to produce the desired tempering effects.

Characterization of Liquid Lead-Bismuth Eutectic for High-Power Neutron Spallation Applications

99504

Francesco Venneri

One of the goals of our project is to acquire the lead bismuth eutectic (LBE) technology from Russia, where it was developed for nuclear submarine propulsion. We expect this technology to lead to (1) powerful and highly efficient neutron sources, (2) proliferation-resistant nuclear reactors, and (3) efficient subcritical systems for nuclear waste destruction. To use LBE technology in the U.S., we must conduct a thorough program of verification of the Russian LBE database. LBE technology was developed in great secrecy, and the materials and methods were quite different from what we are accustomed to in the U.S. The testing of corrosive behavior of materials in LBE and thermal-hydraulics experiments will be needed to confirm the Russian LBE technology as it is acquired. Extending the technology to situations in which proton beams and spallation products are present requires the extension of the database to new regimes (see first figure).

Another major goal is to prepare LANSCE (Los Alamos Neutron Science Center) to receive and test the International Science and Technology Center (ISTC) 1-MW LBE spallation target. This target, the first of its kind worldwide, is being developed in cooperation with the European Union through the ISTC. Our project is directing and monitoring the design and construction of the target for testing in the LANSCE proton beam.

During the past year we acquired important LBE technology from Russia through a series of meetings, common projects, and extended visits of Russian scientists to the Laboratory. Through this exchange, we obtained important and previously unreleased data on materials, thermal-hydraulics, and radiation performance. We also obtained specific competence in design of components for use in LBE systems, visited the Russian Institute for Physics and Power Engineering (IPPE), and extensively discussed LBE coolant technology with IPPE specialists.

We upgraded and restarted the LANSCE LBE loop after an extended shutdown, installed new control and data-acquisition systems, and performed flow measurement experiments. We designed and initiated fabrication of a new loop to complement the first one, extending the range of operation to nonisothermal regimes. Five U.S. candidate steel samples were delivered for testing in the IPPE LBE corrosion test loop, for comparison with the Russian alloys.

Lastly, we completed design of the ISTC 1-MW target experiment (called target complex 1, TC-1) and performed a complete thermal-hydraulic, structural, and neutronic analysis of TC-1 in coordination with international collaborators in France, Sweden, and Russia (see second figure).

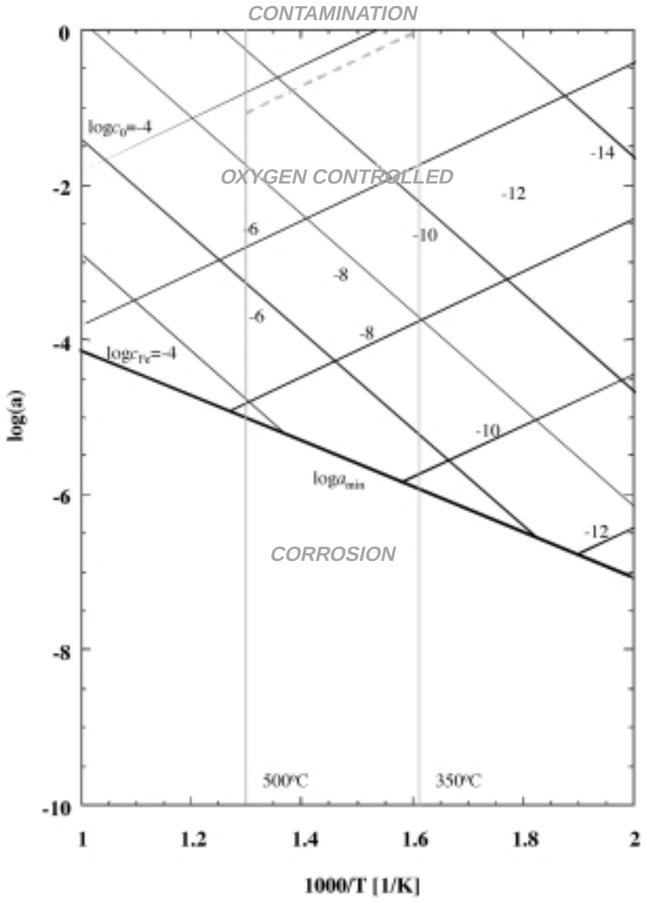

The operating regime of thermodynamic activity of oxygen in LBE for proper oxygen control to prevent corrosion and contamination. Based on LDRD-supported collaboration with the specialists from the Institute of Physics and Power Engineering, Obninsk, Russia, we obtained the free energy of formation for oxides, the solubility of oxygen and steel alloying species in lead-bismuth. These data, which we used to construct this diagram, are critical to the corrosion/contamination-free operation of lead-bismuth coolant systems.

Publications

Li, N., "Liquid Lead-Bismuth Technology Development for Accelerator-Driven Transmutation of Waste," in *Proceedings of the ANS Topical Meeting: Accelerator Applications in Nuclear Systems*, 239 (1998).

Venneri, F., et al., "Disposition of Nuclear Waste Using Subcritical Accelerator-Driven Systems," in *Proceedings of the Uranium Institute 24th Annual Symposium* (London, September 8–10, 1999).

Venneri, F., et al., "Disposition of Nuclear Waste Using Subcritical Accelerator-Driven Systems: Technology Choices and Implementation Scenario" (to be published in *Nuclear Technology*).

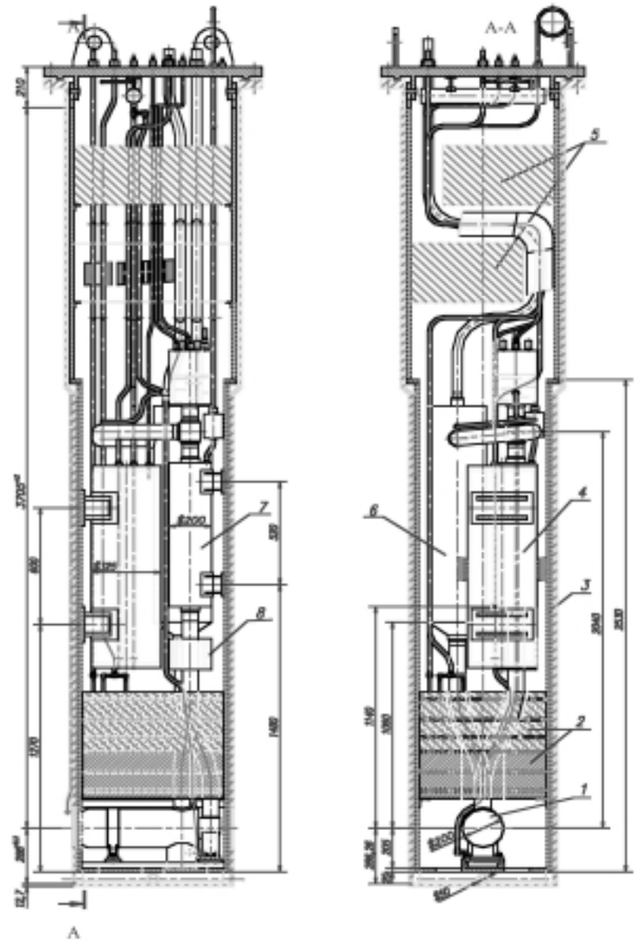

Schematic illustration of the lead-bismuth eutectic (LBE) spallation target designed with our Russian collaborators. The target complex (TC-1) is now under fabrication. Los Alamos is providing the data acquisition and control system that will be used to monitor and control target operations. Los Alamos is also designing the external water and gas systems necessary for removing heat and transferring the LBE into and out of the loop. These systems will be fabricated by the Laboratory in 2000: (1) target (2) shielding (3) frame (4) drainage tank (5) shielding (6) heat exchanger (7) electromagnetic pump (8) flow meter.

Nuclear Materials Management Systems for Proliferation Resistance, Environmental Protection, and Sustainability

99521

Edward D. Arthur

The objective of this project is creation of a nuclear materials management analysis system. The system will include appropriate databases and evaluation metrics that will allow consistent, quantitative, and transparent assessment of present and future nuclear fuel cycles. The assessments will be defined in terms of performance associated with proliferation resistance and safeguardability, environmental protection, and economics.

We have created a flexible linear programming model that allows description and incorporation of any present or future nuclear fuel cycle and its components (see figure). The basis for a multiattribute utility assessment exists to define fuel cycle component combinations optimized for driver objects related to proliferation resistance, environmental attributes, and economics. Our system includes 15 nuclear materials and 39 fuel cycle material processes. We demonstrated the system using nuclear materials flows and management choices (both time independent [a snapshot in time] and time dependent [over decade timeframes]) to optimize economic performance.

A key task initiated this year was creation of metrics and utility functions for proliferation resistance and waste management to be used in the multiattribute utility analysis. We also created initial utility functions related to materials safeguardability that incorporate material inventories, containment, and surveillance approaches. In the environmental area, we are defining metrics through use of analysis codes that integrate waste types and forms, disposal systems, and engineered barriers to quantify performance in terms of dose release, toxicity, and other parameters.

Publications

Krakowski, R.A., "Long Term Global Trade-Offs Related to Nuclear Energy," in *Proceedings of the International Conference on Future Nuclear Systems: Global99* (American Nuclear Society, Chicago, 1999), p. 209.

Krakowski, R.A., and R. Wilson, "What Nuclear Power Can Accomplish to Reduce CO_2 Emission," in *Innovative Energy Systems and CO_2 Stabilization*, R. Watt, Ed. (Cambridge University Press, New York, in press).

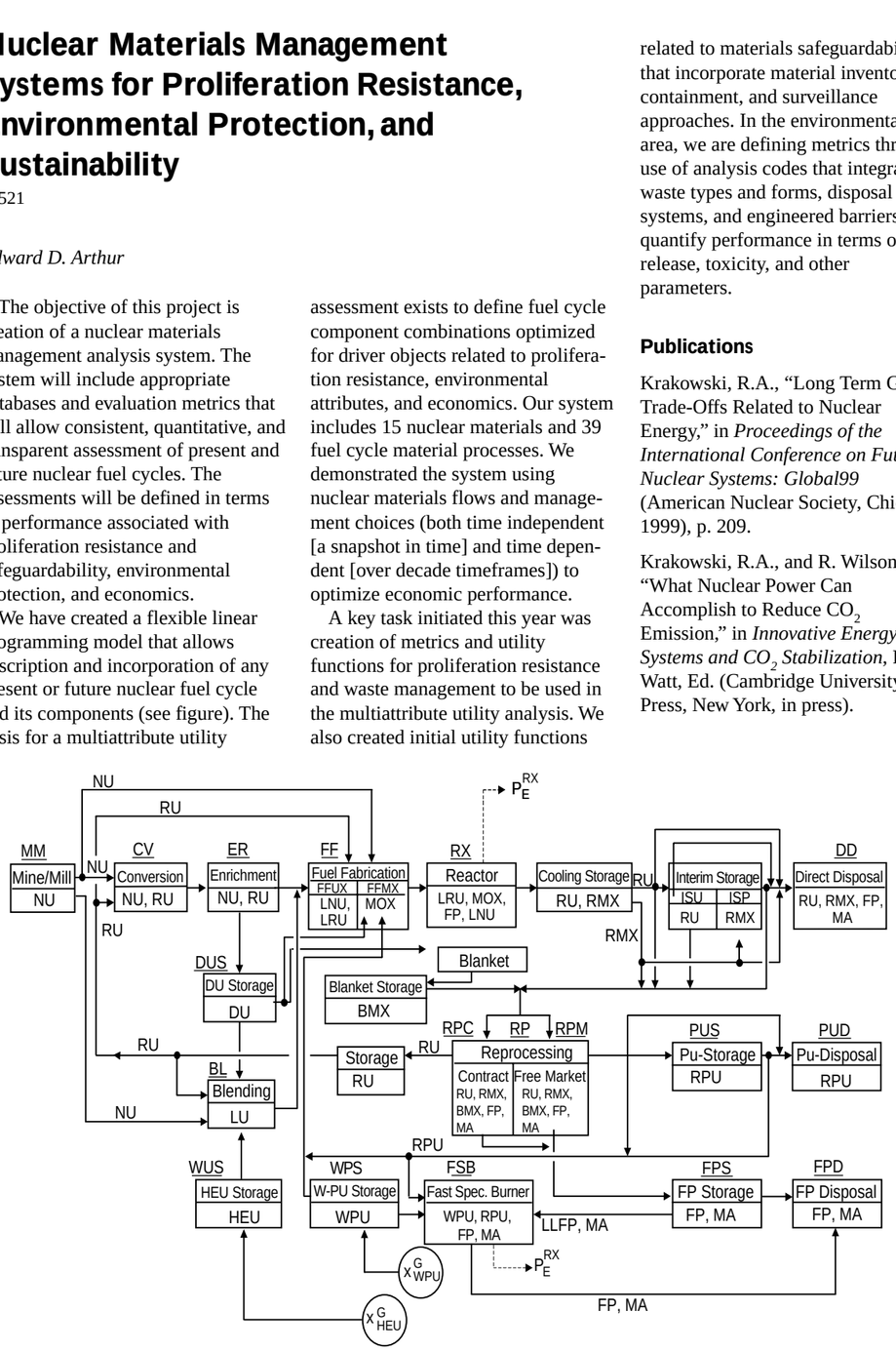

The nuclear fuel cycle model of our nuclear materials management analysis code system.

Hard and Deeply Buried Target Defeat

99510

William Priedhorsky

The "hard and deeply buried target defeat" problem has three integrated phases: target detection, characterization, and neutralization. We studied several technologies that promise improved capabilities in all three phases. To bridge these areas and examine them in a joint sense, we are developing new information integration tools.

Seismic techniques, both active and passive, can find and characterize buried facilities. Research into knowledge discovery in this area can enable us to exploit huge databases, such as the World Wide Web. The development of a wide range of signatures that can be accessed with remote sensors, such as the Sandia/Los Alamos Multispectral Thermal Imager Satellite and wideband radio frequency (rf) collectors, will help us find and characterize hard targets. Tools that use the Laboratory's Advanced Strategic Computing Initiative (ASCI) computing to create three-dimensional models from two-dimensional models of the physical effects of nuclear weapons will quantify these weapons' effectiveness against hard targets.

Using the MUSIC (Multiple Signal Classification) matrix technique, we processed signals from a German seismic array that detected industrial activity from a distance of over 300 km (see first figure). This technique bodes well for passive long-range detection of hard targets.

Active seismic techniques promise more information than passive techniques, at the cost of great intrusiveness. Using a modified Boltzmann lattice gas model, we

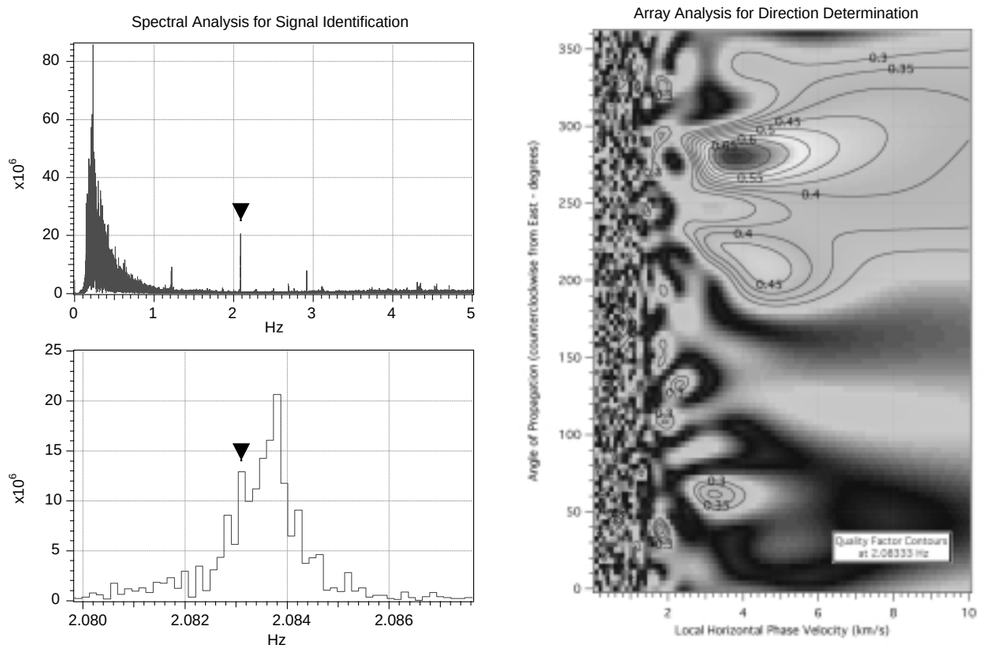

- Narrow-Band Analysis of Continuous Data (Adaptation of MUSIC Technique)
- Two Hours of Data from GERESS Seismic Array (Germany)

Long-range detection of a man-made seismic source via spectral analysis. The strong signal at 2.08 Hz comes from an unknown source 300 km distant.

showed that active seismic imaging is possible in realistic, rough terrain.

We are using a low-frequency infrasound detection system to characterize activities in underground facilities (see second figure). Preliminary results indicate that we can detect signals at practical ranges.

Wideband rf sensors can detect electromagnetic signatures from machinery, such as vent fans, and other activities in underground facilities. We are also using this technique to determine the signatures of conventional explosives.

We are using the Metastable Intermolecular Composites (MIC) technique to investigate energy coupling and partitioning to estimate kill effectiveness. Experiments indicate that up to 44% of the energy expended reaches the target.

We are exploring a concept for a self-contained Rocket Exhaust Thermal Spallation (RETS) penetrator of hard rock. Our new analytical model combines thermal spallation rock mechanics with heat transfer models, ballistic models, and penetrator engineering design parameters.

We developed a new technique of bispectral analysis to produce signal "fingerprints" from data, like seismic signals, that contain a high level of Gaussian noise.

Finally, we are using information integration systems to combine results from these diverse approaches. These systems include a knowledge system that incorporates disparate data types into a geographic/temporal/logical context. The information integration system employs a modular structure that allows incremental upgrades and an open interface for flexibility and manual processing.

Publications

Steck, L.K., et al., "Seismic Characterization of Tunneling Activity at the Yucca Mountain Exploratory Studies Facility," *Seis. Res. Lett.* **70**, 197 (1999).

This compact, unattended infrasound sensor, developed at Los Alamos, has been used to demonstrate infrasound's potential for facility characterization.

Instrumentation and Diagnostics

Advanced Nuclear Measurement Science

98601

Mark M. Pickrell

The purpose of this project is to develop the underlying science for future nuclear material measurements. In the next decade we must be capable of assaying nuclear materials that are highly impure, contaminated, encased in highly shielding matrices, and inhomogeneous. This challenge requires fundamentally new nuclear measurement methods.

This year our efforts at developing fast neutron detectors produced a neutron-detection efficiency greater than 50%. We calculated a neutron die-away time less than 5 μs in simulations of a neutron well-counter consisting of 64 layers of 6Li-scintillator/WLS fiber. We experimentally determined that the neutron-detection efficiency of a single layer of 6Li-scintillator/WLS fiber agreed with the results of single-layer simulations.

We demonstrated techniques for imaging prompt gamma rays produced by active interrogation using californium-252. We also produced fully three-dimensional images and compared experimentally derived gamma-ray production rates with calculations that show that quantitative estimates of gamma-ray production rates can be determined (see the first figure). We have developed state-of-the-art modeling tools and experimental diagnostics for CdZnTe detectors, including an alpha-particle scanner for device characterization. These tools allow us to design advanced detectors, investigate material system and device characteristics, and provide feedback on growth and manufacturing processes. For example, we developed novel detector designs for high-performance gamma-ray spectroscopy (see the second and third figures).

We also contributed to manufacturing and processing techniques through our investigation of surface passivation using energetic oxygen atoms. We focused on emerging safeguards problems and proliferation risk by investigating and characterizing existing inventories of fissile materials, in particular, the minor actinides formed in the commercial fuel cycle.

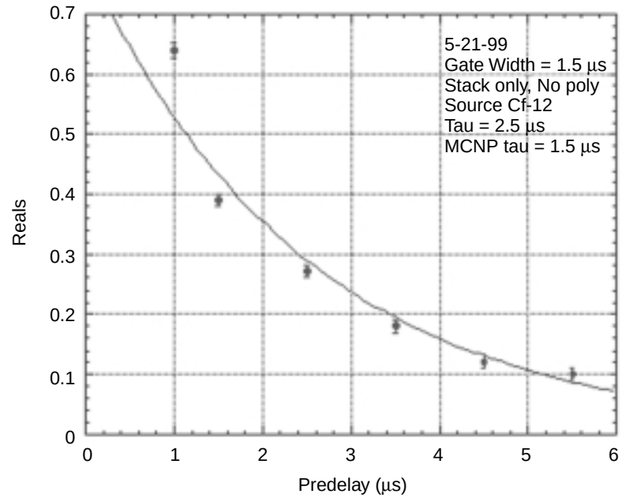

An experimental neutron die-away time "Tau" of 2.6 μs is obtained with a 20-layer test assembly of the 6Li-scintillator/WLS fiber detector from the dependence of the californium-252 coincidence count rate ("Reals") on the delay time coincidence gate ("Predelay"). This is a 20-fold reduction in neutron detection time compared with previous technology.

Our data-fusion efforts included (1) reducing bias in tomographic gamma scanning by including prior assumptions about smoothness of the solution vector, (2) exploring sampling methods to verify alternate nuclear material (neptunium), (3) combining neutron and gamma assays (followup on 1998 experimental results), and (4) studying the effect and possible remedies of measurement error in predictors in nondestructive assays.

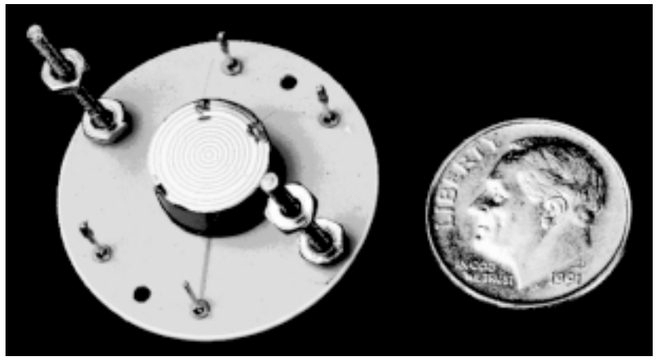

Cylindrical coplanar grid CdZnTe detector designed by Los Alamos National Laboratory and manufactured by an industrial partner. The detector is now commercially available.

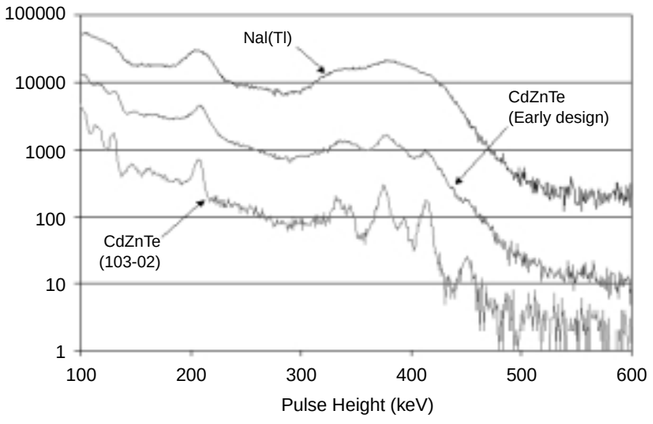

Pulse-height spectra for low-burnup plutonium (plutonium-239, 413.7 keV) measured using a NaI(Tl) detector and two CdZnTe detectors, one of the first coplanar grid detectors (Early design) and a cylindrical coplanar grid detector designed by Los Alamos National Laboratory. Note that the spectra can be compared only in terms of resolution because the counting time and measurement geometry were different in each case. The cylindrical design yields significantly better resolution than the early coplanar grid design.

Publications

Burr, T., and P. Knepper, "A Study of the Effect of Measurement Error in Predictors in Nondestructive Assay" (to be published in *Appl. Radiot. Isot.*).

Burr, T., and T. Prettyman, "Bias Reduction in Tomographic Gamma Scanning: Experimental and Simulation Results," (The 1999 Spring Research Conference on Statistics in Industry and Technology, Minneapolis, MN, June 2–4, 1999).

Burr, T., and W. Stanbro, "Sampling and Statistical Issues in Neptunium Safeguards" (to be published in *J. Nucl. Mater. Man.*).

Burr, T., et al., "Shielding-Related Assay Challenges and Experimental Results in Nuclear Safeguards" (American Nuclear Society 1999 Winter Meeting, Long Beach, CA, Nov. 14–18, 1999).

Dreicer, J.S., "How Much Plutonium Could Have Been Produced in the DPRK IRT Research Reactor?" (to be published in *Science and Global Security*).

Earnhart, J.R.D., et al., "Evaluation of the Compton Camera Method for Spectroscopic Imaging with Ambient Temperature Detector Technology" (The International Symposium on Optical Science, Engineering, and Instrumentation, Denver, CO, July 18–23, 1999).

Ensslin, N., et al., "Performance Calculations for Fast Active Neutron Assay" (The 40th Annual INMM Meeting, Phoenix, AZ, July 25–29, 1999).

Gavron, A., et al., "Development of Safeguards Detector Technology at Los Alamos" (The 21st Annual ESARDA Meeting, Seville, Spain, May 4–6, 1999).

Geist, W., et al., "Testing of a Fiber/Scintillator Neutron Capture Detector" (The 6th Annual Topical Conference on Nuclear Safeguards: The Process-Safeguards Interface, Jackson Hole, WY, September 21–24, 1999).

Mayo, D.R., et al., "Design of a Fiber/Scintillator Neutron-Capture Counter for Assay of Impure Plutonium" (The Institute for Nuclear Material Management Annual Meeting, Phoenix, AZ, July 27–31, 1999).

Miller, M.C., et al., "Evaluation of the BC454/BGO Detector in High Gamma-Ray and Neutron Background Environments" (The 6th NDA Waste Characterization Conference, Salt Lake City, UT, November 17–19, 1998).

Prettyman, T.H., "Method for Mapping Charge Pulses in Semiconductor Radiation Detectors," *Nucl. Instrum. Methods Phys. Res., Sect. A.* **422**, 232 (1999).

Prettyman, T.H., "Theoretical Framework for Mapping Pulse Shapes in Semiconductor Radiation Detectors," *Nucl. Instrum. Methods Phys. Res., Sect. A.* **428**, 72 (1999).

Prettyman, T.H., et al., "Design and Characterization of Cylindrical CdZnTe Detectors with Coplanar Grids" (The International Symposium on Optical Science, Engineering, and Instrumentation, Denver, CO, July 18–23, 1999).

Prettyman, T.H., et al., "Investigation of Charge Collection in CdZnTe Detectors" (The International Symposium on Optical Science, Engineering, and Instrumentation, Denver, CO, July 18–23, 1999).

Prettyman, T.H., et al. "Multielement CdZnTe Detectors for High-Efficiency, Ambient-Temperature Gamma-Ray Spectroscopy," *Trans. Am. Nucl. Soc.* **79**, 108 (1998).

Prettyman, T.H., et al., "Performance of CdZnTe Detectors Passivated with Energetic Oxygen Atoms," *Nucl. Instrum. Methods Phys. Res., Sect. A.* **422**, 179 (1999).

Staples, P., et al., "Imaging of Heterogeneous Materials by Prompt Gamma-Ray Neutron Activation Analysis," *Nucl. Instrum. Methods Phys. Res., Sect. A.* **422**, 906 (1999).

Advanced Dynamic Radiography with Protons

97618

Chris Morris

We are using intermediate energy protons to produce radiographs of explosively driven experiments. Proton beams provide a flexible time format, excellent position resolution, and adjustable contrast for a wide range of experiments. The 800-MeV linear accelerator at the Los Alamos Neutron Science Center (LANSCE) provides short pulses of protons that are dispersed and focused using magnetic lenses. Typically, 50-ns-wide pulses of 4×10^9 protons are dispersed across the 12-cm × 12-cm object plane. The transmitted beam is then imaged on a detector plane using a magnetic lens. The magnet lens system images scattering angles in the object at an intermediate location. Angle collimators at this location were used to optimize the image contrast for specific experiments.

We have used a system of gated CCD cameras to obtain up to seven images per experiment. More time frames can be obtained by using a second proton lens and image plane or by using framing cameras. We have obtained multiple images with pulse spacings as small as 357 ns. The accompanying figure presents recent results in a Cambell-Cox corner-turning experiment that clearly show the motion of the burn front in a detonating high-explosive assembly.

Proton radiography is evolving rapidly. Recent developments include reconfiguring the lenses to magnify each time frame image, replacing the collimators with beam blockers to image the scattered beam rather than the transmitted beam, and developing new detector technologies that will provide more dynamic range and more frames.

Publications

King, N.S.P., et al., "An 800-MeV Proton Radiography Facility for Dynamic Experiments," *Nucl. Instrum. Methods* **424**, 84 (1999).

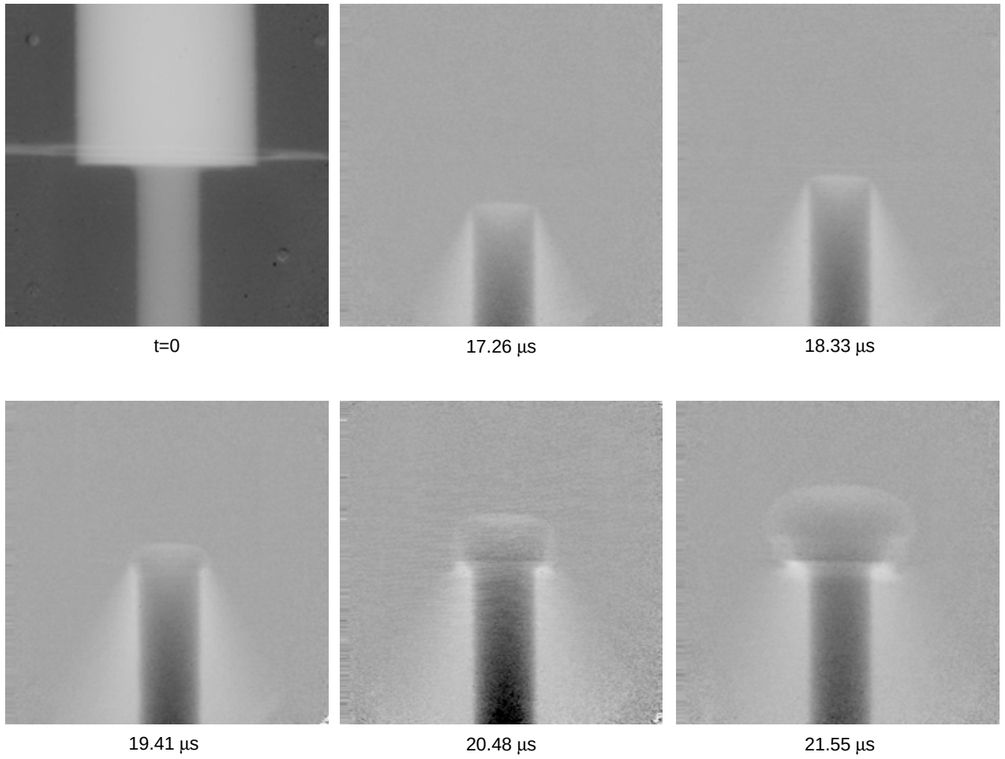

Proton radiographs showing the time evolution of the burn front in detonating PBX-9502 high explosives. The radiographic times are displayed in the figure. The first frame is the "static" frame taken before the detonation. In subsequent frames, the swept-back shadow represents a high-density region created by the shock wave in the air that results from the detonation.

Geoscience, Space Science, and Astrophysics

Algorithm Development for Ocean Models

97808

Len Margolin

The aim of this project is to develop improved numerical algorithms for use in global ocean models. Currently available ocean models, such as the Parallel Ocean Program (POP) and the Miami Isopycnic Coordinate Ocean Model (MICOM), are limited in their ability to resolve the broad range of length and time scales that are important to the study of global climate because of the memory and speed constraints of today's computers. Our project is an algorithmic approach to improving the accuracy and computational efficiency of ocean models. In particular, we are studying the use of nonoscillatory transport schemes to represent the effects of unresolved spatial scales on larger scales of motion. We are also studying a method of averages (MOA) that significantly increases computational efficiency.

We continued our investigation into using nonoscillatory transport schemes as implicit subgrid scale models in numerical large-eddy simulations (LES). We verified these schemes' effectiveness in convective boundary-layer growth and are now studying their use in the growth of shear boundary layers. While these numerical transport schemes represent the effects of transport and dissipation terms of turbulence, a parameterization of the source term is still required. We found that noise (for example, introduced by incomplete convergence of our iterative solver) leads to growth that is qualitatively correct, but that must be "tuned" to achieve quantitative agreement. We are now exploring an analytic model of Kelvin-Helmholtz instability growth as a source, where the unstable perturbation is chosen proportional to the mesh size. An important aspect of this work is that while typical LES models used in ocean simulations have on the order of five parameters that must be retuned for different problems, the nonoscillatory tranport schemes are self-adaptive.

We generalized our analysis of the MOA, which is a computational technique that efficiently simulates problems with multiple time scales. The MOA is a nested algorithm, in which efficiency results from maximizing the number of inner iterations. Our new analysis estimates the number of inner iterations, while including the effects of the interactions between slow and fast scales. Further efficiency results from spatial smoothing in the inner loop and from employing a nonuniform weighting scheme to estimate time-averaged quantities for the outer loop. We implemented the MOA in an idealized code for shallow fluid flow to verify our analytic estimates, as well as in a code for simulating wildfire propagation. The wildfire code includes many physics models relating to combustion and turbulence, and so illustrates the effectiveness of the MOA methodology in a complex geophysical model.

Publications

Chen, S., et al., "Direct Numerical Simulation of the Navier-Stokes Alpha Model" (to be published in *Physica*).

Margolin, L.G., et al., "Large Eddy Simulations of Convective Boundary Layers Using Nonoscillatory Differencing" (to be published in *Physica*).

Reisner, J.M., et al., "Coupled Atmospheric-Fire Modeling Employing the Method of Averages" (submitted to *Mon. Weather Rev.*).

Smolarkiewicz, P.K., et al., "Forward-in-Time Differencing for Fluids: A Hierarchy of Nonhydrostatic Models" (submitted to *J. Atmos. Sci.*).

Solar Terrestrial Coupling through Space Plasma Processes

97803

Joachim Birn

The terrestrial environment is strongly affected by the solar wind, charged particles (plasma) ejected from the Sun that impact on Earth's magnetosphere. This project focuses on the processes that govern charged-particle transport and energization and both microscopic and macroscopic instabilities in the magnetosphere and adjacent regions. Our approaches combine space-data analysis with theory and computer simulations. Our primary regions of interest are those where different plasma populations interact with each other. These are regions of particularly dynamic plasma behavior, associated with magnetic flux, energy transfer, and dynamic energy release. Major regions of the magnetosphere are shown schematically in the accompanying figure.

We studied the basic plasma processes that govern the solar wind, Earth's magnetosphere, and their interface, the magnetopause. Using collisionless plasma theory (particles interact through a mutually induced space-charge field, where collisions have no significant effect), we found a critical condition on the solar wind's electron beta (the ratio of electron pressure to magnetic pressure), resulting from heat flux instabilities. This condition shows fair agreement with observations from the spacecraft Ulysses.

A second project dealt with flux transfer events (FTEs), which are interpreted as manifestations of transient processes connecting the magnetospheric and magnetosheath magnetic fields at Earth's magnetopause (see figure). We determined the interior structure of FTEs by examining high-resolution magnetic field and plasma distribution functions from the ISEE 2 spacecraft. This study confirmed the existence of two distinct regions within an FTE, a central core and a field-draping region, and unambiguously showed reconnection of the interplanetary magnetic field and Earth's magnetic field.

Two phenomena we observed in the magnetotail suggest that transient reconnection akin to magnetopause FTEs also occurs in the magnetotail. These phenomena occur in the plasma sheet and consist of brief occurrences of fast plasma flow (bursty bulk flows) and plasmoids, or magnetic flux ropes, which represent parts of the plasma sheet that have the structure of closed loops or twisted tubes of magnetic field lines (see figure). Using constraints from the two spacecraft observations, we have started modeling such flux ropes. Most of the flux ropes do not fit a model based on the balance between the magnetic stresses and the gradient of an isotropic plasma pressure. This lack of fit indicates that these events are strongly affected by time dependence, anisotropic stresses, or dynamic pressure.

We also investigated the propagation of solar-wind perturbances in the magnetosphere, with ground magnetometer observations. We have installed magnetometers in New Mexico, Colorado, and California, and are currently installing one in Louisiana. Our studies of the propagation of sudden changes (sudden impulses) and irregular pulsations of the ground magnetic field demonstrated that the propagation delays do not always agree with expected delays based on current theories.

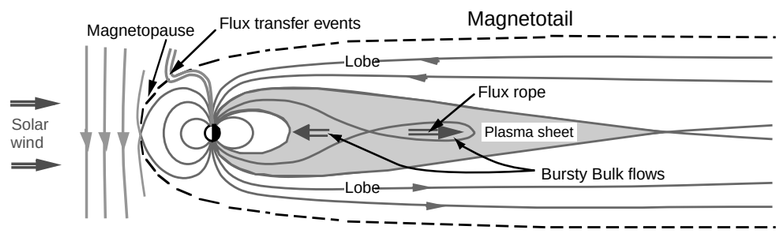

Main regions of Earth's magnetosphere, shaped by their interaction with the solar wind, a stream of charged particles ejected from the Sun. The impact of the solar wind compresses Earth's magnetic field on the day side (solid lines to the left of Earth) and deforms it into a long, comet-like tail on the night side. The interface between the solar wind and the magnetosphere is called the magnetopause. This interface may be penetrated by interconnected magnetic flux tubes called flux transfer events. The magnetic tail includes a layer of plasma (the plasma sheet) embedded between two lobes. The plasma sheet may contain magnetic loops or helical magnetic structures, called plasmoids or flux ropes. The arrows within the plasma sheet indicate plasma flow, which may occur in brief bursts called bursty bulk flows.

Publications

Gary, S.P., et al., "A Lower Bound for Electron Core Beta in the Solar Wind," *J. Geophys. Res*. **103**, 14559 (1998).

Hesse, M., and M.G. Kivelson, "The Formation and Structure of Flux Ropes in the Magnetotail," in *New Perspectives on the Earth's Magnetotail*, A. Nishida et al., Eds. (American Geophysical Union, Washington D.C., 1998), p. 139.

Karimabadi, H., et al., "Magnetic Structure of the Reconnection Layer and Core Field Generation in Plasmoids," *J. Geophys. Res*. **104**, 12313 (1998).

Kinney, R.M., and J.C. Williams, "Turbulent Cascades in Anisotropic Magnetohydrodynamics," *Phys. Rev. E* **57**, 7111 (1998).

Kinney, R.M., et al., "Mechanism for Discrete Arc Breakup by Nonlinear Alfven Wave Interaction," *J. Geophys. Res.* **104**, 19,931 (1999).

Krauss-Varban, D., et al., "Two-Dimensional Structure of the Coplanar and Noncoplanar Magnetopause Transition During Reconnection," *Geophys. Res. Lett.* **26**, 1235 (1999).

Le, G., et al., "The Magnetic and Plasma Structure of Flux Transfer Events," *J. Geophys. Res*. **104**, 233 (1999).

Newbury, J.A., et al., "Electron Temperatures in the Solar Wind: Typical Properties and a Lower Bound at 1 AU," *J. Geophys. Res*. **103**, 9553 (1998).

Omidi, N., et al., "Hybrid Simulation of the Curved Dayside Magnetopause During Southward IMF," *Geophys. Res. Lett.* **25**, 3273 (1998).

Lithospheric Processes

97815

W. Scott Baldridge

Earth's lithosphere is the outer, rocky shell comprising the crust and uppermost mantle. Despite decades of study, many fundamental questions remain regarding the basic structure of the lithosphere, such as thickness of the crust, thickness of the lithosphere, age domains, and various physical properties (density, seismic velocities). These latter properties are partly a function of the age of the lithosphere and of the geothermal gradient. Using both geophysical and geochemical techniques, we focused, in part, on basic characterization of the lithosphere in selected regions. Better characterization is required for an understanding of processes by which the lithosphere is formed and modified over time in various tectonic events. Our studies are also directly related to societal issues such as the Comprehensive Test Ban Treaty and environmental cleanup. In addition, we studied mass and heat transport and fractional crystallization process in selected igneous rock bodies to learn about fluid flow and magma transport in the crust.

Western China is a region of great topographic and structural complexity, where mountain ranges such as the Tien Shan have undergone great deformation and, paradoxically, adjacent areas such as the Tarim Basin have remained relatively stable. Is deformation controlled by the structure of the crust or by physical properties of the crust and/or mantle? While not providing a complete answer, our studies showed that the crust beneath the Tarim Basin is composed of a 42-km-thick "typical" lower to middle crust (i.e., metamorphosed and anhydrous) that is similar to that of the central U.S. and other interior continental regions and is overlain by ~4 km of sediments and sedimentary rocks. The Tarim Basin may remain undeformed because of the presence of this strong "cratonic" lithosphere. In comparison, the crust of the Tien Shan is similar in thickness, averaging 45 to 55 km thick. No thick, low-density crustal root is present. Thus, the high elevation of the Tien Shan may be dynamically supported by low-density (hot) upper mantle. Our seismic studies of the Colorado Plateau in the western U.S. show that its high elevation is the result of dynamic support by low-density mantle and that the structure, density, and seismic properties of the crust vary by age provinces. Our work on isotopic compositions of mantle-derived lavas in eastern Spain confirms that lithosphere was thinned before 10 million years ago during an episode of extension that followed collision with the African plate. No deep mantle plume is required, as has been hypothesized.

Because geochemical and isotopic data from magmatic rocks are typically "inverted" to interpret the composition of the mantle, it is important to understand processes by which magmatic compositions evolve in the upper crust. We studied selected lavas from Hawaii to understand how long magma resides in upper-level chambers. From study of short-lived uranium-series isotopes, we determined that holding times in shallow magma chambers are relatively short (a few hundred years to around 1,000 years) and that contamination of melts by crustal wall rocks is not a major problem.

Elements of Water Resources and Urban Pollution

97812

Charles Keller

We are continuing to strengthen our capabilities and understanding in the area of water resources. Several collaborators are coming together to give a consistent picture of water vapor fluxes from the land and sea surface into the atmosphere.

Using very high resolution (2 meter zones) in the HIGRAD code, we have simulated our lidar observations of evaporation from the tropical ocean surface. The simulations show that the upwelling columns of moisture are surrounded by down-welling drier air, but most importantly they arise and vanish on a more rapid scale than we thought, which has resulting in our changing the timing of the lidar scans. We have implemented and improved a code (SPLASH) that treats the behavior of precipitation at this air/land interface. Four important attributes of SPLASH are (1) physical representation of surface water routing, (2) topographic shading, (3) surface/subsurface hydrological coupling, and (4) physically and biologically based representation of evaporation and transpiration (first figure).

This interface study also included chemical fluxes. Most interesting is the use of the Laboratory's global ocean circulation model combined with explicit bio-geochemical models to produce growth of phytoplankton. We have followed phytoplankton through its life cycle to its production of dimethyl sulfide, which provides cloud condensation nuclei (second figure).

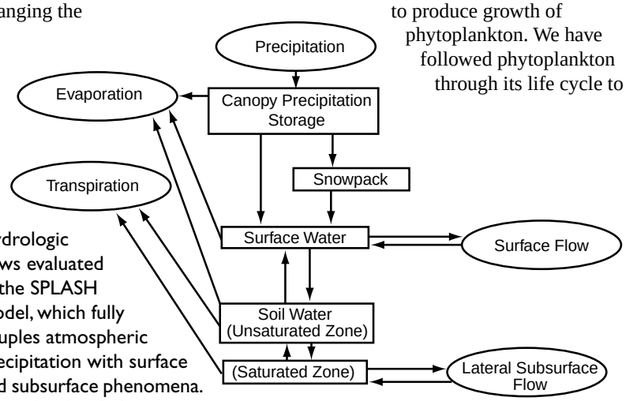

Hydrologic flows evaluated in the SPLASH model, which fully couples atmospheric precipitation with surface and subsurface phenomena. Note the detailed treatments of interactions among the various regimes, including newly appreciated importance of Lateral Subsurface Flow.

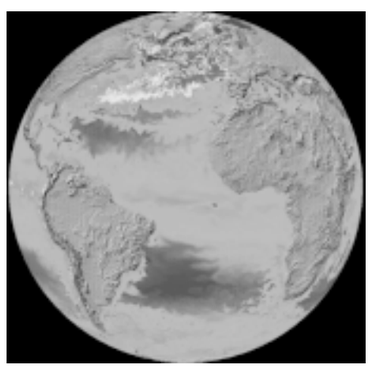

From a multiyear simulation, the springtime bloom of phytoplankton is shown in the North Atlantic Ocean. This rapidly occurring bloom agrees well with satellite observations.

Biomass burning can be compared to anthropogenic emissions. To quantify this comparison, we combine chemistry with the Laboratory's coupled wildfire-micrometeorology model (FIRETEC-HIGRAD) to compute wildfire emissions and assess their impact on global climate change and regional air quality. This computation better represents the heat release process in real fires and improves fire-spread-rate calculations. It also gives us the capability to compute trace gas emissions from wildfires for climate change and regional air quality assessments.

Finally, we are actually modeling regional-scale atmospheric flows and studying how coastal currents affect their moisture-carrying capability. A coupled regional ocean-atmosphere model (ROAM) is essential to a successful simulation of California winter precipitation. The ability of this model to resolve regional-scale California coastal countercurrent provides us with the means to investigate the oceanic impact on sea surface temperature (SST), air-sea fluxes, and, hence, resulting precipitation.

Publications

Huang, Z., and C.-C.A. Lai, "Multidecadal Variations of Monsoon Precipitation in the Southwestern United States between 1895 and 1996" (to be published in *J. Climate*).

Kao, C.-Y.J., et al., "Test of the Volume-of-Fluid Method on Observed Marine Boundary Layer Clouds" (to be published in *Mon. Wea. Rev.*).

Martens, S.N., et al., "Spatial Distributions of Understory Light Along the Grassland/Forest Continuum: Effects of Cover, Height, and Spatial Patterns of Tree Canopies" (to be published in *Ecological Modelling*).

Shao, X.M., et al., "Observations of Precipitable Water Vapor Fluctuations in Convective Boundary Layer via Microwave Interferometry," *J. Geophys. Res.* **104**, 16729 (1999).

Urban Security

97616

Grant Heiken

Urban areas are confronted with many security issues, from crime to natural disasters to pollution. Our goal is to model the vulnerability and response of urban systems to changes in their physical environment, social-political setting, or economy, as well as to malicious attacks. The subsystem models we develop will be integrated with a decision-making model to enhance disaster preparation and recovery. We have initiated a Web-based emergency-planning effort for earthquake preparedness in the Los Angeles area.

We linked models of nonlinear seismic ground response, earthquake damage, and the electrical infrastructure within the city of Los Angeles. These linked models would be used by contingency planners as a planning tool, by responders as a real-time event-specific information source and damage assessment tool, and by both planners and responders to model losses, rapidly determine resources needed, and estimate social-economic impacts of earthquakes.

We also simulated the transport and fate of nitrogen-compound pollutants from auto and industrial emissions through the air-water environment of the Ballona Creek watershed in Los Angeles, California. We tracked the dispersion and chemistry of these pollutants as they were transported by regional winds and eventually deposited, wet or dry, on the ground. We then traced their path as they were entrained into surface water runoff during rain storms and then carried into the receiving water system, where dispersion and biologically mediated chemical reactions take place.

By generalizing two existing urban evolution models, we developed, with collaborators, a Markov Random Field model that estimates the most suitable future land use for any given location. This estimate is based on what was there initially and the land-use pattern in the neighborhood around the location, together with zoning, physical suitability, transportation access, demographics, and economic factors. These growth dynamics are linked to an earthquakes and urban infrastructure project in Los Angeles.

In addition, we developed an integrated modeling system of new and legacy (declassified weapons codes with broad applications) code components that builds upon the strength in scientific modeling and simulation of the Laboratory. This system allows communication among objects written in different languages across address spaces and networks. Any code module, existing or newly developed, may be added to the system.

Publications

Brown, M., "Urban Parameterizations for Mesoscale Meteorological Models," in *Mesocale Atmospheric Dispersion* (submitted to WIT Press, Southhampton, UK).

Brown, M., and M. Williams, "Urban Canopy Parameterizations for Use in Mesoscale Meteorological Models," in 2nd *AMS Symp. Urban Envir.* (American Meteorological Society, Albuquerque, NM, 1998).

Brown, M., et al., "Integrated Air and Water Quality Modeling System: Application to the Los Angeles Metropolitan Area" (2nd AMS Symp. Environmental Applications, Long Beach, CA, January 2000).

Burian, S.J., et al., "Modeling Atmospheric Contributions of Nitrogen Compounds in Urban Stormwater Runoff" (11th AMS and AWMA Joint Conference of the Applications of Air Pollution Meteorology, Long Beach, CA, January 1999).

Burian, S., et al., "Modeling Atmospheric Deposition of Nitrogen Compounds and the Amount Washed Off by Storm Water Runoff" (submitted to *Air, Water, Soil Pollution*).

George, J.E., and D.C. George, "L2F—Legacy to the Future Framework" (ACM 1999 Java Grande Conference Workshop for High-Performance Network Computing, San Francisco, CA, June 12–14, 1999).

Heiken, G., "Modeling Cities: The Los Alamos Urban Security Initiative," *Natural Hazards Observer* **23** (available online, *http://www.colorado.edu/hazards/o/maro99/maro99a.htm#losalamos*, 1999).

Heiken, G., et al., "Modeling Cities—The Los Alamos Urban Security Initiative," *Pub. Works Management Policy* **4**, 198 (1999).

Jones, E.M., and K.B. Olsen, "Broadband Modeling of Nonlinear Soil Response for the 1994 Northridge, California, Earthquake," *Seismol. Res. Lett.* **70**, 226 (1999).

Maheshwari, S., and L.J. Dowell, "Integrated Modeling of Earthquake Impacts to the Electric-Power Infrastructure: Analyses of an Elysian Park Scenario in the Los Angeles Metropolitan Area" (URISA 1999 Annual Conference, Chicago, IL, August 21–25, 1999).

Theoretical and Observational Studies of the Earth's Mantle

97813

Thomas J. Shankland

Our project involves the dynamical transport of heat and matter in the earth's mantle and core. We studied the three-dimensional (3-D) dynamics of the mantle and core through both simulations and analyses of observational data. We also compared fluid dynamic model predictions with field and seismic observations. Our research exercises Laboratory hydrodynamic codes and exposes their operators to a broader world of computational research. It also supports related missions in treaty verification and in the consequences of geological hazards reduction.

A Laboratory cartesian convection code, MC3D, has yielded an unanticipated, exciting result: A supercontinent (such as the one from which our present continents are derived) need not be inherently unstable because it insulates the mantle that it overlies. By incorporating both oceanic and continental plates in our model (see first figure), we found that oceanic plates impose a long-wavelength flow on the regions they overlie, which raises the temperature in the mantle beneath to magnitudes comparable to and even in excess of those observed below a model supercontinent. We conclude that because the mantle is largely internally heated, subcontinental heating results from an absence of subduction rather than the insulation of active upwellings. Accordingly, hotter-than-average regions may evolve below both large oceanic plates and supercontinents. These findings are supported by the vast, hot region in the upper mantle observed by seismic tomography below the Pacific plate.

In calculations we performed using the massively parallel, 3-D, spherical mantle convection code, TERRA, we included extremely large viscosity variations; such viscosity variations

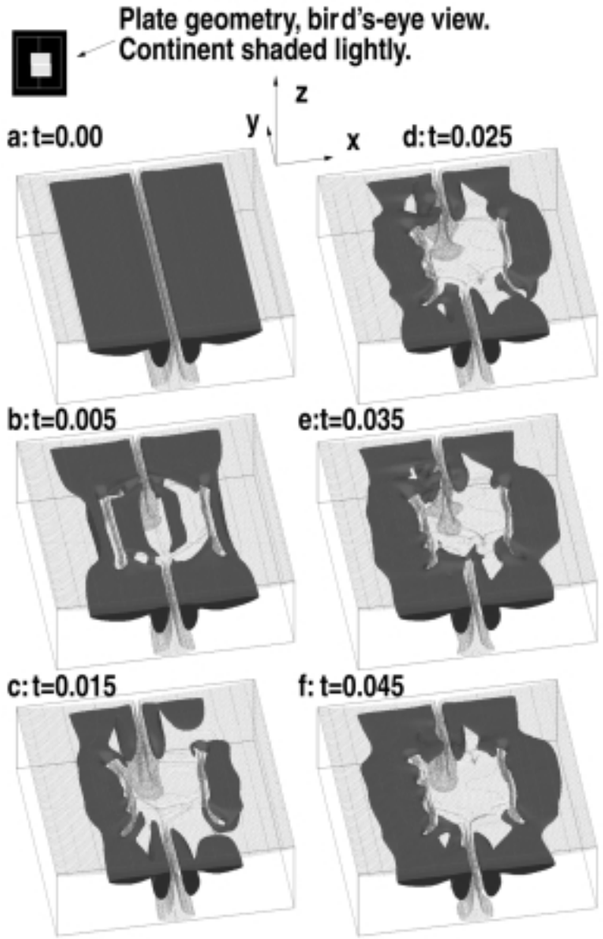

Isosurfaces indicating equal nondimensional temperatures T in the mantle following a continental collision. T = 0.7 (light shaded) and T = 1.09 (dark). The elapsed nondimensional time t is indicated for each frame. At t = 0.0, a continental collision is simulated at a convergent plate boundary (delineated by the light-shaded downwelling in frame a) by introducing the plate geometry (shown in black and gray in the upper left) on top of a temperature field obtained from a model incorporating a pair of symmetric plates. As a result of this collision, the mantle flow reorganizes. However, in contrast to models that do not include oceanic plates, the hottest regions of the mantle (indicated by the dark isosurface) persist below the large oceanic plates.

can be handled flexibly for both temperature- and stress-dependent rheologies. We have used such methods to synthetically image convection models, performing perhaps the most realistic tests of resolution of global seismic imaging to date. The plate-constrained mantle convection models reproduce well many of the features found by seismic tomography, including pronounced high-velocity structures beneath old subduction zones and the large-scale structures of slow and fast anomalies near the core-mantle boundary (see second figure).

In geodynamo simulations, a nonuniform pattern of heat flux imposed over the core-mantle boundary can significantly affect properties of Earth's magnetic field. When the pattern of core heat flux is antisymmetric about the equator, varies significantly in longitude, or has a minimum in polar regions, polarity intervals will be shorter and reversal durations will be longer. Between reversals, the average magnetic-field intensity will be smaller and secular variation will be larger than average.

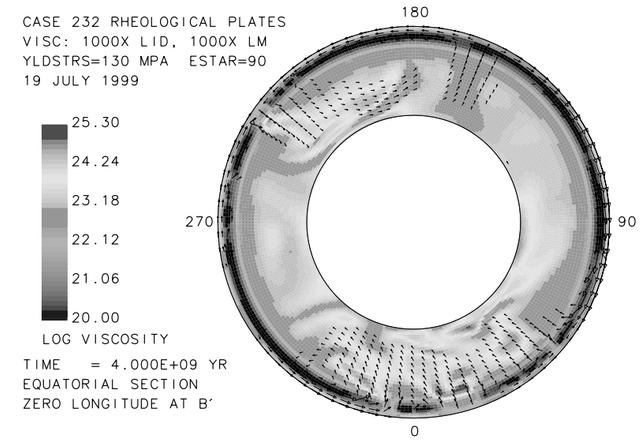

Cross section through the equatorial plane of the TERRA mantle convection calculation showing viscosity in gray scale and transverse velocity with arrows. The viscosity varies throughout the mantle by a factor of 200,000. The surface velocity has platelike coherence over notable angular distances.

Publications

Bunge, H.-P., et al., "Time Scales and Heterogeneous Structure in Geodynamic Earth Models," *Science* **280**, 91 (1998).

Christensen, U., et al., "Numerical Modeling of the Geodynamo: A Systematic Parameter Study," *Geophys. J. Int.* **138**, 393 (1999).

Glatzmaier, G.A., and P.H. Roberts, "Dynamo Theory Then and Now," *Int. J. Engr. Sci.* **36**, 1325 (1998).

Hongre, L., et al., "An Analysis of the Geomagnetic Field Over the Past 2,000 Years," *Phys. Earth Planet. Inter*. **106**, 311 (1998).

Liddicoat, J.C., et al., "Record of the Younger Part of the Pringle Falls Excursion at Long Valley, California," *Geophys. J. Int*. **135**, 663 (1998).

Lowman, J.P., and G.T. Jarvis, "Effects of Mantle Heat Source Distribution on Continental Stability," *J. Geophys. Res.* **104**, 12,733 (1999).

Olson, P., et al., "Numerical Modeling of the Geodynamo: Mechanisms of Field Generation and Equilibration," *J. Geophys. Res*. **104**, 10,383 (1999).

Thompson, P.F., and P.J. Tackley, "Generation of Mega-Plumes from the Core-Mantle Boundary in a Compressible Mantle with Temperature-Dependent Viscosity," *Geophys. Res. Lett.* **25**, 1999 (1998).

van Keken, P.E., and C.J. Ballentine, "Dynamical Models of Mantle Volatile Evolution and the Role of Phase Transitions and Temperature-Dependent Rheology," *J. Geophys. Res.* **104**, 7137 (1999).

van Keken, P.E., and C.J. Ballentine, "Whole-Mantle Versus Layered Mantle Convection and the Role of a High-Viscosity Lower Mantle in Terrestrial Volatile Evolution," *Earth Planet. Sci. Lett.* **156**, 19 (1998).

Zhu, R.X., et al., "Sedimentary Records of Two Geomagnetic Excursions Within the Last 15,000 Years in Beijing, China," *J. Geophys. Res*. **103**, 30,323 (1998).

Space Science and Exploration

99511

David J. McComas

The main goal for this project is to develop Los Alamos techniques, instruments, and ideas sufficiently enough that they can be successfully presented to NASA for space science and exploration missions. This project is intentionally broad based, aimed at exploiting the best opportunities from a wide range of scientific fields.

We are integrating innovative research from five broad scientific and technical areas spanning expertise from across the Laboratory. These areas are space physics and astrophysics, planetary science and resource utilization, astrobiology and biological effects, space nuclear power and propulsion, and space materials and structures.

A partial list of accomplishments this year includes: (1) positive identification of DNA via fluorescent staining in 3-Myr-old mineralized rocks; (2) production of water from iron titanate, a Martian surrogate material that we screened in a hydrogen plasma fluidized bed; (3) production of the first image of fossilized bacteria using atomic force microscopy (first figure); (4) demonstration and testing of a new technique for fabricating reactor heat pipes (second figure); (5) characterization of a beryllium-aluminum alloy, which permits the comparison of multiple properties such as strength/weight ratios against other materials for use on space structures (third figure); (6) experiments that show that enhanced measurement of solar-wind ion mass can be obtained using a surface reflection technique; and (7) characterization of the feasibility of using a pulsed, frequency-doubled laser to acquire both laser-induced breakdown spectroscopy (LIBS) and Raman signals on relevant mineral samples from a single instrument. This success is a major breakthrough because by combining the elemental data from LIBS and laser-induced mass spectrometry (LIMS) measurements with the Raman data, a complete geochemical/mineralogical analysis system can be developed.

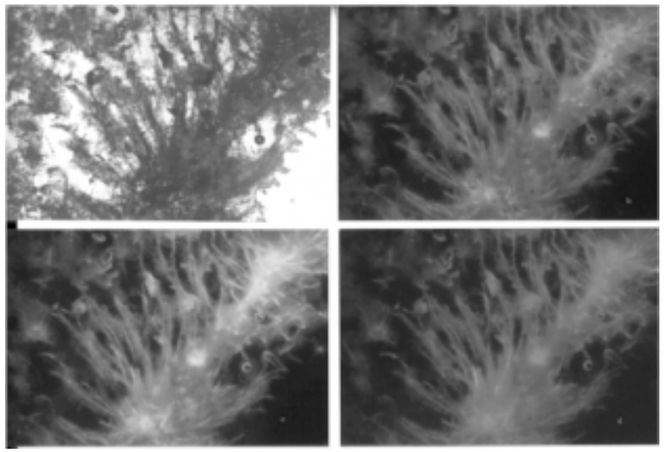

The fluorescent signatures of fossilized biological materials on Earth, which can help us look for similar structures elsewhere in our solar system.

In addition, our "CHEMIN" x-ray diffraction/x-ray fluorescence instrument received an R&D 100 Award, and our LIMS project was accepted by NASA as part of the Planetary Instrument Definition and Development program.

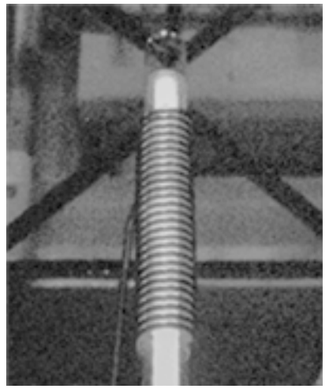

A heat pipe under development for the heat-pipe power system, which is a fission power source intended to provide electricity for deep-space and manned missions.

Publications

Burde, S., et al., "Fluorescent Staining of Microfossils Using Biological Stains," in *Lunar and Planetary Science XXX*, Abstract No. 1811, CD-ROM (Lunar and Planetary Institute, Houston, 1999).

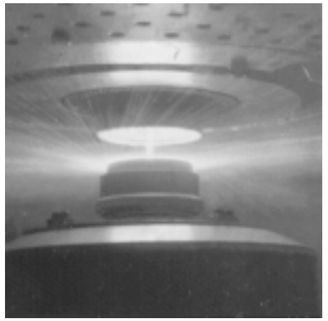

A beryllium-aluminum alloy plasma being converted to a powder via centrifugal atomization. The high strength-to-weight ratio of such advanced materials makes them ideal candidates for space structures.

Currier, R.P., et al., "Hydrogen Plasma Reduction of Planetary Materials" (In-Situ Resource Utilization Technical Interchange Meeting, Houston, February 1999).

Funsten, H.O., et al., "Electronic and Nuclear Stopping of 1-60 keV Ions in Silicon" (Materials Research Society Meeting, Boston, November 1999).

Houts, M.G., et al., "Planetary Surface Reactor Shielding Using Indigenous Materials," in *Space Technology and Applications International Forum—1999, Part 2* (American Institute of Physics, Woodbury, NY, 1999), p. 1476.

Ritzau, S.M., et al., "Damage Induced in Silicon by keV Ions" (Materials Research Society Meeting, Boston, November 1999).

Vaniman, D.T., et al., "Process Monitoring and Control with Chemin, a Miniaturized CCD (Charge Coupled Device)-Based Instrument for Simultaneous XRD (X-Ray Diffraction)/XRF (X-Ray Fluorescence) Analysis," in *Proceedings of the SPIE—The International Society for Optical Engineering*, Vol. 3769 (SPIE, Bellingham, WA, 1999), p. 243.

Coupled Environmental Modeling

98604

C. L. Winter

Coupled systems consist of discrete physical domains (for example, the atmosphere and the land surface) that interact nonlinearly and operate at different time and space scales. The study of coupled systems is leading to a new generation of modeling tools that can be used to predict environmental phenomena. This project has contributed to the visibility of nonweapons research, high-performance computing, and computer simulation in two application areas—prediction of wildfire behavior and prediction of consequences of variations in regional water cycles—that are immediate national and regional needs.

Our project investigates approaches to software integration that link separate codes efficiently without requiring extensive knowledge of the internal structure of the codes. Process codes are treated as internally coherent threads that are loosely coupled by passing objects, such as meshes, through messages. Coupled environmental models also integrate theory and computational science with experimental science and observation by requiring maintenance of large sets of diverse data for simulation, model testing, and validation. In some cases new data must be derived or inferred from other data and must also be assimilated occasionally in existing models. This project is relevant to crisis management and environmental security, as well as to the development of new, integrated approaches to solving basic problems of environmental science and decision making.

Our basic goal is to develop the physical and computational science needed to couple environmental processes that operate at different space and time scales. Our models avoid ad hoc parameterizations and model simplifications by writing interdomain exchanges of mass and energy at fine scales, in which we are confident that the physics of each process is accurately represented. We then up-scale systematically through averaging techniques and sensitivity analysis.

Publications

Bossert, J.E., et al., "A Coupled Modeling System to Simulate Water Resources in the Rio Grande Basin," in Preprints of the 14th Hydrology Conference, AMS 79th Annual Meeting (Dallas, TX, January 10–15, 1999), p. 83.

Brualdi, R.A., and J.G. Sanderson, "Nested Species Subsets, Gaps, and Discrepancies," *Oecologia* 119:256.

Campbell, K., "Linking Meso-Scale and Micro-Scale Models: Statistical Disaggregation Methods," in *1999 Proceedings of the Section on Statistics and the Environment* (American Statistical Association, in press).

Costigan, K.R., et al., "Atmospheric/Hydrologic Models for the Rio Grande Basin: Simulations of Precipitation Variability" (to be published in *Global and Planetary Change*).

Costigan, K.R., et al., "Evaluation of Precipitation Predictions in a

Regional Climate Simulation," in Preprints of the 14th Hydrology Conference (American Meteorological Society 79th Annual Meeting, Dallas, TX, 1999), p. 90.

Linn, R.R., and F.H. Harlow, "Transport Model for Wildfire Propagation" (submitted to the *Inter. J. Wildland Fire*).

Martens, S.N., et al., "Spatial Distributions of Understory Light along the Grassland/Forest Continuum: Effects of Cover, Height, and Spatial Pattern of Tree Canopies" (to be published in *Ecological Modeling*).

Moulton, P.A., and J.G. Sanderson, "Fate of Passeriform Introductions on Oceanic Islands," *Conservation Biology* **13**(4), 1 (1999).

Sanderson, J.G., et al., "Null Matrices and the Analysis of Species Co-Occurrences," *Oecologia* **116**.

Springer, E.P., et al., "Water Resources Simulation in the Rio Grande Basin Using Coupled Models" (26th Annual Water Resources Planning and Management Conference, American Society Civil Engineers, Tempe, AZ, June 6–9, 1999).

Tartakovsky, D.M., and C.L. Winter, "Groundwater Flow in Composite Aquifers under Uncertainty," in *Proceedings of the International Conference "Calibration and Reliability in Groundwater Modeling"* (ModelCARE'99, Zurich, Switzerland, 1999).

Tartakovsky, D.M., and I. Mitkov, "Some Aspects of Head-Variance Evaluation," *Comput. Geosciences* **3**(1), 89 (1999).

Tartakovsky, D.M., and S.P. Neuman, correction to "Transient Flow in Bounded Randomly Heterogeneous Domains, 1. Exact Conditional Moment Equations and Recursive Approximations," by D.M. Tartakovsky and S.P. Neuman, *Water Resour. Res.* **35**(6), 1947 (1999).

Tartakovsky, D.M., and S.P. Neuman, extension of "Transient Flow in Bounded Randomly Heterogeneous Domains, 1. Exact Conditional Moment Equations and Recursive Approximations," *Water Resour. Res.* **35**(6), 1921 (1999).

Tartakovsky, D.M., et al., "Conditional Stochastic Averaging of Steady State Unsaturated Flow by Means of Kirchhoff Transformation," *Water Resour. Res*. **35**(3), 731 (1999).

Tartakovsky, D.M., et al., "Effective Hydraulic Conductivity and Transmissivity for Heterogeneous Aquifers" (to be published in *Math. Geology*).

Zhang, D., and C.L. Winter, "Moment-Equation Approach to Single Phase Fluid Flow in Heterogeneous Reservoirs," *Soc. Petroleum Eng. J*. **4**(2), (1999).

Low-Luminosity Compact Stellar Objects and the Size of the Universe

97811

Richard Epstein

Our goal is to elucidate the nature of high-energy astrophysical systems using experimental and theoretical techniques. Our experimental efforts focused on developing the Milagro gamma-ray observatory. This will be the first facility capable of observing teraelectronvolt radiation from sources over much of the sky, a revolutionary advance in high-energy astrophysics. Our theoretical work was directed at modeling phenomena on compact stars, galactic systems, solar neutrino production, and the overall universe. This work included investigating explosive events on the surface of neutron stars, the regular and chaotic orbits of stars in galactic potentials, and fluctuations in the cosmic microwave background.

With the Milagro observatory we recorded over 9 billion events and honed the computer algorithms to reconstruct the energy and arrival directions of the gamma rays. To calibrate the instrument, we analyzed the image of the Moon. The Moon is not a source of gamma rays and appears as a deficit in the distribution of events from the isotropic flux of cosmic rays. Other data show that Markarian 501, an active galaxy, is a source of teraelectronvolt gamma rays. To study stellar orbits in galactic potentials, we have created a parallel particle-mesh code, and we have developed a numerical solver for the Landau/Fokker-Planck equation. We are now in a position to solve for stellar orbits and accurately compute damping and diffusion coefficients. We have examined whether convective mixing in the Sun's core can explain the so-called "solar neutrino problem": a deficiency of observed neutrinos compared to the predictions of "standard" solar-models. Our preliminary calculations showed that using acceptable values of the stellar opacity and convective mixing length, we could obtain reasonable agreement with both the observed neutrino flux and the observed helioseismic frequencies. We found that the variations in the spin rates of the Crab pulsar and some other neutron stars may indicate the occurrence of "starquakes." As the star spin rate steadily decreases as a result of magnetic braking, the star's equatorial circumference decreases, straining the crust and causing it to crack. We found that these starquakes can suddenly move matter toward the magnetic poles thereby changing the star's symmetry (see figure). The resulting changes in the star's spin rate are clearly discernable in the existing timing data.

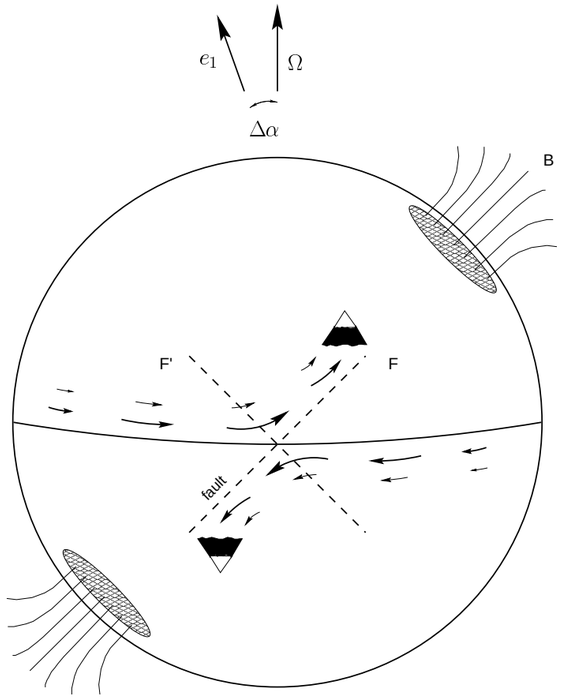

A neutron star with a slowing spin rate W tends to crack along faults *F* or *F´*. The inclusion of the effects of magnetic stresses shows that faults such as *F* that move matter toward the magnetic poles occur preferentially. The accumulated matter, shown as snow-capped peaks (though they are only a few millimeters high), shift the principal axis of inertia by an angle Da.

Publications

Antoniadis, I., et al., "Fractal Geometry of Quantum Spacetime at Large Scales," *Phys. Lett.*, **B444**, 284 (1998).

Blasi, P., et al., "Ultra-High Energy Cosmic Rays from Young Neutron Star Winds"(to be published in *Astrophysical J. Lett.*)

Edwards, B.C., et al., "Demonstration of a Solid-State Optical Cooler: An Approach to Cryogenic Refrigeration," *J. Appl. Phys*. **86**, 6489 (1999).

Franco, L.M., et al., "Quaking Neutron Stars and the Observable Consequences" (to be published in *Astrophysical J.*).

Hoffman, C.M., et al., "Gamma-Ray Astronomy at High Energies," *Rev. Mod. Phys.* **71**, 897 (1999).

Lei, G., et al., "Spectroscopic Evaluation of Yb^{3+}-Doped Glasses for Optical Refrigeration," *IEEE J. Quantum Electron.* **34**, 1839 (1998).

Lei, G., et al., "Spectroscopic Properties of Yb^{3+}-Doped Glasses Important for Optical Refrigeration" *OSA: Trends in Optics and Photonics Series* **19**, *Advanced Solid State Lasers* (1999).

Link, B., et al. "Pulsar Constraints on Neutron Star Structure and Equation of State," *Phys. Rev. Lett.* **83**, 3362 (1999).

Link, B., et al., "Starquake-Induced Magnetic Field and Torque Evolution in Neutron Stars," *Astrophys. J*. **508**, 838 (1998).

Murtagh, M.T., "Compositional Investigation of Yb^{3+}-Doped Heavy Metal Fluoride Glasses for Laser-Induced Fluorescent Cooling Applications," *J. Noncrystalline Solids* **257**, 207 (1999).

Olinto, A.V., et al., "Galactic Ultra-High-Energy Cosmic Rays" in *Proceedings of 26th International Cosmic Ray Conference* (Salt Lake City, UT, September 1999).

J. Qiang, et al., "A Second-Order Stochastic Leap-Frog Algorithm for Multiplicative Noise" (submitted to *Phys. Rev. E*).

Earth Materials and Earth Dynamics

97814

Kristin Bennett

In this project we link experimental, theoretical, and computational research to reveal properties and processes within the earth and events in its history.

This year we furthered our goal to better characterize, through a broadly based, interdisciplinary approach, the current state of the earth and the processes by which it is formed and modified. We used a combination of techniques including numerical modeling, high-precision mass spectrometry, transient optical grating and conventional geochemistry (including electron microprobe, x-ray fluorescence, scanning electron microscope, and ion probe), and resonant ultrasound spectroscopy (RUS) seismic techniques. In addition, this year we used another powerful technique new to the focus, neutron diffraction, at the Los Alamos Neutron Scattering Center (LANSCE) to investigate texture development during deformation and phase transformation of olivine analogs. The strength of this project is the integration of techniques to address specific problems.

Our goals were to quantitatively understand the effects of coupling thermal, chemical, and mechanical processes active during the evolution of hydrothermal fluid-rock systems and how this coupling affects the system's dynamics, resultant mineralogy, and chemistry; how variations in the fluid phase alter the system's behavior; and how these effects would be manifested in the rock record. We achieved these goals primarily by numerical modeling using a computer code, MOR3D, coupled with field and laboratory investigations of fluid infiltrated rocks. Because macroscopic earth materials are highly inhomogeneous, we are exploring the effects of inhomogeneity on the variationally calculated resonances in the RUS technique. We solved a sequence of one-dimensional problems that illustrates the principles involved in implementing the variational technique for inhomogeneous materials. The measured resonance frequencies are the input to an iterative inversion algorithm that finds the best match between the data and a set of resonances generated from a model. RUS has been used successfully to determine the elastic properties of single crystals of minerals found in the earth's mantle. We are extending the applicability of RUS to macroscopic samples of rock.

We also merged technologies of high pressure with temperature research with neutron diffraction and with nonlinear time-resolved spectroscopy to elucidate equations of state and dynamic relaxation mechanisms in earth and planetary systems. At LANSCE and the University of California, Riverside, we used a combination of high-pressure experimental deformation and neutron diffraction techniques to investigate lattice-preferred orientation (texture) in a, b, g olivine analogs during deformation and phase transformation for interpreting observed seismic low-velocity zones at 540- and 670-km depth in the upper mantle (see figure).

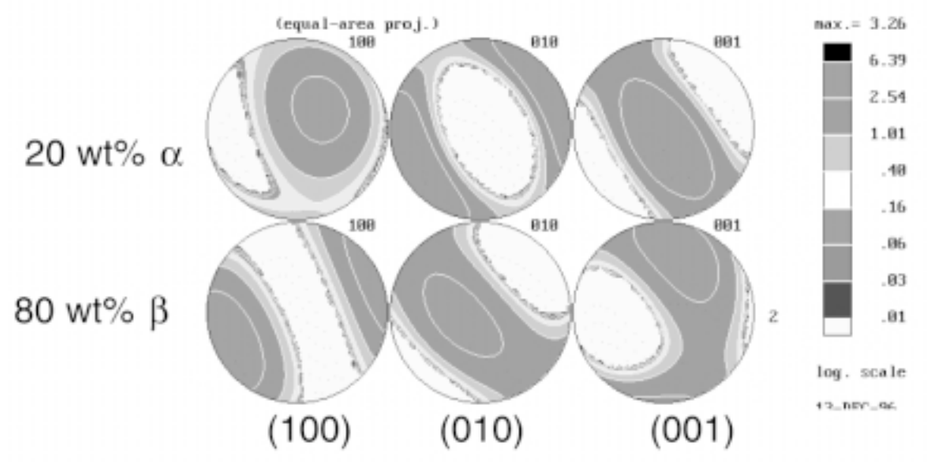

Pole figures (100), (010), and (001) in experimentally deformed a, b, g Mn_2GeO_4 olivine measured by neutron diffraction at Los Alamos Neutron Scattering Center. The pole figures are in equal area projection and the direction of stress is in the center of the figure. We measured 20% in a phase and 80% in b phase in the sample. The phase change from a-b Mn_2GeO_4 is a directional process. Those a grains with (010) orientations transform first. There is an orientation relationship between a-olivine a-axes and b-phase b-axes.

We performed transient grating measurements on fluids under simultaneous high-temperature and high-pressure conditions to probe the equation of state of fluids and solids relevant to planetary interiors of some of the giant planets and icy satellites. Experiment measurements of acoustic dynamics were used to determine elastic constants and the equation of state of fluid ammonia methane and water systems.

Publications

Baer, B.J., et al., "Picosecond Photon Echo and Coherent Raman Studies of Vibrational Dynamics in Molecular Solids under Pressure," in *High Pressure Science and Technology 1999 (*Proceedings of AIRAPT-17, July 1999).

Bennett, K., et al., "HIPPO, A New High Intensity Neutron Diffractometer for Characterization of Bulk Materials*" Proceedings of the Twelfth International Conference on Textures of Materials* (NRC Research Press, Montreal, Canada, 1999), **1**, p. 129.

Dutrow, B.L., and D.J. Henry, "Complexly Zoned Fibrous Tourmaline: A Record of Evolving Magmatic and Hydrothermal Fluids" (to be published in *Can. Mineralogist*).

Dutrow, B.L., et al., "Tourmaline-rich Pseudomorphs after Staurolite: Demarcation of an Infiltration Front," *Am. Mineralogist* **84**, 794 (1999).

Guyer, R.A., and P.A. Johnson, "The Astonishing Case of Mesoscopic Elastic Nonlinearity," *Phys. Today **52***, 30 (1999).

Guyer, R.A., and K.R. McCall, "A Lattice Boltzmann Description of Magnetization in Porous Media" (submitted to *Phys. Rev. B.*).

Guyer, R.A., et al., "Hysteresis and the Dynamic Elasticity of Consolidated Granular Materials," *Phys. Rev. Lett.* **82**, 3280 (1999).

TenCate, J., et al., "Universal Slow Dynamics in Granular Solids" (submitted to *Phys. Rev. Lett.*).

Ulrich, T.J., et al., "Determination of Elastic Moduli of Rock Samples Using Resonant Ultrasound Spectroscopy" (submitted to *J. Acoustical Soc. Am.*).

Zhao, L., et al., "Surface Acoustic Wave Studies of Aluminum (111) and Nickel (100) Surfaces by Impulsive Scattering" (submitted to *J. Chem. Phys.*).

Integrated Remote Sensing Science

99501

Sig Gerstl

The primary objective of the Integrated Remote Sensing Science (RSS) project is to build a Laboratory competency in remote sensing science by performing fundamental science tasks that establish new science capabilities and stretch existing ones. These capabilities will serve as a basis for nonproliferation and environmental/earth remote sensing sciences. The scope of the research encompasses three technical areas: hyperspectral remote sensing, active remote sensing (LIDAR: LIght Detection And Ranging), and new remote sensing concepts.

RSS focuses on detecting gaseous plumes, understanding the atmospheric boundary layer, and developing new tools and techniques for remote sensing. These tasks correlate well with capabilities that we will need for future applications to nuclear, biological, and chemical weapon nonproliferation and to environmental and earth sciences.

We developed (1) technologies to remotely probe natural and man-made chemical plumes and (2) instrumental and computational tools to characterize vegetation and/or atmospheric boundary layer processes, including clouds. We supported five tasks: Raman Lidar, Fourier transform infrared (FTIR) spectrometry, imaging spatial heterodyne spectrometry (ISHS), wide-angle imaging lidar (WAIL), and the multidirectional imaging spectro-radiometer (MISR) and Triana satellite concepts.

Publications

Cooke, B.J., et al., "Analysis and System Design Framework for Infrared Spatial Heterodyne Spectrometers" (to be published in *Proceedings of the International Society for Optical Engineering*).

Cooper, D.I., et al., "Spatial and Temporal Properties of Water Vapour and Flux over a Riparian Canopy" (to be published in *J. Agri. Forest Meteorol.*).

Davis, A.B., "Physical Thickness and Optical Depth of Stratocumulus from Space-Borne Lidar, A Moment-Based Diffusion Method," in *Technical Digest of OSA Topical Meeting on Optical Remote Sensing of the Atmosphere* (Optical Society of America, Washington, DC, 1999), p. 66.

Davis, A.B., and B.W. Smith, "Solar Photon Pathlength Diagnostics from Weak Oxygen Line Profiles, A Challenge for Fourier Transform

Spectroscopy," in *Technical Digest of OSA Topical Meeting on Fourier Transform Spectroscopy: New Methods and Applications* (Optical Society of America, Washington, DC, 1999), p. 186.

Davis, A.B., et al., "Cloud Lidar in the Diffusion Limit, from Inception to 'First Light'" (to be published in *Proceedings of 10th International Workshop on MUltiple SCattering in Lidar Experiments*, MUSCLE 10).

Davis, A.B., et al., "The Lévy-Flight Model for Solar Photon Transport in the Cloudy Atmosphere: Observational Support from High-Resolution Oxygen A-Band Spectroscopy," in *Proceedings of 10th AMS Conference on Atmospheric Radiation* (Am. Met. Soc. Boston, MA, 1999), p. 575.

Davis, A.B., et al., "Off-Beam Lidar: An Emerging Technique in Cloud Remote Sensing Based on Radiative Green-Function Theory in the Diffusion Domain," *Phys. Chem. Earth (B)*, **24**, 757 (1999).

Eichinger, W.E., et al., "Estimation of Spatially Distributed Latent Energy Flux over Complex Terrain from a Raman Lidar" (to be published in *J. Agri. Forest Meteorol.*).

Fuehrer, P.L., et al., "A Statistical-Uncertainty-Based Adaptive Filter for Lidar Signals" (to be published in *J. Appl. Opt.*).

Gerstl, S.A.W., and F.P.J. Valero, "The Triana Satellite Mission from L-1 for Global Vegetation Monitoring," *IEEE IGARSS'99 Proc.* **1**, 14 (1999).

Gerstl, S.A.W., et al., "Angular Signature Retrieval and Comparison with Spectral Signatures from AirMISR Data," *IEEE IGARSS'99 Proc.* **1**, 404 (1999).

Kao, C.-Y. J., and W.S. Smith, "Sensitivity of a Cloud Parameterization Package in the NCAR CCM," *J. Geophys. Res.* **104**, 11961 (1999).

Kao, C.-Y.J., et al., "High Resolution Modeling of Lidar Data: Mechanisms Governing Surface Water Vapor during SALSA" (to be published in *J. Agri. Forest Meteorol.*).

Kao, C.-Y.J., et al., "Test of the Volume-of-Fluid Method on Marine Boundary Layer Clouds" (to be published in *Mon. Wea. Rev.*).

Laubscher, B.E., et al., "The Infrared Imaging Spatial Heterodyne Spectrometer (IRISHS) Experiment Effort" (to be published in *Proceedings of the International Society for Optical Engineering*).

Milligan, S., et al., "Optical Design of an Imaging Spatial Heterodyne Spectrometer," in *Proceedings of the International Society for Optical Engineering* **3698** (Optical Society of America, Washington, DC, 1999), p. 869.

Qin W., et al., "Use of Multiple Scattering Fractions to Estimate Leaf Area Index of Grass Canopies," *IEEE IGARSS'99 Proc.* **1**, 404 (1999).

Shao, X.M., et al., "Observations of Precipitable Water Vapor Fluctuations in Convective Boundary Layer via Microwave Interferometry," *J. Geophys. Res.* **104**, 16729 (1999).

Smith, B.W., and J.M. Harlander, "Imaging Spatial Heterodyne Spectroscopy: Theory and Practice," in *Proceedings of the International Society for Optical Engineering* **3698** (Optical Society of America, Washington, DC, 1999), p. 925.

Smith, B.W., et al., "IRISHS, The Infrared Imaging Spatial Heterodyne Spectrometer: A New Pushbroom Fourier Transform Ultraspectral Imager with No Moving Parts," *Proceedings of the International Society for Optical Engineering* **3698** (Optical Society of America, Washington, DC, 1999), p. 501.

Nuclear and Particle Physics

Nonequilibrium Science: Assessment, Control, and Prediction

98605

Emil Mottola

The next frontier of multiscale science lies in controlling and predicting the statistical properties of the fluctuations intrinsic to complex nonequilibrium systems. We need this capability to go beyond phenomenology and pass information systematically between scales, to assess macroscopic uncertainties, and to develop numerical algorithms to extend the predictive reach of the modeling over the largest dynamic ranges and to the longest time scales. Our strategy is as follows: (1) develop the microscopic theory and the corresponding numerical methods at the finest spatio-temporal scales; (2) identify coherent structures, significant variables, and the spectrum of fluctuations to apply coarse graining techniques in space and time; (3) develop numerical methods to solve the resulting mesoscale stochastic partial differential equations; (4) compare the mesoscale models with microtheory and validate with experimental data; and (5) iterate this procedure to macroscopic length and time scales. Specific applications include shock-induced phase transitions, phase transitions in nuclear matter, and dynamics of topological excitations.

We have developed a new Landau theory for shock-induced phase transitions in iron using the specific volume as the order parameter. The Fokker-Planck equation describing the evolution of the order parameter in thin slabs of the shocked material can be coupled to codes that solve for the macroscopic evolution. We have also developed a theory that includes microscopic inhomogeneities by applying the Lindgard-Mouritsen model to shock-induced transitions for body-centered cubic (bcc) to hexagonal close-packed (hcp) materials. The coupling of Landau-Ginzburg models to macroscale codes, such as finite element, is being investigated. We are developing a symmetry-based density functional formalism as a general formalism to describe structural phase transitions and their dynamics; we have also developed a new error control and error improvement strategy for one-dimensional stochastic partial differential equations.

Publications

Bettencourt, L.M.A., et al., "Controlling One-Dimensional Langevin Dynamics on the Lattice" (to be published in *Phys. Rev. D*).

Chodos, A., et al., "Cooper Pairing at Large N in a 2-Dimensional Model," *Phys. Lett. B* **449**, 260 (1999).

Habib, S., and G.D. Lythe, "Dynamics of Kinks: Nucleation, Diffusion, and Annihilation" (submitted to *Phys. Rev. Lett.*)

Sasik, R., et al., "Thermal Vortex Motion in a Two-Dimensional Condensate" (submitted to *Phys. Rev. Lett.*).

Saxena, A., et al., "Hierarchical Microstructure in Structural Phase Transitions," *Phase Transitions* **67**, 481 (1998).

Shenoy, S.R., et al., "Martensitic Textures: Multiscale Consequences of Elastic Compatibility" (submitted to *Phys. Rev. B*).

Ultracold Neutron Science

98606

Susan J. Seestrom

Fundamental physics that can be performed using with ultracold neutrons (UCNs) includes determination of neutron lifetime and decay parameters that can provide sensitive tests of the standard model of electroweak interactions. We used an existing UCN rotor source as a test bed for developing techniques needed to carry out a UCN research program while simultaneously developing advanced UCN source concepts that concentrated on cryogenic deuterium as the UCN converter.

This year to increase speed, we rewrote the computer codes used to calculate UCN production from cryogenic moderators. This allowed us to expand the code to include calculation of UCN transport out of the source through guides, varying the surface finish on the guide. We also expanded the model to include cold-neutron production by spallation and moderation, including the development of new scattering kernels for the Monte Carlo neutron physics code.

We built and tested a prototype spallation UCN source in which the 800-MeV beam from the Los Alamos Neutron Science Center (LANSCE) accelerator is directed onto a spallation target for about two seconds. The spallation neutrons are moderated in a cold (5 K) polyethylene moderator surrounded by a beryllium reflector at liquid nitrogen temperature. Within the cold polyethylene moderator is a solid deuterium converter (up to 1 liter in volume) held at 5 K. The solid deuterium moderator is connected at the top to a UCN guide tube leading to a UCN storage bottle or detector. While the proton beam strikes the spallation target, an intense pulse of UCN is created and diffuses out of the solid deuterium moderator.

We modified our spallation UCN source (see the first figure) several times to increase the number of UCNs detected. Most recently, because the solid deuterium was not being uniformly cooled, we identified and tested a technique that provided more-uniform cooling to the deuterium. Even with more-uniform cooling, the rate of UCNs produced does not depend strongly on deuterium temperature; this points to a UCN loss mechanism in the deuterium, with a temperature dependence that counteracts the temperature dependence of the upscattering caused by phonons in the deuterium. We also found that the UCN production rate does not scale with deuterium volume as expected. We plotted the number of observed UCNs divided by the deuterium volume (see the second figure). If the deuterium were transparent to UCNs, this would be a constant; in contrast, we find that the UCN density falls more rapidly than expected with deuterium density (plotted as a line for a mean free path of 8 cm).

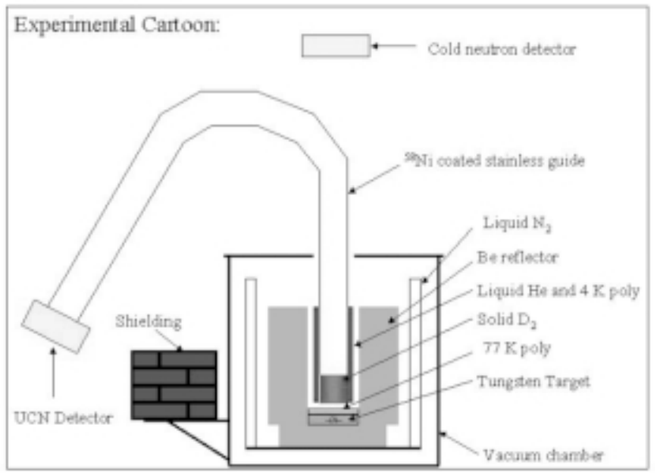

Schematic layout of our prototype UCN spallation source.

Publication

Anaya, J.M., et al., "Performance of the Prototype LANL Solid Deuterium Ultra-Cold Neutron Source" (to be published in *Nucl. Instrum. Methods*).

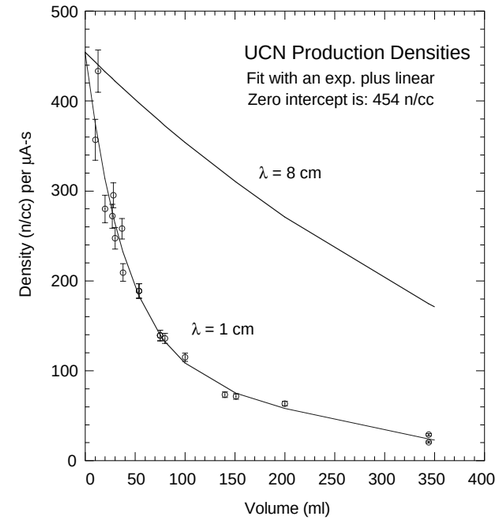

Plot of the number of UCNs detected divided by the of volume of solid deuterium in the test system. The density falls off at a small volume (~ 100 cc), indicating that UCNs are being collected from only a small thickness of the deuterium.

Neutrino Physics Experiments

99514

William Louis

The goal of our project is to explore some advanced technology areas that might significantly enhance or broaden the performance of the Booster Neutrino Experiment (BooNE) at Fermilab and the Sudbury Solar Neutrino Observatory (SNO) in Canada. BooNE and SNO are well poised to resolve the anomalies seen by the Liquid Scintillator Neutrino Detector (LSND) experiment and by solar neutrino experiments and to make precision measurements of the neutrino oscillation parameters involving neutrino masses and mixing angles. Our explorations may well provide answers to some of the most basic questions in fundamental physics that remain to our understanding of the universe, such as the contribution of neutrinos to the mass of the universe and the production of heavy elements in supernova bursts.

On BooNE, new approaches to event reconstruction and background rejection have resulted in improved efficiency in reconstructing events. We have also simplified the design for mounting detector and veto phototubes in the detector tank. Now we will mount the detector phototubes on an opaque barrier that separates the veto region from the detector region and mount the veto phototubes on the tank walls. We have also begun development of electronics and data acquisition systems that will improve the operation of the detector. These systems include a new front-end electronics design that could determine the time of all photoelectrons (not just the first photoelectron); a new trigger electronics system that is faster than the trigger used in the LSND experiment; and a new scheme for performing data acquisition that will involve an array of PCs running LINUX instead of a single multiprocessor computer. Finally, we have computed neutrino cross sections within a large-basis shell-model framework.

On SNO, most of our effort has gone into developing techniques that will better determine the ratio of neutral-current (NC) to charged-current (CC) neutrino scattering processes, which should provide direct evidence as to whether neutrino oscillations are occurring. We have begun developing the analysis tools necessary to characterize the various backgrounds that affect the NC/CC ratio. We have also begun comparing the ability to extract the NC/CC ratio for the pure D_2O, MgCl, and helium-3 array running conditions. Lastly, we have initiated development of the optimal use of sources to better understand the radioactivity background.

Enabling R&D for Future Proton Applications

99520

Henry A. Thiessen

This project involved developing a proton radiography facility plan using a synchrotron to accelerate protons to produce high-quality images of dynamically imploding objects. High-quality motion pictures of a simulated weapon could then be used as a diagnostic for the nuclear stockpile in the absence of actual testing

Efforts in this project focused innovative technological research on four distinct technical areas: (1) advanced containment/confinement concepts; (2) large-aperture superconducting quadrupoles (components of a lens for imaging the protons); (3) accelerator and beam-delivery system concepts at the Los Alamos Neutron Science Center (LANSCE); and (4) magnetic-field measurements.

We have developed concepts for nearly windowless containment/confinement of an explosion that maximize resolution and minimize multiple coulomb scattering by putting window material at the end of long beam tubes, and we have also tested some materials for low-Z windows.

We instituted a study of large-aperture (75-cm-diam) quadrupole design in collaboration with the MIT High-Field Magnet Laboratory, and we produced a cost estimate for a 75-cm-diam superconducting quadrupole in a contract with General Atomics. An experiment to measure the heat input to a superconducting coil is set up at Brookhaven National Laboratory to determine whether the heat is excessive to the point that the coil no longer functions as a superconductor.

We investigated and completed work on several accelerator and beam transport system concepts that were the starting point for a pre-conceptual design report that is now in preparation. In order to make any synchrotron perform as desired, it is necessary to understand the imperfections of the magnetic field. To this end, we have obtained and installed the necessary AC power supplies, refurbished the LANSCE magnet measuring laboratory, and are preparing measuring coils. Our plan is to measure one B1 dipole from Fermilab in Chicago, validate these data, and then turn the magnet measuring laboratory over to the proposed Advanced Hydrodynamics Facility Project for future use in measuring the fields of all of the magnets that will be used in the synchrotron.

Bioscience

Pathogen Detection in the Real World

99516

Babetta L. Marrone

There is a national need for improved strategies and technologies to counter the threat of biological terrorism. However, the lessons learned from battlefield preparedness do not directly transfer to domestic preparedness. The objective of this project is to develop a complete, potentially fieldable system for discriminating biological agents from environmental background. Such an enhanced capability will depend upon improved agent signal detection and understanding of the relevant backgrounds (noise) and their influence on bioagent detection. Our efforts this year focused on three main research areas: pathogen gene discovery, characterization of background environmental aerosols, and smart trigger development.

In the area of pathogen gene discovery, we established the first version of a toxin and virulence database, which assimilated molecular data from several organisms. Entries come from the literature and from experimental projects that involved generating DNA sequences of virulence and potential virulence genes from a variety of pathogens. We developed a new approach to pathogen gene discovery using a membrane microarray and tested it with predicted genes from *B. anthracis* PX01 and PX02. We made a new ligand for the receptor-binding domain of the anthrax protective antigen, preparing it with a biotin tag for testing in a detection scheme. We also tested alternative statistical models for the evolution of influenza. We found a five-parameter statistical model of the hemagglutinin gene sequences (called the Hasagewa model) to be the most accurate.

In the area of characterizing background environmental aerosol, we collected and are analyzing a voluminous amount of outdoor aerosol data, including data from a UV-fluorescence particle analyzer. We performed five campaigns to collect samples of indoor environmental aerosols for analysis. The analyses so far indicate a very low content of biological particles in the ambient aerosol.

In the smart trigger area, we developed and evaluated an improved air-to-air particle concentrator. This concentrator uses acoustic energy to concentrate biological particles for analysis or collection. The concentrator will be coupled to a commercial particle counter (MetOne) for testing. We built a prototype instrument for discriminating between different types of bio- and nonbioaerosol particles on the basis of scattered light by modifying a standard MetOne particle analyzer.

Publications

Burr, T., “Maximally Selected Measure of Space-Time Correlation” (to be published in *Stats. Med.*).

Burr, T., et al., “Confidence Measures for Evolutionary Trees: Applications to Molecular Epidemiology,” in *IEEE Intelligence in Neural and Biological Systems* (IEEE Computer Society, Los Alamitos, CA, 1999), p. 107.

Cirino, N., et al., “Disruption of Anthrax Toxin Binding with the Use of Human Antibodies and Competitive Inhibitors,” *Infect. Immun.* **67**, 2957 (1999).

Integrated Structural Biology Resource

97610

William Woodruff

The purpose of this project is to develop our capabilities in x-ray structure determination, nuclear magnetic resonance (NMR), small-angle scattering, optical spectroscopy, and theory. We envision a five-element Integrated Structural Biology Resource (ISBR) for targeting the structural biology of proteins and their biological functions.

The goals of the protein production and purification resource this year were to develop procedures for cloning, expressing, purifying, and crystallizing proteins on a large scale. The resource has successfully cloned over 150 genes from *Pyrobaculum aerophilum*, expressed 80 of these in *E. coli*, purified 27, and obtained crystals from 10. We can now standardize its protocols and implement a high-throughput protein-production facility.

Our use of x-ray crystallography to determine structure has resulted in major breakthroughs in the understanding ligand binding and catalysis. We determined the 1.4 A resolution crystal structure of a ligand-binding intermediate in carbonmonoxy myoglobin by cryo-crystallography. We saw that the pathway for carbon monoxide binding to the heme includes a stop in a hydrophobic pocket inside the protein next to the heme, revealing that cavities in myoglobin have a functional role in the kinetics of ligand binding and also in determining relative affinities of different molecules. With similar techniques, we observed the structure of an important intermediate in the protonmotive photocycle of bacteriorhodopsin for the first time.

We completed temperature-dependent studies of folding/unfolding in a thermophilic heat shock protein using small-angle scattering. These experiments required modifying the small-angle scattering instrumentation to provide increased capability for studying thermophilic proteins at their native temperatures and at room temperature. We performed scattering of mesophilic and thermophilic forms of an adenylate kinase to show the state of oligomerization of the different forms. The combined theoretical/experimental study of the highly heat stable thermophilic adenylate kinase provided experimental validation of a full solvent molecular dynamics simulation. It also gave us insights into the metal ion-binding-dependent conformational changes in that protein that reveal misleading effects of crystal-packing forces in these proteins.

This year we made a substantial effort to develop vibrational imaging capability for application to biological systems with both Raman and infrared (IR)-based imaging systems. We saw a significant improvement in our ability to enable efficient imaging of cells and tissues, and preliminary efforts to develop such protocols have begun. Using a tunable IR-diode laser as a source for imaging applications has recently been demonstrated elsewhere. The IR laser produces a high-intensity IR beam at a single wavelength, enabling rapid chemical image acquisition. We have purchased a new state-of-the-art imaging microscope and a 256- × 256-element mercury-cadmium-tellurite array detector. We are in the process of assembling this system and developing the appropriate software.

For the theory, modeling, and computation resource, we developed a Monte Carlo method for modeling large biomolecular complexes from low-resolution x-ray, small-angle scattering, fluorescent resonance energy transfer, chemical cross-linking, and site-directed mutagenesis data. This work has demonstrated the strength of combining different modeling methods for developing a high-resolution troponin I/troponin C model that is consistent with experimental observations. We modeled membrane channels and the nucleosome. Using our new theory for hydrophobic effects, we studied the relationships of pressure, ionic effects, chemical composition, and hydrogen/deuterium content in the solution to the strength of the hydrophobic effect. This work addresses the role of solvents in the configuration and flexibility of alpha helical packaging and will be relevant in determining helix packing in membrane channels. We also investigated the effect of solvation in the charging free energy of simple solutes to help us understand changes in protein amino acid residues.

Publications

Chu, K., et al., “Crystal Structure of Photorelaxed Horse-Heart Myoglobin CO Complex,” *Nature* **403**, 921 (2000).

Sass, H.J., et al., “The M Intermediate Structure of Wild-Type Bacteriorhodopsin at 2.2 A Resolution” (submitted to *Nature*).

Bioremediation Science to Meet National Challenges

99500

James Brainard

The remediation of contaminated aquifers is the most difficult of the cold war environmental legacies. Yet, in situ bioremediation offers the potential of solving this problem because of its ability to remediate dilute, diffuse, and inaccessible contaminants cost effectively. This project’s objective is to develop and apply capabilities in bioremediation science first by understanding and improving enzyme catalysis, gene expression, and microbe survival and then by using in situ bioremediation to meet regulations for contaminant destruction.

Our focus has been on understanding catalysis in two important classes of dehalogenases (the hydrolytic alkane dehalogenases and the reductive perchloroethylene [PCE] dehalogenase from Dehalospirillum multivorans) and on developing and applying molecular tools for assessing microbial community structure and dynamics.

This year we developed a hydrolytic dehalogenase assay based on rate of proton release and applied it to the kinetic analysis of the mechanistic similarities and differences in wild type and mutant hydrolytic dehalogenases. We determined a mechanism of halide inhibition in the *Xanthobacter* dehalogenase and identifed site-directed mutants of the *Xanthobacter* enzyme that are not inhibited by halide.

We identified mutants of the *Xanthobacter* enzyme with two-fold increase in k_{cat} and developed a bacterial selection and rapid in vivo screen for hydrolytic dehalogenases. We completed a spectroscopic study of the interaction of trans-DCE with cobalamin and demonstrated that an electron transfer proceeds the binding of the halocarbon to cobalamin.

In addition, we obtained a UV/vis spectra of the PCE dehalogenase from Dehalospirillium multivorans and demonstrated that the corrin is not in the base-off form. We obtained infrared spectroscopic studies of the D. multivorans PCE dehalogenase and obtained preliminary evidence for a conformational change upon binding of an alkane to the protein.

Other accomplishments include identification of new environmental isolates of DCA degrading species and dhlA genes, development and application of Terminal Restriction Fragment Analysis for community level complexity and dynamics in the environment, and application of a quantitative PCR to detect and track indigenous genes.

Publications

Chang, C.-H., et al., “*In vivo* Screening of Haloalkane Dehalogenase Mutants” (to be published in *Bioorg. Med. Chem.*).

Dunbar, J., et al., “Levels of Bacterial Community Diversity in Four Arid Soils Compared by Cultivation and 16S rRNAGene Cloning,” *Appl. Environ. Microbiol.* **65**, 1662 (1998).

Newman, J., et al., “Haloalkane Dehalogenases: Structure of a Rhodococcus Enzyme” (to be published in *Biochemistry*).

Pond, A.E., et al., “Assignment of the Heme Axial Ligand(s) for the Ferric Myoglobin (H93G) and Heme Oxygenase (H25A) Cavity Mutants as Oxygen Donors using Magnetic Circular Dichroism,” *Biochemistry* **38**, 7601 (1999).

Schindler, J.F., et al., “Haloalkane Dehalogenases: Steady-State Kinetics and Halide Inhibition,” *Biochemistry* **38**, 5772 (1999).

Functional Genomics

99518

Michael R. Altherr

This year we initiated a program in functional genomics to evaluate technologies likely to transition DNA sequence information into biologically relevant data without regard to species of origin. We define functional genomics as a collection of activities, procedures, and processes intended to rapidly produce information and resources for characterizing unknown genetic elements. Ultimately, the capabilities we are developing will support a variety of issues of national importance such as bioterrorism threat reduction and the cellular effects of low-dose ionizing radiation.

We are characterizing the coding component of the genome by implementing a strategy for high-throughput cDNA sequencing (see first figure). We identified a collection of cDNA clones localized to the Joint Genome Institute (JGI) target chromosomes and have initiated the complete sequencing of these clones. Several clones have been completed, and several dozen are now in progress. Approximately 1,750 cDNA sequences from IMAGE consortium clones corresponding to the three JGI target chromosomes are being sequenced and annotated with respect to the co-linear genomic sequence.

For global gene-expression analysis, we implemented the technology required to print and read cDNA microarrays using a nylon-based substrate and colorimetric detection (see second figure). Specifically, we have installed the robotics required to allow parallel printing of over 100 microarrays in a single run and used a high-resolution scanner for colorimetric array analysis. Both instruments have been used successfully with human and *Bacillus anthracis* arrays when interrogated by hybridization with appropriately labeled cDNA.

For protein analysis, we formed an alliance with the University of Texas to generate molecular recognition ligands via RNA aptamers. Our focus has been on the expression of a proposed functional homologue of human frataxin in *E. coli* to model a high-throughput protein expression system. We also evaluated a biochemical purification scheme to prepare proteins for analysis by mass spectrometry, a critical tool for analyzing the complete protein content of a cell. Finally, we used a proof-of-principle approach using stem cells to analyze hypothetical gene functions in vivo.

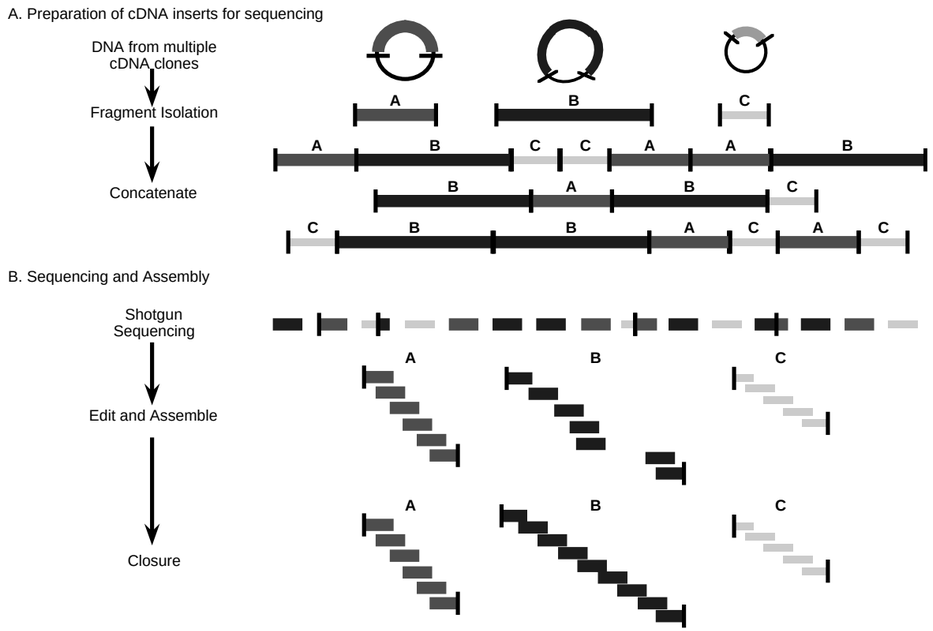

Overview of the concatenation of cDNA sequencing (CCS) strategy for high-throughput sequencing.

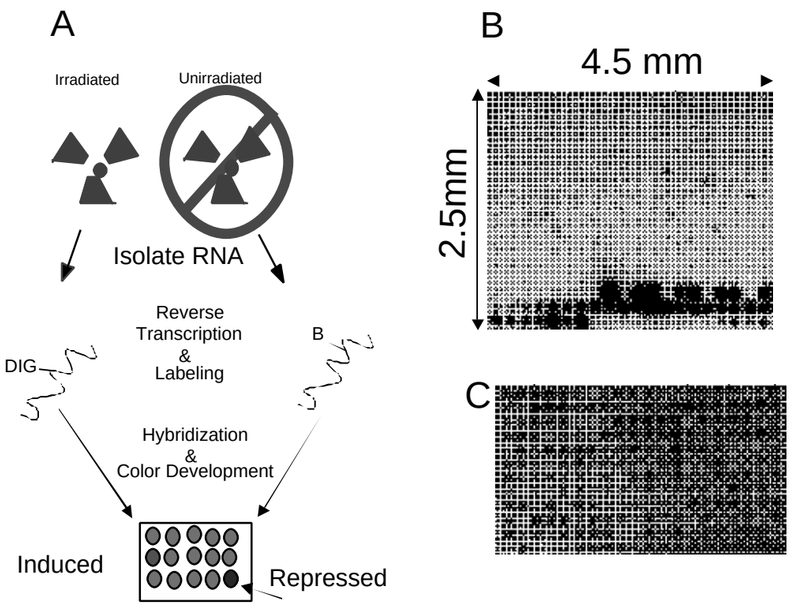

A: Schematic representation of two-color, microarray-based gene-expression profiling. RNA isolated from control and experimental cells is differentially labeled. After simultaneously hybridizing the two labeled probes to a microarray, detection is carried out by enzymatic reactions. B: A test array containing control plant genes and 240 human genes. The array has been hybridized with labeled plant probes generated in vitro to determine the specificity and sensitivity of the approach. Despite the presence of over 200 human gene elements (upper portion of the array), only the plant gene elements corresponding to the hybridized probe are detected. C: Expression profile of 240 human genes. Labeled RNA from human tissue culture cells was hybridized to human test arrays. A range of staining intensity is observed revealing the relative abundance of the transcripts represented on this array.

Optical Biosensor

99506

Basil Swanson

The goal of this project is to develop a biosensor platform that can be used for the environmental detection of protein toxins. Through our research, we hope to better understand the underlying science of optical sensors based on protein-receptor binding, cell membrane mimics, and receptor aggregation that is triggered by protein-receptor recognition. Although aimed primarily at environmental detection, this sensor approach can be adapted to other applications, including early diagnosis of infection and exposure.

We have successfully demonstrated an optical biosensor based on membrane mimetic architectures and protein-receptor recognition in applications to the rapid detection of protein toxins. We have also developed three transduction approaches that involve proximity-based fluorescence changes triggered by receptor aggregation that accompanies protein-receptor recognition.

This new biosensor approach compares favorably with the most laboratory-based immunoassay approach, ELISA, in terms of speed, sensitivity, specificity, and simplicity. This approach has been demonstrated in flow cytometry and has also been used as a miniaturized sensor system based on optical waveguides. We have made progress on several related fronts, including the measurement of fluorescence lifetime changes induced by protein-receptor binding, the mechanism of hybrid bilayer formation, the kinetics and mechanism of multivalent protein-receptor binding on membranes, the preparation of robust tethered bilayer membranes, and the development of new recognition molecules for ricin.

Publications

Bardeau, J-F., et al., "Phase-Transition Based Transduction in a Biosensor Design," *Synth. Met.* **103** (1999).

Eberhardt, A.S., et al., "Defects in Microcontact Printed and Solution-Grown Self-Assembled Monolayers," *Langmuir* **15**, 1595 (1999).

Goldstein B., et al., "The Influence of Transport on the Kinetics of Binding to Surface Receptors: Applications to Cells and BIAcore," *J. Mol. Recognit.* **12**, 1 (1999).

Kelly, D., et al., "Integrated Optical Biosensor based on Planar Optical Waveguides and Fluorescence Resonance Energy Transfer Triggered by Protein-Receptor Binding" (to be published in *Appl. Opt. Lett.*).

Mason, T., et al., "Effective Rate Models for the Analysis of Transport Dependent Biosensor Data," *Math. Biosci.* **159**, 123 (1999).

Myszka, D.G., et al., "Extending the Range of Rate Constants Available from BIACORE: Interpreting Mass Transport Influenced Binding Data," *Biophys. J.* **75**, 583 (1998).

Nolan, J.P., and L.A. Sklar, "The Emergence of Flow Cytometry for Sensitive, Real-Time Measurements of Molecular Interactions," *Nature Biotechnology* **16**, 633 (1999).

Nolan, J., et al., "Flow Cytometry: A Versatile Tool for all Stages of Drug Discovery," *Drug Discovery Today* **4**, 173 (1999).

Nyquist, R.M., et al., "Characterization of Self-Assembled Monolayers for Biosensor Applications" (to be published in *Langmuir*).

Parikh, A.N., et al., "Infrared Spectroscopic Characterization of Lipid-Alkylsiloxane Hybrid Bilayer Membranes at Oxide Substrates," *Langmuir* **15**, 5369 (1999).

Song, X., and B.I. Swanson, "Direct, Ultrasensitive and Specific Optical Detection of Protein Toxins Using Multivalent Interactions," *Anal. Chem*. **71**(11), 2097 (1999).

Song, X., and B.I. Swanson, "An Optical Biosensor Based on Fluorescence Resonance Energy Transfer: Ultrasensitive and Specific Detection of Protein," *J. Am. Chem. Soc.* **120**, 11515 (1998).

Song, X., and B.I. Swanson, "Optical Biosensors Based on Direct Coupling of Recognition, Signal Transduction and Amplification," in *Proceedings of Symposium on Electro-Optic, Integrated Optic and Laser Technologies for Online Chemical Process Monitoring* (SPIE, Bellingham, WA, 1998), p. 280

Song, X., and B.I. Swanson, "Rational Design of an Optical Biosensor for Multivalent Proteins," *Langmuir* **15**, 4710 (1999).

Song, X., et al., "Flow Cytometry-Based Biosensor: Studies of Sensitivities and Kinetics" (submitted to *Anal. Biochem.*).

Song, X., et al., "Optical Transduction triggered by Protein-Ligand Binding: Detection of Biological Toxins Using Multivalent Receptors," *J. Am. Chem. Soc*. **120**(19), 4873 (1998).

Wang, R., et al., "Non-equilibrium Pattern Formation in Langmuir-Phase Assisted Assembly of Alkylsiloxane Monolayers" (to be published in *Phys. Chem. B*).

The Identification of Proteins That Bind to Novel DNA Sequences/Structures

99529

E. M. Bradbury

Interspersed throughout human chromosomes, DNA repeats account for 25% of the human genome. They occur in the regulatory regions of genes, i.e., the 5' and 3' untranslated regions and the intron. They are also present inside the centromere and telomere. The DNA repeats in the regulatory regions of the genes program gene expressions, whereas the DNA repeats in the centromere and telomere are critical in genomic stability. We hypothesized that proteins that specifically recognize these DNA repeats are essential for their biological functions. The main goal of this project is to identify and characterize proteins that bind to DNA repeats in the human genome and to explain on a quantitative basis how such DNA-protein interactions are relevant to gene regulation and genomic instability.

Previously, we demonstrated that hairpin formation by the fragile X (CGG), myotonic dystrophy (CTG), and Huntington (CAG) repeats during replication may account for their expansion. However, it is not known whether any replication or repair protein plays a specific role in triplet-repeat expansion. The human flap endonuclease (FEN-1) is a candidate protein since it is involved in processing the 5' flaps of the Okazaki fragments in the lagging strand. If, however, the 5' CGG/CTG/CAG flaps form stable hairpin structures, they can severely diminish FEN-1 activity which, in turn, may lead to repeat expansion. We have combined nuclear magnetic resonance spectroscopy and binding measurements by surface plasmon resonance to show that the CGG/CTG/CAG repeats in the 5' flap do, indeed, form stable hairpins, and FEN-1 can still bind to the hairpins even though it is incapable of processing them.

Publications

Catasti, P., et al., "DNA Repeats in the Human Genome" (to be published in *Genetica*).

Spiro, C., et al., "Inhibition of FEN-1 Processing by DNA Secondary Structure at Trinucleotide Repeats" (submitted to *Mol. Cell*).

1999

LDRD

Exploratory Research Projects

Novel Approaches to Low-Temperature Thin Film Materials Chemistry: Kinetic Energy Activated Molecular Beam Epitaxy

99040

Mark Hoffbauer

Innovative technologies are critical for developing new materials. Our research objective is to use energetic atomic species to grow thin film materials with improved properties. By controlling the kinetic energy of reactive species, we can grow high-quality thin films at much lower temperatures than with other technologies. The thin films produced are characterized using a variety of techniques for understanding important surface reactions, film physical properties, and the growth/morphology relationships. The goal is to grow very high quality heteroepitaxial crystalline films of nitride and oxide materials by improving upon the state-of-the-art for thin film growth. These materials will then be used to produce prototype electronic and/or optical devices.

This year we emphasized understanding the scientific basis for kinetic energy activated molecular beam epitaxy whereby thin film materials are grown using energetic reactive species. Substantial improvements in our energetic atom source have resulted in vastly improved reliability and performance. In the past, atomic oxygen beams with average kinetic energies of >2.0 eV were produced. Recently, producing an intense nitrogen atom beam with an average energy of >1.0 eV has become routine.

We are focusing on growing thin, passivating oxide layers on compound semiconductors and growing wide band-gap nitride films (e.g., GaN, AlN, InN, and carbon nitride). To examine physical, chemical, and structural properties, we characterize films, using either Laboratory facilities or those of collaborators, with a variety of diagnostic techniques, including surface science and optical spectroscopies, electron and scanning microscopies, and x-ray diffraction. For example, GaN films grown near ambient temperatures on GaAs substrates were analyzed using x-ray photoelectron spectroscopy. Results show the formation of GaN films >10 nm thick, and atomic force microscopy measurements show distinct GaN islands with sizes of ~10 μm covering the surface. Other thin films grown on silicon, aluminum, indium, sapphire, and diamond substrates also show significant nitrogen incorporation and the likely formation of nitride species such as Si_3N_4, AlN, and InN. Oxygen atom surface passivation of $Cd_{1-x}Zn_xTe$ room-temperature radiation detectors has resulted in large improvements in device performance.

These encouraging results are beginning to underscore the important and unique role energetic species have in selectively improving thin film growth. For the first time, these investigations are enabling materials chemistry issues involving energetic atoms to be understood at the atomic level. This understanding will lead to new low-temperature synthetic routes for nitride and oxide thin film materials with finer process control, resulting in improved materials with enhanced performance.

Publications

Prettyman, T.H., et al., “Performance of CdZnTe Detectors Passivated with Energetic Oxygen Atoms,” *Nucl. Instrum. Methods Phys. Res. A* **422**, 179 (1999).

Experimental Determination of Statistical Parameters for Improving a Micromechanical Model of Ductile Fracture

97001

Rich Thissell

The mechanism of ductile fracture consists of void nucleation, growth, and coalescence. Current damage models implemented in hydrocodes are not even remotely accurate in predictive capability and cannot be fitted to multiple experimental measurements under a wide range of experimental test conditions. The purpose of this project is to develop techniques and procedures for extracting statistical parameters from incipiently damaged microstructures to help in developing new models to describe the ductile fracture process.

Project accomplishments include the further development of software for analyzing quantified damage from incipiently damaged flyer plate specimens. We developed new ways of statistically describing these data, including spatially resolved volumetric number densities and size distributions. We implemented a new genetic algorithm technique to improve the validity of inference from planar to volumetric observations.

We performed incipient failure flyer plate experiments at three different impact velocities on two plates of 10100 Cu (>99.99% pure) with near identical chemistries and grain sizes. Significant differences in VISAR (velocity interferometry system for any reflector) pullback signals, shown in the first figure, and damage accumulation behavior occurred that we attribute to subtle differences in second-phase particle number densities and size distributions in the two plates. A summary of Romanchenko-corrected spall strengths shown in the table indicates that grain size does not dominate the resulting spall strength; some other unknown factor is dominant. The unknown factor could be differences in second-phase particle number density and/or size distributions.

We performed microcomputed tomography (MCT) of two incipient failure tests in collaboration with the Naval Research Laboratory. The MCT instrument has a voxel size of ~3 μm, so voids smaller than 10–20 μm in diameter are not detected. One great advantage of using MCT for damage quantification is its ability to describe coalescence behavior of damage in three dimensions.

To assess the cleanliness of the two plates, we performed cold crucible induction melting of samples at the National Physics Laboratory in London, England. The second figure shows a secondary electron image (SEI) of one of dozens of particles observed on the surface of a 5.47 cm^3 sample. Most of the particles are this size or smaller.

Another important result is that the longitudinal porosity distribution of the damage can be described almost entirely by the number density distribution in the Hitachi plate, with only a minor contribution from the median void size distribution. In the Follansbee (Fols.) plate, the median void size longitudinal distribution contributes much more significantly to the porosity distribution.

The following conclusions may be made for very clean, ductile, low-Peierls-energy materials under spallation conditions: (1) damage accumulation is increasingly dominated by void nucleation with increasing material cleanliness; (2) void growth is initially rapid and then decreases as the void increases in size due to inertial effects; and (3) coalescence occurs only via void impingement.

Publications

Thissell, W.R., et al., "Quantitative Microstructural Damage Evolution in Incipiently Spalled 10100 OFHC Copper," in *Proceedings of Plasticity '99*, A.S. Khan, Ed. (Neat Press, Fulton, Maryland, 1999), p. 675.

10100 Cu Spall Strength

Material	Grain Size (μm)	Shock Pressure (GPa)	Romanchenko Spall Strength (GPa)
Fols.	53	2.26	0.92
Fols.	53	2.86	0.95
unknown		2.65	1.29
Hitachi	63	2.88	1.65
Fols.	53	4.05	1.35

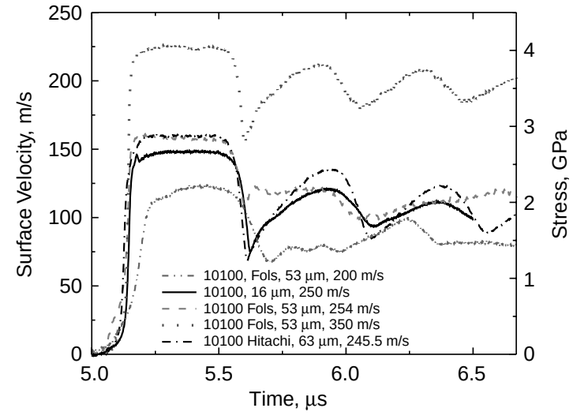

VISAR-measured back surface velocities of several 10100 Cu materials. Note the dramatic pullback difference between the Fols. and Hitachi impacted at about 250 m/s.

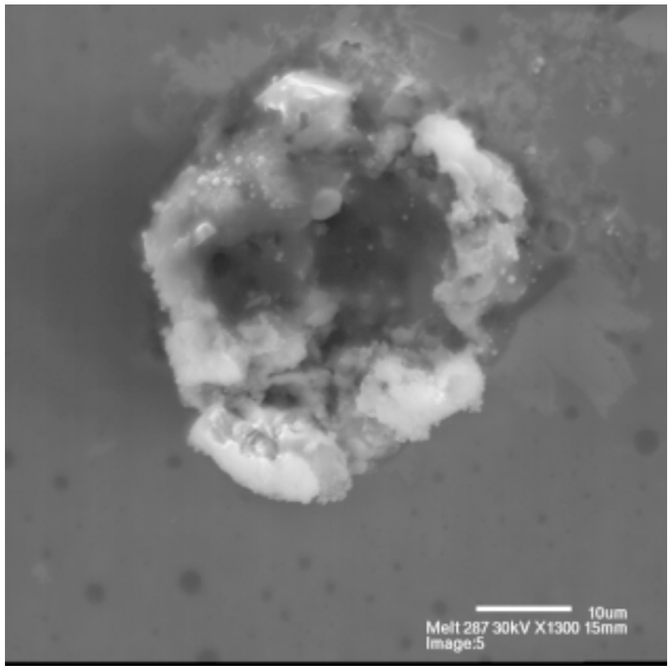

SEI image of a particle in a cold crucible melt specimen. Energy dispersive spectroscopy indicated that this particle consisted of aluminum and silicon.

New Vortex Phases in Irradiated High-Temperature Superconductors

98037

Lev Boulaevskii

We are studying new structures of the vortex state, those that appear when nanometer-diameter amorphous columnar tracks are introduced into anisotropic high-temperature superconductors (HTS) by irradiation with energetic heavy ions. This information is important for all HTS applications because vortex structure and dynamics control losses in the superconducting state.

In highly anisotropic HTS compounds, vortex lines decompose into point-like "pancake" vortices that form a liquid at high temperatures. An array of columnar defects suppresses this transition and changes the nature of the liquid phase of mobile vortices, introducing line-like correlations.

There exist two kinds of pancake liquid with different degrees of interlayer correlations. We are establishing the relationship between c-axis correlations in the vortex state and the c-axis resistivity and the Josephson plasma resonance in HTS with columnar defects. We use both theoretical and experimental approaches to study c-axis correlations as functions of the magnetic field.

The relationship is established between c-axis correlations of pancake vortex positions and the behavior of the c-axis resistivity in oblique magnetic fields. Using this relationship and data for the c-axis resistivity vs magnetic field in the $Bi_2Sr_2CaCu_2O_8$ superconductor with columnar defects, we have uncovered a new vortex liquid phase with line-like correlations of pancakes. Our results allow us to estimate the average length of pieces of vortex lines confined inside columnar defects as a function of the filling factor of columnar defects.

We have developed a theory for the Josephson plasma resonance frequency and line width in the absence of magnetic fields, as well as for the c-axis critical current and the c-axis DC resistivity in d-wave layered superconductors. These theories assume coherent interlayer tunneling and resonant scattering of electrons due to impurities. Our theoretical results provide an explanation for the current-voltage characteristics obtained in stacks of small-area cuprate layers with intrinsic Josephson effect (in small mesas fabricated of $Bi_2Sr_2CaCu_2O_8$ whiskers by using the double-sided ion beam processing technique).

We developed and tested a theory of Josephson plasma resonance in the vortex glass and vortex liquid phases at low magnetic fields and near the critical temperature. Comparing our theoretical results with experimental data for pristine crystals, we conclude that in this region the vortex solid melts into a liquid of vortex lines in contrast with melting into a pancake liquid in the region of high magnetic fields. We found that pinning by columnar defects slightly affects the field dependence of the Josephson plasma frequency near the critical temperature.

We also have developed a theory for the line width of the Josephson plasma resonance in the vortex liquid phase and explained the experimentally observed asymmetric lineshape. In addition, we have developed a theory for the c-axis quasiparticle conductivity in d-wave layered superconductors in the presence of the magnetic field parallel to the layers. We have shown that measurements of the angle-dependent c-axis magnetoresistance, as a function of the orientation of the magnetic field in the layers, provide information on the type of superconducting pairing.

Publications

Artemenko, S.N., et al., "Effect of Quasiparticles on c-Axis Transport in Layered Superconductors," *Phys. Rev. B* **59**, 11587 (1999).

Bulaevskii, L.N., and M.P. Maley, "Vortex States in $Bi_2Sr_2CaCu_2O_8$ Superconductor" (Physical Phenomena at High Magnetic Fields Conference, Tallahassee, FL, October 1998).

Bulaevskii, L.N., et al., "The Effect of an In-plane Magnetic Field on the Interlayer Transport of Quasiparticles in Layered Superconductors," *Phys. Rev. Lett.* **83**, 388 (1999).

Bulaevskii, L.N., et al., "Plasma Resonance at Low Magnetic Fields as a Probe of Vortex Line Meandering in Layered Superconductors," *Phys. Rev. B* **61**, R3819 (2000).

Koshelev, A.E., and L.N. Bulaevskii, "Fluctuation Broadening of Plasma Resonance Line in the Vortex State of Layered Superconductors," *Phys. Rev. B* **60**, R3743 (1999).

Latyshev, Yu.I., et al., "Interlayer Transport of Quasiparticles and Cooper Pairs in $Bi_2Sr_2CaCu_2O_8$ Superconductors," *Phys. Rev. Lett.* **82**, 5345 (1999).

Morozov, N., et al., "Structure of Vortex Liquid in Irradiated $Bi_2Sr_2CaCu_2O_8$ Crystals," *Phys. Rev. Lett*. **82**, 1008 (1999).

Experimental and Theoretical Investigation of Fracture and Deformation of a Revolutionary High-Temperature Gamma-TiAl Alloy

97011

George T. Gray III

The materials used to construct such items as jet engines must be lightweight and flexible, yet strong. The objectives of this study were to understand the deformation mechanisms that lead to low ductility in gamma titanium aluminides (gamma-TiAl) and to explore how to increase their tensile ductility. We examined the anomalous temperature dependence of mechanical twinning (which may additionally provide new concepts and theories of mechanical twinning) and the ductile-brittle transition strain rate in gamma-TiAl.

In the final year of this project, we completed our studies of microcrack nucleation and propagation in both polysynthetically twinned (PST) TiAl crystals and polycrystalline gamma-TiAl alloys. We found that (1) for the soft-mode oriented PST-TiAl crystals, interlamellar microcracks form by a shear mode, while translamellar microcracks are initiated via local tensile stresses during global compressive loading; and (2) in polycrystalline gamma-TiAl alloys, microcracks present either intragranularly or transgranularly are formed via shear displacements along particular crystallographic planes (usually in close-packed planes).

We characterized the mechanical response of polycrystalline gamma-TiAl alloys for a wide range of temperatures and strain rates (see accompanying figure). We documented three temperature regimes of mechanical response for both cast and wrought polycrystalline gamma-TiAl alloys. Tests of pure shear loading, in particular crystallographic directions of PST-TiAl crystals, showed that both the yield stress and the mechanical response of these crystals were different in different crystallographic directions.

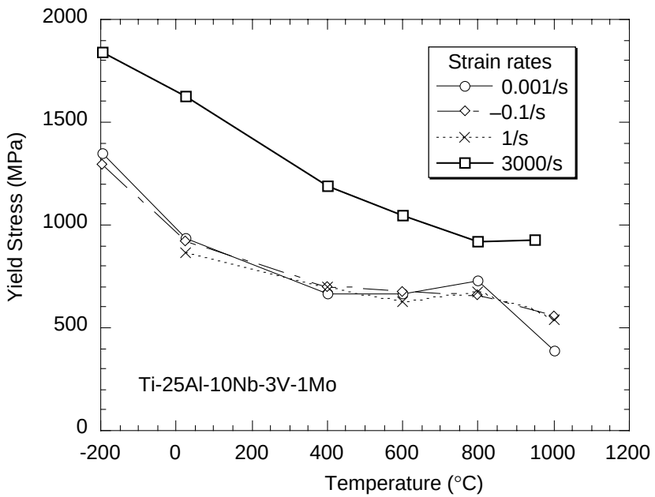

Stress-strain response of Ti-25Al-10Nb-3V-1Mo as a function of temperature for various strain rates of loading in compression.

We performed large-scale molecular dynamics simulations to investigate the dynamical and structural properties of jogged-screw dislocations in gamma-TiAl alloys under external stresses. Our simulations revealed that the critical height for a jog (a shift in dislocation from one plane to another) to move forward nonconservatively is between three and four times the distance of the nearest-neighbor aluminum atoms. We developed a mechanism responsible for the formation of small jogs from the decomposition of large jogs in gamma-TiAl alloys. The competition between the forward nonconservative and the lateral conservative motions of jogs plays a key role in determining the formation of pinning points. We identified the force distribution of the screw and jog segments, which is useful in analyzing the dynamical and structural properties of dislocations. Our modeling simulations showed that interstitial clusters and vacancy tubes are formed during the forward nonconservative motion of small jogs. We also observed stable dipoles during the dynamical process of dislocations and dislocation loops that are formed in the case of intermediate and large jogged-screw dislocations.

Publications

Chen, K.Y., and S.J. Zhou, "Dynamics and Structures of Jogged Screw Dislocations in Gamma-TiAl Alloys Investigated via Molecular Dynamics Simulations" (submitted to *Philos. Mag. A*).

Vaidya, R.U., et al., "A Comparative Study of the Strain Rate and Temperature Dependent Compression Behavior of Ti-46.5Al-3Nb-2Cr-0.2W and Ti-25Al-10Nb-3V-1Mo Intermetallic Alloys" (to be published in *Scripta Mater.*).

Intrinsic Fine-Scale Structure in Complex Materials: Beyond Global Crystallographic Analysis

97016

Albert Migliori

In many materials, such as complex oxides and martensitic alloys, internal fine-scale structures determine the physical properties of the materials. Using resonant ultrasound spectroscopy (RUS), transport measurements, x-ray crystallography, and neutron pair-distribution function (PDF), we studied the formation of these fine-scale structures at phase transitions. By measuring and modeling the interplay of temperature, strains, defects, free energies, and entropy, we are elucidating the dynamics of these structures and the consequences for materials undergoing a phase transformation.

Experimentally, we focused on the cubic martensites AuZn and NiTi. The first figure shows neutron scattering data from AuZn at different temperatures. As the material transitions from austenite to martensite near 60 K, the features corresponding to scattering from larger-scale features (small q) are much less affected than the smaller-scale features (large q), which are smeared out in the martensite (microstructured) phase. This supports the idea of local distortions, which have little effect on global structures.

Detailed low- and high-temperature elastic moduli measurements on both AuZn and NiTi show an anomalously high internal friction at low temperatures in all the martensite alloys, behavior similar to that expected from a glass, suggesting random, small distortions at a local (probably unit-cell) scale. The high-temperature behavior of the moduli is also anomalous, the temperature coefficient being positive, contrary to what may be expected. In NiTi, this behavior holds up to 500°C (second figure). This suggests that even in the austenite phase, where the internal friction is low, the system is slowly changing with temperature to a configuration that has higher elastic constants. Though this may be only subtly different from an exactly cubic configuration, we expect that at a higher temperature, this change would be complete and the temperature coefficient would become negative.

Our models showed that specific signatures in the PDF and x-ray and neutron scattering structure factors, previously ascribed to local structural distortions, could be due to an underlying anisotropic, long-range elastic field. Our results are relevant for interpreting structural data for a wide class of functional elastic materials undergoing structural phase transitions and exhibiting twin-like and tweed-like microstructure. Some examples include martensitic alloys, transition metal perovskite oxides, colossal magnetoresistance manganites, ferroelectric, and relaxor materials.

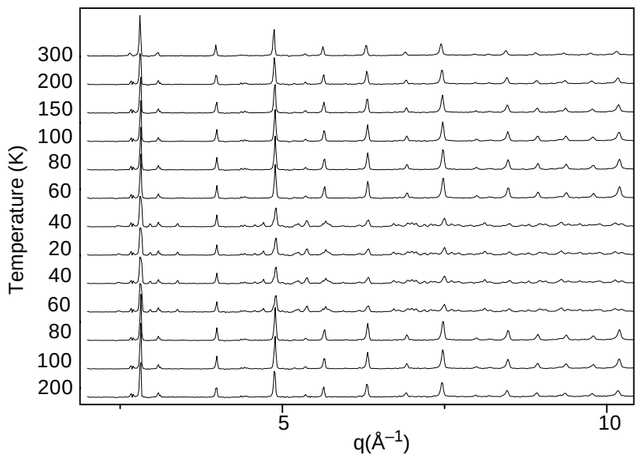

Intensity of scattered neutrons as a function of momentum transfer q, at a sequence of temperatures. The transition occurs below 60 K. The greatest effect is at higher q (shorter range), while longer-range order (lower q) is least affected.

Publications

Lookman, T., et al., "Signatures of Long-Range Elastic Interaction in Textured Materials" (to be published in *Phys. Rev. B*).

Saxena, A., et al., "Defect-Induced Microstructure and Shape Memory in a Continuum Model" (to be published in *Mater. Sci. Forum*).

Saxena, A., et al., "Elastic Compatibility, Martensitic Textures and Weak Plasticity" (in *Proc. Solid-Solid Phase Transformations (PTM'99): The Japan Institute of Metals*), in press.

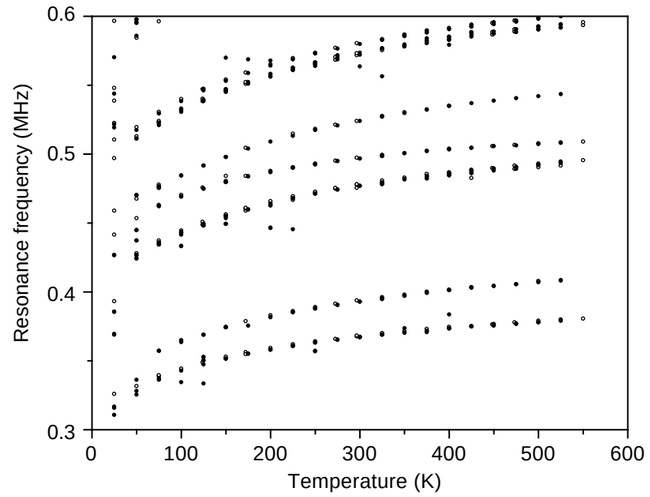

Temperature dependence of the acoustic resonances of polycrystal NiTi. The anomalous variation of the elastic constants with temperature continues to at least 500°C. The lines of data points represent different modes of the sample.

Targetry Development for the Production of Research Radioisotopes

97523

Michael Cappiello

Radioisotopes are important tools in biological and medical research. Their use leads to major advances in our understanding of biological functions and disease processes. Although radioisotopes have been used in medicine to diagnose and treat human maladies since the 1930s, radioisotopes for research and for promising new nuclear medicine products are frequently unavailable or very expensive. The objectives of this project are to develop conceptual designs of a medical isotope target station for operation at the high-energy end (800 MeV) of the Los Alamos Neutron Science Center (LANSCE) accelerator and of a medical isotope target station for operation at the Low-Energy Demonstration Accelerator (LEDA).

We completed a conceptual design for a medical isotope target station at the high-energy end of the LANSCE accelerator. This target station, which will produce a variety of radioisotopes, will accommodate up to 1 MW of beam power continuously and allow for quick remote retrieval of targets. The target station would be located in the thin target area directly downstream of the switchyard, adjacent to the existing hot cell.

The station comprises a tungsten neutron source, a hydraulic system for the retrieval of production targets, cooling lines, and shielding. For some isotopes, embedding their production targets in tungsten enhances their production rate over direct proton irradiation because of the significant production of high-energy spallation neutrons. The hydraulic system provides for the irradiation of up to 20 separate isotope production targets. Each target may be removed separately to the hot cell using hydraulics. The hot cell provides a safe environment for processing or packaging the targets for shipping. The major isotopes we are investigating for production include phosphorus-32, strontium-82, palladium-103, scandium-47, samarium-153, indium-111, germanium-68, copper-67, iodine-127, xenon-127, iodine-125, zinc-62, copper-64, tin-117 metastable, thulium-118, sodium-22, and tungsten-188. Our calculations show that high specific activity and radiopurity are achievable for many isotopes.

To validate our prediction of isotope production quantities, we performed an assessment using existing data from an earlier irradiation. Results show that our design codes, MCNPX and CINDER'90, predict isotope generation rates to within ±40%. This benchmark provides a measure for the calculational uncertainty of our predictions of the isotope production capability of the proposed facilities.

Optimum Design of Ultrahigh-Strength Nanolayered Composites

97042

Hui-Jou Harriet Kung

The goal of this project is to advance our understanding of nanophase materials by investigating their strengthening mechanisms in multilayered metallic composites. Nanophase materials, which have an ultrafine-scale microstructure, often exhibit ultrahigh strength. They can provide the basis for fabricating miniature actuators, springs, and diaphragms and can be used for biomedical or sensor applications. They also have great potential in electrical, thermal, and magnetic applications for which strength and structural integrity are of major concern.

Scientifically, we are working to (1) determine the limits at which conventional Hall-Petch and Orowan descriptions of yielding as microstructural scale reduce to nanometer (10^{-9} meter) scale, (2) characterize the new deformation mechanisms that may apply at these very small dimensions, and (3) clarify and quantify how defects and interfacial bonding strength affect macroscopic mechanical properties. Technically, we must learn how the microscale structure and strengthening mechanisms relate to macroscale properties.

We have examined microstructure, mechanical behavior, and electrical properties as functions of structural length scale in several copper-based multilayered systems. In a series of experiments, we deformed the layers in a controlled manner to determine mechanical properties and then constructed a two-dimensional deformation-mechanisms map to illustrate the regime of different deformation behavior (see first figure). These maps illustrate the relative effects of layer thickness and grain size on the strengthening mechanisms, and serve as guidelines for interpreting the scale-dependent strengthening or softening mechanisms in mutlilayers.

In modeling, we studied phase transformations in nanoscale multilayered thin films. We learned that as we reduce the layer thickness of copper/silver multilayer films, the crystal structure of copper transforms first from face-centered cubic (fcc) to hexagonal close packed (hcp) and then to a body-centered cubic (bcc) structure at a very small layer thickness (see second figure). These results are corroborated by experimental observations in copper/silver as well as in other systems, including copper/niobium and cooper/chromium multilayers. We also studied the interaction of dislocations with interfaces in copper/silver multilayers. We discovered that some dislocations dissociated into the interface, making it very difficult to transport slip through the interface. In other cases, dislocations cross the interface spontaneously without an applied stress. The rationale for the behavior involves the relative orientations of the two materials on either side of the interface and the sign of the moving dislocation.

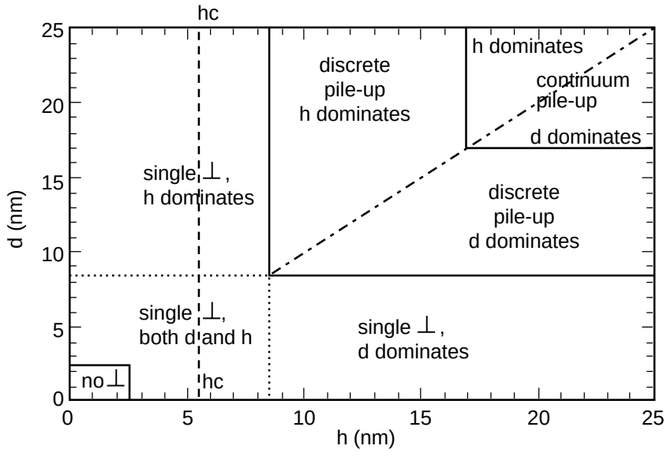

An example of a deformation mechanism map for copper-based multilayers with a misfit of ~2.5%. The map illustrates the different regime of deformation behavior as a function of layer thickness (h) and grain size (d) within the layers. (⊥ = dislocation)

Publications

Fayeulle, S., et al., "Thermal Annealing, Irradiation, and Stress in Multilayers," *Nucl. Instrum. Methods Phys. Res., Sect. B* **148**, 227 (1999).

Keast, V.J., et al., "Elemental Mapping of Nanoscale Cu/Nb Multilayers," in *Electron Microscopy*, Vol. III, H.A. Calderón Benavides and M. José Yacaman, Eds. (Institute of Physics, Bristol, 1998), p. 563.

Misra, A., et al., "Electrical Resistivity of Sputtered Cu/Cr Multilayered Thin Films," *J. Appl. Phys.* **85**, 302, (1999).

Misra, A., et al., "Residual Stresses and Ion Implantation Effects in Cr Thin Films," *Nucl. Instrum. Methods Phys. Res. Sect. B* **148**, 211, (1999).

Misra, A., et al., "Residual Stresses in Polycrystalline Cu/Cr Multilayered Thin Films" (to be published in *J. Mater. Res.*).

Stone, D.S., et al., "Hardness of Thin Films Determined Based on Load and Contact Stiffness," *MRS Sym. Proc.* **522**, p. 257 (1998).

Tambwe, M.F., et al., "Haasen Plot Analysis of the Hall-Petch Effect in Cu-Nb Nanolayer Composites," *J. Mater. Res* **14**, 407 (1999).

Verdier, M., et al., "Plastic Behavior of Cu/Ni Multilayers Deposited on Cu Single Crystals," *MRS Sym. Proc.* **522**, 77 (1998).

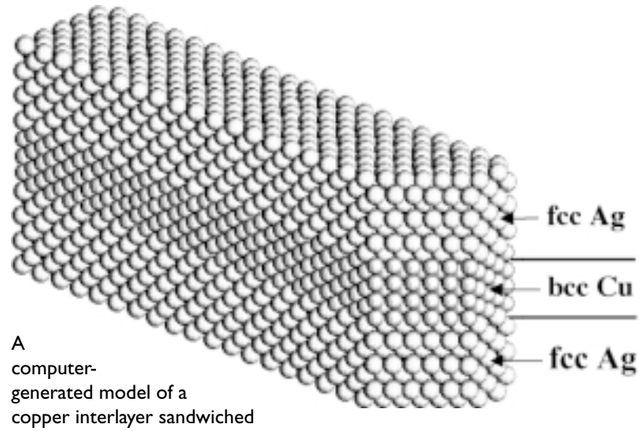

A computer-generated model of a copper interlayer sandwiched between two (very thick) layers of silver. Copper, which is normally a face-centered cubic crystal structure, adopts a body-centered cubic crystal structure as a stable configuration with its {110} planes parallel to the sides of the model.

Plutonium Aging: Investigation of Changes in Weapon Alloys as a Function of Time

98535

Barbara Martinez

As the U.S. stockpile of nuclear weapons ages, it is important that we determine the effects this aging has on plutonium-239. One way to characterize aging effects in plutonium is to accelerate aging by doping plutonium-239 with plutonium-238. The time-dependent phenomena we expect to simulate by plutonium-238 doping are radiation-induced void formation and swelling; ingrowth of helium, uranium, and americium; and phase stability. Our efforts this year focused on preparing the material and the characterization facilities.

We will prepare plutonium-239 metal blended with 5% plutonium-238, which ages at a rate of about 15 years per year, compared with undoped plutonium-239. We will also alloy the doped plutonium metal with gallium to produce a solute-stabilized delta phase. Samples of this alloy will be stored under carefully controlled conditions designed to simulate realistic stockpile storage environments, accounting for self-heating and thermally sensitive aging effects. We will carefully track the results of these fundamental measurements to detect changes as a function of time and to compare these results with those for the freshly cast material.

To prevent cross-contamination of plutonium-238 to other workstations, we isolated our specimen preparation activities in two gloveboxes: one for casting and one for machining. Both gloveboxes required extensive mechanical and electrical systems upgrades prior to their use with plutonium-238. We completed upgrades to the casting glovebox, including seismic upgrades and installation of an inert atmosphere system. We also completed a revamp of the induction heating system, which necessitated the installation of a new solid-state induction power supply. Molds for the enriched castings and incubators for the long-term storage of the enriched plutonium are ready. A new heat treating furnace, lathe, milling machine, and specimen coring punch are ready for installation.

We completed the design and construction of a dilatometer, a plutonium sample-containment vessel and optical platform used for laser-triangulation length measurements. We continued the development of BASIC code for acquiring data from the displacement sensor and temperature controller. For precision density, we developed BASIC code to automate a Mettler balance and a digital thermometer. We acquired the feed-throughs and service panels required for glovebox installation. We also completed the assembly and testing of a Sieverts equilibrium system for helium gas effusion studies, including the vacuum/gas handling manifold, furnace control, data acquisition system, and pressure sensor measurement system.

Organic Electronic Materials under Intense Electrical Injection

99043

Darryl L. Smith

Organic electronic materials are now of great interest both scientifically and technologically. For example, light-emitting diodes are an important application of organic electronic materials that are entering production, and organic electrical injection lasers are being pursued. Understanding the fundamental physics of intense electrical injection in organic electronic materials, in which numerous charge carriers are present, is essential to the development of these kinds of new devices.

The objective of this project is to understand organic electronic materials under intense electrical injection using a tightly coupled synthesis-characterization-modeling approach. Our approach consists of collaborative experimental and theoretical efforts.

The theoretical efforts are divided into two classes: macroscopic device modeling and microscopic theory. There is strong interplay between the classes, with the microscopic theory providing input to the device modeling and the device modeling suggesting interesting questions to be addressed by microscopic theory. We are using both classes to interpret the experimental results and to suggest additional experiments.

There are two principal classes of structures that are being investigated experimentally: vertical injection structures and multilayer charge accumulation structures. The vertical injection structures consist of one or more layers of conjugated organic materials with electrically injecting metal contacts on each side. We apply a pulse bias to the structure and then study the properties of the injected excitations.

The multilayer charge accumulation structures consist of a film of a conjugated organic material with a metal contact on one side and an insulator, such as Al_2O_3 or SiO_2, with a metal contact on the other. When we apply a voltage bias across the structure, carriers accumulate in the conjugated organic material. These structures are being used to determine the steady-state properties of the charged excitations, such as their optical absorption cross sections.

We have enhanced our understanding of how interactions among the injected polarons influence the transport properties of the organic film and of the transport properties of vertical injection structures.

Publications

Campbell, I.H., and D.L. Smith, "Physics of Polymer Light-Emitting Diodes," in *Semiconducting Polymers—Chemistry, Physics and Engineering*, G. Hadziioannou and P. Van Hutten, Eds. (VCH-Wiley, New York, 1999).

Campbell, I.H., and D.L. Smith, "Schottky Energy Barriers and Charge Injection in Metal/Alq/Metal Structures," *Appl. Phys. Lett.* **74**, 561 (1999).

Campbell, I.H., et al., "Charge Transport in Polymer Light-Emitting Diodes at High Current Density," *Appl. Phys. Lett.* **75**, 841 (1999).

Campbell, I.H., et al., "Consistent Time-of-Flight Mobility Measurements and Polymer Light-Emitting Diode Current-Voltage Characteristics," *Appl. Phys. Lett.* **74**, 2809 (1999).

Crone, B.K., et al., "Charge Injection and Transport in Single Layer Organic Light-Emitting Diodes," *Appl. Phys. Lett.* **73**, 3162 (1998).

Crone, B.K., et al., "Device Physics of Single Layer Organic Light-Emitting Diodes," *J. Appl. Phys.* **86**, 5767 (1999).

Saxena, A., et al., "Electronic Transmission Across a Metal/Conjugated Oligomer/Metal Structure: Role of Intrinsic Disorder," *Opt. Mater.* **9**, 461 (1998).

Yu, Z.G., et al., "Dynamics of Electronic Transport in Metal/Organic/Metal Structures," *J. Phys.: Condens. Matter* **11**, L7 (1999).

Yu, Z.G., et al., "Electronic Transmission in Conjugated Oligomer Tunnel Structures: Effects of Lattice Fluctuations," *J. Phys.: Condens. Matter* **10**, 617 (1998).

Yu, Z.G., et al., "Green's Function Approach for a Dynamical Study of Transport in Metal/Organic/Metal Structures," *Phys. Rev. B: Condens. Matter* **59**, 16001 (1999).

Application of High-Temperature Superconductors to Underground Communications

97517

David Reagor

Low-frequency electromagnetic waves are deeply penetrating in conducting media and are typically used for underground or underwater communication. They are normally executed with either wire-based or wireless systems. Currently available wireless receivers use a conventional ferrite-core antenna. These receivers, however, are fairly insensitive to low-frequency magnetic fields when configured into a small, portable package. The goal of this project is to develop a technology base for underground communications using high-temperature superconducting devices. High-temperature SQUID (superconducting quantum interference device) receiver technology is based on Josephson junctions (thin insulators separating superconducting materials) and superconducting loops. Placed in small packages, these receivers can be easily carried by miners underground. The receivers possess the sensitivity and bandwidth needed to carry voice and data in a configuration that is easier to install and maintain than wire-based technology.

We previously demonstrated underground radio reception over a 650-m range. In that case, the transmitter used a large, fixed antenna, and the results established the viability of paging communications. This year the emphasis of our project has shifted to wireless, two-way voice transmission. To attain an economically viable voice technology, we must achieve a number of goals in materials and technology development.

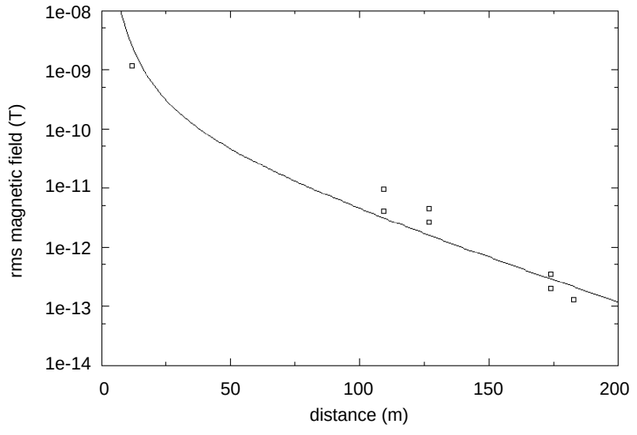

The results of an underground radio-propagation test at the WIPP. The measured magnetic field is plotted vs distance from the transmitter. The solid curve is a fit to the magnetic field predicted from a radiating-dipole model with a skin depth of 35 m.

Our key materials-research results this year are related to improved performance and lower SQUID cost. We achieved an improved passivation method that was used to demonstrate for the first time high-quality, 2-μm technology. This innovation will eventually improve the performance of a receiver by a factor of 3.

Also as part of our materials research, we measured the magnetic noise of superconducting films deposited by a number of standard methods. A new deposition technique increasingly favored for cost-sensitive applications is large-area coevaporation. Intrinsic magnetic field noise results indicate that these coevaporated films are high quality and comparable to the standard films currently used.

The portion of our project relating to underground radio testing focused on low-power transmitter tests appropriate to the problem of portable transmitters. These low-power field tests were performed at the Waste Isolation Pilot Plant (WIPP). The source for the results shown in the accompanying figure is a 200-mW transmitter at a frequency of 3 kHz. Signals at 180-m range were approximately 1 pT, well above the noise floor of the receiver. The distance at which the extrapolated signal-to-noise ratio approaches unity is over 200 m. The transmitter power levels can most likely be increased by one to two decades before reaching portable power limits.

Bulk Ferromagnetic Metallic Glasses

98035

Ricardo B. Schwarz

Currently, about 1% of the total electrical energy produced in the US is lost as heat dissipated by distribution transformers and motors. These losses can be substantially decreased (by a factor of 2 or 3) by the use of more efficient transformers and motors that use ferromagnetic cores made from amorphous (glassy) metals. The optimum implementation of ferromagnetic glasses requires that these materials be prepared in the form of laminas at least 0.3 mm thick. Existing ferromagnetic foils prepared by rapid quenching are at most 40 μm thick. We are addressing the science needed to develop new synthesis routes for bulk ferromagnetic metallic glasses. A recent development at Hydro Quebec (Canada) suggests that iron foils prepared by pulsed-current electrodeposition may have similarly low hysteretic losses under cyclic magnetic excitation. We are also exploring this synthesis route for low-loss ferromagnetic alloys.

We analyzed x-ray diffraction data collected at Brookhaven National Laboratory (BNL) using the SAM-85 press. The first figure shows selected x-ray diffraction patterns obtained at pressures in the range of 22 to 33 kbar, while heating the sample from room temperature to 528°C. At room temperature, the x-ray pattern indicates the presence of aluminum and germanium. With increasing pressure, aluminum and germanium react to form a metastable alloy phase, labeled γ in the second figure. At even higher pressures, the γ phase melts. On decreasing the temperature under applied pressure, the melt becomes a glass that is stable at ambient conditions of pressure and temperature. The second figure shows a tentative pressure-temperature phase diagram for $Al_{30}Ge_{80}$ we constructed with data from three experiments at BNL.

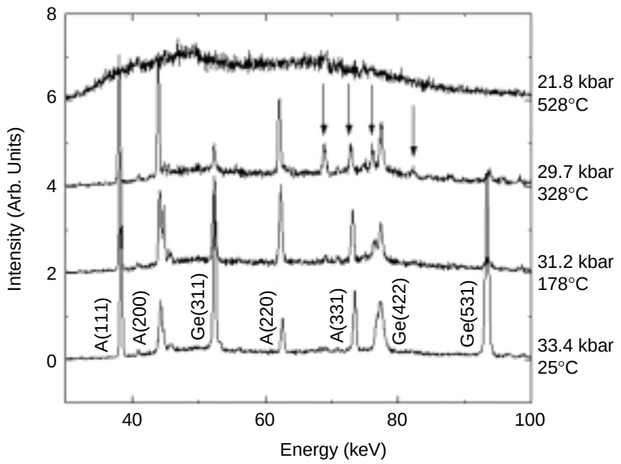

X-ray diffraction patterns of a mixture of aluminum and germanium (molar ratio 3 to 7) obtained during in situ experiments at the SAM-85 press at BNL. The hydrostatic pressure and temperatures for each run are indicated in the figure. The Bragg peaks indicated by the arrows belong to the metastable hexagonal γ phase.

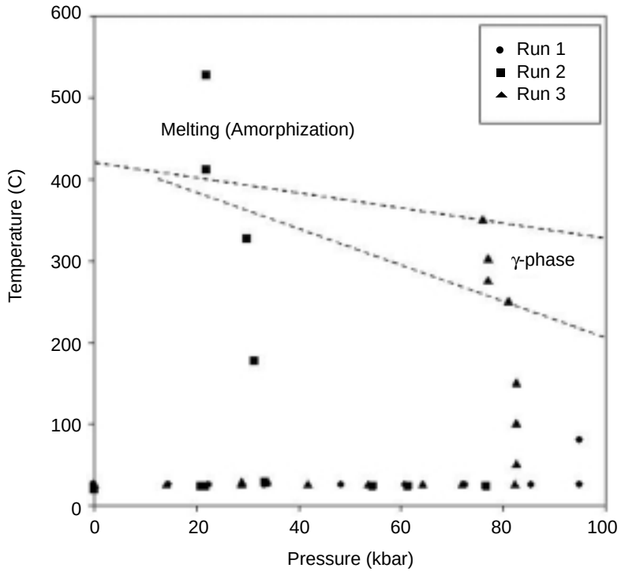

Pressure-temperature phase diagram for $Al_{30}Ge_{70}$ deduced from three in situ synchrotron x-ray diffraction experiments conducted at BNL.

We prepared by mechanical alloying a nanosized mixture of aluminum and germanium and of iron and germanium. These powders were loaded into stainless-steel capsules for shock-wave consolidation experiments.

Pure iron laminas were prepared by pulsed electrodeposition. Two different electrodeposition baths were used to prepare foils with different grain sizes. The electrodeposited laminas were characterized by x-ray diffraction and SQUID magnetometry. The x-ray diffraction data show the films are single-phase iron with nanosized grains in the range 420 to 520 nm. The magnetization data (see the third figure) show a square hysteresis curve with a saturation magnetization in excess of 2 tesla (200 emu/g) and coercivity of 12 Oe. We expect the coercivity will decrease significantly upon annealing the sample under an applied saturation magnetic field.

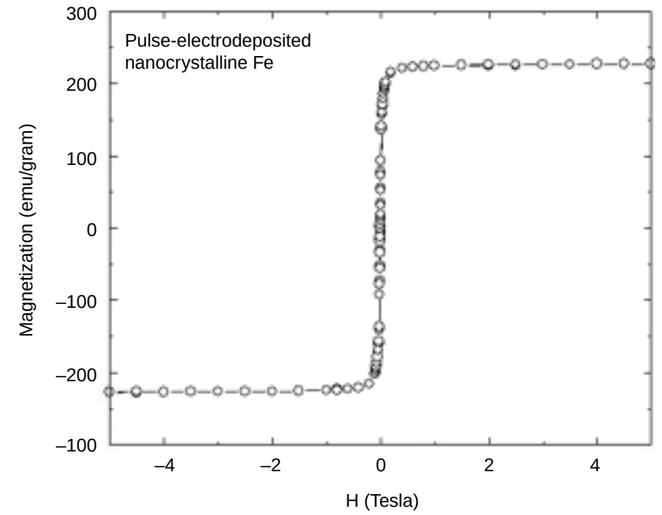

Magnetic hysteresis curve for a fine-grain iron lamina prepared by pulsed-current electrodeposition.

Unusual Metal Behavior in Taylor Microwires

98034

John J. Petrovic

The objective of this research is to develop the Taylor microwire approach and employ it for fundamental studies of both ultrafine-scale and nonequilibrium structures in selected metal alloys. Major goals are (1) to explore fundamental scale aspects of the deformation and fracture of ultra-high-strength materials; (2) to develop an understanding of the synthesis and thermodynamic stability of microwires; and (3) to explore new and unique combinations of electrical, magnetic, and mechanical properties produced by the microwire approach. Possible applications include high-strength/high-conductivity materials, new optical fibers, biological electrodes/sensors, and advanced sensors for enhanced surveillance of nuclear weapons systems.

This year we continued to study microstructures of copper-silver Taylor microwires. We compared atomic resolution transmission electron microscopy images of an silver particle in a copper matrix that was mechanically strained to an 4.8% tensile strain level directly to molecular dynamics atomic position simulation calculations for the same phase configuration. Dislocation structures developed during mechanical straining of the actual material corresponded very well to dislocation structures predicted by the molecular dynamics simulation.

We developed a capability for the tensile testing of Taylor microwires directly in the atomic force microscope (AFM). We also purchased a commercial tensile testing unit that operates in association with the AFM. This tensile testing unit will not only allow a determination of stress-strain curves for Taylor microwires, but also will allow for the direct AFM observation and interrogation of the microwire surfaces during the tensile loading process. This experimental capability will be invaluable in determining Taylor microwire deformation mechanisms.

Publication

Han, K., et al., "Microstructural Aspects of Cu-Ag Produced by the Taylor Wire Method," *Acta Materialia* **46**, 4691 (1998).

Investigation of Experimental Defect Interactions in Materials by Integrating Experimental Techniques with Large-Scale Simulations

99044

Peter Lomdahl

Our project investigates experimentally and theoretically the detailed physics of dislocation-dislocation interactions in face-centered cubic (fcc) materials. Large-scale molecular dynamics simulations with millions of atoms can now reveal details of the core-core interaction of dislocation crossings, and experimental high-resolution transmission electron microscopy (TEM) techniques allow us to observe this process directly in the laboratory. By combining these techniques into a coherent tool, we hope to understand this basic process, which is of vital importance to the study of materials behavior. This work is directly relevant to the Laboratory core competencies in advance materials and simulation.

This year we investigated the properties of dislocations and their short-range interactions with large-scale molecular dynamic simulations, elasticity, and dislocation energetics. These findings provided guidance for later experimental verifications. By analyzing the processes of both repulsive and attractive dislocation intersections, we demonstrated that investigating short-range dislocation interactions requires atomistic simulations. Atomistic simulations can find the physical path in the complicated energy landscape and can determine essential information for macroscopic/mesocopic deformation modeling, such as a critical breaking angle for dislocation intersections.

In addition, we also performed a series of large-scale (up to 54 million atoms) molecular dynamics simulations to investigate the formation of vacancies by a moving jogged dissociated dislocation in copper at low temperatures. We found that the deviation of the jog line causes the formation of vacancies. With the help of dislocation energetics, we uncovered the mechanism responsible for the deviation of the jog line. Because the jog motion has a significant role in dislocation mobility, and consequently the ductility of materials, we also investigated the jog motion in gamma-TiAl. We observed the creation of vacancies, interstitials, and dislocation loops in the moving process of a pair of jogs and determined their structures.

To further understand dislocation loops, we investigated shear circular dislocation loops with elasticity theory and molecular dynamics simulations. The results of the simulations are in good agreement with those of elasticity theory for a loop with radius about 7.5 nm.

Our major experimental instruments include a liquid-nitrogen-cooled straining stage and a charge-coupled device camera. We have performed a number of in situ TEM experiments on pure copper to show that the experiment, while difficult, is quite feasible and should provide very useful information about dislocation intersections and other properties in fcc materials.

Publications

Chen, K.Y., et al., "Atomistic Studies of Jogged Screw Dislocations in γ-TiAl Alloys," (Fall Meeting of the Materials Research Society, Boston, MA, November 30–December 4, 1998).

Zhou, S.J., and D.L. Preston, "Short-Range Dislocation Interactions: Intersections, Junctions and Jogs" (to be published in *Physica* D).

Zhou, S.J., et al., "Investigation of Vacancy Formation by a Jogged Dissociated Dislocation with Large-Scale Molecular Dynamics and Dislocation Energetics," *Materialia*, **47**, 2695, (1999).

Zhou, S.J., et al., "Shear Circular Dislocation Loops Investigated with Elasticity Theory and Atomistic Simulations" (to be published in *J. Comput.-Aided Mater. Des.*).

Bulk Rapid Solidification

99041

Dan J. Thoma

Directed light fabrication (DLF) fuses gas-delivered metal powders within a focal zone of a laser beam to produce fully dense, near-net shape, three-dimensional (3-D) metal components from a computer-generated solid model. The flexibility in power distributions of lasers allows the processing of a variety of materials, ranging from aluminum alloys to tungsten and including intermetallics such as Mo_5Si_3 and NiAl. The DLF-generated microstructures contain microstructural features significantly refined over any other conventional solidification process. We have preliminary indications that the cooling rates are in the regime classified as rapid solidification. Bulk rapid solidification promises enhancement and optimization of the properties of materials. Our project seeks to interpret the solidification behavior in Fe-25Ni with two complementary efforts: experimental and simulation. Our end goal is to mature a technology that revolutionizes manufacturing into a single step (a huge cost savings with reduced environmental impacts). The scientific thrust is defining the remarkable physical properties that surpass conventional techniques.

Using DLF, we processed a complete set of Fe-25Ni samples under a variety of conditions. We examined secondary dendrite morphology in one-dimensional rods as a function of growth conditions.

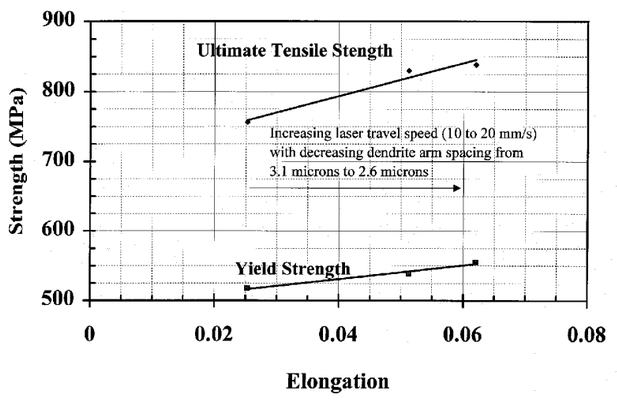

The strength of DLF-processed Fe-25Ni bars and corresponding ductility. The strength and ductility increase with the refinement of the microstructural features.

Independent of the conditions, examination of over 200 dendrite arms in each sample demonstrates that conduction dictates heat transfer through the rod, with average experimental cooling rates up to 1000 K/s. In 3-D blocks, the average experimental cooling rate is much higher, in excess of 10^4 K/s. Because secondary dendrite arms did not develop at these high rates, we investigated primary dendrite arms. We measured the strength of the samples as a function of elongation. As the laser deposition traverse speed increased, the strength and elongation increased as the figure shows, a paradoxical result because material ductility almost always decreases as strength increases. We are currently investigating the microstructural cause of this outcome, a paradox that illustrates how bulk rapid solidification can optimize materials.

Simulation efforts have been equally fruitful. Boundary condition analyses for the input power, once thought to be an ambiguous parameter, are actually bounded and well behaved. We can, for example, couple the absorbed power directly to powder flow rate and sample geometry relatively independent of melt cap height. With the correlation of powder flow and sample radius (for wires) to absorbed power, we can readily correlate the input condition to cooling rate based upon the thermal properties of the samples. This unique feature can provide feedback controls for deposition rates and microstructural tailoring. Currently, calculated cooling rates are on the order of 200 K/s. First experimental iterations demonstrated cooling rates of 150 K/s, in close agreement with the simulations.

Unconventional Superconductivity and Violation of Time-Reversal Invariance

98036

Roman Movshovich

The subject of our project is a recently discovered low-temperature phase transition in nickel-doped bismuth-strontium-calcium-copper oxide (BSSCO), a high-temperature superconductor. This phase transition manifests itself by a sharp drop in thermal conductivity as a function of temperature (by a factor of 3 within 50 mK of the transition temperature of 200 mK). The observation of multiple superconducting phases in high-temperature superconductors is a definitive hallmark of unconventional superconductivity. The new low-temperature state that is observed below 200 mK is expected to possess the very unusual property of violated time-reversal invariance. Our goal is to be able to differentiate between several competing scenarios for the origin of such states.

In our experimental work, we are using thermal conductivity to investigate this 200 mK anomaly. Phonons are present as well as electrons, which contribute to thermal transport, even though phonon contribution is expected to vary as temperature cubed (T^3) for usual crystalline insulators. To separate the low-temperature electronic and phonon mechanisms of thermal transport in high-temperature superconducting BSCCO, we measured thermal conductivity in single crystals of yttrium-doped BSCCO (YBSCCO), an insulating analogue of pure BSCCO, in a temperature range between 40 mK and 2 K (see first figure). Temperature dependence of the thermal conductivity of insulating samples changes from $T^{1.7}$ between 1 and 2 K to $T^{2.6}$ below 200 mK, indicating saturation of the phonon mean free path with decreasing temperature. Overall, thermal conductivity of the insulating samples (which is due entirely to phonons) is strongly suppressed in comparison to that of the superconducting samples. This leads us to conclude that a large (and at the lowest temperature end, predominant) part of total thermal transport in superconducting BSCCO is performed by electrons, which are responsible for the 200 mK transition.

In our theoretical work this year we generalized our ideas developed earlier on the basis of interaction of the d-wave condensate with magnetic impurities into a statement of marginal stability of a $d_{x^2-y^2}$, by considering the effect of magnetic field on the d-wave condensate. We discovered that the d_{xy} component is generated in a d-wave superconductor in the magnetic field. As one enters the superconducting state at finite field, the normal to superconducting transition occurs into bulk $d_{x^2-y^2} + i\, d_{xy}$ state (see second figure). The driving force for the transition is the linear coupling between the magnetic field and the nonzero magnetization of the $d_{x^2-y^2} + i\, d_{xy}$ condensate. The external magnetic field violates parity and time-reversal symmetries, and the nodal quasiparticle states respond by generating the id_{xy} component of the order parameter, with the magnitude estimated to be on the order of few Kelvin. Parity (P) and time-reversal (T) symmetries are violated in this state.

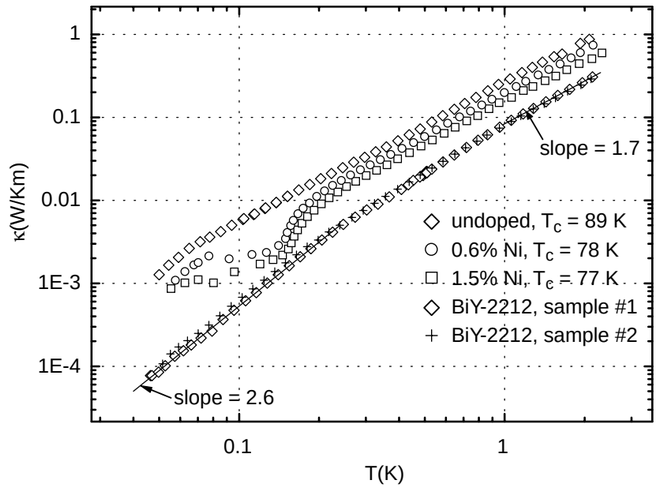

Thermal conductivity of several superconducting BSCCO samples and its insulating analogue BY-2212, Y-doped BSCCO samples. Insulating samples clearly have much lower conductivity than superconducting ones, suggesting that at very low temperature, most of the heat in superconducting samples is carried by electrons.

Publications

Balatsky, A.V., "Field induced $d_{x^2-y^2}+id_{xy}$ State and Marginal Stability of High-T_c Superconductors" (submitted to *Phys. Rev. Lett.*).

Balatsky, A.V., "Spontaneous Parity and Time Reversal Violation in *d*-Wave Superconductors" (to be published in *J. Supercond.*).

Balatsky, A.V., and R. Movshovich, "Marginal Stability of *d*-Wave Superconductor," *Physica B* **259**, 446 (1999).

Jaime, M., et al., "Heat Capacity of Ni-Doped BSCCO Single Crystals" (to be published in *Physica B*).

Mao, W., and A.V. Balatsky, "Finite DOS in a Mixed State of $d_{x^2-y^2}+id_{xy}$ Superconductor," *Phys. Rev. B* **59**, 6024 (1999).

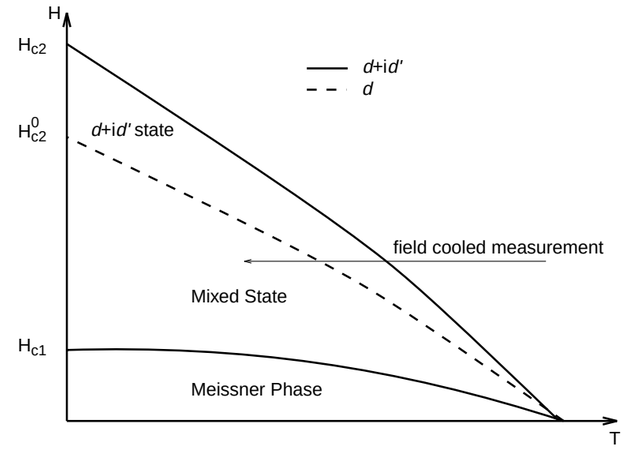

The (H,T) phase diagram of d-wave superconductor. Magnetic field leads to introduction of the $d_{x^2-y^2}+id_{xy}$ state above the usual mixed (vortex) state.

Intrinsic Nonlinear Local Modes in Low-Dimensional Materials

99042

Andrew P. Shreve

Intrinsic localization of vibrational energy to form intrinsic localized modes (ILMs) has long intrigued scientists in fields ranging from biology to condensed-matter physics because of its deep implications for focusing and transport processes in many general classes of materials. However, progress in this field has been largely stalled by poor understanding about how to create and study ILMs experimentally.

This project is aimed at developing and using optical spectroscopic techniques for this purpose. The work requires strong collaboration between experiment and theory. Fully nonlinear and nonadiabatic models must be employed to interpret results and guide new experimental design, while conversely, experimental results, including measurements of dynamics, are needed to benchmark further model development.

We have focused on the class of materials known as halide-bridged mixed-valence transition metals, or MX materials. These materials are characterized by very strong electron-phonon coupling, and the resulting lattice nonlinearities lead to the existence of localized vibrational states. Further, we have shown that, because of the source of the nonlinearity, resonance Raman spectroscopy provides an ideal probe of localized vibrational states in these materials.

This year we completed characterizing spectroscopic observables associated with ILMs in MX materials. We explored the signatures of strong electron-phonon coupling in resonance Raman excitation profiles, that is, in the dependence of the Raman scattering on the excitation energy. This work has required the development of experimental techniques for near-ultraviolet and deep blue resonance Raman experiments. We developed time-resolved Raman capabilities, with initial experiments indicating the occurrence of energy localization (self-trapped exciton formation) in electronic excited states of a particular class of MX materials.

In addition to these spectroscopic studies, we have also made advances in synthesis and theory. Synthetically, we developed new approaches to allow control of defect concentration in general halide-bridged transition-metal materials. In future work this control will allow for direct comparison of intrinsic localization with

defect-induced localization. On the theoretical side, we used exact diagonalization numerical techniques for a small $PtCl_2$ cluster to demonstrate multiphonon localization and signatures in Raman overtone red shifts consistent with experiment. We also studied effects of long-range Coulomb interactions and revealed a novel competition between nonadiabaticity and long-range Coulomb effects as a function of the number of bound quanta.

Publications

Fehske, H., et al., "Local Mode Behavior in Quasi-1-Dimensional Charge-Density-Wave Systems" (to be published in *Physica C*).

Kladko, K., et al., "Intrinsic Localized Modes in the Charge-Transfer Solid PtCl," *J. Phys.: Condens. Matter* **11**, L415 (1999).

Swanson, B.I., et al., "Observation of Intrinsically Localized Modes in a Discrete Low-Dimensional Material," *Phys. Rev. Lett.* **82**, 3288 (1999).

Alkane Chemistry of Ligated (Allyl)Iridium Moieties on Metal Oxide Supports and Multilayer Hydrogen Transport Membranes

99012

R. Tom Baker

Most industrial organic chemicals are prepared from alkenes that are obtained by energy-intensive, catalytic "cracking" of crude oil. Catalytic utilization of alkanes, obtained directly from natural gas, would save large amounts of energy and reduce waste.

Heterogenizing homogeneous catalysts has the potential to combine the qualities of selectivity and tunability found in homogeneous catalysts with the ease of separation afforded by heterogeneous catalysts. For the dehydrogenation of alkanes to alkenes, active homogeneous iridium catalysts are inhibited by the alkene products, which also undergo iridium-catalyzed isomerization to less desirable internal isomers. We are investigating the chemistry of ligated allyl(iridium) moieties on metal oxide surfaces as new alkane dehydrogenation catalysts that can be employed in gas phase reactors to minimize catalyst-product interactions.

In the first phase of this project, we significantly improved the preparation of tris(allyl)iridium and investigated its detailed structure by vibrational and dynamic nuclear magnetic resonance (NMR) spectroscopy and density functional theory. We then studied the reactivity with a variety of ligands. While "hard" ligands such as pyridine, tetrahydrofuran, and chelating diimines were unreactive, "soft" ligands such as phosphines, phosphites, isocyanides, isothiocyanates, and carbon monoxide all gave trivalent complexes in which one or more of the pi-allyl ligands were converted to sigma-allyls. In particular, reactions with mono-, bi-, and tridentate phosphine ligands gave thermally stable products with one, two, and three sigma-allyl ligands, respectively (see figure). While reactions of pi-acid ligands such as phosphites and isocyanides induced reduction of tris(allyl)rhodium to monovalent complexes, the iridium analog gave trivalent products. The increased thermal and redox stability of the trivalent allyliridium complexes, as compared to their Rh analogs, bodes well for the use of metal oxide-supported organoiridium catalysts for alkane dehydrogenation.

Publications

John, K.D., et al., "Chemistry of $M(allyl)_3$ (M = Rh, Ir) Compounds: Structural Characterization of Tris(allyl)iridium Complexes with Phosphorus Ligands" (to be published in *Chem. Commun.*).

John, K.D., et al., "Comparing Ligand Chemistry of $M(allyl)_3$ (M = Rh, Ir)" (submitted to *Organometallics*).

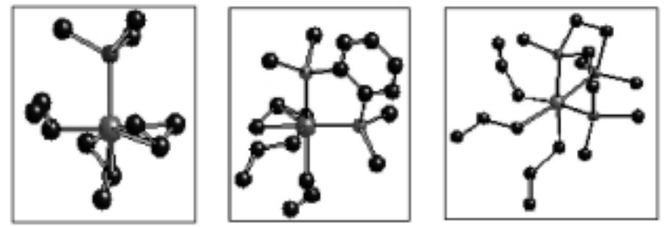

A B C

Ball-and-stick view of the molecular structures of tris(allyl)iridium with monodentate (A), bidentate (B), and tridentate phosphine ligands (C). Phosphine-phenyl groups are represented by a single ball. The ease with which the pi-allyl ligands are converted to the sigma-allyls with increasing substitution demonstrates the electronic flexibility of the tris(allyl)iridium moiety.

Classical Kinetic Mechanisms Describing Heterogeneous Ozone Depletion

97023

Bryan F. Henson

Since the first report of the south polar "ozone hole," field observations and laboratory measurements have established that heterogeneous (gas/surface) reactions on polar stratospheric cloud (PSC) particles activate gas phase chemical reactions and sedimentation processes that are directly responsible for north and south polar ozone depletion. In a stratospheric system of fixed relative humidity and reagent vapor pressures, these reactions will be coupled in a complex manner by the surface concentration of reagents and products.

We have developed a surface sensitive experimental probe of adsorption on ices under stratospheric conditions and a complementary theoretical model of the impact of adsorption on heterogeneous chemistry. We are applying these techniques to the full heterogeneous kinetic mechanism of the coupled system of stratospheric reactions, including the competition between Langmuir-Hinschelwood and Eley-Rideal kinetic rates. This example of the determination of a heterogeneous kinetic mechanism on a complex substrate may illuminate many other applications in environmental chemistry and build a methodology by which other important heterogeneous reaction schemes may be addressed.

Our experiments on the adsorption behavior of a second halogen halide species on ice, HBr, complement and extend the theory and modeling developed for the HCl/ice system, in which we determined the interfacial thermodynamic phase and related it to the bulk phase diagram for the binary HCl/H_2O system. We obtained experimental measurements of the vapor pressure and HBr coverage of ice for a number of temperatures. Analysis indicates that the same relationships between the interface and bulk thermodynamics obtained for HBr apply for HCl. This is a significant improvement in the understanding of the interfacial thermodynamics for both of these species, which together play an important role in atmospheric heterogeneous chemistry.

We have also completed application of our theory for heterogeneous hydrolysis reactions in the lower stratosphere to the literature data. We applied the model to the hydrolysis reactions of chlorine nitrate and dinitrogen pentoxide on nitric acid trihydrate, sulfuric acid tetrahydrate, and sulfuric acid monohydrate ice surfaces. We compared calculations to data taken in several laboratories, as the figure shows. With one exception, the model describes the entire literature data set. As reported, the data display significant nonlinearities as a function of temperature and pressure. In the figure the set has been linearized, according to the model, by plotting the reaction probability, γ, divided by the reaction probability on an ice surface, γ_o, as a function of the coverage, θ.

We have also completed a set of experiments on the uptake of acetone by ice. Acetone is an important tropospheric species that was believed to participate in the chemical cycle controlling OH radical concentrations. Adsorption of acetone on ice has been implicated as a reservoir for acetone, removing it from the gas phase. We have obtained data on the vapor pressure and coverage of acetone on ice, and our analysis indicates that uptake of acetone by ice is much too small to serve as such a reservoir.

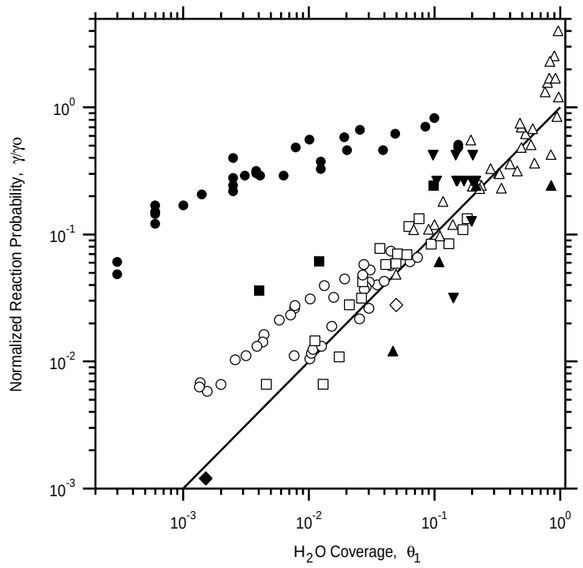

Shown are measurements of the normalized reaction probability for hydrolysis on three different acid hydrate ices as a function of the H_2O coverage on the hydrate surface, theta. The reaction probability is normalized by dividing the observed probability over the hydrate surface by that observed over pure H_2O ice. The data, taken from several laboratories, are a function of temperature and pressure. The solid line is the normalized reaction probability calculated from the model.

Publications

Dubey, M.K., et al., "Measurements of Acetone Interactions with Ice: Are Cirrus Clouds a Sink for Acetone?" (submitted to *Geophys. Rev. Letters*).

Henson, B.F., et al., "Experimental Isotherms of HCl on Ice under Stratospheric Conditions" (submitted to *Nature*).

Fundamental Process in Polymer Light-Emitting Electrochemical Cells

98011

Darryl L. Smith

A polymer light-emitting electrochemical cell (LEC) is a recently invented organic light-emitting device. An LEC consists of a doped polymer layer that is luminescent and ionically and electronically conductive. The polymer is contacted by two metallic electrodes. The polymer layer is doped with an ionic salt. When a sufficient voltage bias is applied to the cell, ions from the dissolved salt are spatially separated. The ions dope the polymer p-type near the anode and n-type near the cathode, making it electronically conductive. An electrochemical junction forms between the p-type and the n-type doped polymer. Electrons injected from the n-type side of the junction recombine with holes injected from the p-type side of the junction emitting light. Polymer LECs offer a number of potential advantages over organic light-emitting devices, including insensitivity to variations in device thickness and to the type of metal used to form the contacts.

The electrochemical junction in an LEC is completely different from a conventional p-n junction in inorganic semiconductors. In a conventional p-n junction, there is a large built-in junction potential at zero bias caused by charge transfer between the p- and n-type doped regions. The charge transfer creates the ionic space-charge region that produces the junction potential. In contrast, in the LEC there is no junction potential at zero bias because the n- and p-type regions in the polymer have not yet been formed. In forward bias in a conventional p-n junction, the bias opposes the built-in junction potential and decreases it but does not reverse its direction. In contrast, in the LEC in forward bias, there is no built-in potential to oppose, and the electric field in the junction is in the same direction as the external bias. The carriers in the LEC junction move by drift in the electric field in the junction.

We performed capacitance-voltage and current-voltage measurements of polymer LECs and compared these results with steady-state device model calculations. The capacitance-voltage characteristic was used to assess the formation and structure of the electrochemical junction in the device. The cell capacitance and current both increase sharply above a threshold voltage as the bias is increased. The steady-state device model is in good agreement with these observations.

We investigated the structure of the electrochemical junction formed during the operation of the LECs using a combination of electrical alternating-current impedance spectroscopy and optical electroabsorption techniques. Using small-signal impedance spectroscopy at frequencies high enough that the electrical response of the LEC is dominated by electrical and not ionic transport, we determined the capacitance that is due to the electrical junction in the LEC. This electronic capacitance determines the effective separation of the electrons and holes forming the junction. The width of the electrical junction is extremely important.

Publications

Campbell, I.H., and D.L. Smith, "Physics of Polymer Light-Emitting Diodes," in *Semiconducting Polymers—Chemistry, Physics and Engineering*, G. Hadziioannou and P. Van Hutten, Eds. (VCH-Wiley, New York, 1999).

Campbell, I.H., and D.L. Smith, "Schottky Energy Barriers and Charge Injection in Metal/Alq/Metal Structures," *Appl. Phys. Lett.* **74**, 561 (1999).

Campbell, I.H., et al., "Charge Transport in Polymer Light-Emitting Diodes at High Current Density," *Appl. Phys. Lett.* **75**, 841 (1999).

Campbell, I.H., et al., "Consistent Time-of-Flight Mobility Measurements and Polymer Light-Emitting Diode Current-Voltage Characteristics," *Appl. Phys. Lett.* **74**, 2809 (1999).

Crone, B.K., et al., "Charge Injection and Transport in Single-Layer Organic Light-Emitting Diodes," *Appl. Phys. Lett.* **73**, 3162 (1998).

Gao, J., et al., "Direct Observation of Junction Formation in Polymer Light-Emitting Electrochemical Cells," *Phys. Rev. B. Rapid Comm.* **59**, R2482 (1999).

Soluble Polymers for Enhancing Biocatalysis

98013

Nancy Sauer

Natural and synthetic soluble polymers have been shown to significantly enhance enzymatic activity and stability, but limited information is available that correlates enzyme functional changes with specific polymer-enzyme interactions. This research develops an understanding of the molecular interactions between soluble synthetic polymers and enzymes affecting biocatalysis, thus increasing the utility of biocatalysts for synthetic, sensor, waste treatment, and decontamination applications.

We used organic and aqueous soluble polyamines of three structural types (linear, branched, and spherical) as backbones for enzyme stabilizing systems. The affinity of these polymers for enzymes and their predominant interaction mode was controlled by incorporation of various functional groups at the amine sites on the polymers. We selected two enzymes for study—yeast alcohol dehydrogenase (ADH) and subtilisn (SUB). These enzymes are capable of numerous chemical conversions on a variety of nonchiral and chiral substrates. We were able to correlate biocatalyst activity and structure in the presence of polymers with the structure and function of the associated polymer. This correlation can identify the critical interactions that result in enhanced biocatalyst activity.

A principal focus this year was the determination of the mechanism of enzyme stabilization by water-soluble polymers. Specifically, we evaluated four polymers with differing ionic, coordinating, and hydrogen-bonding characteristics for stabilization and activation of ADH and SUB. These four are polyacrylic acid (PAA), a commercially available anionic polymer with ionizable carboxylate groups; polyethylenimine (PEI), a commercially available cationic polyamine; and two derivatives of PEI (PEIM [permethylated PEI] and PEI-SO3 [a zwitterionic polymer with approximately 25% of the amines functionalized with alkylsulfonate groups]).

Data on the decay of enzyme activities in the absence of polymers (buffer only) and in the presence of ammonium sulfate and acrylic acid demonstrate that all of the polymers examined stabilized SUB enzyme activities (see first figure). The half-lives for SUB activity are increased 12 to 450 times in the presence of different water-soluble polymers. Notably, cationic (PEI and PEIM), anionic (PAA), and zwitterionic (PEI-SO3) polymers are all capable of stabilizing SUB. Similar results were seen for ADH. For the polymers PEIM, PEI, PEI-SO3, and PAA, the effects of polymer functionality on enzyme stability appear to follow a similar trend for both the ADH and the SUB enzymes. The second figure shows the stability enhancement for each of the polymers for both enzymes. This trend in enzyme stabilization approximates the Hoffmeister order of the charged groups on the polymer.

These observations suggest that (1) the mechanism(s) for enzyme stabilization by water-soluble polymers are similar for ADH and SUB and (2) the mechanism(s) may be related to the well-studied Hoffmeister effects of electrolytes on protein stability.

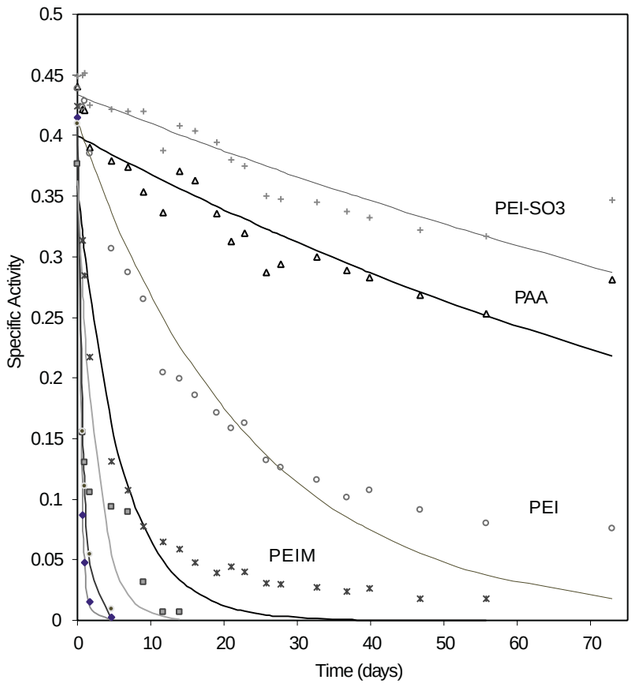

Effect of polymers on subtilisn inactivation.

Publications

Vanderberg, L.A., et al., "Treatment of Heterogeneous Mixed Wastes: Enzyme Degradation of Cellulosic Materials Contaminated with Hazardous Organics and Toxic and Radioactive Metals," *Environ. Sci. and Tech.* **33**, 1256 (1999).

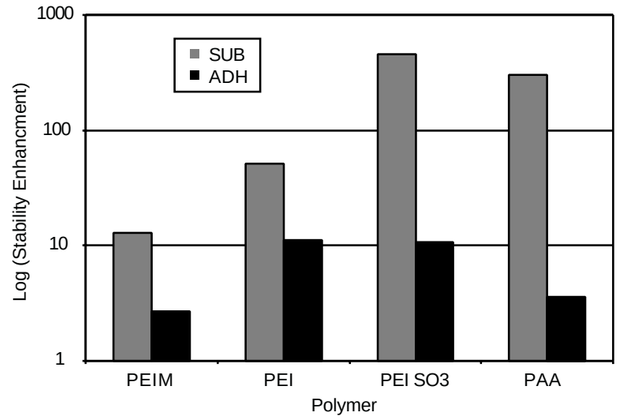

Trend of enzyme stability enhancement with polymer functionality.

Supported Technetium Chemistry

99014

Carol Burns

We seek to apply solid-phase synthesis techniques to investigate the heterogenized coordination chemistry of technetium. Our principal goal is to determine if the analogy between homogeneous (solution) and supported (solid) reactivity can be experimentally validated, or if the local environment within a polymer dramatically affects the reactivity of the metal. Put simply, we want to be able to attach metals to the polymer to test the principle that solid-supported chemistry is a good analogy for solution chemistry. This would permit us to examine a broader range of technetium chemistry while controlling the possible spread of contamination (technetium is a beta-emitter whose oxides are volatile and spread easily).

We identified the means to purify intended polymeric substrates (divinylbenzene cross-linked polystyrene) and developed routes to chemically add functional groups to provide sites for metal attachment. The initial means of attachment we chose to investigate involved the generation of metal-imido linkages by the reaction of a metal oxo species (MO_4^-, $(Me_3SiO)MO_3$, where M = Re, Tc) with a polymer support functionalized by isocyanate groups. Although we investigated several ways to generate isocyanate-containing functional groups on the resins, the most effective way for us to introduce these reactive sites has been the reaction of amine-functionalized resins with triphosgene. We found that the reaction of the metal oxo species with these supports allowed ready attachment of the metal complex to the support. The kinetics of this attachment appears to demonstrate rapid binding.

In collaboration with researchers at Lawrence Berkeley National Laboratory, we studied the mode of attachment of these metal-containing species with x-ray absorption spectroscopy (XAS). Extended x-ray absorption fine structure spectra of $(Me_3SiO)TcO_3$-loaded polymers demonstrate that the technetium remains in the heptavalent oxidation state; these data may be fit to a model consistent with the formation of imido functional groups. Similar studies on rhenium-containing species demonstrate that initial reduction of the rhenium center occurs upon binding. Preliminary leaching studies suggest that the imido linkages are quite robust; we observe little leaching of the metal under acid or base conditions. We also investigated generating polymers functionalized with "linkers" (molecular spacers between the polymer backbone and the metal attachment site). In particular, we chose to investigate the generation of polymers derivatized with cleavable linkers: silyl-containing functional groups that are readily degraded by certain reagents. While chemistry on the solid support is the ultimate goal, it is difficult to characterize the precise chemistry in the solid state. By employing cleavable linkers, we can put the metal-containing species back in solution to facilitate characterization.

Recombination Kinetics: Correcting the Textbooks

97007

Russell T. Pack

Recombination is one of the most basic types of chemical reaction. Current kinetics texts and literature assume that it occurs only by sequences of two-body collisions. We are now doing the first-ever, exact quantum calculations to verify that true three-body collisions are not only important but often dominant for atomic recombination. Our research contributes to the Laboratory's theory, modeling, and high-performance computing core competency. Our calculations are lending new understanding to the fundamental theory of chemistry, requiring the rewriting of kinetics textbooks and changing the way chemists treat recombination. Codes using our new methods will make it possible to compute the rates of reactions that have been previously impossible computationally.

We are getting the word out to physical chemists that atomic recombination involves true three-body collisions. Two major papers appeared. We tested and published our new method for calculating hyperangular surface functions for all total angular momenta.

When we performed approximate calculations for the reaction Ne + Ne + H $\Leftrightarrow$ Ne_2 + H for the three isotopic cases in which the neon dimer formed is $^{18}Ne_2$, $^{16}Ne^{18}Ne$, and $^{16}Ne_2$, we received an unexpected bonus. The resulting rates showed a sizeable anomalous or "mass-independent" isotope effect for the unsymmetric dimer. A very similar effect occurs in the more complicated reaction that forms ozone in the stratosphere—a puzzling effect that has gone unexplained for 20 years. In the present case, because we calculated the full rate coefficient matrix, we were able to determine what caused the effect and explain it fully. We expect in future work to also explain this effect for ozone.

Progress toward exact quantum calculations on the neon reaction just shown continues. We have done much coding and debugging during this year; checked the convergence of the pieces of the program; programmed the different boundary conditions that apply for bound, quasibound, and free states; and put the whole program together. We are very close to fully converged results.

Publications

Kendrick, B.K., et al., "Hyperspherical Surface Functions for Nonzero Total Angular Momentum. I. Eckart Singularities," *J. Chem. Phys.* **110**, 6673 (1999).

Zeman, V., et al., "A Treatment of the tm + D_2 Reaction by the Methods of Quantum Reactive Scattering" (submitted to *Phys. Rev. A*).

Characterization of Propane Monooxygenase

97024

Pat Unkefer

Chlorinated hydrocarbons, which have been widely used by industry, are the cause of widespread soil and ground-water contamination. Because they have been shown to degrade chlorinated compounds, including trichloroethylene (TCE), a number of bacterial strains are being considered as bioremediation agents.

Reports had indicated that the propane monooxygenase (PMO) from Mycobacterium vaccae degraded TCE by a mechanism other than the formation of the epoxide, indicating that it might be an important alternative to methane monooxygenase for bioremediation of TCE-contaminated sites. However, PMO had not been isolated and had remained largely uncharacterized. This project aimed at the first characterization and examination of the PMO mechanism.

Our work on PMO substrate specificity produced results inconsistent with reports of earlier work. Specifically, the unusual character of this enzyme is now in question because the enzyme is, in reality, quite similar to methane monooxygenase (MMO), a very well studied and characterized enzyme. We concluded that the published literature describing previous work on PMO contains errors relating to the key differences in substrate specificity between PMO and MMO. Thus, our postulation that the chemical mechanism for PMO is distinctly different from the MMO mechanism was incorrect. PMO's distinct lack of unique character causes us to forgo further study.

Utilization of High-Nitrogen Compounds

99053

Michael A. Hiskey

The high-nitrogen compound 3,6-dihydrazino-s-tetrazine (DHT) can be used as a pyrotechnic fuel that requires small amounts of metal salts for coloring the flame. In addition, DHT pyrotechnic formulations using nonmetallic oxidants, specifically ammonium perchlorate and ammonium nitrate, produce little smoke when burned. These mixtures are more environmentally friendly than traditional mixtures, which are heavily formulated with metallic salts. Our research on these pyrotechnic formulations received a 1998 R&D Award. As a follow-on to this research, we have extended our focus to two other high-nitrogen fuels, bis-(1(2)H-tetrazol-5-yl)-amine monohydrate (BTAw) and 5,5'-bis-1H-tetrazole (BT), and their salts as likely candidates for low-smoke pyrotechnic fuels. This research is also an offshoot of our high-nitrogen synthesis project to synthesize insensitive high-nitrogen explosives and gas generants.

We prepared three high-nitrogen substrates and their salts and investigated their utility in low-smoke applications. Two of the three substrates, BTAw and BT, can react with basic amines to form mono- and diaminated salts and with metal carbonates or hydroxides to form metal salts. The third substrate, DHT, reacts with certain acids to yield potentially useful flame-coloring ingredients.

To compare high-nitrogen with traditional flames, we gathered the spectral data of a large variety of burning high-nitrogen and traditional formulations. We then converted this data into useful C.I.E. (International Commission on Illumination) 1931 color coordinates, which is a standard method of characterizing visually observed color in a two-dimensional coordinate system. We found that mixtures of high-nitrogen fuels and oxidant ammonium perchlorate require only 1–7 wt % metal colorants to achieve purer flame colors. This level of metal content is approximately an order of magnitude less than that found in traditional pyrotechnic formulations, which can be as high as 50 wt % or more.

Traditional formulations are known to burn with abundant smoke, and often ash as well, which are attributed to partial combustion and the generation of nongaseous products, particularly metal oxides. Furthermore, some traditional formulations use chlorinated polymers for color enhancement, and this has done little to decrease the amount of noxious smoke. The Laboratory has submitted a patent application entitled "Low-Smoke Pyrotechnic Compositions." The patent is primarily concerned with the use of BTAw, BT, and their salts as low-smoke pyrotechnic fuels.

In addition to spectral analyses, we performed a variety of sensitivity tests to provide baseline hazards for these high-nitrogen pyrotechnic ingredients, as well as thermogravimetric analyses to provide stability data.

Publications

Chavez, D.E., et al., "High-Nitrogen Fuels for Low-Smoke Pyrotechnics," *J. Pyrotech.* **10**, 17 (1999).

Chavez, D.E., et al., "The Utility of High-Nitrogen Compounds in Explosive, Pyrotechnic, and Propellant Applications" (Life Cycles of Energetic Materials, Orlando, FL., Sept. 1999).

Ultrafast, Solid-State Electron Transfer in Donor-Acceptor Conducting Polymers

97025

Duncan McBranch

Electron transfer in conducting polymers is a promising new field of photochemistry. In these systems, charge transfer occurs in less than 200 fs, with near unity quantum efficiency, and is metastable with an asymmetry in the forward and back transfer rates of up to 9 orders of magnitude. We are applying femtosecond spectroscopy to study the dynamics of charge transfer: the excitation events, the charge transfer itself, and the stabilization mechanism. These data will allow us to determine the nature of the excited state, to understand the mechanisms resulting in asymmetry in the forward and back transfer rates, and to design chemically modified, optimized charge-transfer systems.

This year we finished a comprehensive study of the photoexcitations in conjugated polymers, including excitons and charge-transfer excitations created by both donor-acceptor electron transfer and interchain electron transfer intrinsic to undoped polymers in the solid state. We identified universal features in the transient absorption spectra and dynamics that are common to many different fluorescent polymers in the polyphenylene vinylene family. In addition, we observed a new spectral feature in the mid-infrared spectrum caused by "hot" excitons and observed, for the first time in oriented polymer samples, the conversion of intrachain excitations polarized along polymer chains to charge-transfer excitations polarized transversely to the chains. This work forms the basis for a complete understanding of the optical excitations in these polymers.

In addition, we discovered a novel and extremely powerful manifestation of ultrafast charge transfer in solution: subpicosecond donor-acceptor electron transfer in systems consisting of anionic (negatively charged) polymers, together with cationic (positively charged) electron-acceptor molecules such as methylviologen. In these water-soluble polymers, we observed a million-fold amplification of sensitivity to electron-transfer quenching, relative to the quenching observed for small molecules with similar chemical structure. We harnessed this amplified sensitivity to design a new class of sensitive and selective biological sensors.

Publications

Chen, L., et al., "Highly-Sensitive Biological and Chemical Sensors Based on Reversible Fluorescence Quenching in a Conjugated Polymer" (to be published in *Proc. Natl. Acad. Sci. U.S.A.*).

Kirova, N., et al., "Excitations and Optical Properties of Phenylene-Based Conjugated Polymers," *Synth. Met.* **101**, 188 (1999).

Kraabel, B., et al., "A Unified Picture of the Photoexcitations in Conjugated Polymers: Universal Spectral and Dynamical Features in Subpicosecond Transient Absorption" (submitted to *Phys. Rev. B.*).

McBranch, D.W., et al., "Signatures of Excitons and Polaron Pairs in the Femtosecond Excited-State Absorption Spectra of Conjugated Polymers and Oligomers," *Synth. Met.* **101**, 291 (1999).

McBranch, D.W., et al., "Universal Ultrafast Photoexcitation Signatures in Conjugated Polymers" (SPIE Conference, Organic Light-Emitting Materials and Devices, Denver, CO, July 1999).

Wang, H.-L., et al., "Controlled Unidirectional Energy Transfer in Luminescent Self-Assembled Conjugated Polymer Superlattices" (to be published in *Chem. Phys. Lett.*).

Xu, S., et al., "Ultrafast Relaxation of Excitons in Polyfluorene" (submitted to *Phys. Rev. Lett.*).

Novel Surfactants and Micellar Chemistry for Enhanced Reactivity and Separations

99013

John G. Watkin

We are developing an environmentally benign, energy-efficient method for carrying out catalytic reactions using aqueous two-phase micellar catalysis without organic solvents (i.e., employing water and dense-phase CO_2 only). This program brings together expertise in synthesis, catalysis, micelle and surfactant chemistry, and physical characterization to develop and understand new micelle-forming catalyst systems.

Our research will demonstrate an important new scientific concept for catalyst use and recovery. The combination of micellar catalysis with transition metal–mediated chemistry will lead to a set of new surfactants, modified catalysts, and chemical processes. New catalytic techniques developed during this project should help overcome major economic and environmental challenges to catalysis science and practice. They are expected to produce significant economic and environmental benefits by reducing the use of hazardous solvents, by improving the recovery of expensive and possibly toxic catalysts, and by minimizing waste generation and energy utilization.

To demonstrate the advantages of water/CO_2 emulsions for biphasic homogeneous catalysis, we have begun to initially study the hydrogenation reaction of olefins, using the catalyst $RhCl(tppds)_3$, where tppds is tris(3,5-disulfonatophenyl)phosphine ligand (L). We used three different surfactants that we have found to form water/CO_2 emulsions: (a) anionic surfactant perfluoropolyether ammonium carboxylate, (b) cationic Lodyne 106A, and (c) neutral poly(butylene oxide)-*b*-poly(ethylene oxide). Using optical microscopy, we measured the PBO-*b*-PEO and PFPE micelles to be 3 to 5 µm, whereas the Lodyne 106A was found to be 10 to 15 µm. We obtained the time profile, using the formation of product ethyl benzene, for the hydrogenation of styrene for the three surfactants and in control experiments run in two-phase water/CO_2 and water/toluene systems without surfactants (see figure). The two-phase water/CO_2 is clearly more reactive than the water/toluene system. The reaction rate for styrene hydrogenation increases significantly upon addition of surfactant and emulsion formation.

Phase separation and catalyst recycle have also been investigated. During the reaction at 4000 psi, the system is a milky white emulsion. When the reaction is complete, the pressure is decreased and the pump and magnetic stirring are stopped. After standing for about 10 min, complete phase separation occurs with supercritical CO_2 above the aqueous catalyst phase. The product, which is soluble in CO_2 above certain pressures, can be recovered by transfer and subsequent pressure letdown, also allowing for CO_2 recycle. The lower aqueous phase contains the rhodium, ligand, and water-soluble surfactant, in the case of PBO-*b*-PEO or Lodyne 106A. For the water-insoluble PFPE surfactant, a third phase that is due to the high density of the surfactant forms below both the CO_2 and aqueous phases. Catalyst recycle was demonstrated by transferring the product-containing CO_2 phase under pressure to a separate high-pressure reactor and then charging the aqueous phase, still containing the catalyst and surfactant, with more H_2, CO_2, and alkene. Using this method, we have found that the catalyst activity remains essentially constant for at least three cycles, demonstrating efficient catalyst recycle.

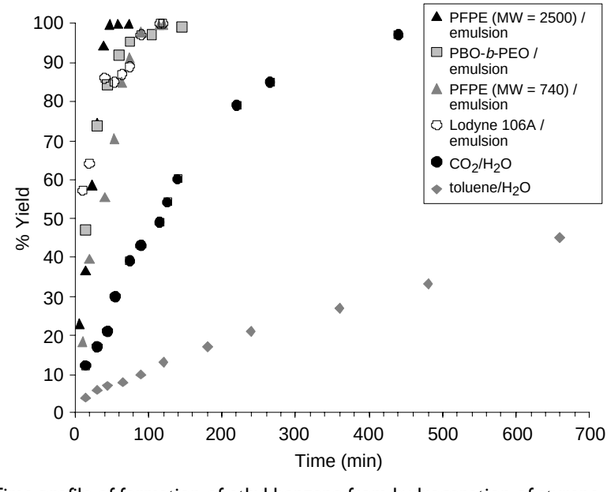

Time profile of formation of ethyl benzene from hydrogenation of styrene performed in biphasic water/toluene, biphasic water/CO_2, and in water/CO_2 or CO_2/water emulsions, using four different surfactants. Reaction conditions are 50/50 wt % water/CO_2 (4.75 g each), 1.5 wt % surfactant, 80 mM styrene, 1 mol % catalyst, Rh/L = 1/6, 40°C, and 4000 psi.

Publications

Jacobson, G.B., et al., "Enhanced Catalyst Reactivity and Separations Using Water/Carbon Dioxide Emulsions," *J. Am. Chem. Soc.* **121**, 11902 (1999).

Unraveling Heterogeneous Surface Reaction Kinetics

98012

William Patrick Ambrose

When a system of molecules is heterogeneous in nature, a bulk measurement masks the behavior of molecules that are different from the mean. Unexpected heterogeneous behavior was uncovered recently in nominally homogeneous systems only by examining individual molecules. We have built optical microscopes that we have used to investigate the optical properties of single molecules. In this project we are observing and studying the nature of the interactions between single immobilized and single solvated molecules. The unique concept that sets this work apart from other surface reaction techniques is that interesting details will be uncovered that are normally masked by bulk averaging. This analysis technique will be useful in the interpretation of the operation and improved design of sensors based on molecular binding and recognition.

This year we explored three types of total internal reflection (TIR) excitation and imaging of single molecules and found that prism TIR produces the best signal-to-background ratio, while through-objective TIR excitation produces the best total signal before photo-bleaching.

We also developed a flow cell compatible with the requirements of single molecule detection while using total internal reflection excitation (optical access to a wall of the flow cell for excitation and imaging with a high numerical aperture objective and obtaining a low optical background). We performed preliminary experiments showing binding of individual molecules to a wall of the flow channel under flowing conditions.

Publications

Ambrose, W.P., et al., "Single Molecule Detection with Total Internal Reflection Excitation: Comparing Signal to Background and Total Signals in Different Geometries," *Cytometry* **36**, 224 (1999).

Ambrose, W.P., et al., "Single Molecule Fluorescence Spectroscopy at Ambient Temperature," *Chem. Rev. Thematic Issue: Chemical Analysis in Small Domains* **99**, 2929 (1999).

Brooks, S.A., et al., "Micron Dimension Derivatization of Biosensor Surfaces Using Confocal Dynamic Patterning," *Anal. Chem.* **71**, 2558 (1999).

Nonadiabatic Processes in Chemical Reactions

99015

Brian K. Kendrick

In the past, most theoretical methods for treating chemical reactions were based on the simplifying adiabatic approximation that ignores nonadiabatic processes. In recent years, it has become clear that the discrepancies between experiments and theoretical treatments of reactions as simple as $H + D_2 \rightarrow HD + D$ may be the result of theoretical treatments that ignore these nonadiabatic processes. Treating these processes properly from a theoretical standpoint has been very difficult and computationally challenging, but we have developed some novel methods that may allow for an accurate treatment of these processes for the first time. We expect to develop new techniques that will help to resolve the current discrepancy existing between recent experimental results and previous theoretical treatments for the above reaction at high energies. This work contributes to the fundamental understanding of chemistry and to competency in theory, modeling, and high-performance computing.

We have made great progress this year. We finished developing our methods for including the nonadiabatic processes that occur at low collision energies and applied them to the reaction, $H + D_2 \rightarrow HD + D$. We have completed calculations for the first six values of total angular momentum (i.e., the values of J from 0 to 5). Our results show that the effects of nonadiabatic processes cancel out at low energies when the contributions from each value of J are added together (see first figure). These results were quite unexpected, but they are consistent with recent high-resolution experiments. In order to make direct comparison with experimental results, many more values of J must be included (i.e., all values of J that are less than 45). These calculations will require significant computational resources on massively parallel machines.

We have also applied our new methods to compute the rovibrational spectra of $Na_3(X)$ for values of J less than 2. The effects of low-energy nonadiabatic processes are quite significant in this system. Our preliminary results predict significant shifts in the energy levels (see second figure). We are currently using quantum chemistry codes to develop an improved potential energy surface for this system that will make our rovibrational energy levels more accurate.

Publications

Kendrick, B.K., et al., "Comment on 'On the Longuet-Higgins Phase and Its Relation to the Electronic Adiabatic-Diabatic Transformation Angle,' " *J. Chem. Phys.* 110, 7594 (1999).

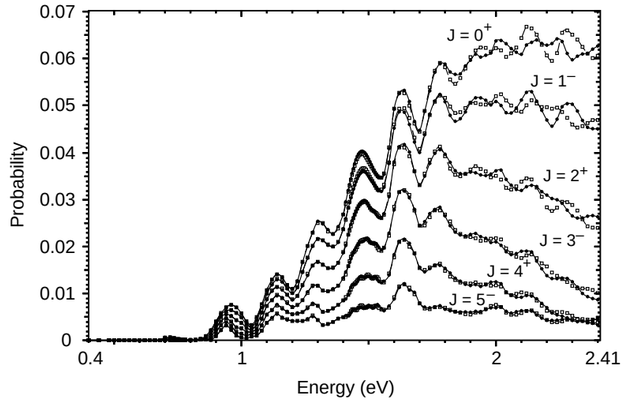

Reaction probability for H + D_2 (v=0 j=0) → HD(v′=I j′=0) + D for several values of total angular momentum J. The solid data points include nonadiabatic processes, whereas the open squares do not. The two kinds of data alternate "phase" between even and odd values of J, leading to a complete cancellation of the nonadiabatic effects.

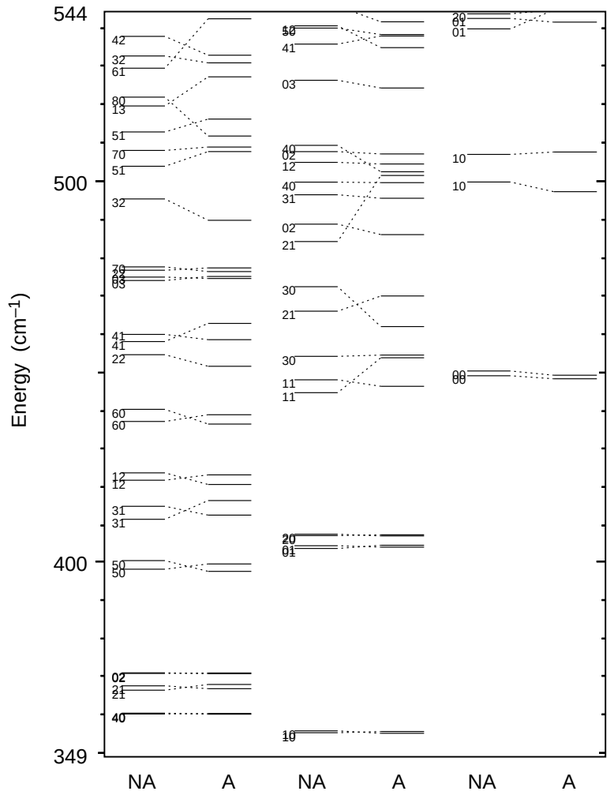

Vibrational energy levels of $Na_3(X)$ for J=0. The energy levels that lie above the NA include nonadiabatic processes, whereas those that lie above the A do not. Nonadiabatic processes give rise to large shifts in the energy levels, resulting in a reordering of many levels.

Description of Complex Adsorption from a Simple Equation of State

99016

Bryan F. Henson

We are developing new equations of state to describe the adsorption and interfacial thermodynamics of volatile systems, such as aerosols or ice particulates. We have developed a nonlinear light-scattering technique to measure surface coverage under the unique, high-pressure conditions necessary for the stability of these systems. With this technique we have begun to determine the equations of state for some important environmental systems. As a fundamental extension of this work, we are developing an equation of state for surface melting in homogeneous systems, an important and poorly understood phenomenon.

We are studying chemical systems of direct relevance to atmospheric aerosols. The theoretical and experimental work will illuminate the important role of aerosols in global change, atmospheric chemistry (ozone depletion), and the transport of pollutants and chemical and biochemical warfare agents.

We have modeled data from Los Alamos and other laboratories on multiple-layer adsorption in heterogeneous, volatile systems (e.g., methane on ice and water on acid hydrates), using the Brennauer, Emmett, and Teller equation of state with a surface equilibrium constant formulation derived at Los Alamos. It has been shown that energies of adsorption in the heterogeneous system are thermodynamically consistent with energies of sublimation and vaporization in the pure components. We have finalized the new theory of quasi-liquid formation, have shown that the thickness and coverage of a quasi liquid may be calculated as a polynomial in the activity of the vapor/solid system, and have verified this against data for H_2O and toluene. The derivation is interesting and, since it is formulated in terms of the bulk solid and liquid energies, will pertain to the proper thermodynamic description of the quasi-liquid phase. In the three accompanying figures, we show the second harmonic intensity from the surface of ice, vapor pressure measurements for amorphous and crystal ices, and the possibility of a new regime of surface liquid formation at the amorphous/crystalline phase transition, respectively.

Development continues on a resonant nonlinear optical capability to enhance our nonresonant, second harmonic generation (SHG) technique. Using SHG, we obtained data on the amorphous and crystalline phases of H_2O and methylbenzene ices. Data on H_2O ice revealed the transition from amorphous solid water to ice (ASW/I_c) and an equilibrium feature of large signal near melting, which may be associated with the quasi liquid.

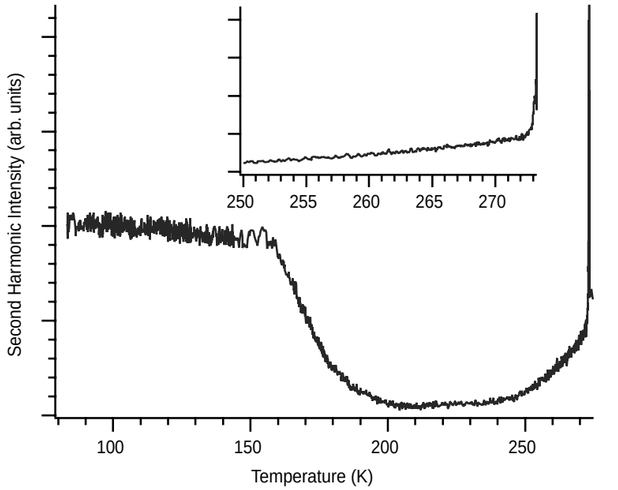

SHG intensity during the heating of a low-density ASW sample. The decrease in signal at approximately 160 K is correlated with the ASW/I_c transition. The signal increase near melting (expanded scale) is a reversible, equilibrium feature, which may be correlated with quasi-liquid formation.

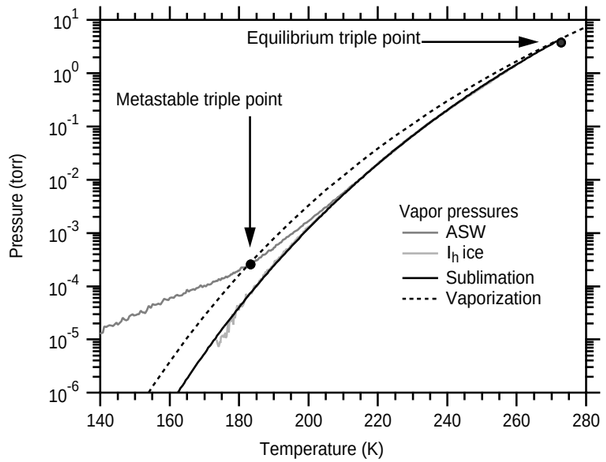

The graph shows pressure data obtained by mass spectrometry over the ASW and ice I_h phases: the calculated sublimation and extrapolated vaporization pressures for H_2O, the equilibrium triple point at 273.16 K, and temperature of the proposed metastable triple point at 160–180 K.

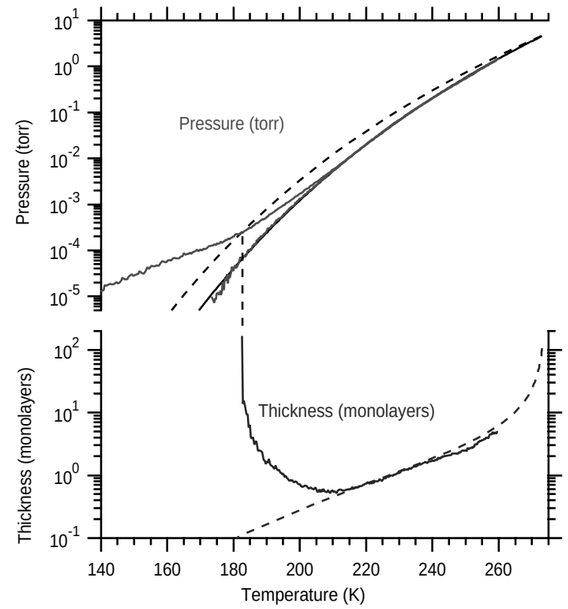

The top panel shows pressures of the ASW/I_c system. The bottom panel shows the calculated thickness, in monolayers, of a quasi-liquid phase as a function of the measured pressure (solid line) and the ice I_h sublimation pressure (dashed line).

Solvation Dynamics of Ion Pairs

98010

Antoinette Taylor

An unsolved but critically important scientific problem is the dynamics of how a solvent responds to a solute. Our project objective is to determine the mechanisms and time scales involved in both the formation and the dynamic behavior of ion pairs in solution. To accomplish this goal, we are developing the technique of femtosecond terahertz time-domain spectroscopy for the study of dynamic molecular interactions in liquids and tying the spectroscopic results obtained to the molecular dynamics calculations.

This year we measured the complex dielectric function for the following polar liquids: water, methanol, ethanol, acetone, acetonitrile, propylene carbonate, and ethylene glycol. We found for all liquids studied (except water) that a Debye-based relaxation model of the dielectric function is inadequate because significant resonant absorption occurs throughout the frequency range from 0.2 to 1 THz. Electronic structure calculations for methanol revealed that the resonant absorption corresponds to the vibrational frequencies of molecular clusters.

Extension of the frequency range of these measurements to frequencies that are low enough that they fall in the microwave range (<50 GHz) is important. We have redesigned our system so that a broadband spectrum yields the dielectric function for frequencies as low as 50 GHz. Further, we have developed a new narrowband terahertz source based on the multiple optical-pulse excitation of terahertz emitters. This source yields tunable narrowband terahertz radiation with frequencies as low as 10 GHz.

Initial measurements of the dielectric function of ionic salt solutions revealed that terahertz spectroscopy may be a useful probe of solvent clusters. We performed terahertz spectroscopy measurements of propylene carbonate with varying concentrations of salt solutions of lithium triflate (Li Tf) and lithium bis(trifluoromethane sulfonyl)imide (Li TFSI). The resonant absorption features of pure propylene carbonate disappear as relatively low (0.1 M) concentrations of Li TFSI are added to the solution, whereas for Li Tf, resonant absorption, although somewhat damped, is substantial for salt concentrations up to 0.5 M. Resonant absorption features are suppressed less in the triflate solution because the solvent does not participate as effectively in lithium ion solvation, leaving the extended clusters intact.

These results indicate that terahertz spectroscopy may be useful in revealing cluster interactions in molten salts, ion pairing systems, and other polymer electrolytes.

Publications

Asaki, M.L., et al., "Dielectric Response of Polar Liquids in the Terahertz Frequency Range" (submitted to *Phys. Rev. Lett.*).

Park, S.-G., et al., "High-Power, Narrowband Terahertz Generation Using Multiple-Pulse Excitation of Photoconductive Antennas" (to be published in *Proc. Soc. Photo-Opt. Instrum. Eng.*).

Mathematics and Computational Science

Scalable Algebraic Multilevel Preconditioning for General Sparse Systems Using Sparse Approximate Inverses

99039

Michael DeLong

The project objective is to build on previous work in sparse approximate inverses to construct a parallel preconditioner that is scalable for systems of linear equations in which the coefficient matrix is neither structured nor symmetric positive definite.

The work contributes to research areas that need to solve large sparse linear systems arising from finite-difference or finite-element discretizations of partial differential equations over unstructured grids. It is particularly useful for computational models of the diffusion of heat, radiation, or contaminants through a heterogeneous system such as a metal structure made of several different materials, a piece of equipment having parts of different shapes, or a piece of land containing rocks, sand, and clay.

We have completed a serial code that we will use to test the components of an approximate Schur complement preconditioner using sparse approximate inverses. It includes code to construct coarse problems algebraically using sparse approximate inverse methods, code to do intergrid transfer, and code to solve the coarsest problem. It also includes a generalized minimal residual solver.

We also did some theoretical work, focusing on the problem of how to construct sparse approximate inverses so that the range of the resulting transfer operators includes very smooth error modes. We found that for some test problems, we could transfer nearly constant error very well, but we have not found a strategy that works well in general.

Finally, with the help of two collaborators, we developed and implemented a simpler variant of the preconditioner mentioned above using only two levels, but which runs in parallel. This code was developed and tested on the Los Alamos Nirvana cluster, incorporated into our team's code base, and delivered to other teams within the Laboratory. It performs well for problems of up to a few million equations so long as the separator set induced by the graph partitioner is small. This condition is generally true for two-dimensional problems but is more difficult to achieve for three-dimensional problems. This approach is fast for many test problems but is not scalable.

Publications

Benzi, M., et al., "Parallel Preconditioning with Factorized Sparse Approximate Inverses," in *Proceedings of the Ninth SIAM Conference on Parallel Processing for Scientific Computing*, B. Hendrickson et al., Eds. (SIAM, Philadelphia, PA, 1999).

Benzi, M., et al., "A Two-Level Parallel Preconditioner Based on Sparse Approximate Inverses" in *Iterative Methods in Scientific Computation II*, D. Kincaid and A. Elster, Eds. (IMACS Series in Computation and Applied Mathematics, IMACS, Piscataway, NJ, in press).

DeLong, M., et al., "Multilevel Methods for LANL ASCI Problems: Current Status" (Copper Mountain Multigrid Conference, Copper Mountain, CO, April 4–8, 1999).

Diffusion in Porous Media and Stochastic Advection

97033

Shi-Yi Chen

We combined numerical simulation and theoretical research to study diffusion by intermittent stochastic velocity fields. Although principally applied to diffusion of substances in porous media, this study will also have an impact on pollutant diffusion in the atmosphere or oceans and on chemical reactions in fluids. We are exploiting the unmatched parallel-computation capability at Los Alamos, together with recent advances in the analytical treatment of anomalous scaling phenomena in passive scalar turbulence advection, to increase our knowledge of the advective process and to improve its modeling. The technical aspect that distinguishes this work is the development of sound analytical and numerical treatment of advection by extremely intermittent stochastic advection velocities.

We analytically developed two levels of mapping closure to handle the changes in flux, or velocity field, induced by strongly non-Gaussian fluctuations in the diffusivity of a porous medium subjected to external pressure heads. We coded the simpler level and subjected it to numerical tests, with good qualitative and fairly good quantitative results in test cases in which the diffusivity fluctuations have a lognormal distribution. Here the lognormal diffusivity field is represented by a nonlinear mapping of a Gaussian fluctuation field.

The use of mapping approximations to represent the statistics of a passive scalar field advected by a prescribed, highly intermittent velocity field is a more difficult problem than that faced with the Gaussian field. Even the statistics of a passive scalar field advected by a Gaussian velocity field are still controversial among researchers. One case is a straightforward extension of the Gaussian case, in which the eddy diffusivity exerted by the velocity field changes slowly in space compared with the spatial scales of the scalar field. In this example, the scalar statistics are those of an ensemble of scalar fields advected by Gaussian velocity fields of different intensities. The more interesting case is one in which all spatial scales are comparable. For this case we have some analytical mapping formulations, although it is unclear whether they will be successful.

We also explored the utility of alpha equations (in which we change the nonlinear term by introducing a dispersive relation) in providing a subgrid model for fluid turbulence. Our principal results are comparisons of direct numerical simulations of fluid turbulence using several values of the parameter alpha, including the limiting case in which the Navier-Stokes equations are recovered. Our studies show that the large-scale features, including statistics and structures, are preserved by the alpha models, even at coarser resolutions in which the fine scales are not fully resolved. We also described the differences that appear in simulations. We provided a summary of the principal features of the alpha equations and offered some explanation of the equations' effectiveness when used as a subgrid model for three-dimensional fluid turbulence.

Publications

Cao, N., et al., "Statistics and Structures of Pressure in Isotropic Turbulence," *Phys. Fluids* **11**, 2235 (1999).

Chen, S., et al., "The Camassa-Holm Equations as a Closure Model for Turbulent Channel Flow," *Phys. Rev. Lett.* **81**, 5338 (1998).

Chen, S., et al., "A Connection between the Camassa-Holm Equations and Turbulence Flows in Channel and Pipes," *Phys. Fluids* **11**, 2343 (1999).

Chen, S., et al., "Direct Numerical Simulations of the Navier-Stokes Alpha Model" (to be published in *Phys. D*).

Gong, H., et al., "An Analysis of Subgrid-Resolved Scale Interaction with Use of Results from Direct Numerical Simulation," *Acta Mech. Sinica* **15**, 108 (1999).

He, G., et al., "Scalings of Dissipation and Enstrophy Induced by Random Strained Vortices in Fluid Turbulence," *Phys. Rev. Lett.* **81**, 4636 (1998).

A Theoretical Description of Inhomogeneous Turbulence

97018

Leaf Turner

We developed a state-of-the-art analytical and numerical model of spatially inhomogeneous turbulence. Our objective was to obtain a fundamental understanding of such turbulence by properly treating the effects of spatial variations of pressure and other fluid quantities. These variations are absent in most theoretical work that generally limits itself to the analysis of spatially homogeneous turbulence or treats inhomogeneous turbulence only through phenomenological assumptions. As a result, we were able to study the effects of coherent macroscopic structures due to boundaries on the turbulence.

We discovered how a local mean flow can develop out of turbulent fluctuations when no such flow is present initially. This work has implications for improved phenomenological models for engineering applications that extend from drag forces on transportation vehicles, energy efficiency in automotive combustion, and meteorological phenomena to forest fires, volcanic eruptions, and weapons physics.

In fluid turbulence theory, one often specifies a state of a system by specifying some set of spectral coefficients, {c(**k**)}. Often one assumes an ensemble of identical systems and imposes the condition that $<c^*(\mathbf{k})c(\mathbf{k}')>$ vanishes if k is not equal to **k′**, in which the brackets denote an average taken over the members of an ensemble. However, when actually performing direct numerical simulations, one usually deals with a number of realizations, say *N*, in an ensemble smaller than the number of spectral coefficients specifying the physical configuration. Since the number of orthogonal vectors cannot exceed the number of realizations, the theoretical condition above is vitiated.

We have derived an analytical formula that replaces the previous condition when the spectral coefficients have random phases (see dashed line in accompanying figure). Inhomogeneous Navier-Stokes dynamics data (from direct numerical simulations) appear consistent with random phases (see solid line in the figure).

To demonstrate realizability when using an Eddy-Damped Quasi-Normal Markovian closure in the two-fluid-like case of magnetohydrodynamic (MHD) turbulence, one must demonstrate that the turbulent fluid energy spectrum remains positive at all times, that the turbulent magnetic energy spectrum remains positive at all times, and that the cross-helicity spectrum, a measure of the correlation of the magnetic and velocity fluctuations critical to the turbulent MHD dynamo, satisfies a Schwarz inequality. In the absence of mean fields, we demonstrated this using the Elsasser field variables, **v**+**B** and **v**–**B**.

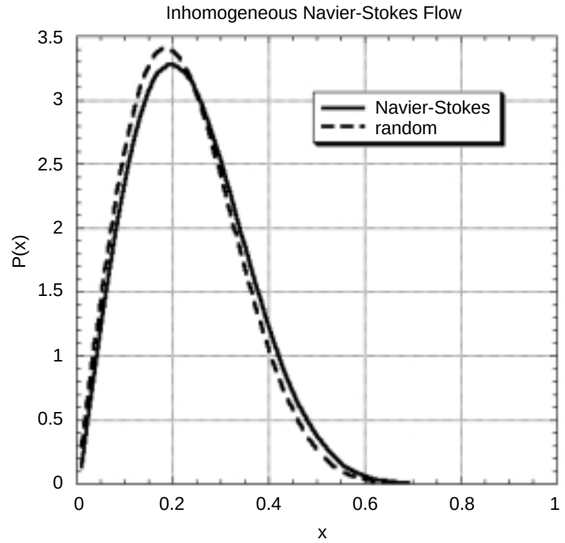

Randomness of Navier-Stokes channel-flow data obtained from an ensemble of numerical simulations is demonstrated by comparison with the theoretical prediction based on randomness. The discrepancy is due to the presence of a finite viscosity.

Publications

Turner, L., "Macroscopic Structures of Inhomogeneous, Navier-Stokes Turbulence," *Phys. Fluids* **11**, 2367 (1999).

Turner, L., "Using Helicity to Characterize Homogeneous and Inhomogeneous Turbulent Dynamics," *J. Fluid Mech.* **408**, 205 (2000).

Turner, A. M. and Turner, L. "Manifestation of Random Phase in a Finite Ensemble of a Turbulent Fluid," *Phys. Rev. Letters* **84**, 1176 (2000).

Ulitsky, M., et al., "Testing a Random Phase Approximation for Bounded Turbulent Flow," *Phys. Rev. E* **59**, 5511 (1999).

Efficient Multilevel Iterative Methods for Nonlinear PDEs

98029

Dana Knoll

As the field of numerical simulation matures, it is moving from an interpretive capability to a predictive capability. This progression requires nonlinearly consistent time integration and fine grid resolution. Jacobian-free Newton-Krylov methods with multigrid-based preconditioners offer a robust and efficient algorithmic approach for the progression to predictive capability. Our goal is to develop a hybrid numerical solution algorithm for nonlinear systems of partial differential equations (PDEs) that has Newton-like nonlinear convergence properties, multigridlike efficiency, and Krylov-like dependability.

Jacobian-free Newton-Krylov methods offer a general-purpose approach for integrating nonlinearly consistent time to a wide variety of multiple time-scale problems. These methods obtain Newton-like nonlinear convergence without forming or inverting the Jacobian matrix. The effects of the Jacobian matrix are probed through the approximate matrix-vector products required in the Krylov method. Because the viability of these methods for large-scale, multi-physics simulations depends on the efficient preconditioning of the Newton-Krylov iteration, we are developing multigrid-based preconditioners that will scale well under grid refinement.

By applying the Jacobian-free Newton-GMRES (General Minimal Residual) method to three-dimensional (3-D) magnetohydrodynamics, we substantially increased the simulation efficiency and resolution used to study the magnetic reconnection on the day side of the earth's magnetosphere.

In nonequilibrium radiation hydrodynamics, we demonstrated that physics-based operator splitting works well as a preconditioner to the Jacobian-free Newton-Krylov method. We also demonstrated that low-complexity, multigrid methods are effective at approximating the inverse of the resulting elliptic systems. Using operator splitting as a solver (where the nonlinear residuals are not converged) can lead to nearly nonconvergent algorithms under time-step refinement.

We have demonstrated that distributed relaxation multigrid methods are good preconditioners for incompressible and compressible Euler equations. We are incorporating our results on the incompressible Navier-Stokes equations into a 3-D, parallel simulation tool for molding and casting processes. Our results on compressible Euler equations are in a 3-D, parallel atmospheric-flow solver that we are developing for wildfire simulation.

Finally, we contributed to multilevel Newton-Krylov development for a 3-D simulation of the ion distribution function in inertial electrostatic confinement fusion. This is a nonlinear, integrodifferential problem. This simulation tool is producing first-of-a-kind physics results by converging nonlinearities on a fine grid.

Publications

Chacon, L., et al., "An Implicit Energy-Conservative Newton-Krylov Solver for 2-D Fokker-Planck Problems" (to be published in *J. Comput. Phys.*).

Knoll, D.A., and V.A. Mousseau, "On Newton-Krylov-Multigrid Methods for the Incompressible Navier-Stokes Equations" (submitted to *J. Comput. Phys.*).

Knoll, D.A., and W.J. Rider, "A Multigrid Preconditioned Newton-Krylov Method," SIAM *J. Sci. Comput*. **21**, 691 (2000).

Knoll, D.A., et al., "An Efficient Nonlinear Solution Method for Nonequilibrium Radiation Diffusion," *J. Quant. Spectros. Radiat. Transfer* **63**, 15 (1999).

Knoll, D.A., et al., "A Multilevel Iterative Field Solver for Implicit, Kinetic, Plasma Simulation," *J. Comput. Phys.* **149**, 377 (1999).

Knoll, D.A., et al., "A New Nonlinear Solution Method for Phase Change Problems," *Numerical Heat Transfer* **35**, 439 (1999).

Knoll, D.A., et al., "Nonlinear Convergence, Accuracy, and Time Step Control in Nonequilibrium Radiation Diffusion" (submitted to *J. Quant. Spectros. Radiat. Transfer*).

Mousseau, V.A., et al., "Physics-Based Preconditioning and the Newton-Krylov Method for Nonequilibrium Radiation Diffusion" (submitted to *J. Comput. Phys.*).

Rider, W.J., and D.A. Knoll, "Time Step Size Selection for Radiation Diffusion Calculation," *J. Comput. Phys.* **152**, 790 (1999)

Rider, W.J., et al., "A Multigrid Newton-Krylov Method for Multimaterial Equilibrium Radiation Diffusion," *J. Comput. Phys.* **152**, 164 (1999).

Extending the Theory of Resonant Perturbations to Partial Differential Equations, with Applications to Nonlinear Optics

98030

Roberto Camassa

Fiber-optical communication systems require much greater capacities today than ever before because of the rapid growth in communication and the development of the next-generation Internet. Our leadership in this area is crucial to maintain the nation's technological edge and to address the Laboratory's needs for new, high-speed supercomputer interconnects. One of the most promising future carriers of information in fiber telecommunication systems is optical solitons. These are stable, solitary pulses of light that can propagate in an optical fiber over a long distance without changing shape.

The key technology of modern, high-bit-rate optical telecommunications is wavelength-division multiplexing. This technology divides the fiber-optical transparency window of a frequency domain into many separate frequency channels and transmits data streams in parallel through these channels. However, there is strong experimental evidence indicating that the capacity of a system based on this technology is limited by two types of resonances. One resonance is due to interchannel interaction, and the other resonance is due to pulse interaction with the periodical structure of a transmission link with in-line optical amplifiers. We demonstrated that optical solitons are capable of controlling such resonances. This technology exploits the periodic variation of fiber chromatic dispersion (dispersion management technique) to compensate for optical pulse broadening in fiber links. In order for us to fully exploit the potential of this new technique, a fundamental understanding through mathematical modeling is required.

This year we investigated the resonance interaction of solitons with the structure of a fiber-optical transmission line under periodic dispersion management. Periodic dispersion management consists of periodically alternating optical fibers with positive and negative dispersion values. An optical pulse propagates in a fiber and broadens in width because of the effect of dispersion. Then the pulse enters a fiber containing a sign opposite to that of the dispersion and is compressed. At the end of this fiber, the pulse is restored to its original width. This process repeats periodically along the transmission line.

We also considered wavelength division multiplexing (WDM), in which data streams are allocated to different optical frequency channels. In WDM, solitons of different "colors" collide because of different group velocities in different frequency channels. These collisions are characterized by the length of soliton interactions. Periodic dispersion management and amplification introduce external forcing that can lead to resonance with the interacting solitons. This resonace typically manifests itself as the persistent excitation of frequency sidebands, components of the so-called four-wave mixing (this mixing refers to additional radiation that is generated as the result of a nonlinear interaction of the pulses propagating in different channels). This mixing effect eventually destroys the ordered pattern of the bit streams, causing unacceptable errors. Our early research provided a first attempt to explain theoretically how dispersion management, by suppressing the primary resonance, can dramatically reduce the accumulation of four-wave mixing and therefore stabilize a bit pattern. We later followed up by studying the phenomenon that occurs when dispersion variation around a nonzero average is assumed to be small. We found a new evolution equation and an explicit form of the four-wave interaction term in an expansion of the governing Hamiltonian that combines averaging, normal form expansion, and diagrammatic techniques.

We also implemented a parallel code for the simulations of massive WDM data transmission and developed algorithms for solving the direct scattering problem for the Lax operator associated with the governing equation. These codes allow the simulation of a state-of-the-art WDM system with up to 100 channels and complement raw numerical runs by providing diagnostics for soliton evolution and dispersive wave generation during propagation along fiber transmission systems.

Publications

Lvov, Y., and I. Gabitov, "Dispersion Management in Optical Fiber Links: Integrability in Leading Nonlinear Order" (submitted to *Phys. Lett. A*).

Burtsev, S., et al., "NRZ-to-Soliton Data Conversion Problem" (submitted to *J. Opt. Soc. Am. B*).

Simulation of Thin-Film Formation

97513

Robert B. Walker

The immediate purpose of this project is to develop computer simulation tools that will allow collaborators in the United States semiconductor industry to predict how thin films of various materials are formed in their manufacturing processes. One part of this effort is to develop a predictive, fully three-dimensional software simulator that describes the physical and chemical processes that are important in determining the shape, thickness, and uniformity of deposited thin films. The software being developed is called TopoSim-3D. Incorporating a knowledge of the fundamental processes that occur on the molecular time and distance scales at the surface of a growing thin film, TopoSim-3D attempts to describe the geometry of the deposited film for time and distance scales that are thousands to millions of times larger.

This year there have been two major improvements in the capabilities of TopoSim-3D. First, we have improved the way the code describes the transport of materials throughout the volume of space contained in the simulation, in conjunction with how that transport affects the models for the surface chemical reactivity of these transported materials. Second, we have improved the way the code handles the mathematical description of the motion of material surfaces as a result of the growth of new deposited materials at interfaces. These code enhancements make it possible to simulate more-realistic reactor conditions during processing.

An example of the current simulation capability is illustrated in the accompanying figure. The top drawing shows the geometry of the material/vapor interface in a structure consisting of two rectangular trenches that meet at a corner with a small cylindrical hole at the bottom of the corner. The simulation code is used to model the uniformity of deposition of metal in the hole and in the trenches, and this metal creates wires that connect various circuit components together. The lower drawing shows a cross-sectional view of the geometry of a thin seed layer of metal (the darker gray material) that has been deposited.

To provide fundamental data to describe the metal deposition process, we have completed a series of large-scale atomistic simulations to describe the scattering of metals from metal surfaces. These calculations determine the energy and angular dependence of scattered materials from copper surfaces after bombardment with copper or argon ions. We have also analyzed the effect of trapping copper atoms on copper surfaces when the incident atoms hit the surface at grazing angles. The results of these atomic-scale calculations are then used directly by TopoSim-3D to simulate deposition on the micrometer scale.

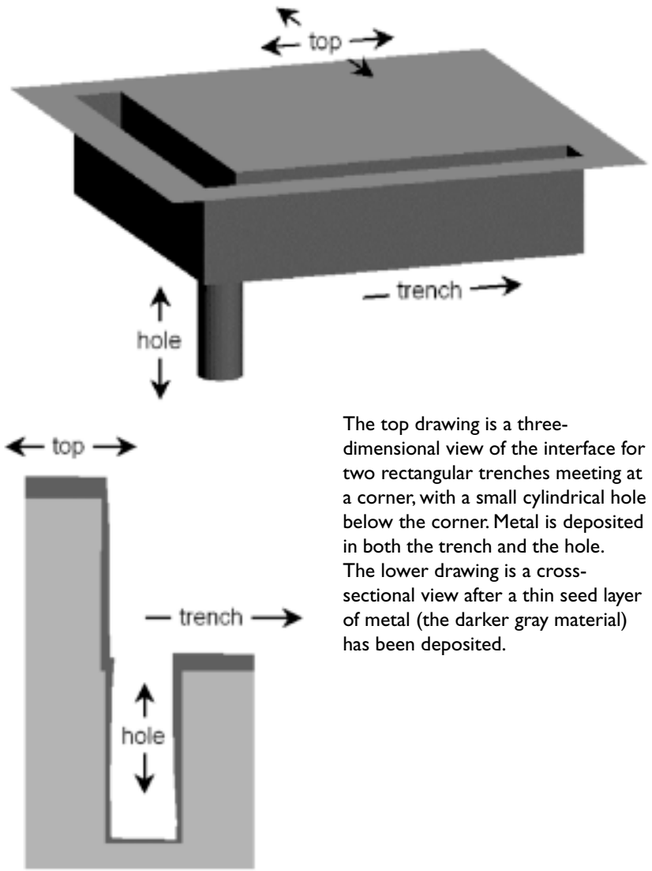

The top drawing is a three-dimensional view of the interface for two rectangular trenches meeting at a corner, with a small cylindrical hole below the corner. Metal is deposited in both the trench and the hole. The lower drawing is a cross-sectional view after a thin seed layer of metal (the darker gray material) has been deposited.

Publications

Hanson, D.E., et al., "Trapping and Desorption of Energetic Cu Atoms on a Cu (111) Surface at Grazing Incidence," *Phys. Rev B.* **60**, 11723 (1999).

Kress, J.D., et al., "Molecular Dynamics Simulations of Cu and Ar Ion Sputtering of Cu (111) Surfaces," *J. Vac. Sci. Technol. A.* **17**, 2819 (1999).

Walker, R.B., and J.D. Kress, "TopoSim-3D: A 3D Feature-Scale Profile Simulation Tool" (MRS Workshop on Advances in Thin Film Simulations and Experimental Verification, San Jose, CA, June 23–25, 1999).

Unitary Symmetry, Discrete Mathematics, and Combinatorics

98032

William Chen

This year we continued to focus our study of combinatorics in relation to physics on research into (1) group representation theory, which is widely used in comprehensive studies of the spectra of many-particle quantum systems (molecules, atoms, nuclei, particles), and (2) the properties maps of the interval, a mathematical technique used to model the behavior of discrete dynamical systems.

Earlier in this project, we discovered that the classical combinatorial result known as MacMahon's master theorem underlies the structure of binary recoupling coefficients, objects that recur throughout physical applications. This year we continued our studies of the theorem's role in recoupling theory and its relationship to pairs of binary trees, which are related to cubic graphs. Our goal is to classify all such recoupling coefficients by their associated cubic graphs.

Our new work is based on our earlier discovery that the multiplication law for group representations depends not on group structure, but on a combinatorial identity among multinomial coefficients, which allows the extension of such representations to polynomials defined over arbitrary commuting variables. That discovery led us this year to a method for dealing with noncommuting variables and to the first comprehensive theory of tensor operators, objects that are the basis of interactions in physical systems.

The theory of words on two letters is basic to the description of the mathematics of maps of the interval and its application to discrete dynamical systems. In our earlier research on this subject, we observed that the parity of certain words, even or odd, is a significant property for the evolution of such maps. We were able to outline a proof of the parity property, but it was only this year that we obtained the complete details. This parity property of words is important to the general theory of such maps of the interval, their bifurcation points, cycles, and so forth.

Publications

Chen, W.Y.C., and J.D. Louck, "The Combinatorics of a Class of Representation Functions," *Adv. Math.* **140**, 207 (1998).

Chen, W.Y.C., and J.D. Louck, "Enumeration of Cubic Graphs by Inclusion-Exclusion," *J. Combin. Theory* **151** (1999).

Chen, W.Y.C, et al., "Adjacency and Parity Relations of Words in Discrete Dynamical Systems" (to be published in *J. Combin. Theory A*).

Chen, W.Y.C., et al., "Angular Momentum, Umbral Calculus, and Combinatorics" (to be published in *Int. J. Comp. Math.*).

Chen, W.Y.C., et al., "The Flagged Double Schur Function" (to be published in *J. Algebraic Combin.*).

Louck, J.D., "Power of a Determinant with Two Physical Applications," *Internat. J. Math. and Math. Sci.* **22**, 745 (1999).

Louck, J.D., "Unitary Group Theory and the Discovery of the Factorial Schur Functions" (submitted to *Ann. Combin.*).

Louck, J.D. , and M.L. Stein, "Relations between Words and Maps of the Interval" (submitted to *Ann. Combin.*).

Louck, J.D., et al., "Combinatorics of 3n-j Coefficients," *Phys. At. Nuclei* **61**, 1868 (1998).

Louck, J.D., et al., "Generating Functions for SU(2) Binary Recoupling Coefficients" in *Proceedings of the Fifth Conference on Symmetry and Structural Properties of Condensed Matter*, T. Lulek et al., Eds. (World Scientific, Singapore, 1999), p. 112.

New Ways of Representing Functions

97034

George Zweig

An understanding of how the atomic structure of plutonium changes while aging is useful in establishing the functionality and safety of stockpiled nuclear weapons. In this project we used the fine structure observed in the energy dependence of the total absorption cross section of x-rays in plutonium to determine the relative distances between neighboring atoms for plutonium samples of different age. This method exploits the interference of electrons directly ionized by the x-rays with those undergoing additional scattering off neighboring atoms after initial ionization.

This year we developed a new, nonparametric, superresolution method of Fourier analysis that exploits the sparseness of plutonium ionization centers in the crystal to transform x-ray absorption fine structure (EXAFS) data of aged and newly processed plutonium. This method, called LIFT, creates a sparse expansion of an underlying sum of complex exponentials by minimizing the l_1 norm of the expansion coefficients. Each complex exponential in the sum corresponds to the position of an atom in the crystal. LIFT increases interatomic spatial resolution by a factor of 64 over that delivered by a windowed Fourier transform. The anomalous site in newly processed plutonium observed by Conradson using a windowed Fourier transform is also observed with LIFT, but with greatly improved resolution and at a larger site separation. The newly processed plutonium is a slightly modified form of δ-plutonium. The anomalous site is not present in aged plutonium. This site seems to disappears as plutonium ages. However, to establish changes in plutonium crystal structure with age, we must make repeated EXAFS measurements on the same sample as it ages.

3-D, Unstructured, Hexahedral-Mesh S_n Transport Methods

97035

Jim E. Morel

The purpose of this project is to develop a discrete-ordinates, or S_n, method for solving the radiation transport equation on three-dimensional (3-D) hybrid finite element meshes consisting of arbitrary combinations of hexahedra, wedges, pyramids, and tetrahedra. The use of these meshes will allow us to efficiently model radiation transport in complex 3-D geometries. To our knowledge, this is the first S_n algorithm ever developed for hybrid finite element meshes.

We adopted a new approach to developing a parallel solution technique for our hexahedral-mesh S_n equations because our original approach, which was based on a standard decomposition of the spatial domain that seeks to obtain a minimum surface-to-volume ratio, proved inadequate. Our new approach is based on finding a near-optimal spatial domain decomposition that is specific to the equations that we are solving. We found that such a decomposition is very different from a standard decomposition.

As part of the overall iterative solution process, a separate equation must be solved for each discrete direction. Although it is not difficult to define an optimal decomposition for each equation, only one decomposition can be used for all of the equations, and the optimal decomposition for one equation can be quite poor for another equation. The most important aspect of our new algorithm is the definition of a spatial decomposition that is near-optimal for the entire set of equations. We have coded our new approach and are now testing it. The algorithm should scale properly if it successfully defines near-optimal decompositions.

This year we also developed S_n spatial discretization schemes that possess certain critical asymptotic properties required for radiative transfer calculations. However, so far these schemes have been successful only for tetrahedral cells. Developing similar discretization schemes for cells in the form of hexahedra, wedges, and pyramids has proved to be quite difficult.

Publications

Wareing, T.A., et al., "A Diffusion Synthetic Acceleration Method for the S_n Equations with Discontinuous Finite Element Space and Time Differencing" (Int. Conf. on Math. and Comp., Reactor Physics, and Environ. Analyses in Nuclear Apps., Madrid, Spain, Sept. 27–30, 1999).

Wareing, T.A., et al., "Discontinuous Finite Element S_n Methods on 3-D Unstructured Grids" (Int. Conf. on Math. and Comp., Reactor Physics, and Environ. Analyses in Nuclear Apps., Madrid, Spain, Sept. 27–30, 1999).

Wareing, T.A., et al., "Discontinuous Finite Element S_n Methods on 3-D Unstructured Grids" (submitted to *Nucl. Sci. Eng.*).

Completely Parallel ILU Preconditioning for Solution of Linear Equations

97036

Wayne Joubert

The most computationally expensive part of many modeling and simulation processes is solving the sparse systems of linear equations that arise from finite-difference or finite element discretizations. They are generally solved by using the powerful incomplete Cholesky or incomplete lower-upper (ILU) preconditioners. Unfortunately, these preconditioning techniques are sequential and thus ineffective in parallel computer platforms. We have developed completely parallel versions of these preconditioners that solve an important class of linear systems: those involving large-scale modeling and simulation applications. In this project, we plan to apply these parallelization techniques to a broad range of structured problems, to perform basic research on the convergence properties and parallelization possibilities of ILU preconditioners, and to explore the possibility of using these techniques for the preconditioning of unstructured problems.

This year we completed our analysis of the effects of orderings on ILU preconditionings. We developed a preconditioning strategy suitable for unstructured matrix problems on parallel computers. This method is an adaptive strategy for determining the required subgrid overlap for overlapping additive or multiplicative Schwarz preconditioners. While more naturally suited to sparse approximate inverse preconditioning, this method can be used for ILU preconditioning as well. This method should be particularly effective for solving matrices arising from two-dimensional (2-D) or three-dimensional (3-D) heterogeneous simulation problems, for which it is important to model the physical interaction between subdomains in a parallel environment.

In the area of ILU/multilevel methods, we have developed an effective parallel coarsening strategy for algebraic multigrid methods and hybrid ILU/multigrid algorithms. The problem of parallel coarsening has been recognized by many as a key unsolved problem for multilevel methods. Our new strategy has been tested on a variety of 2-D and 3-D problems and has been shown to be effective.

Publications

Benzi, M., et al., "Can Incomplete LU Factorizations Give Both Robust and Parallel Preconditioners?" in *Iterative Methods in Scientific Computation,* D. Kincaid and A. Elster, Eds. (IMACS, New Brunswick, NJ, 1999), Vol. IV, p. 155.

Benzi, M., et al., "Numerical Experiments with Parallel Orderings for ILU Preconditioners," *Electron. Trans. Numer. Anal.* **8**, 88 (1999).

Joubert, W., et al., "Fully Parallel Global M/ILU Preconditioning for 3-D Structured Problems" (to be published in *SIAM. Sci. Comput.).*

Design of an Indexing Scheme for Knowledge Management at Los Alamos National Laboratory

98566

Stacey Gerhart

Legacy data archives are becoming critical links between nuclear weapons simulation, verification, and experimentation. Los Alamos archival holdings are estimated to include over 42 million records in various file formats and media types (for example, paper, aperature cards, radiographs) and include records that have been transferred from Mound Pinellas and Rocky Flats.

Our project objective is to develop a state-of-the-art indexing scheme for dramatically improving how we manage and retrieve information from such systems. We will also examine application programming interfaces needed for such a scheme. During the past year we developed an overview of the project and defined four critical tasks: (1) identify data sources for crucial information, (2) identify metadata (descriptive information about the data), (3) provide data population (the automatic upload of information from defined data sources into the corresponding data fields), and (4) reconcile the data (automatically select the "best" from all the available data).

We defined a standard set of metadata fields for the nuclear weapons complex and identified data sources that will provide valuable information during the automatic population of metadata fields. After making provisions to store, organize, provide entry of, and maintain the data, we determined the mapping from the defined data sources to the identified metadata fields.

Statics and Dynamics of Granular Media

99034

Eli Ben-Naim

Granular materials such as powders, grains, and explosives are ensembles of macroscopically sized particles. The mathematical description of these ubiquitous materials remains incomplete, so the goal of our project is to develop appropriate continuum equations and improved numerical modeling techniques based on statistical investigations of the dynamics of granular flow and the statics of granular packing. Better mathematical and statistical descriptions of granular packing and granular flow will translate into improved geophysical and earth sciences models.

Granular materials are characterized by two unique features: strong dissipative interactions and macroscopic particles. We have concentrated on how these characteristics influence freely evolving granular gases and excited granular matter. Our numerical studies employ parallel and serial large-scale (10^7 particles, 10^{11} collisions) computations using event-driven simulations and traditional molecular dynamics. To this end, we have introduced a relaxation method that successfully overcomes singularities associated with dissipative collisions.

In freely evolving granular gases, we have investigated velocity statistics in one, two, and three spatial dimensions. The one-dimensional case produced promising results. We found that weakly dissipative granular media is characterized by a homogeneous phase and a clustering phase. Furthermore, the long-time asymptotic behaviors of overall temperature scale, velocity, and spatial distributions are independent of the degree of dissipation and are all in remarkable agreement with a simple continuum theory, the Burgers equation (see first figure). The clustering process reflects the formation of shocks in the velocity profile. We also verified predictions of this theory in higher dimensions (see second figure). These results resolve many of the open issues in the theory of freely evolving granular gases.

We examined the effects of the particles' macroscopic size using excited granular materials. We numerically studied order-disorder transitions in vibrated granular monolayers and showed that as the vibration strength approaches a critical value, the energy, collision frequency, and fluctuations in the position of the particles sharply decrease, reminiscent of a phase transition. Furthermore, while the velocity distribution is purely Gaussian in the gas phase, a bimodal distribution characterizes the crystal-gas coexistence phase (see third figure), in agreement with recent experimental studies.

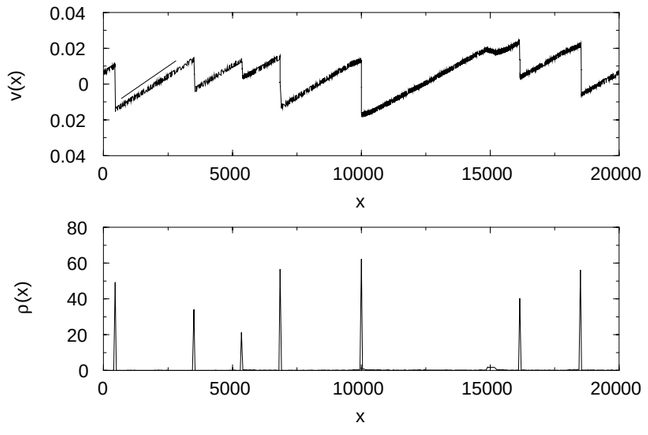

Shock formation in simulations of one-dimensional inelastic gases. Shown are the velocity and the density as a function of space. Statistical properties of the shocks agree with the asymptotic predictions of the Burgers equation.

Publications

Ben-Naim, E., et al., "Multiscaling in Inelastic Collisions," *Phys. Rev. E* **61**, R5 (2000).

Ben-Naim, E., et al., "Shocklike Dynamics of Inelastic Gases," *Phys. Rev. Lett.* **83**, 4069 (1999).

Ben-Naim, E., et al., "Slow Relaxation in Granular Compaction," *Physica D* **123**, 380 (1998).

Chen, S., et al., "Clustering Kinetics of Granular Media in Three Dimensions" (to be published in *Phys. Lett. A*).

Nie, X., et al., "Dynamics of Vibrated Granular Monolayers" (submitted to *Europhys. Lett.*).

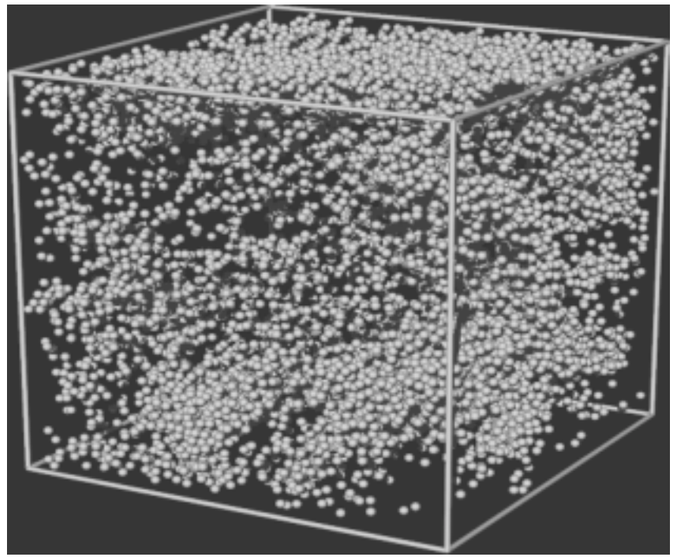

Development of density inhomogeneities in freely evolving granular media. Shown is a subset of a large-scale, parallel, molecular-dynamics simulation.

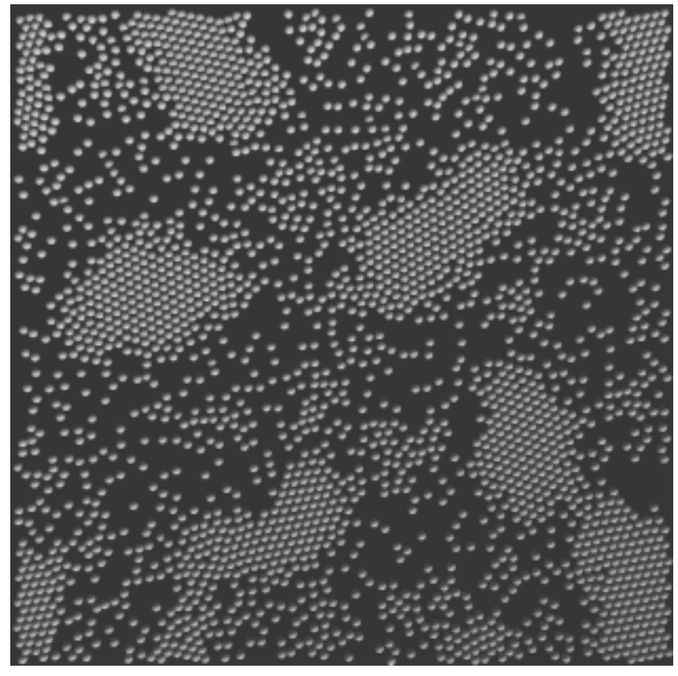

Coexistence of crystal and gas phases in a vibrated granular monolayer. Details of this phase transition are in agreement with the experimental data.

National Transportation System Analysis Capability

98556

Douglas Anson

The success of the Laboratory's Transportation Analysis and Simulation System (TRANSIMS) in modeling regional transportation systems raised the question of whether TRANSIMS could be extended to national transportation. We are examining the feasibility of using TRANSIMS as a prototype for a National Transportation Network Analysis Capability (NTNAC) (see first figure).

The desired NTNAC prototype must be a single, integrated, multimodal, simulation-based decision-analysis tool that can deal with national-level transportation policy, investment, capacity, and intermodal issues. It must also be able to examine defense issues such as "civil competition" during national emergencies, transportation sector vulnerabilities, and, eventually, interdependencies with other U.S. infrastructure sectors (e.g., energy and communication).

This year we determined the technical feasibility of simulating national commodity movement, beginning at the individual load and carrier level. We also completed a prototype simulation that demonstrates this feasibility (see second figure). In addition, we showed that simulations could, at the national level, do the following: (1) generate intermodal movement at the individual carrier and load level, with a focus on freight and the highway and rail systems; (2) generate random hourly freight demand at the county level; (3) generate carrier and commodity trip plans over a one- to three-week time horizon; (4) dynamically couple the highway and rail (sub)systems; (5) generate Department of Transportation freight system performance indicators; and (6) describe extensions to air and marine freight modes and passenger travel.

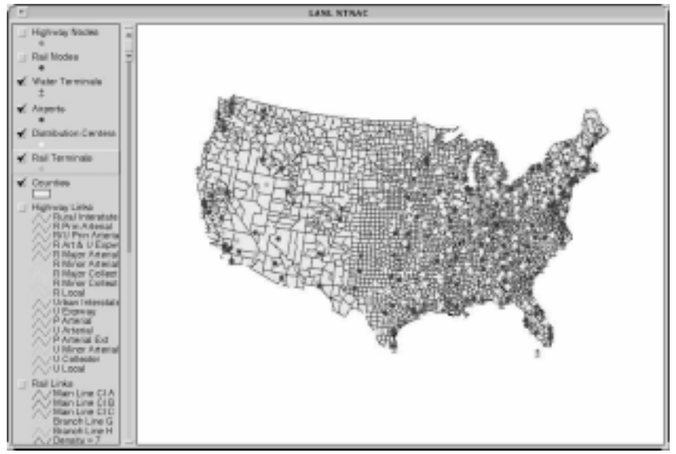

Geographical information system view of water ports, airports, rail terminals, and truck distribution centers overlaid on 3,000 U.S. counties. These are some of NTAC's input data.

A view of the NTNAC simulation of multimodal (truck, air, and rail) commodity shipments from Los Angeles County over a six-day period in May.

New Perspectives in Mathematical Modeling of High-Bit-Rate Fiber-Optical Telecommunications

99038

Ildar Gabitov

To keep up with the exponentially growing demand for optical-fiber system capacity, U.S. industry must develop ever-faster communication (at least in the terabit-per-second regime). In recognition of this demand, a huge multiagency effort has begun to develop significantly better bandwidth solutions. Indeed, no existing network and fiber technology is even close to being sufficiently robust and affordable to link DOE's supercomputing sites. The proposed development of the scientific background for ultrahigh-bit-rate telecommunications at Los Alamos would be an essential component to perform this challenging task. This project also coordinates interactions in optical sciences between theoreticians and experimentalists at Los Alamos.

This year we investigated pulse dynamics in optical-fiber links with dispersion management. We developed both a general description of these phenomena and a simplified asymptotic approach. The simplified model is a system of three first-order ordinary differential equations, and it approximates with high accuracy the results of direct numerical simulations of the general model.

We also obtained higher-order corrections to this general model in the spectral (frequency) domain and illustrated the evolution of dispersion-managed solitons for a specific symmetric dispersion map. The result holds for a dispersion map of arbitrary strength.

An alternative Hamiltonian approach was developed for a similar model in time-coordinate representation. This approach allows one to effectively remove rapid variation of the dispersion coefficient in the original nonlinear Schrödinger equation describing pulse evolution in optical links with dispersion management.

We also developed a new technique for evaluating bit-error rates in soliton systems with saturable in-line amplifiers. Our technique was applied successfully in Europe during the field trial between Madrid, Spain, and Merida, Portugal.

In related work, using a technique developed for modeling pulse propagation in fiber links, we studied pulse dynamics in lasers with absorber-dominated optical cavities. We also discovered new regimes of stable pulse generation that can be used as a soliton pulse clock in soliton transmission systems.

Publications

Gabitov, I., et al., "Lie-Transform Averaging in Nonlinear Systems with Strong and Rapid Periodic Dispersion Variations" (to be published in *Phys. Lett. A*).

Lvov, Yu., and I. Gabitov, "Dispersion Management in Optical Fiber Links: Integrability in Leading Nonlinear Order" (submitted to *Phys. Lett. A*).

Shaulov, G., et al., "Pulse Dynamics in Absorber Dominated Optical Cavities" (to be published in *Opt. Commun.*).

New Dispersive Models of Fluid Turbulence

99037

Darryl Holm

Flows in nuclear weapons, ocean circulation, and other real-life applications have features that make traditional turbulence modeling ineffective. These features include transient forcing, strong anisotropy and inhomogeneity, multiphase flow, and coherent structures. This project combines new elements of theory, numerical simulation, and modeling.

We are exploiting a new analytical approach for both numerical algorithm development and physical modeling. The new approach results in a nonlinear dispersive system of flow equations referred to as the Navier-Stokes alpha model. The Navier-Stokes alpha model shows promise as a subgrid model for turbulent fluid flows.

By direct numerical simulations, we found that the length scale alpha truncates the turbulent cascade without interfering with the fluid motion on scales that are larger than alpha. Thus, the constant parameter alpha in our model defines the boundary between resolved scales and subgrid scales. By comparing direct numerical simulations of fluid turbulence using several values of the parameter alpha (including when alpha equals zero, which is where the original Navier-Stokes equations are recovered), we found that the large-scale features, including statistics and structures, are preserved by the alpha models, even at coarser resolutions. Thus, our model provides an accurate coarse-grained description of the fluid motion at the resolved scales and truncates the subgrid scales.

We discovered an intriguing connection between the Navier-Stokes

alpha model and large-eddy simulation (LES) codes being developed at Los Alamos. These LES codes are based on nonoscillatory algorithms and turbulence estimation methods. They have already proved effective at modeling turbulence (e.g., in planetary boundary layers). The truncation analysis of these nonoscillatory algorithms reveals terms that are nearly identical to the nonlinear dispersion terms in the Navier-Stokes alpha model.

In addition, we found an apparently cubic falloff in the kinetic energy wave-number spectrum by direct numerical simulations of the Navier-Stokes alpha model for driven turbulence in a periodic domain.

Publications

Cendra, H., et al., "Lagrangian Reduction, the Euler-Poincaré Equations, and Semidirect Products," *Transl., Ser. 2, Am. Math. Soc.* **186**, 1 (1998).

Chen, S., et al., "The Camassa-Holm Equations and Turbulence in Pipes and Channels," *Physica D* **133**, 49 (1999).

Chen, S., et al., "A Connection between the Camassa-Holm Equations and Turbulence Flows in Pipes and Channels," *Phys. Fluids* **11**, 2343 (1999).

Chen, S., et al., "Direct Numerical Simulations of the Navier-Stokes Alpha Model," *Physica D* **133**, 66 (1999).

Duan, J., et al., "Variational Methods and Nonlinear Quasigeostrophic Waves," *Phys. Fluids* **11**, 875 (1999).

Holm, D.D., "Fluctuation Effects on 3D Lagrangian Mean and Eulerian Mean Fluid Motion," *Physica D* **133**, 215 (1999).

Quantum Physics Algorithms

99035

Emanuel Knill

Recently, quantum computation has undergone a dramatic evolution. From being a subject of essentially academic interest, it has become a field with enormous potential to revolutionize computer science, affect issues of national security, and have a potential economic impact. Keys for this transformation have been the discovery of interesting quantum algorithms that would be much faster than their classical counterparts, the implementations of individual quantum gates, and the discovery of quantum error-correcting codes. Surprisingly, quantum computations, such as quantum physics simulations, that require only a modest number of quantum bits (~40) on a quantum computer are impossible to do on the biggest present-day classical computers because they require 2^{40} bits. This project aims at advancing the state of the art in the area of quantum physics algorithms.

The question of what additional computational power is provided by quantum physics is largely unanswered. To attempt to learn more about this question, we considered a physically motivated model of computation in which only one quantum bit is initially in a known state, with all others being random. This one-bit model is, in effect, available in ensemble systems at room temperature using nuclear magnetic resonance (NMR). We showed that this model is capable of supporting complex physics simulations and can yield spectral densities for local Hamiltonians.

To begin to determine the feasibility of implementing quantum physics simulations of available physical systems, such as nuclear spins in molecules controlled by NMR techniques, we collaborated with researchers at the Massachusetts Institute of Technology to formulate the general problem. A simple example involving the simulation of a harmonic oscillator using spin 1/2 systems was successfully implemented using an NMR quantum computer. We then described and implemented a proper three-particle Hamiltonian with equal success.

Publications

Knill, E., and R. Laflamme, "On the Power of One Bit of Quantum Information," *Phys. Rev. Lett.* **81**, 5672 (1998).

Somaroo, S., et al., "Quantum Simulations on a Quantum Computer," *Phys. Rev. Lett.* **82**, 5381 (1999).

Tseng, C.H., et al., "Quantum Simulation of a Three-Body Interaction Hamiltonian on an NMR Quantum Computer" (to be published in *Phys. Rev. A*).

Invariant Discretizations for Computational Gas Dynamics

98031

Mikhail Shashkov

The primary goal of this project is to formulate finite-difference methods whose coefficients depend only on the coordinate invariant characteristics of the computational grid, such as edge lengths, face areas, cell volumes, and angles between edges. These coefficients would not contain components of vectors and tensors related to some fixed coordinates system. These new methods will more accurately preserve the symmetries and group properties of the underlying differential equations and can be applied to modeling problems, in which preservation of symmetry is very important. Small departures from spherical symmetry because of discrete errors can lead to unacceptably large errors in systems with large convergence ratios. Also, the uncertainty as to whether a nonsymmetric result is due to numerical errors or to physical design severely limits the predictive capabilities of such systems, as well as our understanding of their dynamical behavior.

This year we developed and implemented a "modified gradient" approach in which forces are locally changed according to the expected symmetry in the flow. This approach preserves exact symmetry but does not conserve momentum when symmetry is absent. We have demonstrated the robustness of this new method with numerical experiments.

We continued development of a method based on a curvilinear grid that we devised during the first year of this project. In particular, we developed a way to reconstruct a curvilinear grid in three dimensions, which reconstructs exactly planes, spheres, and cones. We continued to test two-dimensional methods on curvilinear grids, using realistic problems. In particular, we investigated convergence for problems with analytical solutions and for plane Rayleigh-Taylor instability problems.

Publications

Caramana, E., et al., "The Construction of Compatible Hydrodynamics Algorithms in Multiple Dimensions Utilizing Conservation of Total Energy" (30th AIAA Fluid Dynamics Conference, Norfolk, VA, June 28–July 1, 1999).

Liska, R., et al., "Smoothly Blending Circular Interpolants in Two- and Three-Dimensions" (submitted to *Comput. Aided Geometric Des.*).

Multigrid Homogenization of Heterogeneous Porous Media

98033

Joel E. Dendy

We are developing new, efficient, numerical, multilevel methods for homogenization in models of flow through heterogeneous porous media. The numerical simulation of flow through these media has become a vital tool in forecasting reservoir performance, analyzing groundwater supply, and predicting the subsurface flow of contaminants. Consequently, the computational efficiency and accuracy of these simulations is paramount. However, the parameters of the underlying mathematical models (for example, permeability and conductivity) typically exhibit severe variations over a range of significantly different length scales. Thus the numerical treatment of these problems relies on a homogenization or upscaling procedure to define an approximate coarse-scale problem that adequately captures the influence of the fine-scale structure. Inherent in such a procedure is a compromise between the competing objectives of computational efficiency and numerical accuracy. Although techniques that balance these conflicting demands exist for a few specific fine-scale structures, this is not the case in general. Moreover, upscaling has been identified as a crucial and open problem.

Our motivation is derived from the observation that multiple-length scales are captured automatically by robust multilevel iterative solvers, such as the multigrid method that was developed at Los Alamos. In recent work on two-dimensional (2-D) single-phase saturated flow for periodic heterogeneous media, we developed an algorithm based on the operator-induced variational coarsening of black box multigrid that offers a significant improvement in the compromise between accuracy and efficiency.

In any simulation that employs upscaled or homogenized (tensor)

coefficients, a measure of their accuracy is critical. It was determined that the multigrid homogenization (MGH) method naturally computes an upper bound of the homogenized coefficient. Moreover, in 2-D we extended the method to compute a lower bound as well. In practice these bounds are quite good; preliminary calculations indicate that the use of both bounds provides a significant improvement in the accuracy of the simulation.

We are extending the MGH method to 3-D, and preliminary results are encouraging. Once again, the upper bound is obtained naturally by the MGH method. Preliminary investigation of a lower bound demonstrates that its computation is possible but more difficult than in 2-D; many questions remain.

Signal Integrity Verification

98555

David Cartwright

We are developing an understanding of the relevant high-frequency physical electromagnetic regimes, new algorithms, and associated software for accurately predicting the electromagnetic time-delay and crosstalk in three-dimensional (3-D) structures composed of multiple dielectrics. This project will substantially extend capabilities in modeling, simulation, and high-performance computing in the areas of 3-D, static, and time-dependent electromagnetic simulations of complex structures of general shapes. The new finite-difference time-domain (FDTD) codes developed in this project provide an improved, validated field solver for the time-dependent Maxwell's equations that can be used in various Laboratory programs in threat reduction.

This project has two separate but related components dealing with 3-D electromagnetic simulations: (1) capacitance extraction from complex 3-D structures and (2) a new FDTD code for accurately predicting the high-frequency electromagnetic fields in complex 3-D structures.

We developed a new tool for calculating the capacitance matrix for complex 3-D interconnect structures involving multiple layers of irregularly shaped interconnect imbedded in different dielectric materials. This method uses a new 3-D adaptive unstructured grid capability developed at the Laboratory called LaGriT and a linear finite element algorithm. What is new and different in this approach is that the capacitance is determined from the minimum in the total system energy as the nodes are varied to minimize the error in the electric field in the dielectric(s). This code has been validated against a large number of analytical and numerical test cases.

A new 3-D FDTD field solver was written and partially tested against results from an existing 3-D field solver in the Laboratory's Applied Physics Division. This code is being generalized to include important physical effects that occur at high frequency (greater than 1 GHz) in various electronic devices. We are incorporating the new LaGriT software into this code to take advantage of its elaborate "bookkeeping" and 3-D graphical capabilities and are preparing documentation describing the code in its present version.

Publications

Cartwright, D.C., et al., "Capacitance Extraction from Complex 3-D Interconnect Structures," in *Technical Proceedings of the 2nd International Conference on Modeling and Simulation of Microsystems (MSM99)*, (Computational Publications, Boston), p. 159.

Atomic, Molecular, Optical, and Plasma Physics, Fluids, and Beams

Quantum Feedback Control: Methods and Applications

99004

Salman Habib

The main goal of this project is to develop a theoretical and computational framework for the design and analysis of quantum feedback control systems. Quantum feedback control is expected to play an essential role in promoting technological applications of mesoscale quantum systems that operate at the interface of classical and quantum mechanics. Investigation and understanding of system dynamics in this intermediate regime is also one of the aims of our project. Theoretical techniques developed as part of our effort will be applied to the experimental paradigm of cavity quantum electrodynamics with laser-cooled atoms. A special-purpose compute engine will be built in order to simulate the experiment and the action of the quantum feedback control loop.

Our theoretical effort currently focuses on understanding the role of analogies between classical control theory and the quantum control problem. In cases when these can be made mathematically precise, classical optimal control results can be applied directly to quantum systems. It is therefore of interest to know under what conditions this is possible. As part of the theoretical effort, we are also investigating the question of optimality with regard to the measurement process, an aspect unique to the quantum control problem.

Our computational effort involves the simulation of feedback control in quantum systems. We have written parallel-supercomputer code for performing such simulations and for investigating the relative merit of various simulation methods. The purpose of the simulations is to explore feedback control algorithms that may be performed under real experimental conditions. As far as this practical part of the project is concerned, we have developed a tentative design for the experimental implementation of the feedback and have begun examining such state-estimation and control algorithms as are within the reach of the experiment. We have designed and are constructing the Quantum Control Virtual Testbed for simulating the actual experiment and controlling it using dedicated control hardware based on the use of DSP (digital signal processing) and FPGA (field programmable gate array) chip sets.

Our work toward understanding continuous quantum measurements applied to nonlinear dynamical systems has led to the formulation of the conditions under which classical mechanics is obtained from quantum dynamics. We have succeeded in obtaining the classical Lyapunov exponents from an analysis of the quantum trajectories obtained from quantum measurement theory. This is a key milestone in showing how classical chaos emerges from the underlying quantum substrate.

Publications

Bhattacharya, T., et al., "Continuous Quantum Measurement and the Emergence of Classical Chaos" (submitted to *Phys. Rev. Lett.*).

Strongly Coupled Dusty Plasmas

97003

Dan Winske

This project uses dusty plasmas to study fundamental properties of strongly coupled plasmas. Strongly coupled plasmas occur in many situations in nature, such as the interiors of white dwarfs, neutron stars, and giant planets. Dusty plasma is produced by injecting micron-sized particulates (dust grains) into an rf discharge plasma. Using laser scattering to observe the motion of individual grains, we studied their alignment into strings and lattices and measured the spacing between grains to compare with strongly coupled plasma theory for the interaction potential between nearby grains. We then modeled the experiments with molecular dynamics simulations that incorporate these interactions.

During this final year of the project, we measured the spacing between dust grains of a known size that are injected into our dusty plasma chamber and subsequently form into vertical chains. Using a relatively simple model for the plasma sheath above the lower electrode, where the grains reside, we are able to predict the particle spacing as a function of the interaction potential between nearby grains and parameters of the plasma discharge. We found that the wake potential that forms behind grains because of the flow of ions toward the electrodes is important in the alignment process and contributes in a major way to the type of crystalline structures that are produced. We investigated the properties of the wake potential using plasma simulation techniques that treat the plasma ions as discrete particles, the plasma electrons as a fluid, and the dust grains as stationary objects. On a much longer time scale, we used molecular dynamics simulations to study the dynamics of grain to grain interactions and their alignment into strings. We found reduced spacing between grains as the rf-power applied to the electrodes is increased, in agreement with the experiments. Overall, we conclude that to fully understand the dynamics of dusty plasmas, we need to use plasma properties beyond the simple models in typical strongly coupled plasma theories and calculations.

Publications

Hammerberg, J.E., et al., "Directional Ordering and Dynamics in Dusty Plasmas," in *Proceedings of the 2nd International Conference on the Physics of Dusty Plasmas*, Y. Nakamura et al., Eds. (Elsevier Science, Amsterdam, in press).

Hammerberg, J.E., et al., "Molecular Dynamics Simulations of Dusty Plasma Crystal Formation: Preliminary Results," in *Strongly Coupled Coulomb Systems*, G. Kalman et al., Eds. (Plenum Press, New York, 1998), p. 237.

Murillo, M.S., "Longitudinal Collective Modes of Strongly Coupled Dusty Plasmas at Finite Frequencies and Wavevectors," *Phys. Plasmas* **6**, 33 (2000).

Murillo, M.S., and H.R. Snyder, "Measurement and Modeling of Particle Spacing in Strongly Coupled Dusty Plasmas," in *Proceedings of the 2nd International Conference on the Physics of Dusty Plasmas*, Y. Nakamura et al., Eds. (Elsevier Science, Amsterdam, in press).

Winske, D., et al., "Dust Wake in a Collisional Plasma," in *Proceedings of the 2nd International Conference on the Physics of Dusty Plasmas*, Y. Nakamura et al., Eds. (Elsevier Science, Amsterdam, in press).

Winske, D., et al., "Numerical Simulation of Dusty Acoustic Waves," *Phys. Rev. E* **59**, 2263 (1999).

Geometric Phase, Spatial Resonance, and Control in Spatially Extended Nonlinear Systems

97002

Robert Ecke

Thermal convection with rotation provides a unique system for the study of novel phenomena in nonlinear dissipative systems. In particular, a one-dimensional, nonlinear traveling wave that we discovered is well described by the Complex Ginzburg-Landau (CGL) equation. This state is a thermal wave confined near the walls of a cylindrical convection cell and is effectively one-dimensional in the azimuthal coordinate. It has azimuthal symmetry in the base state and is characterized by a wavelength and a wave speed.

We used this state to conduct an experimental search for the geometrical phase in dissipative systems, which was previously shown to apply to Hamiltonian systems, both quantum mechanical (Berry Phase) and classical (Hannay Angle). A second experiment is a model for topographic forcing of wave motion that can arise in geophysical systems.

We computed the geometric phase for a model CGL equation with experimental coefficients, demonstrated the existence of the geometric phase in the model, and compared the computed and experimental results (see figure). There is quite good agreement between the predictions and the experiment, although the scatter in the experimental data should be reduced. We also showed the existence of the geometric phase as an average quantity in the chaotic regime of the CGL equation.

We are causing the base state to respond to a more general application of temporally and spatially distributed perturbations, allowing for the possibility of controlling a spatially extended nonlinear system. Such control is extremely important in manufacturing, in process control in chemical engineering, and in the broader area of engineering control theory and application.

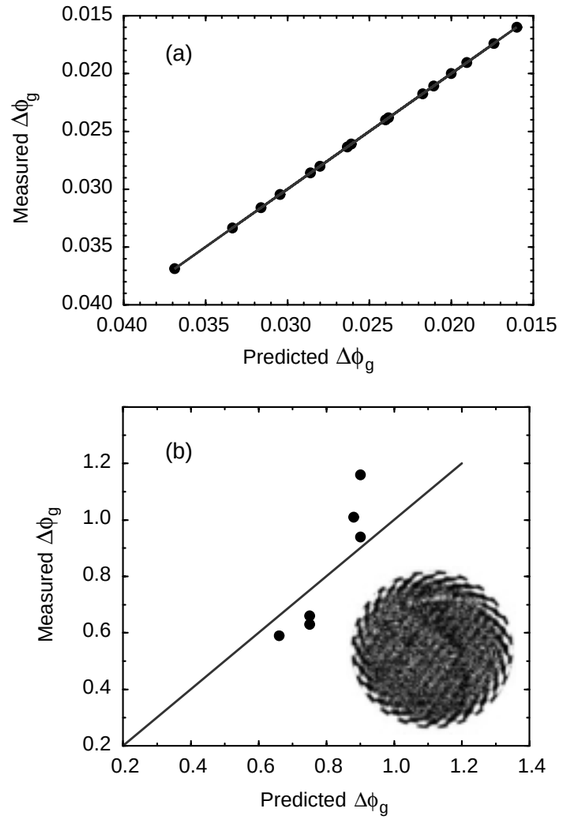

Comparison of (a) the numerically computed geometric phase for the CGL model and (b) the measured experimental phase with the predicted geometric phase from an analytic expression derived from the CGL model. The numerical and experimental data are the solid circles and the theoretical expectations are the solid lines. The inset in (b) is the experimental state of side-wall convection.

Artificial Atoms Probed by Femtosecond Pulses: Evolution of Optical Properties during the Bulk-Atomic Transformation

98001

Victor Klimov

In our project we study the evolution of electronic and optical properties of materials during the gradual transformation from the atomic to bulk-crystalline regimes. This year we concentrated on the effect of spatial confinement and surface properties on depopulation dynamics of electron and hole quantized states in CdSe quantum dots (QDs). Understanding carrier relaxation behavior in QDs is an important step toward developing efficient light-emitting, nonlinear-optical, and photovoltaic devices based on quantum-confined nanostructures.

Because of an enhanced surface-to-volume ratio, carrier dynamics in strongly-confined QDs are strongly affected by surface states (intrinsic and/or defect-related). In the case of surface-dominated relaxation, electron and hole relaxation paths are different. To separately study electron and hole dynamics, we use femtosecond transient absorption (TA) in the visible and infrared (IR) spectral ranges. Visible interband TA spectroscopy provides information on electron relaxation, whereas the application of the IR probe tuned in resonance with intravalence-band transitions allows one to study hole relaxation behavior.

The time-resolved broadband TA spectra of CdSe QDs show that, in the visible spectral range, TA is dominated by state-filling induced bleaching of optical transitions at 2.26 and 2.4 eV involving the lowest 1-S electron and the two lowest S-symmetry hole states (see the figure). TA signals in the near-IR range are due to excited-state intraband absorption. A striking feature of the spectra is the much faster relaxation of IR TA than visible TA. Because of a high density of valence-band states, interband TA (visible spectral range) is dominated by electrons, whereas in the near-IR range, TA is due to intravalence-band transitions. Therefore, relatively slow relaxation of visible TA signals (sub-100-ps initial decay) and very fast relaxation of IR TA (subpicosecond time scale) are due to depopulation of electron and hole quantized states, respectively.

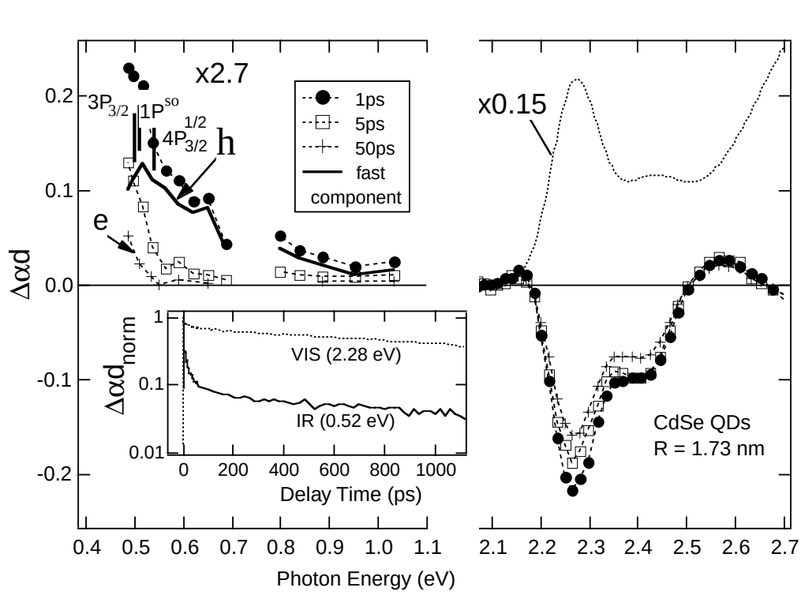

Visible-near-IR TA spectra (symbols) of CdSe colloidal QDs (mean radius 1.7 nm) recorded at different delay times between pump and probe pulses. Dotted line is the linear absorption spectrum. Inset: Comparison of visible (2.28 eV) and IR (0.52 eV) TA dynamics.

Our studies of samples with different surface passivations indicate that initial electron relaxation depends strongly on QD surface properties, suggesting this is due to trapping at surface defects. On the other hand, the hole dynamics are practically unaffected by the degree of surface passivation and remain very fast in all types of samples, including QDs overcoated with a layer of a wide-gap semiconductor. This strongly indicates that subpicosecond hole dynamics are not due to trapping at surface defects, but rather are a result of relaxation into intrinsic QD states.

Publications

Klimov, V.I., et al., "Electron and Hole Relaxation Dynamics in II-VI Semiconductor Nanocrystals," in *Microcrystalline and Nanocrystalline Semiconductors, Proc. Materials Research Society*, M.J. Sailor et al., Eds. (Materials Research Society, Warrendale, PA, 1999), Vol. 536, p. 155.

Klimov, V.I., et al., "Electron and Hole Relaxation Pathways in Semiconductor Quantum Dots," *Phys. Rev. B* **60**, 13740 (1999).

Klimov, V.I., et al., "Femtosecond Inter- and Intraband Spectroscopy of Semiconductor Quantum Dots," in *Quantum Electronics and Laser Science Conference, 1999 OSA Technical Digest*, (Optical Society of America, Washington, DC, 1999), p. 16.

Klimov, V.I., et al., "Ultrafast Dynamics of Inter- and Intraband Transitions in Semiconductor Nanocrystals," *Phys. Rev. B* **60**, R2177 (1999).

Torres-Martinez, C.L., et al., "Biomolecularly-Capped Uniformly Sized Nanocrystalline Materials: Glutathione-Capped ZnS Nanocrystals," *Nanotechnology* **10**, 340 (1999).

Direct Observation of Individual, Optical Energy-Transfer Events

99005

William Patrick Ambrose

Optical energy transfer is used to obtain information about changes in molecular orientation and distance on a length scale between 1 and 10 nm. Extracting donor-acceptor distances often requires assumptions about the underlying distributions of dipole orientations, vector displacements, and dipole approximations in energy-transfer theory.

In this project we plan to experimentally observe interactions between individual pairs of molecules at optical energies, free from ensemble averaging. We will scan individual molecules relative to one another using fine-positioning techniques. The results should allow us to directly test approximations used in energy-transfer theories.

The technical impact of the proposed work is the ability to produce optical images at wavelength l with a resolution better than l/100 = 5 nm, far below the diffraction limit (l/2). This capability can then be used to guide the design of surface-based sensors with molecules embedded in thin films, such as those needed for the DOE Chem-Bio Nonproliferation Program.

This project is in the design phase. The main activity involves construction of a fine positioner with low mechanical vibration and position feedback in three dimensions. We have numerically evaluated the position-noise level needed to achieve short-range optical energy-transfer imaging; we expect that 0.1-nm relative-position noise will be required. We have designed a three-dimensional, wide-range scanner with position feedback in all axes to reduce drift, hysteresis, and position noise. Custom scanner parts are on order for the horizontal fine positioner.

We have conceived a new idea for short-distance feedback sensing and control in the metrology loop that should achieve less than 0.1-nm noise in the vertical position. Two stages of vibration isolation can be used to reduce mechanical vibration above a few hertz to less than 0.1 nm of noise. The first stage of isolation is commercially available and is on order. We have preliminary designs for the second stage of vibration isolation with ~0.3-Hz cutoff.

Publications

Ambrose, W.P., et al., "Single Molecule Detection with Total Internal Reflection Excitation: Comparing Signal to Background and Total Signals in Different Geometries," *Cytometry* **36**, 224 (1999).

Ambrose, W.P., et al., "Single Molecule Fluorescence Spectroscopy at Ambient Temperature" (to be published in *Chem. Rev.*).

Dynamical Stability and Quantum Chaos of Ions in a Linear Trap

99002

Daniel James

This project investigates the optimization of emergent quantum technologies such as ion trap quantum computers in the light of quantum dynamic instabilities. Our specific goal is to investigate dynamical quantum instabilities and quantum chaos for ions confined in a linear ion trap, and to develop experimental tests using the ion trap apparatus currently under construction at Los Alamos for the quantum computation project. Quantum chaos is the study in the quantum domain of systems that, in the domain of classical mechanics, are chaotic. Single or multiple ions confined in a linear trap interacting with a near-resonant laser field are examples of such a system ideally suited to both theoretical and experimental study. The apparatus built for the trapped-ion quantum computer experiment at Los Alamos can, with little or no modification, be adapted to study in the quantum domain systems that classically display chaotic behavior.

To achieve a meaningful experimental program, we are developing theoretical models for a wide class of dynamical quantum instabilities and of quantum chaos for ions confined in a linear ion trap. Developing the requisite theoretical and experimental techniques allows us to establish a very important new direction in modern science, namely dynamical stability and spectroscopy of quantum chaotic systems.

The work performed in the first year of this project was wholly theoretical. We made good progress toward a thorough understanding of the dynamic stability of the driven harmonic oscillator and how it may be realized in the quantum domain using cold-trapped ions. In particular, we examined both analytically and numerically the quasi-energy spectroscopy in the regions of weak- and strong-quantum chaos. Also we worked out in detail the theoretical description of the sort of laser-ion interactions required for realizing this system experimentally. We also analyzed the potential problems that may occur in the experimental system.

Further, we investigated the stability of an ion in a linear ion trap using Husimi function approach, studying the "quantum phase space" of a harmonic oscillator interacting with a plane monochromatic wave. In the regime of weak chaos, the quantum system has the same symmetry as the classical system. Analytical results agree with the results of numerical calculations. We also studied in detail, analytically and numerically, the regular regime and the regime of weak chaos inside a stochastic web. Areas of analysis included quantum-classical correspondence, quantum phenomena of tunneling between the resonant cells, diffusion via the quantum separatrices, and nonmonotonic influence of weak chaos on a diffusion rate. We also derived conditions for experimental realization of quantum chaos in this system.

Publications

Berman, G.P., et al., "Dynamical Stability and Quantum Chaos of Ions in a Linear Trap" (submitted to *Phys. Rev. A*).

Berman, G.P., et al., "Symmetry of Quantum Phase Space in a Degenerate Hamiltonian System" (submitted to *CHAOS*).

Gulley, M.S., et al., "A Raman Approach to Quantum Logic in Calcium-like Ions" (submitted to *J. Opt. Soc. Amer. B*).

Quantum Computation and Nuclear Magnetic Resonance

98004

Raymond Laflamme

All of today's computations can be understood in terms of variants of a simple computer model, the Turing machine. The model implicitly assumes the classical laws of physics and is therefore often referred to as "classical computing." By changing this assumption to one based on the more fundamental laws of quantum mechanics, a new paradigm for computation is obtained, quantum computing. Until recently a subject of essentially academic interest, quantum computing has become a field with an enormous potential to revolutionize computer science, impact issues of national security, and offer economic returns. A key event has been the discovery of quantum-error-correcting codes and implementations of individual quantum gates. The goal of this project is to push forward quantum gates using liquid-state nuclear magnetic resonance (NMR).

This year we have experimentally demonstrated quantum teleportation, using the molecule of trichloroethylene dissolved in deuterated chloroform (see accompanying figure). The nuclear spin of the hydrogen and the two carbon-13 atoms formed the quantum bits. The experiment consisted of demonstrating that we had enough control over the behavior of these nuclei to implement simple quantum algorithms.

Our recent experiments have increased the number of qubits for liquid-state NMR from 3 to 7. At present, this is a world record for the control of a prototype quantum computer. Using a solution of crotonic acid in deuterated chloroform, we have defined a benchmark of 7 qubits for quantum computation. This benchmark is adaptable to other devices but was illustrated using NMR technology.

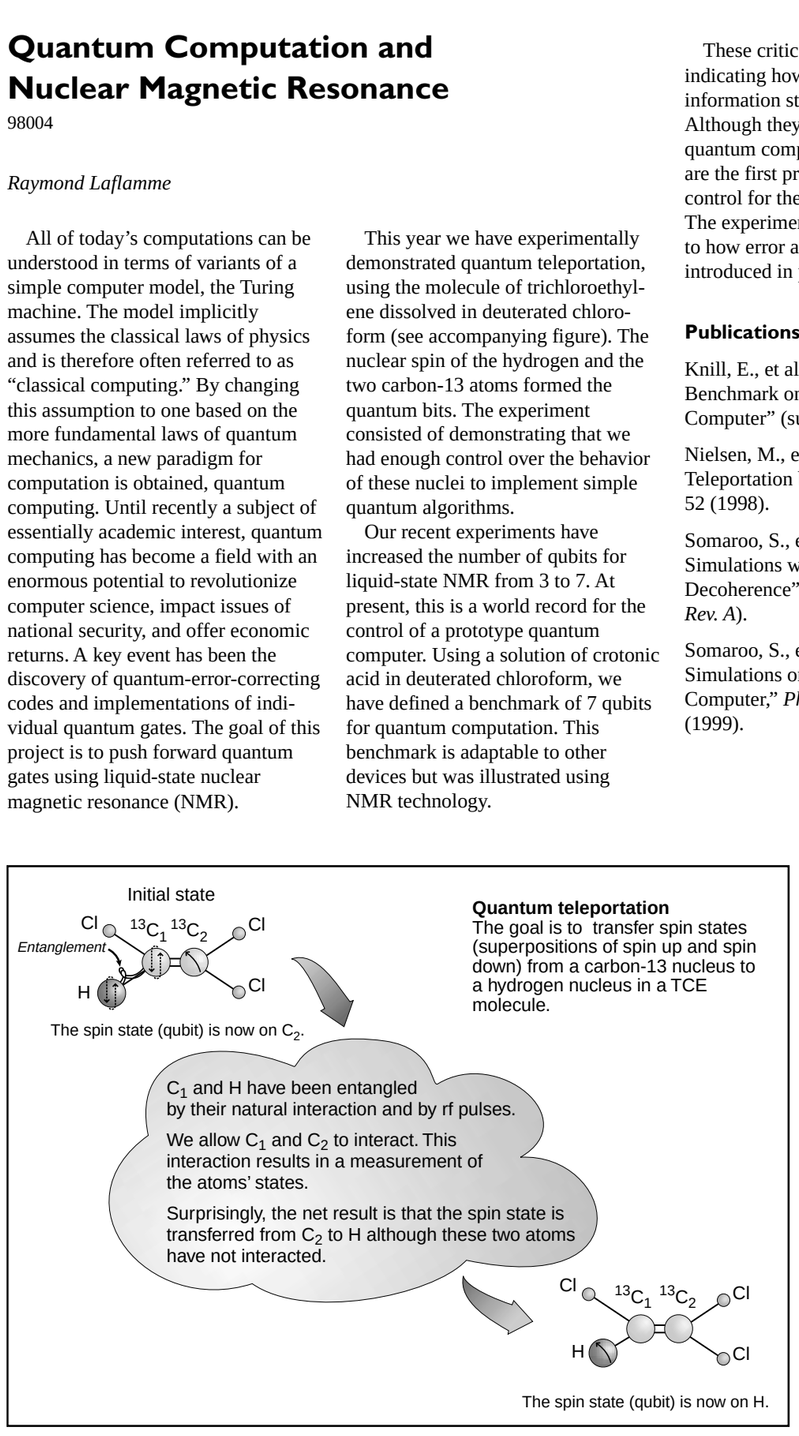

Pictorial demonstration of quantum teleportation. The goal is to transfer spin states (superpositions of spin up and spin down) from a carbon-13 nucleus (C_2) to a hydrogen nucleus (H) in a TCE molecule without having interaction between them.

These critical experiments are indicating how much we can control information stored at the atomic level. Although they fall short in building a quantum computer, these experiments are the first proof of principle of control for the quantum information. The experiments also give us a clue as to how error and imperfections are introduced in physical devices.

Publications

Knill, E., et al., "A Cat State Benchmark on a 7-bit Quantum Computer" (submitted to *Nature*).

Nielsen, M., et al., "Quantum Teleportation by NMR," *Nature* **396**, 52 (1998).

Somaroo, S., et al., "Quantum Simulations with Natural Decoherence" (submitted to *Phys. Rev. A*).

Somaroo, S., et al., "Quantum Simulations on a Quantum Computer," *Phys. Rev. Lett.* **82,** 5381 (1999).

High-Gain Self-Amplified Spontaneous-Emission Experiments in the Infrared

98054

Dinh C. Nguyen

This project conducted self-amplified spontaneous-emission (SASE) experiments in the infrared wavelength range aimed at achieving very high gains, close to saturation, using the high-brightness electron beams that are available at the Los Alamos Advanced Free-Electron Laser (FEL) Facility. The success of this experiment will have a significant impact on the direction of research and development leading to the construction of the Linac Coherent Light Source at the Stanford Linear Accelerator Center (SLAC).

The basic method for generating coherent x-rays, SASE, is a new, high-gain concept that uses no mirror but relies on beam guiding in a long undulator to amplify spontaneous noise all the way to saturation. Los Alamos National Laboratory, working closely with SLAC, the University of California at Los Angeles (UCLA), and other DOE laboratories, has taken the lead role in the initial demonstration of the basic SASE physics at infrared wavelengths.

In FY98 the first demonstration of very high SASE gains in the infrared at Los Alamos was achieved using the Advanced FEL's high-brightness electron beams and an undulator with an effective length of 1 m (see the first figure for the SASE experimental setup). Subsequent experiments, which were performed at Los Alamos in collaboration with UCLA and SLAC and which used the same electron beam but with a 2-m undulator built at UCLA, achieved a single-pass gain at 12 μm of 3×10^5, the highest single-pass gain ever achieved in the infrared. These SASE experimental results validated the physics of this new high-gain FEL and demonstrated for the first time excellent agreement between theoretical predictions and experimental measurements of exponential dependence of power on current, optical gain guiding in the undulator, pulse-to-pulse amplitude fluctuations, and electron microbunching at an infrared wavelength.

Our effort this year was aimed at modifying the 2-m undulator to obtain higher magnetic fields and increasing the SASE interaction to achieve saturation in a single pass. To this end, we removed the undulator magnets from the undulator housing, reduced the gap between the magnet pole tips (to increase the on-axis magnetic field), and reassembled the undulator. We also made corrections to the undulator field errors to obtain a straight electron-beam trajectory through the undulator. Our measurements indicate the modified undulator is suitable for the SASE experiment.

Our initial calculations show that the SASE experiment in the present configuration will saturate in less than 2 m of undulator length (see the second figure). If successful, this experiment will show the highest gain ever achieved in a single pass and allow us to study the physics of SASE at saturation level.

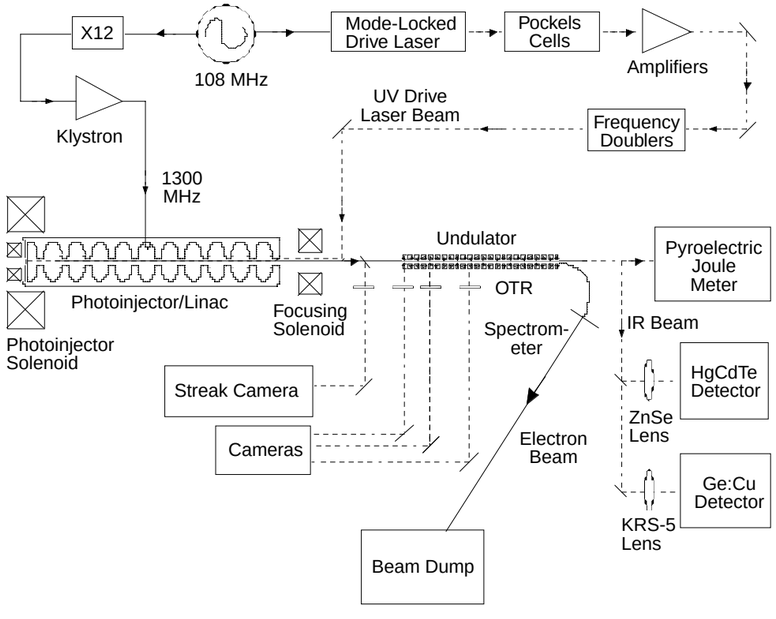

Schematic of the high-gain SASE experiment (OTR is optical transition radiation).

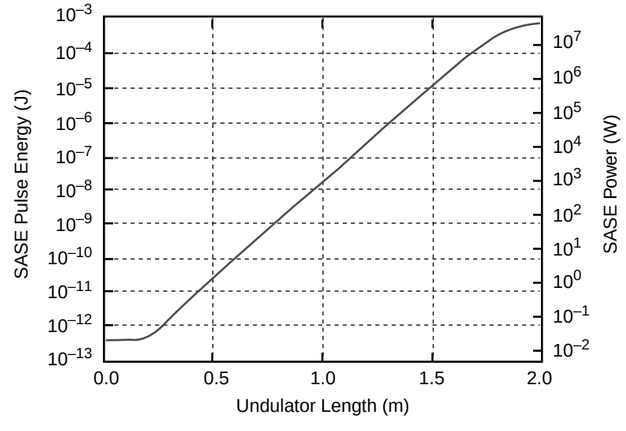

Calculated SASE power versus length of the modified undulator.

Publications

Tremaine, A., et al., "Measured Free-Electron Laser Microbunching Using Coherent Transition Radiation," *Nucl. Instrum. Methods Phys. Res., Sect. A* **429**, 209 (1999).

Laser Cooling of Solids

97015

Tim Gosnell

Existing methods for cooling detectors in satellites suffer significant disadvantages such as excessive size and weight, noise-generating vibration, short working life, and high cost. We have directed our recent research toward developing a long-lasting and vibration-free cryogenic refrigerator, building upon last year's record-breaking accomplishment of cooling a sample fiber to –37°C. We have also demonstrated for the first time the cooling of crystalline material.

We have discovered a method to cool solid materials with laser light that is analogous to the well-known process for laser cooling of gas-phase atoms. By using a rare-earth-doped fluoride glass as a working substance, we have executed the world's first demonstration of solid-state laser cooling, a method equally applicable to other substances such as impurity-doped insulators and stoichiometric insulating crystals and potentially applicable to semiconductors. This project allowed us to pursue our investigations into the optical and solid-state physics of candidate refrigerants, to discover the minimum temperature to which a solid can be optically cooled, to develop a theoretical understanding of photon thermodynamics as applied to laser-cooled solids, and to help develop the techniques required to construct a practical optically driven cryogenic refrigerator.

As a result of our research, we have made the best measurements to date of absorption and stimulated emission cross sections for trivalent ytterbium and discovered that trivalent thulium impurities are especially deleterious to the laser-generated cooling effect. In related results that have significantly improved experimental reproducibility and rationalization of results, we have independently determined sample emissivity, built new sample mounts that combine ultralow thermal conduction with vibration isolation, and incorporated vacuum-compatible translation stages and internally mounted optical components for precise optical positioning and alignment of samples within the evacuated sample chamber.

Publications

Gosnell, T. R., "Laser Cooling of a Solid by 65 K Starting from Room Temperature," *Opt. Lett*. **24**, 1041 (1999).

Create and Study Quantum Degenerate Systems

99001

David J. Vieira

Our main goal in this project is to sympathetically (collisionally) cool a Fermi gas of even-mass rubidium atoms to the quantum-degenerated regime with a rubidium-87 Bose-Einstein condensate (BEC). We will study ultracold Fermi-Fermi and Fermi-Bose collisions along with a variety of predicted quantum mechanical effects.

Beyond the exciting developments in the production and study of cold, dilute alkali BEC systems in rubidium-87, sodium-23, and lithium-7, there is a growing interest in exploring Fermi-degenerate systems, which are made from atoms with half-integer total spin. Lithium-6 and potassium-40 are the only stable alkali isotopes in nature with half-integer total spin. Although several groups around the world are attempting to study these Fermi-degenerate systems, it is not known whether either lithium-6 or potassium-40 has the desired collision properties that are needed to reach full Fermi degeneracy.

We are exploring the use of radioactive rubidium isotopes for studies of Fermi-degeneracy systems. In particular, recent theoretical calculations indicate that rubidium-84 (half-life = 33 days) and rubidium-86 (half-life = 19 days) have favorable collision properties between them and with ultracold rubidium-87. Consequently, both are considered to be excellent candidates for Fermi-degeneracy studies. We have thus developed an experiment to trap rubidium-84 or rubidium-86 atoms in a time-orbiting-potential magnetic trap and to collisionally cool these species down to the Fermi-degenerate regime using an overlapping cloud of ultracold rubidium-87 BEC. If sympathetic cooling is successful, we will investigate the quantum mechanical nature of such macroscopic, ultracold fermionic systems and explore the interactions between mixed fermion-boson quantum degenerate systems. This work may also lead to additional research involving the development a very bright and coherent atomic source called an atom laser.

As an initial step, we recently trapped rubidium-84 in a magneto-optical trap (MOT) for the first time (see first figure). We have also trapped rubidium-83 (half-life = 86 days) for the first time, but our sample was too weak to attempt the trapping of rubidium-86. By overlapping a cloud of 3×10^5 cold rubidium-84 atoms with a large cloud of 7×10^7 rubidium-87 atoms, we were also able to set a limit on the rate of mixed-isotope inelastic collision loss from the trap, which could affect the rubidium-84 trapping lifetime (see second figure). Under our trapping conditions, our measurements showed that this loss rate was small enough to represent no problem for the sympathetic-cooling experiment.

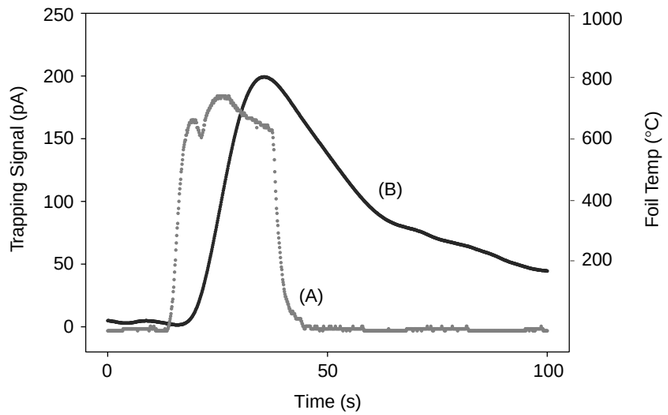

A trapping signal showing a time sequence for the pulsed release and trapping of rubidium-84 that has been implanted into a yttrium catcher foil for several minutes. Trace A is the foil temperature measured with an optical pyrometer. Trace B shows the trapping signal as rubidium-84 fills and is lost from the magneto-optical trap. The peak signal corresponds to ~20,000 trapped rubidium-84 atoms.

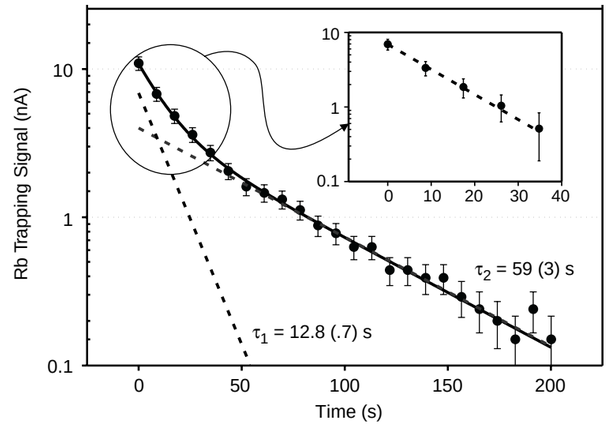

A plot showing the trapping signal time dependence for a million rubidium-84 atoms trapped in our MOT. The data fit a double exponential decay (solid line), indicating that there are two loss mechanisms that dominate for different density regimes. At high densities (short times), light-assisted collisions between trapped atoms dominate. This gives rise to the short-lived component. As the number of trapped atoms depletes, light-assisted losses become negligible and only hot background gas collisional losses remain, corresponding to the long-lived component. The inset shows a fit to the short-lived component when the long-lived component has been subtracted from the trapping signal. We observed no difference in the short-lived component when we overlapped a large cloud of rubidium-87 with rubidium-84.

Quantum Coherence and Decoherence: Trapping a Schrödinger Cat

99003

Wojciech H. Zurek

The purpose of the project is to investigate decoherence in the context of atom and ion trap experiments. Ion traps are a promising implementation of quantum computers. They also offer a possibility for carrying out experiments that will shed new light on the process of decoherence, which is responsible for the transition from quantum to classical behavior. Atomic traps were recently used to observe Bose-Einstein condensation, a symmetry-breaking phenomenon, which involves basic quantum considerations at a fundamental level. In both settings Schrödinger cat states—very quantum superposition—will be implemented. We are investigating loss of quantum coherence analytically in situations relevant for the forthcoming experiments. Such decoherence must be understood if quantum computers are to be implemented in the ion trap setting; it will be the ultimate source of errors, present even after all the more mundane design imperfections have been successfully dealt with.

We have studied formation of topological defects in Bose-Einstein condensates. Some of the conclusions of the mean field theory (obtained previously by one of us in the setting of superfluids) were recovered in a much more rigorous treatment. We have also studied quantum chaos in time-dependent potentials, which can be implemented in ion traps. The pronounced effect of decoherence on the evolution of quantum chaotic systems was observed, and the entropy production rate caused by decoherence was recovered. Last but not least, we have studied decoherence in an as yet unexplored regime, where it actually selects discrete quantum energy eigenstates.

Publications

Paz, J.P., and W.H. Zurek, "Quantum Limit of Decoherence: Environment Induced Superselection of Energy Eigenstates," *Phys. Rev. Lett.* 82, 5181 (1999).

Zurek, W.H., "Decoherence, Chaos, Quantum-Classical Correspondence, and the Arrow of Time," *Acta Phys. Pol.* 29, 3689 (1998).

Zurek, W.H., "Decoherence, Einselection, and the Existential Interpretation (the Rough Guide)," *Philos. Trans. R. Soc. London,* A 356, 1793 (1998).

Stochastic Resonance in Arrays with Tunable Nonlinearity and Coupling

98003

Alp Findikoglu

Stochastic resonance (SR), a phenomenon in which random noise plays a constructive role and enhances a nonlinear system's response to a deterministic signal, has been observed in a wide range of physical and biological systems. Our project combines a novel experimental technique with extensive theoretical analysis to investigate array-enhanced and threshold-free SR. We are incorporating tunable coupling and strong exponential nonlinearities in the design of arrays of stochastic resonators, and hence are opening new opportunities for the technological exploitation of SR. Furthermore, the Laboratory has played a central role in the recent, vigorous development of the theory of nonequilibrium nonlinear dynamics. However, quantitative comparison with experiment had largely been lacking. This project provides such comparisons.

To study the effect of noise on nonlinear response, we designed and fabricated 8-cm-long coplanar waveguides with strong dielectric nonlinearities. We have used these devices as generic, distributed nonlinear resonators (essentially, building blocks for arrays) and characterized them extensively as functions of various noise, bias, and signal inputs. In parallel with this experimental effort, we have developed a theoretical model that uses a set of coupled partial differential equations in a nonlinear medium with two boundaries. We have used our experimental results to parameterize the model, which, in turn, has successfully predicted the deterministic aspects of our waveguides.

The ongoing research focuses on the stochastic effects on the nonlinear response. In our experimental work with the waveguides, we have observed the largest stochastic effects for biases that lead to minimum first-order harmonic generation (i.e., small biases that cancel out extrinsic voltage drops and lead to zero intrinsic electric field). Under such optimal biases, the first-order harmonic power increases monotonically with increasing input noise until a sharp drop in harmonic power is observed due to heating effects. Also, by using various high- and low-pass filters, we have been examining the effect of frequency content of the noise on the observed effects. To simulate stochastic effects, we are currently incorporating noise into the input of our model of our nonlinear system. Preliminary results indicate that the addition of noise does indeed lead to enhancement of the first-order harmonic power.

Publications

Burtsev, S., et al., "Numerical Algorithms for the Direct Spectral Transform with Applications to Nonlinear Schrödinger-Type Systems," *J. Comp. Phys*. **147**, 166 (1998).

Camassa, R., et al., "Nonlinear Waves and Solitons in Physical Systems," *Physica D* **123**, 1 (1998).

Findikoglu, A.T., et al., "Electrodynamic Properties of Coplanar Waveguides Made from High-Temperature Superconducting $YBa_2Cu_3O_{7-x}$ Electrodes on Nonlinear Dielectric $SrTiO_3$ Substrates," *J. Appl. Phys*. **86**, 1558 (1999).

Findikoglu, A.T., et al., "Electrodynamic Properties of Single-Crystal and Thin-Film Strontium Titanate" (submitted to *Integr. Ferroelec*.).

Findikoglu, A.T., et al., "Pulse-Shaping Using Nonlinear Dielectric $SrTiO_3$," *Appl. Phys. Lett*. **74**, 1770 (1999).

Moro, E., and G.D. Lythe, "Dynamics of Defect Formation," *Phys. Rev. E* **59**, R1303 (1999).

Laser-Plasma Interactions in Diffraction-Limited Beams

98002

David S. Montgomery

We are performing an experimental, theoretical, and computational investigation of laser-plasma interactions with a near-diffraction-limited beam in a well-characterized plasma. This investigation, which is the first of its kind in this field, measures the saturated levels of stimulated Raman scattering (SRS) and stimulated Brillouin scattering (SBS), in both the presence and absence of laser self-focusing. The eventual outcome of this work will be the development and benchmarking of reduced models that can be incorporated into laser fusion design codes.

This year we performed a three-week series of experiments on the Trident laser. We fielded a new time-resolved spectrometer to measure SBS spectra, fielded an angularly resolved imaging spectrometer to study the transmitted beam spectrum, fielded a near-backscatter imager to diagnose light scattered directly outside the lens cone, and measured Thomson scattered spectra from the diffraction-limited beam. The experiments focused on obtaining data for Mach 0 and Mach ≥1 transverse flow to examine beam steering and filamentation and their effect on SRS and SBS.

An important result from this series of experiments was that we obtained the first direct evidence of the stabilization of filamentation by supersonic transverse flow. This effect has been predicted by nonlinear fluid simulations but had not been observed experimentally. The data show that for Mach ~0, the transmitted beam sprays out to large angles, indicative of filamentation. The angularly resolved spectra show a broad spectrum (~2–3 Å) for this case.

Experiments for Mach ≥1 show that the transmitted beam undergoes beam steering but is confined to within roughly the original beam cone. The angularly resolved spectra show a resolution-limited spectra (~0.8 Å), which indicates that the beam is dynamically stable. Initial three-dimensional (3-D) fluid simulations are in qualitative agreement with the data.

We have further developed our 3-D fluid model and have compared the simulations to the experimental beam steering results for Mach 2. The simulations are in good quantitative agreement with the experiments for the beam-deflection centroid and are in good qualitative agreement with the measured bow-like features in the transmitted beam distribution.

Finally, a mesoscale model of SRS Langmuir turbulence has been developed and tested in one dimension and two dimensions (2-D). A 2-D fluid code for SRS is being developed to incorporate this mesoscale model, which will be compared to the fully nonlinear 2-D fluid model for SRS.

Publications

Montgomery, D.S., et al., "Characterization of Plasma and Laser Conditions for Single Hot Spot Interaction Experiments," *Laser Part. Beams* **17**, 348 (1999).

Montgomery, D.S., et al., "Flow-Induced Beam Steering in a Single Laser Hot Spot" (submitted to *Phys. Rev. Lett.*).

Plasma-Wakefield Accelerator

97010

Bruce Carlsten

Current acceleration methods limit the gradient to about 100 MV/m in accelerators for high-energy linear colliders and short-wavelength free-electron lasers. Achieving higher gradients requires new methods in future accelerators. High-density plasmas excited by lasers have been shown to support gradients in excess of several tens of gigavolts per meter (GV/m); however, it is not easy to excite such large gradients in plasmas with the phase and amplitude control needed for accelerator applications.

In this project, we plan to demonstrate that an electron-driven plasma-wakefield accelerator (PWA) can achieve 1-GV/m gradients. The advantage of this type of PWA over a laser-driven PWA is that the plasma oscillation phase is easily controlled. In addition, we intend to demonstrate high transformer ratios and other second-order effects required to scale the PWA to a practical device.

This year we have assembled a differential interferometer that can measure transient plasma densities of 10^{16} cm^{-3}. From ionization cross sections of the noble gases, we determined that xenon should be the best gas for our PWA. We have run with this gas and demonstrated energy loss in our drive electron beam. These experiments are ongoing, and we hope to maximize this energy loss and therefore the plasma-wakefield gradient. We will also try other noble gases to confirm our choice of xenon.

Development and Engineering of the Ion-Cut and Low-Temperature Direct-Bonding Process

98015

Michael Nastasi

The goal of this research is to develop an innovative integrated circuit (IC) engineering technology that will allow for the development of effective and economical silicon-on-insulator (SOI) materials technology. The ability to produce SOI materials is critical to the production of (a) high-performance radiation-hardened ICs, (b) ICs that can operate at low power, and (c) three-dimensional IC chips with densities 250 to 500 times higher than conventional chips.

Our approach uses recent technological breakthroughs in the areas of plasma processing, ion beam stimulated cleaving of single crystalline silicon, and plasma stimulated low-temperature direct bonding of silicon to SiO_2. We are developing a plasma-source ion implantation chamber to implant hydrogen into single-crystal silicon. Implanted hydrogen stimulates the cleavage of a thin layer of silicon, which will be bonded to an insulating substrate. We will also study the fundamental materials physics of the ion stimulated cleaving process.

During the past year we studied the formation of hydrogen-induced surface cleaving (blisters) in <100> n-type silicon as a function of boron doping and preimplantation. The silicon substrates had four different n-type dopant levels, ranging from 10^{14} cm^{-3} to 10^{19} cm^{-3}. These substrates were implanted with 240 keV B^+ ions to a dose of 10^{15} cm^{-2}, followed by a rapid thermal anneal at 900°C for 30–60 s to force the boron atoms into substitutional lattice positions (activation). The samples were then implanted with 40 keV H^+ to a dose of 5×10^{16} cm^{-2}. The implanted H^+ distribution peaks at a depth of about 475 nm, whereas the distribution in the implanted B^+ is broader and peaks at about 705 nm.

To evaluate the role of the B^+ implantation, we prepared control samples implanted with H^+ only. We then vacuum annealed all the samples at 390°C for 10 minutes. We observed blisters resulting from subsurface cracking at depths of about 400 nm in most of the B^+ implanted samples, but not in the samples implanted with H^+ only. This study indicates that the blistering results from the coalescence of the implanted hydrogen into bubbles. The doping with boron facilitates the short-range migration of the hydrogen and the formation of bubbles. A comparison of the observed crack depth with the depth of the damage peak resulting from the H^+ implantation (evaluated by the computer code TRIM) suggests that the nucleation of hydrogen bubbles occurs at the regions of maximum radiation damage, and not at the regions of maximum hydrogen concentration. For given values of B^+ and H^+ doping, the blister density decreased with increasing n-type doping, when the boron is activated. We also observed blister formation in B^+ implanted samples that had not been activated. In this case, the blister density increased with increasing value of n-type doping.

In addition, we made significant progress on the development of the plasma source ion implantation chamber for the ion implantation of hydrogen into single-crystal silicon. Our goal is to understand the effect of plasma generation methods on the molecular state of hydrogen ions. We are installing a new high-voltage modulator in the chamber, which will allow plasma-based implantation studies up 100 kV.

Publications

Hochbauer, T., et al., "The Influence of Boron Ion Implantation on Hydrogen Blister Formation in N-Type Silicon," *J. Appl. Phys.* **86**, 1 (1999).

The Plasma Fluidized Bed

97026

Robert P. Currier

We are developing fluidized-bed technologies that use cold plasmas. The basic concept is to couple radio-frequency or microwave energy into the fluidizing gas to form a nonequilibrium plasma. Depending on conditions, the plasma may contain high concentrations of ions and free-radical species, all at modest bulk temperatures. We intend to use these species to initiate or promote desired chemistry in extractive metallurgy, plasma-assisted thin-film deposition, and surface modification of solids. Potential programmatic applications include "dry" processes for actinide recovery from contaminated solids, coatings of specialty ceramics, and use of the fluidized bed as a tool for validating plasma-hydrodynamic codes.

Our effort this year included fluidized-bed hydrodynamics, extractive chemistry, and electromagnetic design. In order to probe hydrodynamic conditions, we conducted laser light-scattering experiments in inductively coupled systems using both fine particles (<15 μm) and larger particles (>100 μm). We discovered that fine particles introduced into the plasma region can become trapped in regions near the wall and remain there for extended periods. For larger particles, the number density of particles in the bed increases (by as much as a factor of 4) as compared with that in a nonplasma bed under the same conditions. We believe there is a complicated interaction between the drag forces, the Coulombic charging on the particles, and the electromagnetic fields that gives rise to these phenomena. We also established, using Langmuir probe measurements, that the existence of a strongly coupled fluidized plasma may be possible.

We measured pressure fluctuations in both nonplasma and plasma fluidized beds as a probe of the dynamics. Clear differences between the two can be seen in the resulting (Fourier and power) spectra. The superficial gas velocity at which transition to a turbulent fluidized bed occurs is higher in the plasma fluidized-bed case. We are completing a time-series analysis of the two data sets to further quantify changes in the underlying dynamics (e.g., by determining the underlying attractor dimensions).

We also examined hydrodynamic-plasma coupling in a circulating fluidized-bed system operating in the so-called fast fluidized regime. We discovered that under flow conditions in which kinetic-energy and hydrodynamic-drag considerations should overwhelm the effects of charging, particle flow patterns are still significantly affected by the plasma. Specifically, we found that the plasma can effectively "focus" the particles toward the center of the cylindrical tube housing the fluidized bed.

In hydrogen-rich plasmas, we examined extractive chemistry using solid compounds such as titanium dioxide and silicon monoxide and glassy materials such as dunite (an olivine-class magnesium silicate). We found that extraction of oxygen in the form of water proceeds at a regular rate over extended periods (as determined by mass spectral analysis). The solid particles pass through the various sub-oxide phases as they are reduced toward the base metals (as determined by x-ray diffraction). We also examined the effect solid-particle size has on the conversion rates and found only a weak dependence. This result, together with the steady production of water, attests to the diffusivity of atomic hydrogen, which can penetrate directly through the lattice. Scanning electron micrographs of the treated solids typically showed significant amounts of surface reconstruction, with an apparent increase in porosity. Surface-area measurement are under way to better quantify these plasma-induced changes.

In addition, we examined the nitriding of a metal (silicon) in a nitrogen-rich plasma fluidized bed. We found that silicon nitride could be produced at bulk temperatures of approximately 200°C. However, both the alpha and beta phases were produced in approximately equal amounts. We also found that at high power inputs, the particles tended to fuse into a free-standing fractal-like structure. Experiments with other metals did not show this effect, suggesting that reaction bonding of the particles may be an important contributing factor (as opposed to just microdischarges, which could "weld" particles together upon contact).

Our electromagnetic design efforts focused primarily on issues related to the ultimate scale-up of the laboratory reactors. We refined our design for an annular reactor configuration suitable for establishing and maintaining a glow discharge. This design should permit operation at much higher pressures (even approaching atmospheric), which will improve the global kinetics associated with the chemistry of interest.

The Compliance Method for Measuring Residual Stress

97017

Michael Prime

The purpose of this project was to develop a method for measuring residual stress in materials. We determined this stress by extending a slot into the material to the stressed region and measuring the released strains. Our goal was to turn this fledgling method into a proven and versatile technique that could fill the gaps in current residual-stress measurement technology. In addition, the extended measurement capabilities resulting from our project will help us develop and verify predictive stress models, which are relevant to many applications.

Our major accomplishment this year was measuring the spatial variation of residual stresses in a metal-matrix composite. No existing technique is able to measure these critical stresses. The accompanying figure shows a narrow slot that was carefully cut between the 180-μm-diameter tungsten fibers in a Kanthal matrix while a gauge measured surface strains. We subsequently developed the analytical tools to account for the anisotropic material behavior of the composite. These measurements will be used to predict the loads that will cause the fiber to debond from the matrix, a crucial issue, for example, in NASA's use of these composites in deep space probes.

Also this year, we experimentally proved a new conceptual idea for measuring a cross-sectional map of residual stresses. On a steel test specimen, we measured the contour of the surface created by cutting the part in half (whereas the compliance method measures surface strains after increments of slot cutting). In an analytical model, the deformed surface was forced back to its original state, and the original residual stresses along the surface were correctly revealed. This method is analytically simpler than the compliance method, yet it provides a more complete map of residual stresses. Much more effort is needed to develop this new method to its full potential, but we have at least proven that it will work.

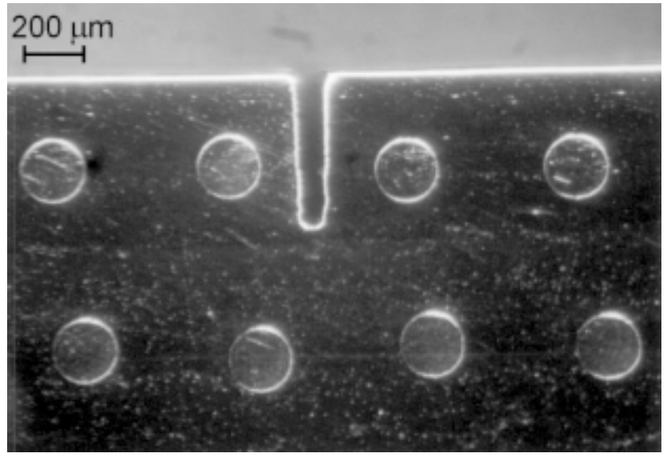

Cross section of an 80-μm-wide slot made between the fibers in a metal-matrix composite. The slot was made by electric discharge machining with a 30-μm-diameter tungsten wire, and strains were measured on the top surface.

Publications

Prime, M.B., "Measuring Residual Stress and the Resulting Stress Intensity Factor in Compact Tension Specimens," *Fatigue Fract. Eng. Mater. Struct.* **22**, 95 (1999).

Prime, M.B., "Residual Stress Measurement by Successive Extension of a Slot: The Crack Compliance Method," *Appl. Mech. Rev.* **52**, 75 (1999).

Prime, M.B., et al., "Residual Stress Measurement and Prediction in a Hardened Steel Ring" (to be published in *Mater. Sci. Forum*).

Rangaswamy, P., et al., "Comparison of Residual Strains Measured by X-ray and Neutron Diffraction in a Titanium (Ti-6Al-4V) Matrix Composite," *Mater. Sci. Eng.* **A259**, 209 (1999).

Highly Constrained Bandwidth Combinational Algorithm for Transmission of Speech (HC-BATS)

99019

John Hogden

We are developing information extraction techniques to transmit large quantities of sensor data using a relatively low number of bits. Because modern sensors such as satellites are capable of collecting large quantities of data and are often used remotely, data must be as compressed as possible. Our focus this past year was on combining Laboratory-developed speech compression algorithms with state-of-the-art data compression algorithms to show that information can be more effectively extracted from a complex signal (speech) as demonstrated by a reduction in the bit rate needed to transmit the signal. A success for speech transmission should translate to more data compression in other domains.

We measure success by the reduction in bit rate needed to transmit a signal. The Laboratory's algorithms should decrease the number of bits required to transmit vector quantization (VQ) codes. With VQ, consecutive feature vectors are first constructed from windows of a signal, which are the signal's successive short-time chunks, e.g., 20 ms. Then a nearest-neighbor scheme is used to find the closest representative vector in a set of representative vectors. This closest vector is then transmitted using a binary code; e.g., if there are 256 representative vectors, then an 8-bit code is used to transmit each vector.

Current compression schemes ignore information about the probability of sequences of VQ codes, information that can potentially decrease bit rates. We are studying a Laboratory-developed technique called MALCOM for its potential to find low-bandwidth signals that can encode VQ code sequences using additional "error bits." The error bits encode the VQ code at time *t* using information in the low-bandwidth signal at *t*. Results show that VQ code sequences are highly predictable given the MALCOM-derived signals, but the total number of bits still exceeds the bits used to transmit the VQ codes; thus, we have not yet improved on the very efficient VQ coding scheme with our limited exploration of the MALCOM parameter space. Nonetheless, we have reduced the necessary bits by about 8% from our first tries and fully expect to succeed as we refine the technique.

Acoustic-Network Refrigerators

98017

William Ward

The acoustic-network refrigerators that we are developing are descendants of the thermoacoustic refrigerator developed at the Laboratory during the past 15 years. The acoustic-network refrigerator shares the thermoacoustic refrigerator's simplicity, but it uses acoustic-network principles to achieve Stirling cycle efficiencies without the complexity inherent in traditional Stirling refrigerators. This helium-charged, CFC (chlorofluorocarbon)-free technology also elevates the application of the Stirling cycle to the temperature range of domestic, industrial, and military cooling uses, where it can have the most significant impact on economics and energy use. This project will also impact ecological systems when, for example, CFC-coolant systems such as chillers on naval vessels can be replaced with these improved models.

This year we built a laboratory-scale refrigerator capable of several hundred watts of cooling at temperature lifts of 30°C. Mean flow across the regenerator, or Gedeon streaming, is identified as one of the primary reducers of cooling power and efficiency. To enhance efficiency, we suppressed this flow with a pair of miniature electric fans, which allowed for continual suppression adjustment.

We also incorporated continuous impedances of a transmission-line nature to tune the acoustic circuit. This type of circuit element is more compact and reduces minor losses generated in lumped-impedance elements for the same application.

Our computer models of acoustic-network refrigerators and other network feedback thermoacoustic systems improved steadily over the year, but we still find significant discrepancies with the results of the experiment, particularly at higher amplitudes. We attribute these discrepancies to conventional acoustics streaming, minor losses in acoustic flows, and other nonlinearities. We continue working to identify and minimize these effects.

Virtual Bandwidth via Stochastic Polyspectra

97028

Murray Wolinsky

The Shannon reconstruction theorem establishes that a continuous time signal can be perfectly reconstructed from a set of its (discretely) *sampled* values when the samples are taken at a rate at least twice that of the highest frequency present in the signal. If this condition is violated—if the original signal is sampled at a rate less than the Nyquist frequency—then the samples do not contain all the information present in the original signal, and we can no longer reconstruct it. Reconstructing a continuous signal from these samples results in an *aliased* signal that differs from the original signal. However, this aliased signal is, in general, a perfectly reasonable signal that might have been the source of the original samples. For this reason (and others), aliasing is generally thought to be undetectable.

This year we showed that under conditions very common in practice, aliasing *can* be detected; for the class of signals under consideration, aliased samples are measurably different from unaliased samples. We originally relied on the bispectrum, a higher-order version of the power spectrum, to resolve a long-standing controversy about its use in detecting aliasing. In particular, we confirmed that the region marked 2 in the first figure will only be present (nonzero) if the original (assumed stationary) signal is aliased. Our work this year also demonstrated, without using the bispectrum, that the detection of aliasing is possible.

To increase our understanding of what is possible with bispectra, we must establish the conditions of *joint realizability* of power spectra and bispectra and determine the amount of power required to transmit a given bispectrum. We made limited, but significant, progress. For the first time, we were able to obtain lower bounds on the power for transmitting a given bispectrum using a particular class of time series models. Although our efforts to generalize these results to obtain model-independent bounds have not yet been successful, we did learn that a very common inequality used to normalize the bispectrum is invalid, a result with considerable significance for the practical use of the bispectrum. In particular, although the "noise immunity" of the bispectrum has made it attractive for certain applications (see the second figure), this improper normalization may have diminished its usefulness in many situations. The properly normalized bispectrum for "real-world" measurements may be considerably more significant than is generally regarded; therefore, this research may lead to considerably greater employment of bispectra in noisy measurements.

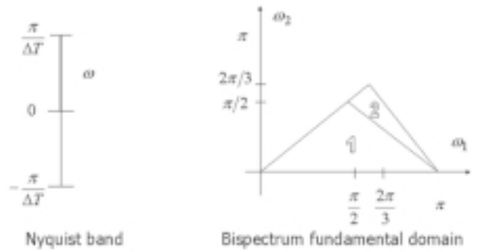

The fundamental domain for the power spectrum (left) and for the bispectrum (right).

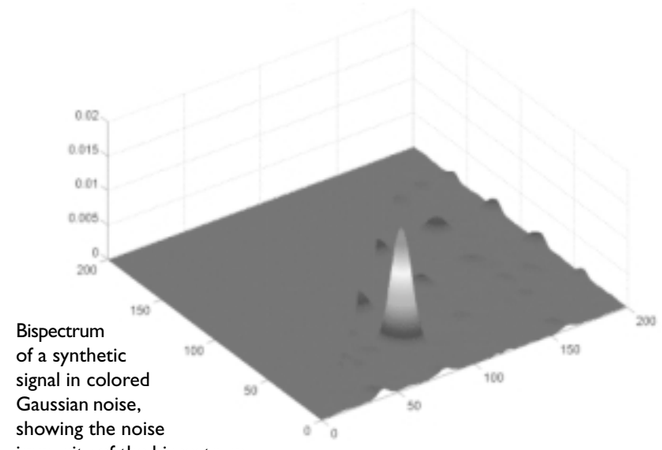

Bispectrum of a synthetic signal in colored Gaussian noise, showing the noise immunity of the bispectrum.

Publications

Vixie, K.R., et al., "The Bispectral Aliasing Test: A Clarification and Some Key Examples" (Fifth Annual International Symposium on Signal Processing and Applications, Brisbane, Australia, August 22–25, 1999).

Vixie, K.R., et al., "Detection of Aliasing in Persistent Signals" (submitted to *IEEE Trans. Sig. Proc.*).

Tritium Recovery and Isotope Separation Using Electrochemical Methods

97027

R. Scott Willms

The primary goal of this project was to demonstrate a new tritium separation technology using ceramic electrochemical pumps based on solid oxide proton conductors. Techniques for the recovery of tritium gas and the removal of tritium from hydrocarbon gases are crucial in order to maintain the nation's nuclear stockpile. The recovery of tritium from the mixed waste amassed in the nuclear weapons complex is also of great national importance.

This project included the design, construction, and testing of the secondary containment glovebox for tritium separation experiments. The glovebox gas-handling subsystems have been tested, and electrical and computer connections are in the process of being completed. We executed and documented a full Failure Modes and Effects Analysis. The primary purpose of this glovebox is to provide secondary containment for the tritium permeation experiments, and two methods of detecting tritium that is being electrochemically pumped through the ceramic membrane have been incorporated into the system to provide for redundancy: a low-volume flowmeter and a pressure, volume, and temperature system. The experimental procedure for the tritium permeation experiments has been documented.

We focused additional work on the design of the permeation experiments and construction of the permeation test cells. Several cells had to be built because the high radiation environment of the permeation experiments prohibits the cells' reuse. Several proton-conducting samples have been prepared this year, including ceramic powders of Ba-Yb-Ce-O, Sr-Y-Ce-O, Sr-Yb-Ce-O, and Sr-Yb-Zr-O perovskites, which have been synthesized, characterized, and formed into dense solid electrolyte membranes. Various glass seals have been formulated and studied to provide the best seal between the ceramic proton conductor and the ceramic tubes used to collect the pure tritium permeated from the retained waste stream.

Publications

Mukundan, R., et al., "Tritium Conductivity and Isotope Effect in Proton-Conducting Perovskites," *J Electrochem. Soc.* **146** (6), 2184 (1999).

Pulse Shaping in Explosive-Pulsed Power

98016

Michael V. Fazio

This project has involved the development of pulse-shaping hardware to allow compact, explosive-power systems to properly drive loads such as high-power microwave tubes. Explosive-pulsed-power systems have milliohm source impedances with exponentially rising waveforms. High-power microwave tubes and other loads of interest require fast-rising, square-pulse outputs of several hundred kilovolts and a few ohms to a few hundred ohms impedance.

This year we developed two different pulse-shaping systems. These two approaches show promise in furthering the use of explosive-pulsed power—each with its own advantages. The first approach involves an air-core, high-efficiency transformer that is capable of up to 300 kV of output at 200 kA of current. The second approach involves an explosively formed fuse. This "opening-switch" is capable of interrupting millions of amperes of current and, coupled with a programmable turn-off resistance curve, can generate high-voltage square pulses into a variety of loads.

The transformer that we developed has performed very well. It is capable of taking a 6-MA, 70-kV input pulse and delivering several hundred kilovolts and hundreds of kiloamperes to a load. This compactly designed, air-core unit has a greater than 0.9 coupling factor and is readily produced.

The explosively formed fuse (EFF) that we developed is capable of generating hundreds of kilovolts at hundreds of kiloamperes with a square pulse into a variety of loads. Although more complex than the transformer, the output allows compact, pulsed power to drive loads that no other source can provide.

This year we built and tested both systems to determine the operating parameters. Combining these two different systems will allow a variety of loads to be powered by explosive-pulsed power, which was previously not possible.

Next-Generation High-Power Microwave Source

99021

Clifford Fortgang

The goal of this project is to design, build, and test a working prototype 17-GHz, 100-MW microwave source. The source is similar to that used by a free-electron laser, but will operate in a new regime with a reversed-axial guide magnetic field in addition to the usual wiggler magnetic field. Two important and distinct applications for this microwave source are as a radio-frequency source for the next-generation electron-positron particle-beam accelerator and as a design for a radio-frequency weapon to attack vulnerable solid-state electronic packages.

This year we finished the design and began the fabrication of the source's electron gun. We have a vacuum chamber with all metal seals with which we have obtained a vacuum of 10^{-10} torr. We have installed and heated an 8-in. thermionic cathode, the largest of its kind ever fabricated. The accompanying photos show both the vacuum vessel and the electron gun.

We have made measurements on the temperature uniformity of the cathode surface. This is important to producing a low-emittance beam, which enhances the microwave-tube performance. We have also made detailed measurements of the cathode emissivity, which is important for predicting the heater power requirements of the cathode.

We have begun some design work for the microwave tube itself and have written a simple computer code that calculates the resonance condition for various operational parameters. We have estimated the complicated effects due to space charge and have obtained a more comprehensive computer code to help guide us toward a final design of the microwave tube.

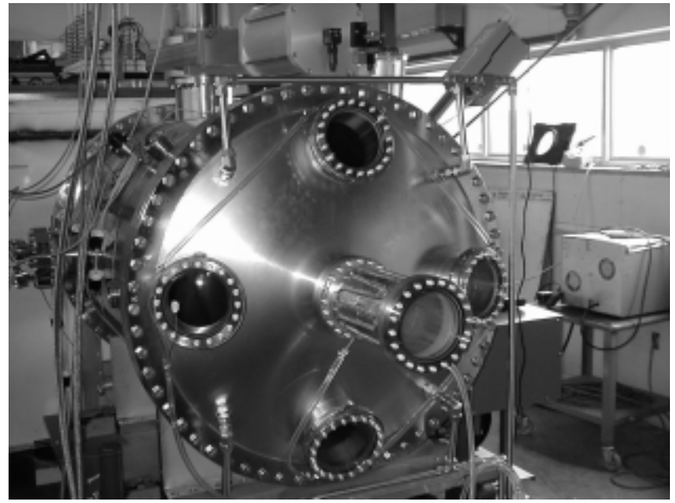

The vacuum vessel that houses our thermionic electron gun.

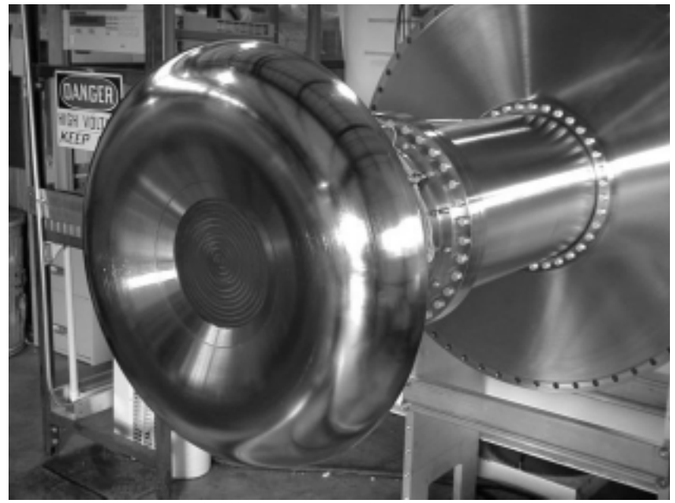

Our electron gun itself: an 8-in. thermionic cathode is surrounded by a stainless steel focusing electrode.

Use of Directed Light Fabrication for Fabricating Functionally Gradient Materials

99017

Gary Lewis

The focus of our work is to enable our Directed Light Fabrication (DLF) process to fabricate metal parts that have functionally placed or graded compositions. DLF is a one-step process that allows us to build up a part by depositing metal powder to the focal zone of a laser beam. A solid model of the part that defines its geometry and material placement boundaries controls the laser beam's motion and the delivery of metal powders from four feeders (see first figure). We have enhanced the process's versatility by integrating finite element design analysis with DLF's solid model, motion path, and process parameter controls. As a result, a designer can combine or change materials in specific areas of a part to improve localized material properties, such as wear or strain resistance. This capability will reduce the cost of fabricating nuclear weapons parts by eliminating multiple processing steps and the need for joining their products.

Using the DLF process, we have demonstrated the capability to place materials where they are specifically required during the fabrication of metal components. We used Abacus finite element modeling to model a commercially pure nickel (nickel-200), 4-point bend specimen, loaded in simulation of an overstress condition to establish a plastic deformation zone (see second figure). We eliminated the plastic zone at the same load on the specimen by replacing this zone with a nickel-30 copper (Monel K400) alloy having higher yield strength than the nickel-200. To fabricate the specimen, we extracted the coordinates of the nickel-200 plastic zone from the finite element analysis model and used them to redefine the zone in the solid model used to produce the deposition motion path. Discretely defined volumes for each zone are necessary to ensure that the materials and process parameters are changed appropriately in each deposition plane.

We enhanced the DLF system to provide the capability to change powders abruptly (see third figure) or to program a compositional gradient that is called from the motion path to control four separate powder feeders (see second figure). These capabilities were demonstrated with transitions among three different metals, nickel, nickel-30 copper, and nickel-30 copper + aluminum, titanium (Monel K500). The yield strength of these materials varied from 138–758 Mpa (20–110 KSI). By implanting the K500 alloy, we produce local precipitation hardening via heat treatment to precipitate gamma prime, forming the highest strength and hardness locally in the part. Additionally, we are using x-ray and neutron diffraction to measure and characterize the residual stress of these functionally graded parts and for input into the finite element analysis of the part under service conditions.

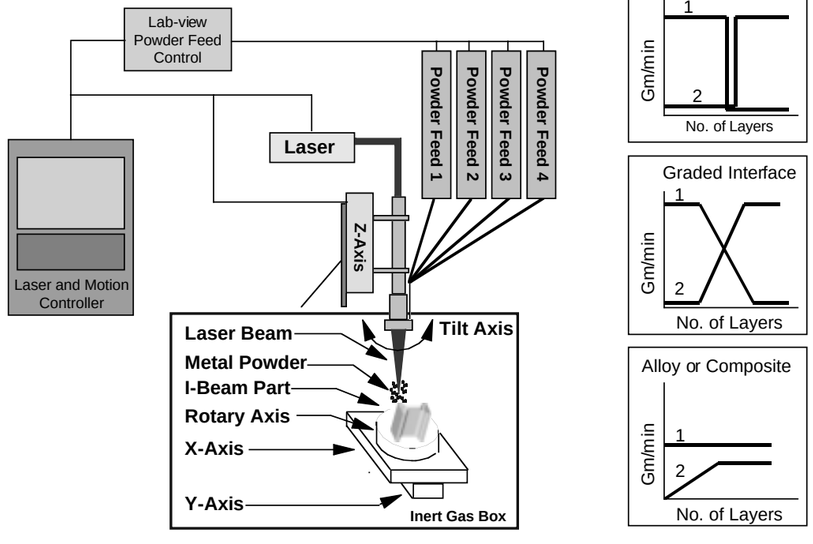

The motion path developed from a solid model defining both the part geometry and material placement boundaries controls four feeders that deliver metal powder to the focal zone of a laser beam. Compositional gradients are formed by ramping two or more feeders; sharp boundaries are formed by changing from one feeder to the other; and alloys and composites are formed by simultaneously feeding two or more feeders.

Publications

Lewis, G.K., et al., "Fabrication of Functionally Graded Metal Deposits," in *Proceedings of the 1999 World Conference on Powder Metallurgy and Particulate Materials* (MPIF, Princeton, NJ, 1999).

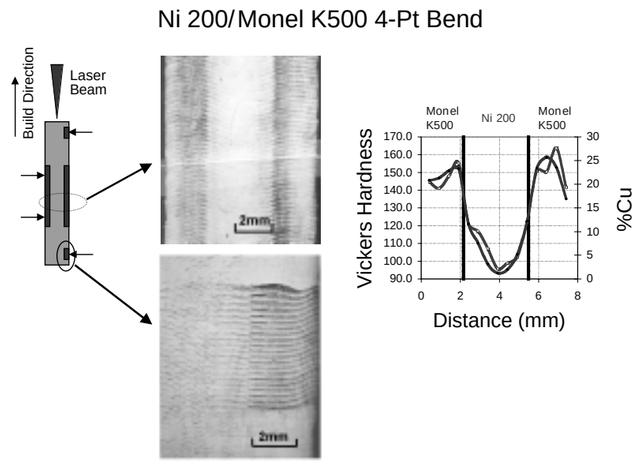

A 4-point bend sample is fabricated from nickel-200—yield strength 138 MPa (20 KSI)—and Monel K500, a precipitation-hardened nickel-30 copper alloy—yield strength 758 MPa (110 KSI)—when heat treated. The plastic zone of a nickel-200 test sample was modeled and then replaced with K500, with no yielding occurring at the same load. The process microstructure, hardness, and copper concentration are shown.

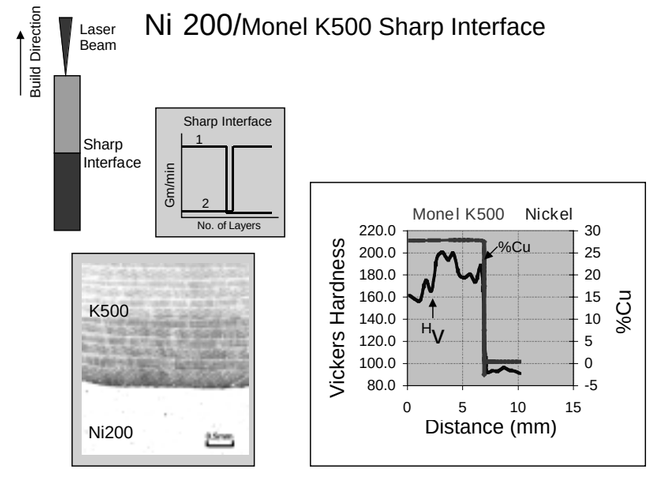

A sharp transition from nickel-200 to Monel K500 (nickel-30 copper) is made by commands placed in the motion path program to change powder feeds into the laser focal zone within one deposition layer. The microstructure at the transition, hardness, and copper concentration indicate the sharp change in properties within the bar.

Hydrogen Storage in Intermetallic Alloys

99020

Dan J. Thoma

Methodologies do not exist for designing complex intermetallic alloys useful in applications that require lightweight materials with large hydrogen-to-metal atom ratios. The resultant trial-and-error approaches severely limit our ability to create these alloys and to tailor such materials for given engineering applications.

Our purpose in this project is to demonstrate a newly developed methodology that uses (1) geometric models for hydrogen-site accommodation and (2) electronic structure calculations for available electronic-state occupancy on a class of intermetallic phases to develop new strategies for optimizing hydrogen capacity. Our research addresses the need to develop a priori methods for predicting chemical reactions and hydrogen capacities in an engineering product. The development of new geometric and electronic models (known in simpler forms to have an influence on hydrogen-storage capability) will provide an enabling strategy for designing chemical species without numerous experimental evaluations.

To date, we have made significant progress designing and testing intermetallics with the desired hydrogen-storage characteristics. The most significant development is the use of geometric models to predict the thermodynamic response of alloys. For example, we have developed accurate geometric models that actually predict the alloying limits of Laves-phase intermetallics.

The use of an alloying theory that substitutes for interstitial alloy theory (as found for hydrogen storage) was the next concept for us to address. An interesting but unexplained consequence of geometric space-filling models is distinct enthalpies of formation as a function of metallic diameter ratios of the atoms forming the stoichiometric phase. The enthalpy of formation correlation to size ratio also translates to an enthalpy of hydride formation. Therefore, based upon thermodynamic tie-line equilibria, we can use geometric models to predict the capacity of an alloy based on only the size ratios of metallic atoms forming the Laves phase. When we plot the heat of formation for hydrides as a function of diameter ratios, distinct lines of behavior develop, as confirmed by experimental measurements. We are using electronic structure theory to establish the fundamental principle governing this result.

The usefulness of this work provides an a priori methodology for designing hydrogen-storage characteristics in intermetallics. Our current hypothesis suggests that the location of the Fermi level on the density of states will dictate both the capacity and the plateau pressure. With the proof of this hypothesis, we have developed first-principles methodologies as well as geometric models for tailoring hydrogen response to any alloy. We are also incorporating these models into hydrogen-isotope applications.

Composite Films Made with Metallic Carbon Nanotubes

99018

Brian Fishbine

Our objective is to suspend metallic carbon nanotubes in polymer matrix in order to produce thin (~1-mm-thick) films that have low reflectivity in the microwave region. Because of their high length-to-radius ratios (up to 10^4 or more) and low resistivity (≤30 μohm·cm), these nanotubes should strongly absorb microwave radiation.

To obtain low reflectivity, however, such films must also closely match the impedance of free space. We plan to address this problem by increasing the dielectric constant of the film with increasing depth to form a gradient in the dielectric constant, the principle of pyramidal absorbers found in anechoic chambers.

In addition to defense uses, these thin films have potential for replacing paint on structures and vehicles, thus reducing the costs and environmental hazards associated with paint.

In the past year we developed a computer code to calculate the electromagnetic properties of individual metallic carbon nanotubes as well as the bulk properties of composite materials made with these nanotubes, such as the complex dielectric constant e_{comp} and the microwave absorption a_{comp}. By comparing the values of a_{comp} calculated from e_{comp} with those obtained from the nanotube concentration in the composite and the single-nanotube extinction cross-section—the sum of the scattering and absorption cross-sections—we verified that the code is consistent to a high degree of accuracy. We have also validated the code against experimental data published in the open literature.

Using scanning electron microscopy and transmission electron microscopy, we found that the quality of nanotube material obtained from different sources varies widely. Microscopy and other characterization techniques have allowed us to select the most promising nanotubes for further study.

We measured e_{comp} primarily with a coaxial dielectric probe, which is wideband (0.2–20 GHz) but requires comparatively thick samples (≥1 cm). This technique has allowed us to evaluate various composite fabrication techniques as well as the quality of nanotubes from various sources. However, the technique cannot easily be used to measure films as thin as we ultimately hope to make. Nor can it accurately measure small values of the imaginary part of e_{comp}. Fortunately, highly absorbing materials often have high values of the imaginary part of e_{comp}, although the ability to measure small values would help us understand absorption well below the percolation limit. Percolation occurs when the concentration of nanotubes is high enough to form conducting paths throughout the volume of a sample. Percolation can dramatically change the properties of composite materials.

Using the coaxial dielectric probe, we measured e_{comp} for composites of nanotube material suspended in organic liquids, aqueous solutions, and solid paraffin. We also used a single-frequency waveguide perturbation technique to make preliminary measurements on small pieces of composites consisting of nanotube material suspended in polysulfone and poly(methylmethacrylate), two common plastics.

Using Metallic Glasses in Ceramic-Metal Joining

98014

Rajendra Vaidya

Our primary objective for this project was to demonstrate the feasibility of using metallic glasses in joining ceramics to metals. Residual stresses due to mismatches in the thermal expansion properties of ceramic/metal joints can lead to failure at the joint or within the brittle ceramic. Low-temperature brazing techniques combined with ductile interlayers can alleviate this problem. However, the use of precious-metal-based brazes and an interlayer add to the complexity and cost of the joining process. To overcome these problems, we proposed the use of metallic glass brazes, an innovation that eliminates the need for separate interlayers in ceramic/metal joining. Metallic glasses can be bent and twisted into complicated shapes, and they melt more uniformly at lower temperatures compared with the base metal they are derived from.

We were successful in joining molybdenum disilicide to a stainless steel 316-L alloy using a metallic glass. The brazing process was reactive and resulted in the formation of intermetallic precipitates, and we expected this microstructure to provide excellent high-temperature creep resistance. Pushout tests performed on brazed samples indicated an average interfacial shear strength of 72.3 MPa. In most of these samples, failure on pushout occurred in a ductile manner within the braze.

We used one of two braze setups depending on the experiment to be performed and the shape of the stainless steel. For the disk-shaped samples used in the preliminary experiment, the brazing foil and substrates were arranged in a block-foil-block orientation, and the entire assembly was placed into a loading device. For the ring-shaped samples used in the pushout tests, the setup consisted of a holder with a recess that contained a stainless steel ring, a tube, and the brazing foil. Additional brazing material was fed into the ceramic/metal gap by using a brazing foil taller than the joint components. With minor modifications, both of these techniques can be adapted to produce industrial-size joints. Preliminary evaluations indicate that the residual stresses introduced into these joints with either technique are not great enough to induce catastrophic failure of the molybdenum disilicide.

Publications

Vaidya, R.U., et al., "Use of Metallic-Glasses in $MoSi_2$-Stainless Steel Joining" (submitted to *Mater. Sci. Eng. A*).

Instrumentation and Diagnostics

Stable Polymeric Light-Emitting Devices

98025

DeQuan Li

Polymeric LEDs (light-emitting diodes composed of layers of polymers) have attracted tremendous scientific and technological interest because (1) they are brighter and more colorful than liquid crystal displays; (2) they can be easily deposited onto large-area substrates, thereby yielding low-cost displays; and (3) they offer flexibility in materials and device design because they permit virtually unlimited structural variations that allow for tunability of bulk and interfacial properties.

Technologically, defense-related devices and instruments continue to require better and higher-performance LEDs. For example, fighter jets need ultrabright displays when in strong sunlight. Polymeric LEDs can also be fabricated into flexible, thin films and adapted for use in many unusual places where conventional, inorganic LEDs cannot be applied (e.g., a roll-up display).

We have synthesized light-emitting polymers with good thermal stability. Unlike conventional conjugated polymers, our polymers are soluble in water and hence can be processed into thin films. By using electrostatic interaction in an aqueous environment, we have fabricated these luminescent polymers into multilayer structures. The thickness of these self-assembled multilayers can be controlled by the number of layers or the number of deposition cycles.

Photoluminescent studies indicate that the polymers emit blue photons in the spectrum region of 380–430 nm. Compared with solution photoluminescents, which are centered around 370 nm, these polymers exhibit a red shift because of the solid-state packing effects of the multilayer films. We have characterized the films with x-ray reflectivity, and they showed remarkably well-defined, layered structures, with the interfaces between two alternating organic layers clearly distinguishable. The bilayer thickness was about 2.6 nm, which is the smallest unit that we can control in terms of device structures.

Current versus voltage (I-V) measurements showed that these polymers are somewhat semiconducting, with a resistivity of $\rho = 10^5\,\Omega$/cm. The contacts between the electrodes and the organic polymer layers are Ohmic in character.

We have fabricated new polymers with novel structures. Because of their design, these polymers are conjugated and may be processed without introducing soluble side chains. It is extremely rare to possess both complete conjugation—i.e., delocalized π-electrons along polymer chains—and good solubility. Therefore, we expect new and interesting phenomena from our polymers.

Publications

Hunag, W., "Synthesis, Characterization, and NLO Properties of a Phenothiazine-stilbazole Monolayer," *Langmuir* **15** (19), 6510 (1999).

Mashl, R.J., "Theoretical and Experimental Adsorption Studies of Synthetic Polymers on an Oppositely Charged Surface," *J. Chem Phys*. **110**, 2219 (1999).

Soliton Optical Communications

97005

Antoinette Taylor

We sought to establish a scientific foundation for the construction of a supercomputer fiber-optic interconnect that will support a sustained data flow of 10^{12} bits per second. More specifically, this project is a joint experimental/theoretical effort to investigate the physical limits of high bit-rate propagation of nonlinear optical pulses called solitons. The theoretical effort applies nonlinear-dynamical-systems analysis to the study of soliton propagation in optical-fiber transmission systems. The experimental effort relies on a powerful new diagnostic—originally conceived at Los Alamos—that measures the exact electric-field envelope and optical phase of ultrashort optical pulses as functions of time. This diagnostic makes possible for the first time characterization of the temporal evolution of optical solitons in fiber-optic waveguides. We will use this diagnostic to measure the characteristics of soliton propagation as functions of pulse width and interpulse separation.

This year we demonstrated that single-shot, second harmonic generation frequency-resolved optical gating (SHG-FROG) is a valuable tool for the analysis of the temporal and phase profile of shaped pulses. We demonstrated the ability to characterize the phase and amplitude of pulses with energies less than 20 pJ with a high dynamic range. Further, temporal reconstruction has been demonstrated for pulse durations in excess of 1 ps.

By changing the input intensity of the 150-fs, 1.55-μm pulses input into a 10-m optical fiber, we observed the transition from the low-intensity, linear-dispersive-broadening regime to the high-intensity soliton regime.

The figure reveals the reconstructed intensity and phase profiles of these pulses (left column) and the corresponding profiles obtained through numerical simulation (right column). The experimentally measured phase and intensity agrees quantitatively with the numerical simulations. With increasing pulse power, temporal narrowing is seen to occur as the nonlinearities counteract the linear dispersion that dominates at low power and the phase changes from a quadratic form corresponding to linear dispersion to a flat phase indicative of a soliton. At higher intensities, where the soliton is forming, the dynamics of the phase and amplitude are associated with the dispersive energy corresponding to the initial chirp on the pulse, leaving the soliton in a series of periodic bursts. Note how the ability to measure the phase profiles strongly cross-checks the comparison between simulation and experiment, which enables a full understanding of the pulse dynamics. The application of this method will enable a deeper understanding of the physical mechanisms governing ultrashort pulse propagation in fibers.

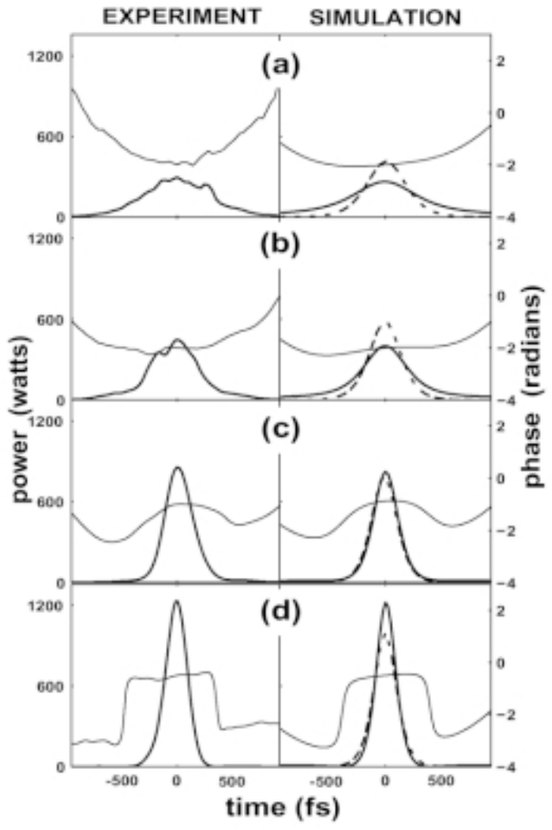

Reconstructed intensity and phase profiles of the FROG traces of the output pulses after traversing 10 m of fiber as the input energy increases from (a) 228 pJ, (b) 255 pJ, (c) 294 pJ, and (d) 318 pJ (left column) and the corresponding profiles obtained through numerical simulation (right column). The dashed line in the right column shows the intensity profile of the asymptotic soliton, whereas in both columns the thinner solid line represents the phase and the thicker solid line represents the intensity.

Publications

Nicholson, J.W., et al., "Evolving FROGs: Phase Retrieval from Frequency-Resolved Optical Gating Measurements by Use of Genetic Algorithms," *Opt. Lett.* **24**, 490 (1999).

Nicholson, J.W., et al., "Full-Field Characterization of Femtosecond Pulses Using Spectrum and Cross-Correlation Measurements" *Opt. Lett*. **24**, 1774 (1999).

Omenetto, F.G., et al., "Genetic Algorithm Pulse Shaping for Optimum Propagation in Optical Fibers" *J. Opt. Soc: B* **16**, 2005 (1999).

Omenetto, F.G., et al., "Observation of Chirped Soliton Dynamics at λ=1.55 μm in a Single Mode Optical Fiber Using Frequency-Resolved Optical Gating" *Opt. Lett.* **24**, 1392 (1999).

Omenetto, F.G., et al., "SHG-FROG Analysis of Low-Intensity Shaped Femtosecond Pulses at 1.55 μm" *Opt. Lett.* **24,** 1780 (1999).

Omenetto, F.G., et al., "Single-Shot SHG-FROG of Ultrashort Pulses at 1.5 Microns, in a Compact Folded Shaper," *in Ultrafast Electronics and Optoelectronics* 1999, *Vol. 28 of Trends in Optics and Photonics Series* (Optical Society of America, Washington, DC, in press).

Siders, C.W., et al., "Multipulse Interferometric Frequency-Resolved Optical Gating," *IEEE J. Quantum Electron.* **35**, 432 (1999).

Subpicosecond Electron-Bunch Diagnostic

97009

Steve Russell

Scientists developing advanced materials for a wide variety of products require knowledge about how atomic or quantum structure changes on ultrafast timescales. Therefore, we require probes that can reveal behaviors with a duration of only 1 trillionth of a second, or 1 ps. One approach for developing these probes is to develop electron accelerators capable of producing electron beams with bunch lengths as short as 0.3 mm or less. When we direct one of these beams onto a target, the beam generates a light or x-ray pulse capable of revealing fast atomic and quantum phenomena. A key obstacle to developing these electron accelerators is the absence of electron-beam diagnostics that can measure bunch lengths reliably, inexpensively, and with resolutions below 0.5 ps.

Our objective is to develop new subpicosecond bunch-length diagnostic techniques that are nonintercepting, are simple and inexpensive, and have resolutions that will scale below 0.5 ps. The specific goals of this project are (1) to build and test a diagnostic based on a transversely deflecting radio-frequency cavity and a nonintercepting beam-position monitor, (2) to test a diagnostic based on coherent Smith-Purcell radiation, and (3) to verify the results using the conventional streak camera method.

This year we demonstrated a radio-frequency cavity and beam-position monitor technique and achieved a resolution of 2.5 ps root-mean squared (rms). We believe that we can improve the resolution to about 0.4 ps rms and hope to pursue this goal during the remainder of the year. We also used an emittance diagnostic developed as part of our work on the radio-frequency cavity to measure the emittance growth because of coherent synchrotron radiation and the noninertial space-charge force as the beam was bunched. This important measurement verified theories developed at the Laboratory and was the subject of an invited paper at the 1999 Particle Accelerator Conference. We are currently collaborating with the Brookhaven National Laboratory in an experiment to investigate the Smith-Purcell diagnostic.

Publications

Russell, S.J., and B.E. Carlsten, "Measuring Emittance Growth due to Magnetic Bunching of an Electron Beam Using the Second Moment of Its Image Charge," *Proceedings of the 1999 Particle Accelerator Conference* (IEEE, New York, 1999), p. 477.

Electron Tunneling Spectroscopy of Buried Interfaces

99033

Ian H. Campbell

The aim of this project is to develop a new, spatially resolved spectroscopic technique to measure the fundamental electrical properties of an emerging class of electronic materials that have strong electron-lattice coupling. Examples of these materials and their applications include transition metal perovskite oxides like $LaMnO_3$, which have potentially important magneto-resistive properties, and conjugated organic materials, which are becoming important for optoelectronic applications.

We are using scanning tunneling microscopy techniques to inject electrons with well-defined and adjustable energy into these materials. Our spectroscopy is a valuable new technique in building a foundation for the technological development of this important class of electronic and magnetic materials.

This year we developed and built a derivative spectroscopy system that will allow us to answer fundamental questions concerning charge injection and transport. This system modulates the bias voltage between a scanning tunneling microscope (STM) tip and the material to be investigated at a frequency, *f*. In this approach, the position of the STM tip is controlled by a feedback circuit so that the tunneling current is held constant during the voltage modulation. The current in the material is measured at frequencies *f* and 2*f* using phase-sensitive measurement techniques. The measurements at *f* give the first, and at 2*f* the second, voltage derivative of the current with respect to the injection bias voltage. The current as a function of bias voltage exhibits changes in slope when a new transport channel becomes available. Measuring voltage derivatives makes these changes in slope apparent and thus enhances the sensitivity and energy resolution of the spectroscopy.

We also began a theoretical study of tunneling in materials with strong electron-lattice coupling. This study predicted that coupling can lead to significantly enhanced tunneling for electrons with energies in the energy gap of an insulator. We can find the energy barriers to charge injection from metal contacts to other materials and, by comparing the minimum voltage for electron and hole injection, we can determine the single-particle energy gap. Enhanced tunneling because of strong electron-lattice coupling will greatly influence the design of electronic devices based on these materials.

We also began to investigate the effects of disorder (irregularity in the occupation of lattice sites) on electron transport in these materials. This new class of materials can have significant intrinsic disorder, which can greatly affect the materials' electrical transport properties. An understanding of the electron-lattice coupling in them is essential for a science-based design strategy for the electronic and magnetic devices that are made from them.

Publications

Campbell, I.H., and D.L. Smith, "Schottky Energy Barriers and Charge Injection in Metal/Alq/Metal Structures," *Appl. Phys. Lett.* **74**, 561 (1999).

Campbell, I.H., et al., "Charge Transport in Polymer Light-Emitting Diodes at High Current Density," *Appl. Phys. Lett.* **75**, 841 (1999).

Kozhevnikov, M., et al., "Effect of Electron Scattering on Second Derivative Ballistic Electron Emission Spectroscopy in Au/GaAs/AlGaAs Heterostructures," *Phys. Rev. Lett.* **82**, 3677 (1999).

Kozhevnikov, M., et al., "Ordering-Induced Band Structure Effects in $GaInP_2$ Studied by Ballistic Electron Emission Spectroscopy" (submitted to *Appl. Phys. Lett.*).

Yu, Z.G., et al., "Dynamics of Electronic Transport in Metal/Organic/Metal Structures," *J. Phys. Cond. Mater.* **11**, L7 (1999).

Yu, Z.G., et al., "Green's Function Approach for a Dynamical Study of Transport in Metal/Organic/Metal Structures," *Phys. Rev.* **B59**, 16001 (1999).

Imaging Time-of-Flight Ion Mass Spectrograph

97008

Herbert Funsten

In conventional time-of-flight (TOF) mass spectrometry, the short gating time over which ions are injected into the TOF tube results in a low duty cycle, limiting the spectrum acquisition time and accuracy. We have developed and patented an imaging TOF ion mass spectrograph that enables a 100% duty cycle.

In our TOF spectrograph, the position of an ion on the detector is correlated with a known, time-varying electric field that deflects the ion at the entrance of the TOF tube, thereby uniquely deriving the time that the ion entered the tube (t_1). Using the time that the ion was detected (t_2), we can determine the ion's time of flight in the TOF tube ($t_2 - t_1$). By detecting the position of the ion, we also gain an accurate measure of the distance that it traveled in the tube (*d*), which is necessary to calculate the ion speed, $d/(t_2 - t_1)$. The accompanying schematic shows the basic elements of our TOF mass spectrograph. If we know the ion's energy, *E*, we can calculate its mass, *m*. Because this spectrograph technique enables a 100% duty cycle, we derive a considerably faster spectrum acquisition time and greater accuracy than are currently achievable. Our TOF mass spectrograph is particularly suited for ions with masses greater than several hundred atomic mass units, including chemical and biological warfare agents, and is useful for large biomolecule identification.

In a second part of this project, we developed and demonstrated a chicane mass filter, which provides control of the mass range of ions entering a TOF tube. This filter significantly increases the signal-to-noise ratio by rejecting major species while allowing minor or trace species to pass into the TOF tube. We have a patent pending for this filter.

This year we assembled and tested a prototype spectrograph that uses a micro-channel plate detector with a two-dimensional position-sensitive resistive anode. Our second figure shows a TOF spectrum for a continuous beam of helium-4 that we obtained with this apparatus using a circular raster pattern with a frequency of 20 kHz, which is low enough that we can use audio amplifiers and off-the-shelf function generators to drive the raster plates. The clear advantage of this mass spectrograph over a traditional gated TOF system, with a duty cycle of less than 1%, is that ions are continuously admitted into the TOF tube, enabling fast spectrum acquisition and high accuracy. Additionally, we can easily adjust the mass range and resolution by modifying the raster pattern and frequency.

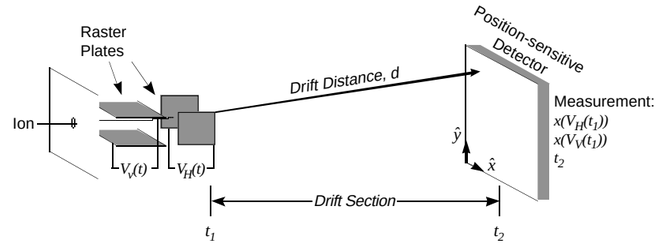

Schematic of the basic operation of our time-of-flight mass spectrograph. An ion is deflected by raster plates with voltages $V_V(t_1)$ and $V_H(t_1)$ when it enters the TOF tube at time t_1. The ion is eventually detected at time t_2 at the position (*x,y*). The detected position (*x,y*) provides unique information about the voltages $V_V(t_1)$ and $V_H(t_1)$ at the time t_1 that the ion passed the raster plates, so t_1 can be uniquely determined. Also, the distance *d* traveled by the ion is accurately measured using (*x,y*). Ion speed is obtained using $d/(t_2 - t_1)$.

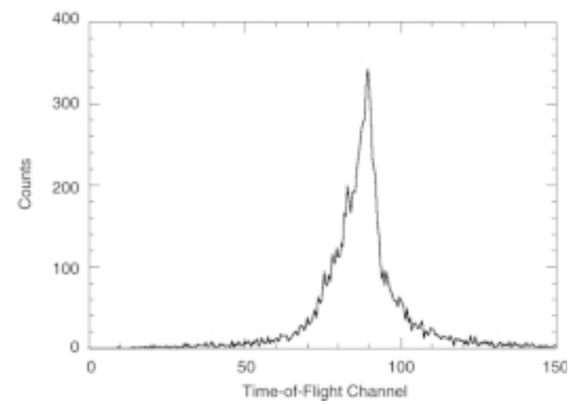

A time-of-flight spectrum of a beam of helium-4 produced by a prototype of our spectrograph.

Novel Signal Processing with Nonlinear Transmission Lines

97031

David Reagor

Nonlinear dielectrics offer uniquely strong and tunable nonlinearities that make them attractive for current devices (for example, frequency-agile microwave filters) and for future signal-processing technologies. The goal of this project is to understand pulse propagation on nonlinear coplanar waveguide prototype devices. We are (1) performing time-domain and frequency-domain experimental studies of simple waveguide structures, (2) pursuing a theoretical understanding of the propagation of signals on these nonlinear waveguides, and (3) investigating signal-processing concepts such as pulse shaping, time-domain filtering, distributed amplification, and self-directed switching.

At low temperatures our prototype devices exhibit strong dielectric nonlinearities and negligible series resistive losses up to at least a few gigahertz, making them interesting for many applications at radio and microwave frequencies. The applications fall into two categories: quasi static and dynamic. Devices in the quasi-static category, such as frequency-agile microwave filters, use the dielectric nonlinearity as a means of controlling the device's small-signal (linear) response. In the dynamic category, the devices are in the large-signal (nonlinear) regime and thus can be used for harmonic generation and mixing, parametric amplification, pulse shaping, and so forth.

To realistically assess the potential applications, we used a time-domain measurement and analysis technique developed during this project to perform a broadband electrodynamic characterization in terms of nonlinear, dispersive, and dissipative effects. The 8-cm-long coplanar waveguides made from high-temperature superconducting electrodes on single-crystal strontium titanate (STO) substrates have exhibited large dielectric nonlinearities. The waveguides, which were essentially dispersionless under zero bias, became dispersive under bias. With bias, the tan∂ has also increased. At present, we still need to learn whether all these effects are caused by purely intrinsic properties of the STO material.

Finally, by using parameters determined from small-signal (linear) transmission characteristics of the waveguides as a function of dc bias, we have constructed a phenomenological nonlinear model equation. This equation—combining nonlinearity with bias- and frequency-dependent dissipation and bias-dependent dispersion—has accurately predicted the large-signal (nonlinear) behavior, for example, pulse-shaping effects, that we observed experimentally (see accompanying figure). The central result of this study is the accurate modeling of propagation on these nonlinear transmission lines.

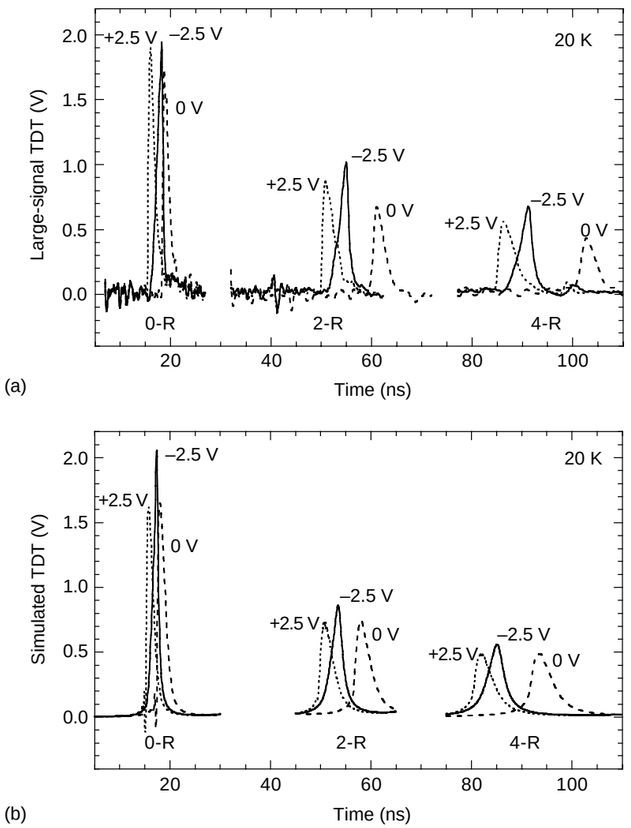

Large-signal impulse time-domain transmission (TDT) at 20 K for different biases (0 V, +2.5 V, –2.5 V) with zero, two, and four reflections (0-R, 2-R, 4-R) at device boundaries, with corresponding propagation lengths of *L*, 3*L*, and 5*L*, respectively. (a) Experiment (b) Simulation.

Publications

Cai, D., et al., "A Perturbed Toda Lattice Model for Low Loss Nonlinear Transmission," *Physica D* **123**, 291 (1998).

Findikoglu, A.T., et al., "Electrodynamic Properties of Coplanar Waveguides Made from High-Temperature Superconducting $YBa_2Cu_3O_{7-x}$ Electrodes on Nonlinear Dielectric $SrTiO_3$ Substrates," *J. Appl. Phys*. **86**, 1558 (1999).

Findikoglu, A.T., et al., "Electrodynamic Properties of Single-Crystal and Thin-Film Strontium Titanate" (to be published in *Integ. Ferroelec*.).

Findikoglu, A.T., et al., "New Potential Applications of Nonlinear Dielectrics: Microwave Solitons and Stochastic Resonance," *Integ. Ferroelec.* **22**, 779 (1998).

Findikoglu, A.T., et al., "Pulse-Shaping Using Nonlinear Dielectric $SrTiO_3$," *Appl. Phys. Lett.* **74**, 1770 (1999).

Jia, Q.X., et al., "Improvement in Performance of Electrically Tunable Devices Based on Nonlinear Dielectric $SrTiO_3$ Using a Homoepitaxial $LaAlO_3$ Interlayer," *Appl. Phys. Lett.* **73**, 897 (1998).

Jia, Q.X., et al., "Integrated Films for Josephson Junctions, SQUIDs and Electrically Tunable Microwave Devices," *Ceramic Trans.* **86**, 61 (1998).

Lu, P., et al., "Effects of Homo-Epitaxial $LaAlO_3$ Layer on Microstructural Properties of $SrTiO_3$ Films on $LaAlO_3$ Substrates," *Thin Solid Films* **348**, 38 (1999).

Rasmussen, K.O., et al., "Higher-Order Effects on Shapiro Steps in Josephson Junctions," *Phys. Rev. B* **59**, 58 (1999).

Rasmussen, K.O., et al., "Soliton Motion in a Parametrically AC-Driven Damped Toda Lattice," *Phys. Rev. E* **58**, 6695 (1998).

Thermal Detection of DNA and Proteins during Gel Electrophoresis

97032

Roger Johnston

Gel electrophoresis, one of the most important investigative techniques in science and biotechnology, is used in biological and biomedical research, polymer chemistry, forensics, law enforcement, disease control, national defense, anthropology, biometrics, genetic counseling, botany, agriculture, and animal husbandry. It is used in both low-technology laboratories and at state-of-the-art facilities. Recent ultrasensitive refractive index measurements suggest there may be a simpler, more sensitive way to detect DNA fragments during gel electrophoresis based on thermometry and local Joule self-heating. This method would permit simple, inexpensive, ultrasensitive detection of DNA and proteins in real time during gel electrophoresis. Our project involves developing the appropriate instrumentation, performing a proof of principle, optimizing the technique, and establishing the detection sensitivity.

This year we constructed a gel electrophoresis assembly using microthermistors instead of the larger conventional thermistors used in the previous year. The microthermistors permitted us to make the most sensitive thermal measurements to date during gel electrophoresis. Despite this level of sensitivity, we were unable to detect any significant local Joule heating when a DNA band entered the probe region of the gel. Our sensitivity exceeded 10 μK vs. the theoretically predicted temperature rise of as much as 1 K for the larger DNA bands. As a result of this work, we now reject Joule heating as a likely mechanism for the anomalous large refractive index (RI) decrease seen when a DNA band enters the probe volume.

The two remaining hypotheses, that the anomalous RI is caused by gel matrix expansion or by salt ion exclusion, remain to be tested. This year a third possible explanation emerged based on collaborations within the Laboratory. According to the new argument, the anomalous RI decrease may be caused by a Frohlich resonance. We crudely modeled this possibility, though the hypothesis remains untested. We concluded this year's work by devising ways that we can experimentally test each of the remaining three hypotheses.

An Integrated Solid-State Optical Device with High-Speed Scanning, Variable Focusing, and Frequency-Doubling Capabilities

98027

Quanxi Jia

The incredibly rich range of linear and nonlinear optical properties exhibited by ferroelectrics, such as lithium niobate and lithium tantalate, has enabled us to perform basic operations with light, such as high-speed scanning, focusing, and frequency conversion, all in one material. These operations depend on our ability to manipulate the ferroelectric domain structure on a micron scale. The goal of this project is to develop an integrated device that will act as the basis for a new generation of integrated, solid-state optical devices that will incorporate a variety of functions. These devices include electro-optic lenses, scanners, and second-harmonic generators and will be integrated on a single crystal of ferroelectric lithium niobate and/or on a lithium tantalate wafer. This integration may lead to the development of a comprehensive, solid-state platform with various optical components.

This year we continued to develop discrete components, such as scanners, lenses, and second-harmonic-generation lasers on lithium tantalate wafers, with improved device performance. We have fully characterized some integrated-wafer devices that contain multiple electro-optic lenses and scanners on a single-crystal, lithium tantalate chip. We fabricated six devices on a single crystal 17 mm × 10 mm × 225 μm (see accompanying figure). Our investigation has established the relationship among the design parameters and characteristics of the devices.

We also studied in real time with electro-optic imaging microscopy (EOIM) the nucleation and growth of 180° ferroelectric domains in congruent lithium tantalate under an external electric field. We observed that the measured domain-wall velocities are an order of magnitude higher than those reported earlier using ex situ (as opposed to real time) techniques. The merger of growing domains creates serrated fronts that show another order of magnitude increase in wall velocity.

We also optimized processing conditions to grow high-quality lithium niobate films on sapphire substrates. By x-ray diffraction and transmission electron microscopy, we systematically studied the structural and ferroelectric properties of epitaxial lithium niobate films. This study establishes a technical foundation for the design and development of integrated solid-state optical devices in thin film forms.

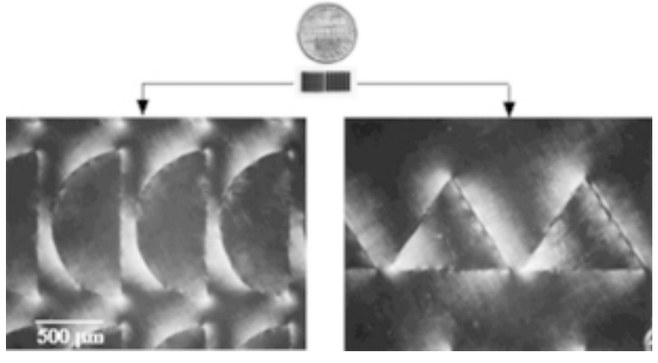

Images obtained with polarized light microscopy of the ferroelectric domains of a portion of the lens (left side) and of the scanner (right side). Six integrated, electro-optic lens/scanner devices (represented by the half circles and triangles) were fabricated on a single crystal 17 mm × 10 mm × 225 mm.

Publications

Gahagan, K.T., et al., "Integrated Electro-Optic Lens/Scanner in a $LiTaO_3$ Single Crystal," *Appl. Opt.* **38**, 1186 (1999).

Gim, Y., et al., "Growth of $LiNbO_3$ Films on Sapphire Substrates Using Pulsed Laser Deposition," *Integrated Ferroelect.* **25**, 91 (1999).

Gopalan, V., and T.E. Mitchell, "In Situ Video Observation of 180-Degree Domain Switching in $LiTaO_3$ by Electro-Optic Imaging," *J. Appl. Phys.* **85**, 2304 (1999).

Gopalan, V., et al., "Ferroelectric Domain Kinetics Congruent $LiTaO_3$," *Integrated Ferroelect.* **27**, 137 (1999).

Gopalan, V., et al., "In Situ Observation of 180° Domain Kinetics in Congruent $LiNbO_3$ Crystals" (submitted *Appl. Phys. Lett.*).

Gopalan, V., et al., "In Situ Video Measurement of 180° Domain Mobility in Congruent $LiTaO_3$ Using Electro-Optic Imaging Microscopy," *J. Appl. Phys.* **86**, 1638 (1999).

Gopalan, V., et al., "Switching Kinetics of 180° Domains in Congruent $LiNbO_3$ and $LiTaO_3$ Crystals," *Solid State Commun.* **109**, 111 (1999).

X-Ray Refractive Optics for Astrophysics and Nonproliferation

99029

Don Casperson

Recent preliminary experiments demonstrate the promise of focusing x-rays with lenses in the same manner as visible light. These lenses have immediate applications, such as focusing synchrotron beams to very high intensities, as well as future applications like high angular-resolution x-ray imaging of astrophysical sources from a satellite platform. Until now, x-ray focusing has required very expensive and difficult-to-manufacture diffractive or figured grazing-incidence *reflective* optics. However, *refractive* x-ray optics (lenses that transmit and focus x-rays over a particular energy range) offers an inexpensive and much simpler alternative. Our project investigates using refractive lenses to focus soft x-rays in the few kiloelectronvolt to few tens of kiloelectronvolt energy range. Because the x-ray refraction effect is quite weak in a single lens, a series of elements—a compound refractive lens (CRL)—focuses soft x-rays over practical focal lengths, typically 1 m to 2 m. The first figure shows a cross-sectional view and the submillimeter spatial scale of a single biconcave lens and a 16-element CRL suitable for focusing x-rays in this energy range. Future practical lenses will consist of an array of CRLs to increase collection area.

This year we acquired a license for and implemented ZEMAX, an optical ray-tracing code that includes the important effect of x-ray absorption in the lens material. With ZEMAX we generated a practical CRL design for x-rays at two interesting energies: 8.04-keV x-rays from copper K_α emission available at laboratory x-ray sources for characterizing the x-ray lenses' focusing properties and the 6.0-keV x-rays resulting from iron line-emission in astrophysical sources of interest.

Experimentally, we chose polystyrene ($C_6H_5CH\,CH_2)_x$ as a low atomic number lens material to minimize x-ray absorption. We developed several techniques to manufacture parabolic lenses suitable for x-ray focusing, including molding biconcave lenses with diamond-turned parabolic mandrels fabricated at the Laboratory. We used a Laboratory optical interferometer to determine the accuracy and quality of the parabolic profiles of the mandrels and lens surfaces, as part of the overall effort to construct our first practical CRL. The second figure shows an example of an interferometer scan.

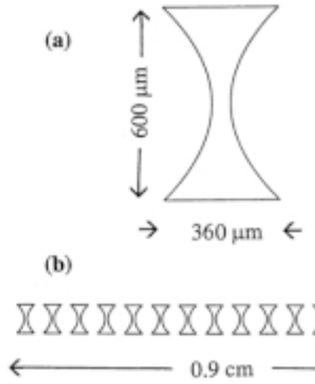

(a) Cross-sectional view of a biconcave parabolic x-ray lens, showing the submillimeter spatial scale. Unlike visible light, the index of refraction for x-rays in polystyrene is less than one, and so we must use *concave* lens surfaces to generate a real image. (b) Cross-sectional view of a CRL with 16 biconcave elements, designed for focusing 6-keV x-rays over a focal length of 1.45 m.

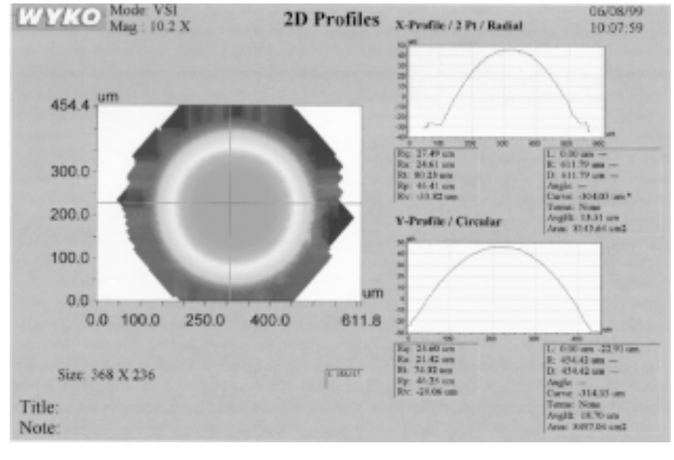

Optical interferometer scan of the surface of a micro-machined parabolic mandrel for molding polystyrene x-ray lenses.

An Integrated Optical Biosensor

99031

Karen M. Grace

In the event of a bioterrorist attack, rapid identification of biological agents and presymptomatic diagnosis of infection are critical to assist response by emergency and medical personnel. The focus of this project is to develop the technologies and underlying science that would permit the development of a miniature biodetection system. The system combines biomolecular recognition surfaces (phospholipid membranes embedded with optically tagged toxin receptors) currently under development at Los Alamos with highly sensitive evanescent-fluorescence detection using planar optical waveguides. Our ultimate goal is to provide a detection platform for the simple and rapid detection of a multitude of biothreat agents, including ricin, anthrax, botulinum, and envelope viruses such as influenza. This work contributes to the capability to deter, detect, and respond to proliferation threats involving biological or chemical weapons.

This year we have developed an optical biosensor laboratory system for detecting multivalent proteins. This biosensor is illustrated in the first figure and is based on optically tagged glycolipid toxin receptors imbedded within a fluid, phospholipid, bilayer membrane formed on the surface of a planar optical waveguide. The coated waveguide is embedded within a fluid cell cartridge, where light from a laser diode is optically coupled into the waveguide via a diffraction grating. Light propagating through the waveguide produces an evanescent optical field that excites the fluorescently tagged receptors. Injection of a multivalent protein toxin such as cholera into the fluid cell causes the toxin to bind to multiple receptors and triggers a fluorescence resonance energy transfer (FRET). The FRET signal results in a two-color optical change that is measured above the waveguide surface using a fiber-optic spectrometer. Changes observed in the FRET signal as the concentration of cholera toxin is increased are shown by the data in the second figure.

Our preliminary results indicate that this biosensor will be highly sensitive and specific. In contrast to intensity-based fluorescence detection, our biosensor is based on a ratiometric measurement of fluorescence emission intensities, which provides sensor immunity to nonspecific binding of interferent proteins, temperature fluctuations, and system variations. This sensor technique also allows for the direct analysis of "dirty" samples, responds within minutes, and does not require the addition of reagents to facilitate detection.

The long-term goal of this project is to develop a waveguide-based biological sensor platform that in the future can be miniaturized and adapted for the simultaneous detection of multiple biological agents. Such a biosensor platform will enable the future development of miniature, field-worthy biodetection systems that are compact and simple to operate, yet rival the sensitivity of current laboratory-based detection methods.

Publications

Kelly, D., et al., "Integrated Optical Biosensor for Detection of Multivalent Proteins," *Opt. Lett.* **24** (23), 1723 (1999).

Kelly, D., et al., "Integrated Optical Toxin Sensor" (to be published in SPIE *Proceedings of Advanced Materials and Optical Systems for Chemical and Biological Detection*).

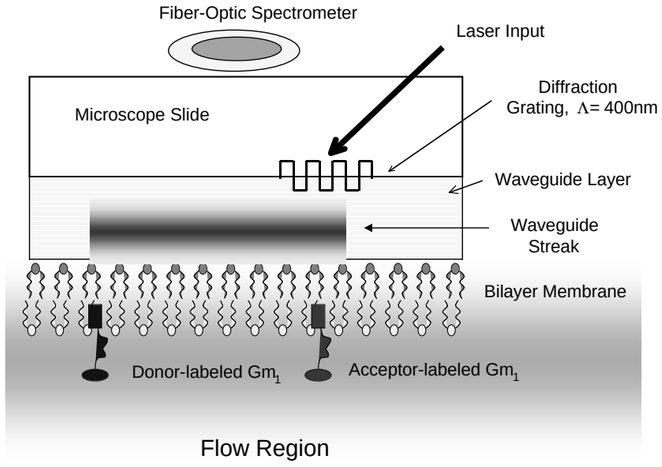

Overhead schematic view of integrated optical biosensor laboratory prototype.

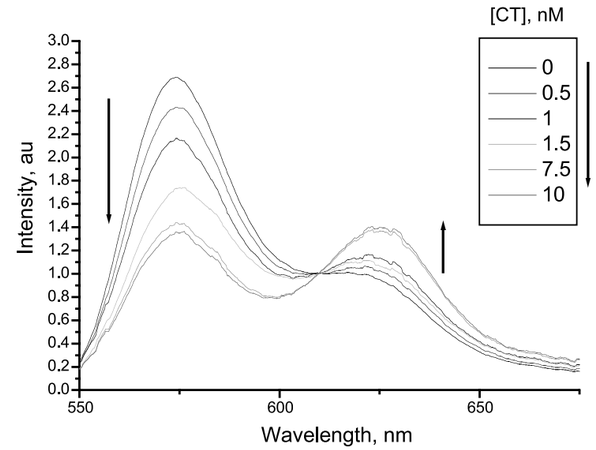

FRET signal as a function of cholera toxin concentration. The arrows emphasize a decrease in the intensity of the first spectral peak and a corresponding increase in the second peak for increasing concentrations of cholera toxin [CT].

Time-Resolved Photon Migration Tomography and Spectroscopy

99030

John S. George

We are developing a system for time-resolved photon migration tomography and spectroscopy. This system is based on the remote ultralow-light-level imaging (RULLI) detector—a novel photon-counting imager developed at Los Alamos. As pulsed laser light is delivered to the surface of biological tissue, the RULLI detector measures the time history and amplitude of light that subsequently emerges from the surface. We will use this time-resolved data to reconstruct tissue absorption and scattering properties.

Time-resolved optical methods offer the prospect of tomographic imaging and localized spectroscopy that are sensitive to biochemistry and physiology. Our system can be used to characterize intracranial bleeding or stroke, to map optical changes associated with neural activation, and to explore the feasibility of optical screening procedures for mammography. Photon migration tomography and spectroscopy techniques also have value for the characterization of highly scattering media, from high explosives to waste containers to suspended aerosols.

This year we used an existing RULLI detector to demonstrate its feasibility for use as a detector for time-resolved optical tomography. We conducted a series of tomographic imaging experiments, using an experimental phantom designed to approximate the light-scattering characteristics of biological tissue. In a variation on this experiment, we imaged a fixed goat brain. These experiments were successful and provided useful insight into practical instrument configurations.

We made significant progress toward the development of the next-generation detector, which will use a smaller-format image intensifier and an integrated crossed delay line (CDL). Several CDLs have been produced with laser machining techniques, and we are testing them for compatibility with the high-temperature vacuum processing required for intensifiers.

We designed and are building a new data acquisition system. We have working prototypes of key system components, software, and PC boards. Using optical fiber bundles, we designed a fiber-optic array for data collection around the human head.

We made detailed characterizations of optical signatures of brain physiology from invasive measurements. Our analysis has identified signals associated with cerebral blood flow and oxygenation, as well as fast light-scattering changes associated with neural activation.

Cryptographic Key Generation Using Long-Base-Line Radio Interferometry

98028

Richard Hughes

There is a growing need for convenient, demonstrably secure methods to generate and distribute the secret random number sequences, known as cryptographic keys, which are used to initialize encryption hardware and software for secure communications. Present day methods of key distribution are subject to ever increasing computational challenges, and so it is essential to develop new, highly secure key distribution technologies. We are developing a method for two parties to generate a shared secret key, on-demand, from simultaneous observations of the correlated radio noise from astronomical objects. The digitized bit strings will be subjected to an information theoretically secure procedure of "advantage distillation," error correction, and "privacy amplification," to distill secret, error-free keys. Although the abstract mathematical formalism for key generation from partially correlated noise sources was developed several years ago, our project is the first practical demonstration of this new technique.

We have constructed two high-gain dish-antenna systems with precision controllers that point and accurately track astronomical radio sources. The 1420-MHz outputs of low-noise preamplifiers at each antenna are fed to two phase-locked radio receivers that we constructed. An output signal from each receiver has a frequency equal to the difference between the frequency of the radio source and that of a local oscillator. The output signal is digitized and then used to produce a set of random numbers, which can then be used to distill key bits. This system is sensitive enough to detect the correlated radio noise in joint observations of bright astronomical radio sources such as Cygnus A, and we have observed correlations with several other radio sources. We are currently working with short base lines between the two observing stations and have developed the data acquisition hardware for key generation.

Development of Radial Probe Instrumentation for Use in DNA Sequencing

98026

Joe Gatewood

We are developing a new method for DNA sequencing based on sensors that are radially positioned around a DNA-sized pore. Our proposed device will monitor tunneling currents through individual DNA bases while electrophoresis is used to move the DNA past the sensors. If the tunneling signatures of the bases are distinct, as predicted by theory, the DNA sequence can be deduced from the measured tunneling profiles.

Our major focus this year was on pore production. We chose as substrates undoped silicon wafers with a silicon oxide coating. With this substrate, we produced pyramidal pits that came to a point that had atomic dimensions. We then exposed the apex of the pyramidal pits to produce a pore. Using this approach, we have produced pores less than 1000 Å in diameter.

We continued development on our electrophoresis cell to reduce noise and to include chip electrical contacts. The noise contribution from the cell and contacts is less than 0.2 pA rms.

We also wrote the prototype software that will be used to control the electrophoretic current and the data acquisition process.

High-Quantum-Efficiency, Silicon-Integrated, Tunable-Band-Gap Infrared-Detection Devices Based on Rhenium Molybdenum Disilicide

99032

Terence E. Mitchell

We are investigating a new class of narrow-band-gap semiconducting rhenium disilicide and rhenium-molybdenum disilicide materials for applications in infrared-detection devices. These infrared sensors may have higher quantum efficiency than platinum silicide–based detectors and may be more easily integrated with silicon technology than detectors based on mercury cadmium telluride. Such sensors are vital components in detection and imaging systems for numerous critical applications such as security, surveillance, environmental monitoring, astronomy, military activities, and industrial process control.

This year we used the solid-phase epitaxy technique to synthesize rhenium-molybdenum disilicide films and performed transmission electron microscopy to characterize both the defect structures in films and the quality of epitaxial growth. Our work resulted in three key findings: (1) Voids occur at the interface (removal of these voids is crucial). (2) Thin films of rhenium disilicide contain a high density of faults (see the figure), in contrast with the "chimney-ladder" structures we discovered in bulk crystals of the same material. (3) For films containing molybdenum, a highly regular-period, compositionally modulated superlattice exists. This superlattice may have interesting optoelectronic properties.

To measure the infrared properties, we set up an optical measurement apparatus with a dual-grating monochromator (with an infrared blackbody source) that gives output over a wide spectral range. The apparatus also includes zinc sellenide optics to focus and steer the beam through a sample holder and onto a liquid nitrogen–cooled mercury cadmium telluride detector. Transmission measurements are made first with a reference substrate and then with the sample film/substrate. In this manner, we can calculate the absorption coefficient as a function of wavelength (or energy) and fit it to extrapolate the band-gap energy for the given sample composition.

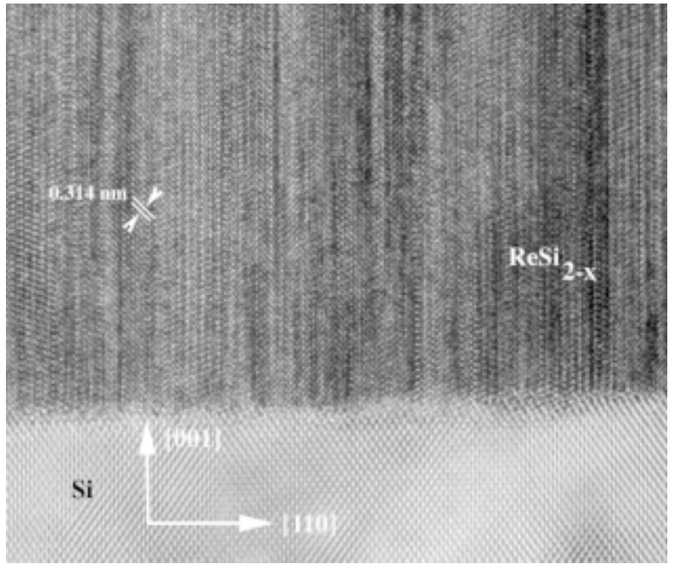

Atomic resolution image of the interface between epitaxial rhenium disilicide film and silicon substrate. The good matching obtained between the silicide lattice planes and the film indicates a high-quality epitaxial film. Planar defects in the film are faults caused by the collapse and shear of missing silicon planes, formed to accommodate the silicon deficiency of the film.

Publications

Misra, A., and T.E. Mitchell, "Twinning in Incommensurate and Commensurate Structures of $ReSi_{2-x}$ Alloys," in *International Symposium on Advances in Twinning*, S. Ankem, Ed. (The Metals, Minerals, and Materials Society, Warrendate, PA, 1999), p. 253.

Misra, A., et al., "Defect Structures in Semiconducting $ReSi_{2-x}$ Epitaxial Thin Films," *Microsc. Microanal.*, **5**, 726 (1999).

Misra, A., et al., "Incommensuration and Other Structural Anomalies in Rhenium Disilicide," *Philos. Mag. A* **79**, 1411 (1999).

Mitchell, T.E., and A. Misra, "Unusual Incommensurate, Modulated and Disordered Structures in Refractory Metal Disilicides," in *Electron Microscopy and Analysis*, C.J. Kiely, Ed. (Institute of Physics, Bristol, 1999) p. 23.

Geoscience, Space Science, and Astrophysics

New Windows on Gamma-Ray Bursts

98020

Ed Fenimore

Since their discovery at Los Alamos in 1973, gamma-ray bursts have become one of the biggest mysteries in astronomy. They are the largest explosions in the universe since the Big Bang. During the few seconds that they are active, they can generate 1% of the luminosity of the entire universe. Although more than 4,000 bursts have been observed, we have measured distances and associated luminosities for only about six.

As a part of the Los Alamos effort in theory, modeling, and high-performance computing, we are unraveling the physics behind these events. We use the time variability to understand how the burst evolves from rapid variations to a smooth afterglow. The observed pulse widths are a diagnostic tool to indicate the distance to the events.

Our analysis of the time variability in the burst phase has revealed a Hubble-like relationship that we can use to find the distance to many bursts. The Hubble relationship relates the pattern of redshifts observed in the spectrum of a galaxy to its distance. It has been used with distant supernovae to map the universe when it was young. Our relationship relates the absolute luminosity of the peak gamma-ray emission to the amount of "spikiness" in the gamma-ray flux. When combined with the observed flux, we can determine distances. We define the "variability" of the gamma-ray flux to be the average significance of the change in flux from one 0.064-second time sample to the next. The logarithm of this variability is directly proportional to the logarithm of the absolute luminosity. Since gamma-ray bursts can be three orders of magnitude brighter than supernovae, we can use gamma-ray bursts to map the universe to even greater distances than we can with supernovae, to get closer and closer to the time when stars and galaxies were beginning to form.

Our other studies of the temporal variability found that millisecond variations are common and that the spectral lag as a function of energy is not a strong function nor is it consistent with synchrotron radiation. We studied the gamma-ray burst that Los Alamos discovered early, the bright optical emission from GRB990123, and found evidence in the temporal variability that the gamma-rays must originate from a central engine.

Publications

Fenimore, E.E., and E. Ramirez-Ruiz, "The Observational Basis for Central Engines in Gamma-Ray Bursts," in *Gamma-Ray Bursts: The First Three Minutes: Proceedings of a Workshop Held at Graftavallen, Sweden, 6-11 February 1999*, J. Poutanen and R. Svensson, Eds., Astronomical Society of the Pacific conference series, v. 190 (Astronomical Society of the Pacific, San Francisco, 1999).

Fenimore, E.E., et al., "GRB990123: Evidence that the Gamma-Rays Come from a Central Engine," *Astrophys. J. Lett.* **518,** L73 (1999).

Ramirez-Ruiz, E., and E.E. Fenimore, "Temporal Evolution of the Pulse Width in GRBs," *Astron. & Astrophys. Supplement Series* **138**, 521 (1999).

Walker, K.C., et al., "Gamma-Ray Bursts Have Millisecond Variability" (to be published in *Astrophys. J.*).

Wu, Bobing, and E.E. Fenimore, "Spectral Lags of Gamma-Ray Bursts from *Ginga* and *Batse* Data" (submitted to *Astrophys. J.*).

A New Method for Modeling Wave Propagation in Strongly Heterogeneous Media: Applications to Seismic Wave Propagation in the Earth

98024

Michael C. Fehler

Modeling seismic wave propagation in the earth, which is important for fossil energy exploration and nonproliferation detection, can be accomplished using a variety of analytic and numerical methods. Analytic methods give reliable results even when media contrasts are strong, but solutions are not available for many media of interest. Numerical methods give reliable results for only weakly heterogeneous media. Most numerical methods cannot account for variations in surface topography caused by real-earth features such as mountains and canyons. Strong heterogeneities and surface topography can have significant influences on seismic wavefields propagating in the earth, but we currently have no reliable means to model their influences.

We have developed a novel microscopic approach, termed the phononic lattice solid by interpolation (PLSI), for modeling wave propagation in strongly heterogeneous media, including those with irregular surface topography. The goals of this project are to further develop this method and investigate its reliability.

We made progress in three areas: we validated the approaches used to model free-surface and absorbing boundaries (necessary at the nonfree surfaces to limit model sizes); we validated PLSI by comparing results with those obtained from other approaches; and we developed a new method, called Lattice BGK (LBGK), which is computationally faster and will provide a feasible framework for developing a three-dimensional (3-D) modeling approach.

For validation of free-surface and absorbing boundary conditions, we compared waveforms reflected from these features with the known waveform character for various angles of incidence. For a flat free surface, we can analytically calculate the reflected waveform using a mirror image of the source located the same distance above the surface as the source is below. We found that the reflected wave amplitude agreed very well with that calculated using the mirror-source approach. The goal of an absorbing boundary condition is to pass outgoing waves without reflection so that the medium appears to be infinite even though it is spatially limited. We found that the boundary conditions we developed were efficient at absorbing waves without reflection.

For extension to 3-D problems, we must find a more efficient method to model particle interactions at each lattice node. The PLSI approach has rather complicated interaction rules in two-dimensions, which become more complex in 3-D. We have investigated and tested a new set of particle interaction rules, called LBGK, which require fewer computations per interaction step and will be more tractable in 3-D. We found that the method has an additional advantage that it can model inelastic absorption of wave energy, which is important to model for real-earth problems.

Publications

Huang, L.-J., et al., "Absorbing Boundary and Free Surface Conditions in the Phononic Lattice Solid by Interpolation," *Geophys. J. Int.* **40**, 147 (2000).

Sato, H., et al., "Scattering and Attenuation of Seismic Waves in the Lithosphere," in *Handbook of Earthquake and Engineering Seismology* (Academic Press, Orlando, in press).

Astrophysics with the Sloan Digital Sky Survey

99055

Warner A. Miller

Our multidisciplinary team has been involved in the commissioning of the Sloan Digital Sky Survey (SDSS) located in the Sacramento Mountains of southern New Mexico. SDSS, under final construction and commissioning at Apache Point Observatory, will systematically map one-quarter of the entire sky, producing a detailed image of it and determining the positions and magnitudes of more than 100 million celestial objects. It will also measure the distance to a million of the nearest galaxies, giving us a three-dimensional picture of the universe through a volume one hundred times larger than that explored to date. The sky survey will also record the distances to 100,000 quasars, the most distant objects known, giving us an unprecedented knowledge of the distribution of matter to the edge of the visible universe.

The SDSS photometry team is building the SDSS standard star system. The technique uses a dedicated 20-in. telescope to observe bright primary standard stars to define the new photometric system and fainter secondary star fields that will provide the link between the photometric system and the observations taken by the 2.5-m survey telescope. The 1-deg field of view of the 20-in. telescope is inscribed by a 2048-sq CCD that is the heart of the photometry camera system. One of our team members has contributed to the photometry mission plans as well as to the reduction techniques used in the reduction pipeline along with his collaborators at Johns Hopkins University. He has also performed engineering work on the photometry instrumentation.

Another project member has been working with the Fermilab-based controls and interlock team to extend the capabilities of the SDSS telescope control system. He was a participant and presenter in the SDSS Controls Operational Readiness Review held at Fermilab in July 1999. The successful integration of the Experimental Physics and Industrial Control System (EPICS) toolkit was co-developed at Los Alamos.

The Genesis and Evolution of Basalt on the Moon

99022

William C. Feldman

We are investigating the origin and evolution of basalt on the Moon with data measured by our Lunar Prospector neutron and gamma-ray spectrometers. These data and their analysis provide a first demonstration of the utility of neutron spectroscopy for remote sensing of planetary surfaces, which supports our ability to meet our DOE programmatic activities in the area of nuclear treaty verification.

So far we have developed the first global map of thorium on the Moon. The distribution of thorium suggests that the Moon has a single hot spot near the surface that faces Earth. This hot spot implies a global redistribution of all radioactive elements that have contributed to heating the Moon and hence the observed distribution of lunar volcanism, which preferentially occurred on the near side of the Moon.

We have found that the hydrogen content of permanently shaded craters near the south pole of the Moon is enhanced by a factor of 35 relative to the hydrogen content contained in soils at equatorial latitudes. This ratio is sufficiently high that it is most likely explained in terms of water-ice deposits. However, we cannot rule out an explanation in terms of hydrogen implanted by the solar wind.

We have delineated and quantified the chemistry of the different lunar terranes using measurements of fast-neutron fluxes and the ratio of thermal/epithermal neutron fluxes, respectively. It turns out that both data sets provide useful indices that discriminate between basaltic (mafic) compositions normally found in the lunar maria and anorthositic compositions normally found in the lunar highlands.

We have also studied the distribution of gadolinium and samarium by combining our thermal neutron data with measurements of the abundances of iron and titanium. These measurements were derived from the UV/VIS spectral-reflectance data gathered by a camera aboard the Clementine mission. The distribution of gadolinium and samarium closely matches that of thorium as measured by our Lunar Prospector gamma-ray spectrometer.

Publications

Elphic, R.C., et al., "Determination of Lunar Global Rare Earth Element Abundances Using Lunar Prospector Neutron Spectrometer Observations" (to be published in *J. Geophys. Res.*).

Feldman, W.C., et al., "The Chemical Information Content of Lunar Thermal and Epithermal Neutrons" (to be published in *J. Geophys. Res.: Planets*).

Feldman, W.C., et al., "Polar Hydrogen Deposits on the Moon" (to be published in *J. Geophys. Res.: Planets*).

Lawrence, D.J., et al., "High Resolution Measurements of Absolute Thorium Abundances on the Lunar Surface from the Lunar Prospector Gamma-Ray Spectrometer," *Geophys. Res. Lett.* **26** (17), 2681 (1999).

Lawrence, D.J., et al., "Thorium Abundances on the Lunar Surface" (submitted to *J. Geophys. Res.: Planets*).

Maurice, S., et al., "High-Energy Neutrons from the Moon" (submitted to *J. Geophys. Res.: Planets*).

Ices on Titan: Laboratory Measurements That Complement the Huygens Probe

97030

Jeanne M. Robinson

The composition of the cold bodies in the outer solar system may hold some of the key molecular clues to the composition of the prestellar molecular cloud that gave rise to the solar system. We studied the physical chemistry and heterogeneous (gas/surface) reactivity of extraterrestrial ice analogs on the surface of Saturn's largest moon, Titan. This project coupled surface spectroscopic techniques with physical adsorption measurements. We addressed several of the pressing questions regarding Titan: Is storage of hydrocarbons in Titan's water ice crust feasible? Do heterogeneous processes influence the atmospheric chemical composition of Titan? Are phase transitions to be expected? These data can be incorporated into photochemical models, with the goal of improved modeling of the chemical composition and meteorology of Titan's atmosphere. Titan will be probed by the Cassini-Huygens Mission; our results on Titan ice analogs can be used to help interpret the mission data.

This year we studied the feasibility of hydrocarbon storage in Titan's porous water ice crust. Methane is thought to be the main climatological fluid on Titan, analogous to water on Earth. Models of methane photolysis on Titan suggest that the atmospheric inventory of methane would, over the age of the solar system, have been depleted many thousand times. It has been proposed that methane is stored in the porous water ice regolith, that is, in the impact-shattered layer of ice detritus that is thought to cover most of Titan.

We measured the uptake of methane on ice films that simulate the regolith at temperatures from 85 K to about 100 K and found that the uptake of methane is greatly enhanced by capillary absorption via the Kelvin effect, compared with multilayer physical adsorption. The Kelvin effect describes the depression of the vapor pressure of a liquid over a curved surface (i.e., a pore) compared with a flat surface. In simple terms, capillary absorption is the condensation of a gas to a liquid at a lower vapor pressure in a pore than over a flat surface. The first figure compares the uptake of methane we observed at 89 K with the uptake of argon. The second figure shows methane adsorption isotherms at several temperatures. The relative methane humidity at which capillary absorption begins is very sensitive to temperature, as shown in the third figure. At temperatures below about 93 K, the onset of capillary absorption following multilayer absorption is readily apparent. As the surface temperature on Titan fluctuates about this 93-K point, large quantities of methane evaporate or condense. From our measurements, we calculate that sufficient quantities of methane could be stored in a 2-km-thick regolith to buffer the photolytic loss.

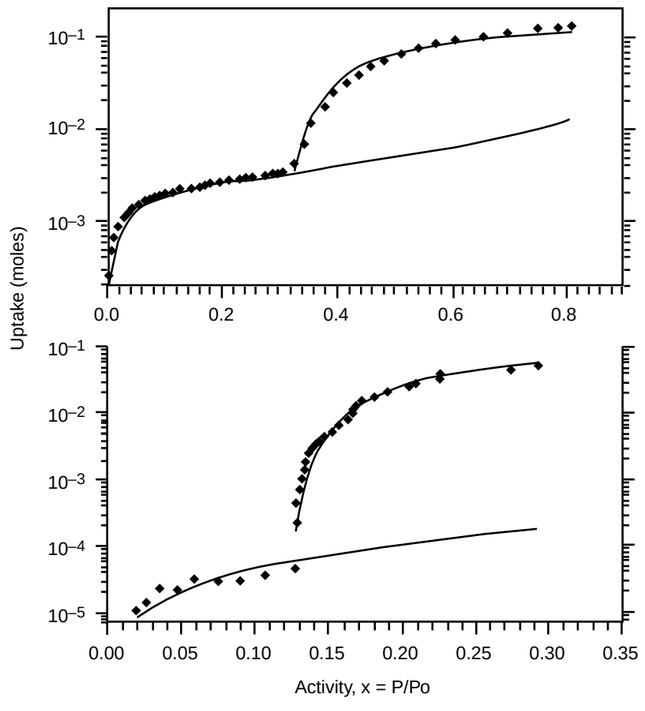

The measured uptake of argon (top) and methane (bottom) on porous ice, illustrating their behavior during multilayer physical adsorption and subsequent capillary absorption. The solid lines are fits to the Brunnauer-Emmett-Teller equation for multilayer physical adsorption and the Kelvin equation during capillary absorption.

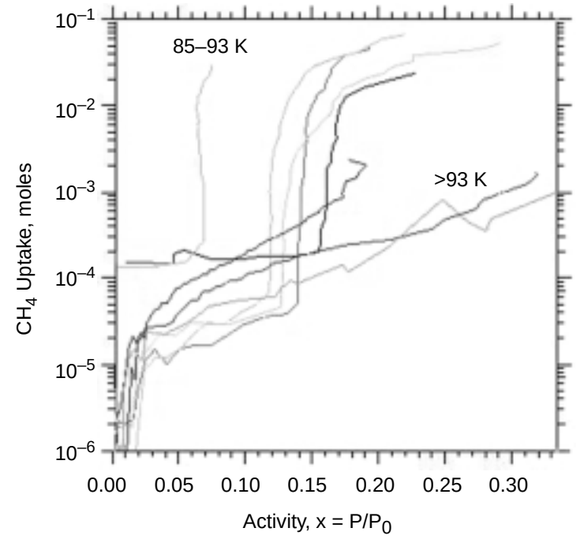

The temperature dependence of the measured uptake of methane as a function of the relative humidity of methane ($x = P/P_0$). P is the measured vapor pressure of methane over the porous ice film and P_0 is the condensation pressure of methane.

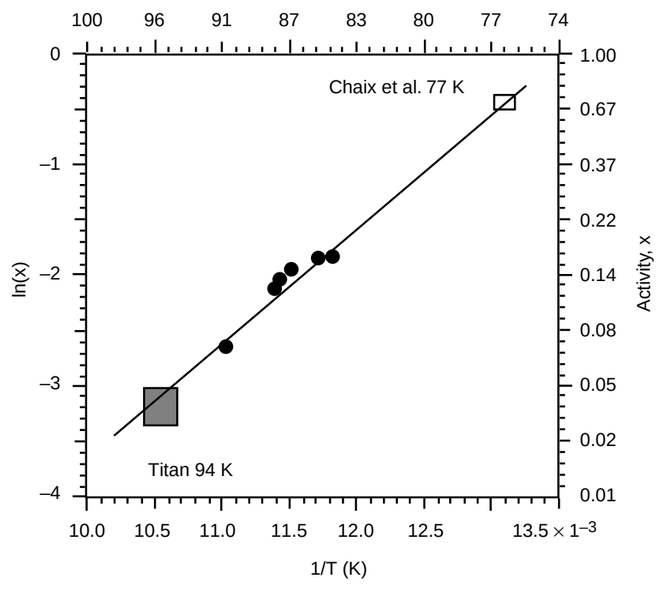

The inverse temperature dependence of the relative humidity of methane at which capillary absorption begins. The line through the data obeys the form of the Kelvin equation. The data suggest that capillary absorption near and above Titan's surface temperature of 94 K occurs at a relative methane humidity of much lower than 5%, in agreement with our measurements of methane uptake.

High-Pressure Crystal Chemistry of Hydrous Minerals

98019

Yusheng Zhao

We are studying the crystal chemistry and stability field of hydrogen-bearing minerals at high pressures and temperatures, specifically at the pressures and temperatures found in the earth's mantle. This study of hydrous minerals will clarify the effects of pressure and temperature on absorption and desorption of hydrogen and on the kinetics of hydrogen-release processes. An increased understanding of the dehydration process helps us to model deep earthquake processes and mantle convection patterns. We are using neutron diffraction to study bond lengths and vibrational features of the hydrogen bond under mantle pressure and temperature conditions.

We conducted neutron diffraction experiments on the deuterated hydrous mineral brucite $Mg(OD)_2$, which we synthesized in a sealed platinum capsule at 300°C for 12 hours. Neutron diffraction is sensitive to the hydrogen (deuterium) position, allowing us to study the details of the crystal structure of hydrous minerals. We refined the crystal structure of the deuterated sample using the Rietveld technique, and then determined the atomic position and thermal vibrations. We compared the refinement results with previous experimental results and got very good agreement.

There are two sets of crystal structures with different crystallographic models for brucite. In the traditional view of brucite, the hydrogen atoms are positioned at the (*2d*) site with a full occupation of 1.0, while the new view has hydrogen occupation of 1/3 at the (*6i*) site (see first figure). It is quite challenging to distinguish these two crystallographic models experimentally. The high-resolution time-of-flight neutron diffraction pattern we collected at LANSCE for the brucite sample covers a wide range of *d*-spacing from 0.4 Å to 4.0 Å, which makes the accurate determination of the crystal structure possible. We were able to refine the thermal vibration of different atoms.

For both models of the deuterated brucite $Mg(OD)_2$, the Mg atom does not vibrate much, as indicated by a small U_{iso} value, while the oxygen atom has a median U_{iso} value, and the deuterium atom has the highest U_{iso} value. We believe that in the case of $Mg(OH)_2$ the hydrogen atom may have a much higher thermal vibration than the deuterium atom because of the mass difference between the two (see second figure).

One significant difference between two models is that the observed thermal vibration for the (*2d*) site is a rather large value for room temperature measurement; while the vibration measure observed for the (*6i*) site is more realistic. The observation of thermal motion of hydrogen atoms plus the quality of the fit (as indicated by χ^2) suggest that the new prospect is a better structural model for the brucite.

Publications

Zerda, T.W., et al., "Structure of Carbon Black Particles," in *High Pressure Molecular Science*, R. Winter and J. Jonas, Eds. (Kluwer Academic Publishers, Netherlands, 1999), p. 225.

Zhao, Y., et al., "A High P-T Cell Assembly for Neutron Diffraction up to 10 GPa and 1500 K," *High-Pressure Res.* **16**, 161 (1999).

Zhao, Y., et al., "Correction of Diffraction Optics and P-V-T Determination Using Thermoelastic Equations of State of Multiple Phases," *J. Appl. Crystallogr.* **32**, 218 (1999).

Zhao, Y., et al., "High P-T Structural Aspects and Thermoelastic Equations of State of Clinopyroxenes" (submitted to *Phys. Chem. Minerals*).

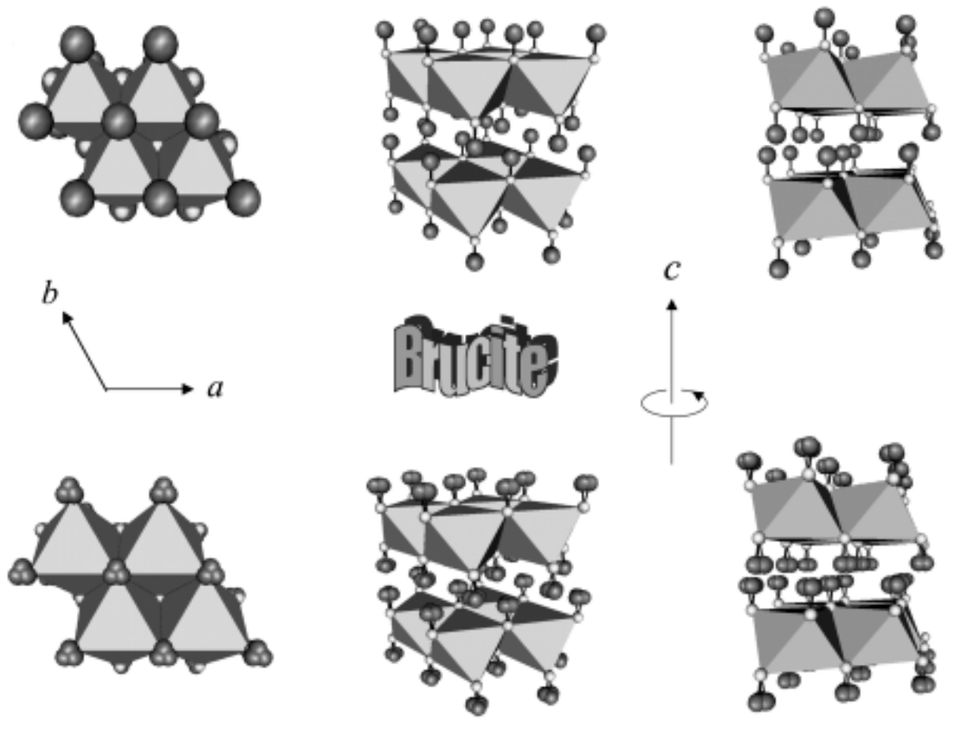

Structural models for brucite $Mg(OH)_2$. The MgO_6 octahedral has shared edges, and the hydrogen is the tangling atom. The top images show the traditional view of brucite, where the hydrogen atoms are positioned at the (*2d*) site with a full occupation of 1.0, while the bottom images show the new prospect of hydrogen occupation of 1/3 at the (*6i*) site.

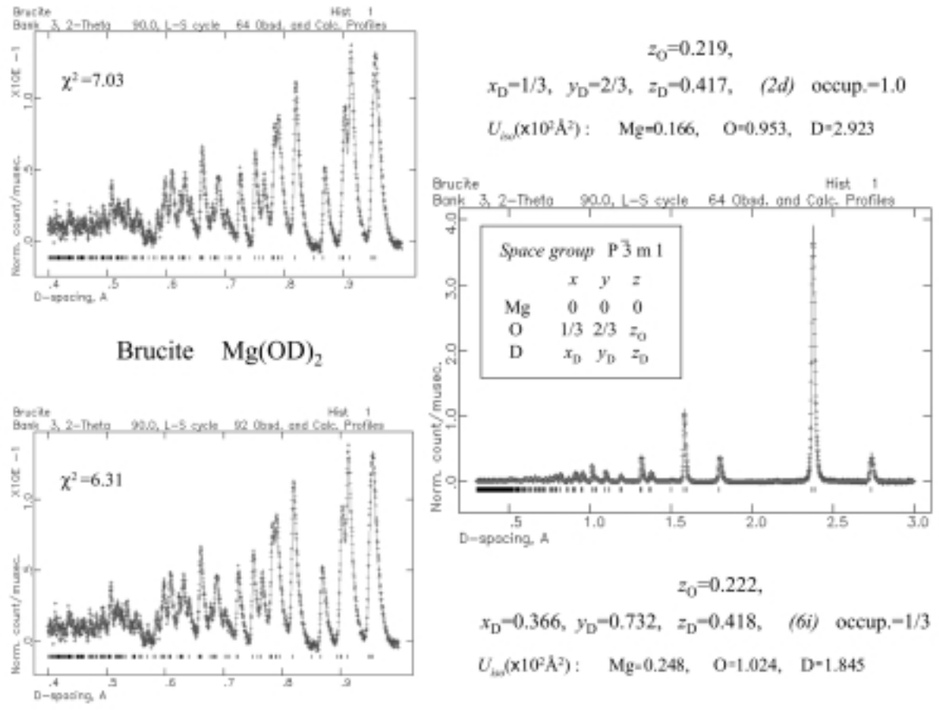

Structural refinement results of neutron diffraction of $Mg(OD)_2$. The right side shows the overall diffraction pattern and the left side shows detailed spectra at small *d*-spacing. The peak positions of the diffraction pattern reveal the information about lattice dimensions, while the peak intensities (especially those at small *d*-spacing) can be used to refine atomic positions and thermal vibrations.

Tsunami from Asteroid and Comet Impacts

98022

Jack G. Hills

Asteroid and comet impacts are among the greatest known threats to the survival of humanity. One serious consequence of such impacts occurring in the ocean is a tsunami. We are using Los Alamos computer capabilities and professional expertise to model the tsunami waves expected from asteroid encounters. We are motivated to reduce the threat from asteroid impacts both by providing a risk assessment of the amount of damage expected from them and by identifying coastal areas that are particularly vulnerable to such impacts. We are simulating large asteroid impacts in mid ocean to identify coastal areas that are most vulnerable. To estimate the damage expected in these vulnerable areas, we run Monte Carlo simulations of impacts in the ocean over a range of asteroid sizes.

We made considerable progress in the past year identifying coastal areas that are most vulnerable to flooding from asteroid impacts. We improved the boundary conditions in our computer code so that a typical computer simulation now runs about twice as long as the travel time of a tsunami across an ocean. This long duration is important because we find that reflections off coastal areas and island groups can greatly increase tsunami damage. We made computer-based movies from these simulations that helped us understand the tsunami dynamics.

An interesting case is the flooding of Florida. Our previous work showed that most of the tsunami energy would be reflected off Florida's shallow continental shelf. It showed little flooding by the time we had to terminate the calculations because of problems with the boundary conditions. However, we find much more flooding when we are able to run the code for a much longer time. Two factors are responsible for this late-stage flooding: the slowing down of the tsunami as it enters the shallow waters off Florida causes a mesa of water to slowly build on this shelf. Then a tsunami wave reflects off the Bahamas chain and piles up on top of the mesa of water produced by the first tsunami wave. When the mesa of water collapses, it floods Florida.

The first accompanying figure shows the maximum depth of flooding due to an asteroid hitting at three different points in the mid Atlantic. The simulated asteroid is the size of the one that is thought to have caused the extinction of the dinosaurs (10 km in diameter), and we see that most of Florida is inundated. The second figure shows the maximum tsunami height throughout the Atlantic Ocean basin for one of the asteroids. It shows areas that are protected by shallow water and seamounts (underwater mountains) and areas where a tsunami is reflected.

One of the most interesting findings from our Pacific simulations has been the extreme vulnerability of Tokyo and the flat plain around it to an asteroid-generated tsunami. No matter where we simulate the asteriod impact in the Pacific, the resulting tsunami floods Tokyo.

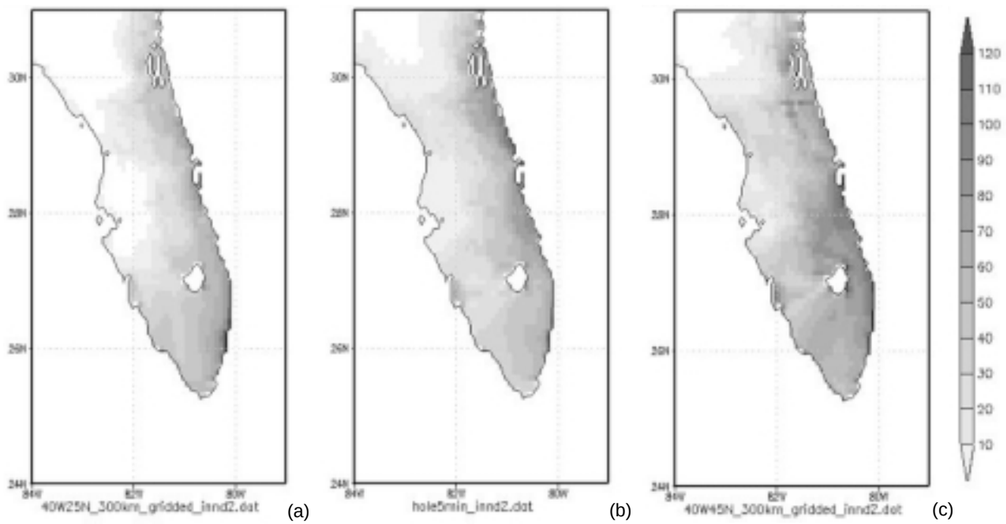

The maximum depth of inundation in Florida as the result of a 10-km-diam asteriod impacting at (a) longitude 45 degrees West and latitude 25 degrees North, (b) 45 degrees West and 35 degrees North, and (c) 45 degrees West and 45 degrees North. The depths are recorded as meters above local ground level.

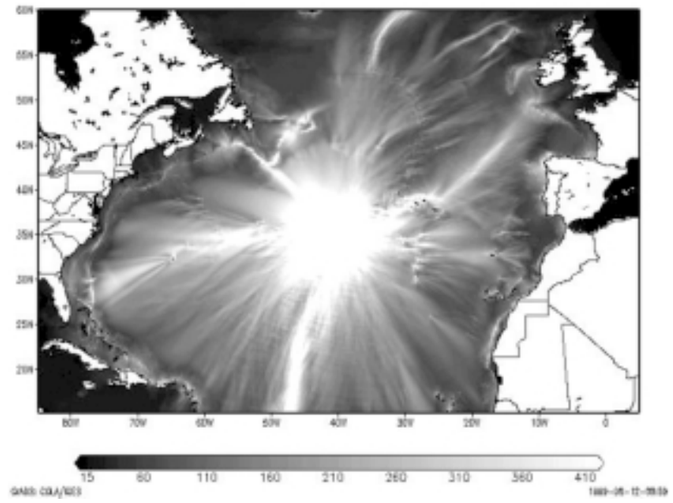

Maximum water height in meters above mean sea level as the result of tsunami waves produced by an asteroid impact at 45 degrees West and 35 degrees North. Note how the topology of the ocean bottom channels and reflects the tsunami. Note the tongue of high water channeled toward Florida.

Publications

Hills, J.G., and M.P. Goda, "Damage from Comet and Asteroid Impacts with Earth" (to be published in *Phys. D*, Special Issue on Predictability).

Hills, J.G., and M.P. Goda, "Tsunami from Asteroid and Comet Impacts: The Vulnerability of Europe," *Sci. Tsunami Hazards* **16**, 3 **(**1998**)**.

Determining the Mass of the Universe

97013

Michael S. Warren

The average mass density of the universe, parameterized by Ω, is the most sought after single number in cosmology. It can determaine the ultimate fate of the universe because it indicates whether the universe is open and expanding forever (Ω < 1) or closed, eventually recollapsing (Ω > 1). Unfortunately, after a half century of research, Ω is still uncertain by at least a factor of 5. We have the tools at hand to significantly improve our measurements of the mass of the universe.

We have continued to refine our data analysis capabilities to enable data mining from the very large data sets we are currently able to generate and to enable comparisons with the largest observational data sets such as those from the Las Campanas Redshift survey and the forthcoming Sloan Digital Sky Survey. A paper comparing our N-body code with the dozen leading cosmological codes in the world has been accepted by the *Astrophysical Journal* and shows that our numerical methods provided the highest-resolution simulation among all of the participants. A large parallel N-body simulation, which we performed locally on the Avalon cluster for this project, won the 1998 Gordon Bell Prize for superior effort in practical parallel processing research.

Publications

Frenk, C.S, et al., "The Santa Barbara Cluster Comparison Project: A Comparison of Cosmological Hydrodynamics Solutions" (to be published in *Astrophys J.*).

Warren, M.S., "Avalon: An Alpha/Linux Beowulf Cluster Achieves Unprecedented Price/Performance for Astrophysical Simulations and Data Analysis," *Bull. Am. Astron. Soc*. **30** (4), (1999).

Galactic and Extragalactic Magnetic Fields: Their Origin and Manifestation in Accretion Disks around Supermassive Black Holes

99024

Warner A. Miller

This project is concerned with magnetic fields generated in the accretion disks expected during the formation of every supermassive black hole in nearly every galaxy of the universe. We propose to understand the following: (1) Its origin via an alpha-omega dynamo driven by Keplerian shear and by star-disk collisions. (2) The formation of large-scale magnetohydrodynamic (MHD) jets that transport the binding energy of the black hole. (3) The origin of the magnetic flux and magnetic energy in our universe. This research will further our understanding of the enormous power-generating mechanisms at the heart of the active galaxies.

The Rossby vortex mechanism of a purely hydrodynamic alpha disk viscosity has been confirmed with linear theory; our nonlinear simulations are partially done and have given preliminary results (see the first figure). Using kinematic dynamo calculations, we have simulated the alpha-omega dynamo due to the expected star-disk collisions in the black hole accretion disk (see the second figure). The kinematic dynamo calculations have confirmed the formation of the alpha-omega dynamo in the Couette flow with driven plumes as planned in the liquid sodium dynamo experiment.

Our initial calculations of the magnetic helix formed by the saturated alpha-omega dynamo of the black hole accretion disk show the expected jet formation, which explains both the active galactic nuclei (AGN) phenomenon and the distribution of the magnetic flux of the universe.

Further calculations on modeling the multiwavelength AGN observations (from radio to teraelectronvolt) are done, and both the kinetic equation and Monte Carlo codes are fully developed and tested.

Our analysis of radio Faraday rotation measures indicates an entirely new and demanding source of magnetic flux ($\times 10^4$) and magnetic energy ($\times 10^7$), greater than that believed typical within galaxies. This explains the missing energy of black hole formation within the universe and increases the astrophysical motivation for understanding the black hole accretion disk dynamo.

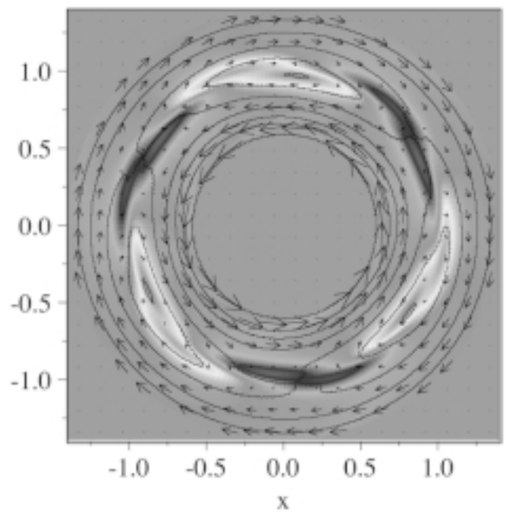

The three "anticyclones" of closed streamlines when the Rossby wave instability is excited in thin accretion disks. The gray scale indicates the high and low surface density regions, respectively. The contour lines and the arrows show the velocity field as seen by an observer corotating with the disk at Omega(r_0).

Publications

Colgate, S.A., and H. Li, "Dynamo Dominated Accretion and Energy Flow: The Mechanism of Active Galactic Nuclei" (to be published in *Astrophys. Space Sci.*).

Colgate, S.A., and H. Li, "The Origin of the Magnetic Fields of the Universe and the Black Hole Accretion Disk Dynamo," at "Highly Energetic Physical Processes and Mechanisms for Emissions from Astrophysical Plasmas," an *Astronomical Society of the Pacific Conference Series*, Intl. Astronomical Union Symposium, P.C.H. Martens and S. Tsuruta, Eds. (Montana State University, Bozeman, MT, July 6–10, 1999), Vol. 195.

Colgate S.A., et al., "The Origin of Galactic and Metagalactic Magnetic Fields: The Black Hole Accretion Disk Dynamo," *Am. Astronomical Soc.* Meeting no. 193 (1998).

Gary, S.P., and H. Li, "Whistler Heat Flux Instability at High Beta" (to be published in *Astrophys. J.*).

Kusunose, M., et al., "High Energy Emission from Compton Scattering: Comparisons between Monte-Carlo Simulations and Escape Probability-Based Kinetic Codes" (submitted to *Astrophys. J.*).

Li, H., and M. Kusunose, "Temporal and Spectral Variabilities of High Energy Emission from Blazars Using Synchrotron Self-Compton Models" (submitted to *Astrophys. J.*).

Li, H., et al., "On the Particle Heating and Acceleration in Black Hole Accretion Systems," a review at "High Energy Processes in Accreting Black Holes," in *Astronomical Society of the Pacific Conference Series*, J. Poutanen and R. Svensson, Eds., Vol. 161, 349 (1999).

Li, H., et al., "Rossby Wave Instability of Thin Accretion Disks—II. Detailed Linear Theory" (submitted to *Astrophys. J.*).

Lovelace, R.V.E., et al., "Rossby Wave Instability of Keplerian Accretion Disks" *Astrophys. J.* **513**, 805 (1999).

Pariev, V., et al., "Numerical Simulations of Star-Disk Collisions Magnetic Dynamo," AAS Meeting no. 194 (1999).

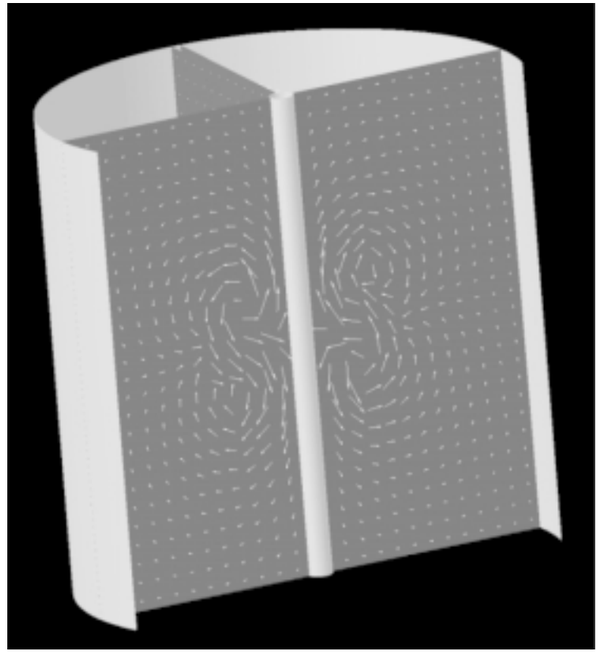

The poloidal magnetic fields generated by either the star-disk collision dynamo or the liquid sodium plume-driven dynamo. We use three-dimensional kinematic dynamo code to model the growth of the magnetic field. Together with differential Keplerian flow or Couette flow, the motion caused by star-disk collisions of driven plumes leads to the exponential growth of the seed magnetic field and to the excitation of the quadrupole-like poloidal magnetic field.

Lightning in the Atmosphere and in the Solar Nebula

98018

J. E. Borovsky

Our project objectives are to develop a model for lightning stepped leaders in Earth's atmosphere and to develop a methodology to scale this model into the conditions of the solar nebula. We are basing the model on the dynamics of charge flow in the lightning channel near the leader tip and using recent theoretical results about the electrodynamic properties of lightning channels.

This year we added nonlinear terms (representing the effects of lightning-channel heating and radiation and the effects of charge migration off the channel into the surrounding air) to the simplified differential equation that describes the electrodynamic propagation of charge down a conducting lightning channel. The changes in the properties of the propagation owing to these nonlinear terms were examined by computationally solving the nonlinear differential equation. We uncovered a surprising dilemma: the effects produced by charge migration off the channel are insufficient to slow down the propagation of charge to the velocity observed for lightning dart leaders. Our search for the correct effect continues.

Advanced Computational Analysis of Disordered Materials and Clay Minerals

98021

David Bish

X-ray and neutron diffraction are the most powerful methods for elucidating the crystal structures of solids; existing crystal structure refinement methods are restricted to ordered materials, and disorder parameters cannot be refined presently.

We are developing a revolutionary new method for diffraction analysis of the structures and types/degree of disorder of disordered materials, either in single-phase form or in mixtures with ordered materials. The method combines accepted Rietveld refinement methods with a new treatment of disorder that completely describes scattering over all parts of reciprocal space sampled in a diffraction experiment. The calculation of intensity diffracted by a disordered crystal involves independently determining the intensity at every measured step in a digital powder diffraction pattern. This new methodology allows Los Alamos researchers to quantitatively analyze disordered materials, such as zeolite and clay catalysts, superconductors, and nanocomposites, and represents a major breakthrough in our ability to understand the structures of polycrystalline disordered materials.

This year we developed algorithms for crystal parameters to describe disordered materials: crystal size in three dimensions, crystallite-size distribution for both coherent and turbostratic portions of the crystal, a variety of specific rotations of individual structural units, and variations in structural vacancies. We modeled silicate clay minerals first, as they make up the most important group of natural disordered materials. Disorder in the mica/smectite mineral group is reasonably well understood, and application of existing theories in our algorithms provided calculated diffraction patterns that agree very well with experimental data. Not so for the kaolin minerals, one of the technologically most important clay minerals. Consequently, we had to develop new disorder theories. We modified our disorder/diffraction code to compute in any symmetry. The program now produces excellent agreement between experimental and calculated diffraction patterns for a variety of clay minerals.

We also wrote algorithms to compute the effects of fixed translations in structural units. This model works well for some materials, but not for others, because it allows unfavorable electrostatic interactions for some translations. A modification of this model that interstratifies structural units with their enantiomorphs and produces phase shifts very close to $+b/3$ eliminates the electrostatically unfavorable shifts.

We developed a treatment to incorporate the effects of random displacements in the X-Y plane to account for the existence of broad energy minima across interlayer interfaces. To simulate these effects, we used an integrated Gaussian distribution of translations whose components in the X-Y plane are diminished by a simple sine correction, which in turn, is based on the angle that a plane hkl makes with respect to c^*. Application of this algorithm produced realistic diffraction patterns, but no combination of the model parameters matched all observed data for all materials. Thus we will continue to develop additional theories.

Publications

Bish, D.L., and S.J. Chipera, "Analysis of Clay Mineral Crystallite-size and Strain Broadening in X-ray Diffraction Patterns" in *Proceedings of Euroclay 1999: Conf. of the European Clay Groups Assoc.* (European Clay Groups Association, Editorial Office: Institute of Geological Sciences PAN, Krakow, Poland, 1999), p. 64.

Reynolds, Jr., R.C., "Illite/Smectite in Three Dimensions" in *Proceedings of Euroclay 1999: Conf. of the European Clay Groups Assoc.* (European Clay Groups Association, Editorial Office: Institute of Geological Sciences PAN, Krakow, Poland, 1999), p. 125.

Low-Energy Neutral-Atom Imaging: Watching Magnetospheric Dynamics

99027

Herbert Funsten

Imaging of energetic neutral atoms (ENAs), which are generated when energetic ions in the magnetosphere are neutralized by charge exchange with cold geocoronal neutrals, is a powerful method of remotely viewing the structure and dynamics of the earth's magnetosphere. This project involves analyzing and interpreting data from a low-energy neutral-atom prototype (LENA-P) imager that Los Alamos built in collaboration with industrial partners. The LENA-P imager, launched in 1997, is the first instrument to image ENA emission from the bulk magnetosphere.

Our study focuses on identifying temporal transients and their correlation with geomagnetic activity, mapping the spatial extent of structure, analyzing spectral distributions of structures and transients, and modeling ENA data to infer three-dimensional structure. We have implemented a data archival and retrieval system, identified several spectral transients, and are studying correlations between the ENA fluxes and geomagnetic activity.

The LENA-P instrument continues to return raw ENA imaging data from collaborators. This year we developed software to convert the raw data to differential angle and energy ENA distributions using the instrument response, archived the data with its ephemeris in the National Center for Supercomputer Applications' hierarchical data format, and developed a sophisticated, Web-based data-retrieval system.

One interesting feature is that observed flux is strongly dependent on the local time of the measurement. The highest count rates are observed between approximately 12–24 hours local time, although low count rates can be observed at any local time. We found no strong correlations in the data of the high-count-rate periods on latitude and L shell (the distance from the earth in terms of the earth's magnetic field topology). Typically, we did not see the very highest count-rate times above about 55°. If the data are consistent with the plasma ions' local production of ENAs, this analysis will allow us to map the location of the earth's plasma sheet and its variations with time and geophysical conditions.

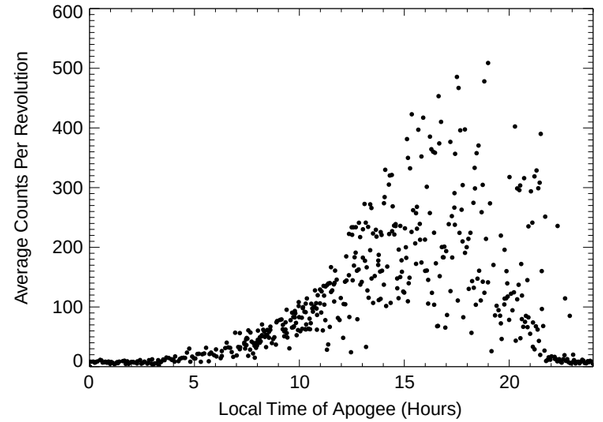

Data from LENA-P, December 5, 1997, through July 26, 1999, showing the average number of counts per minute per spacecraft orbit as a function of the local time apogee. The high-count times may be a direct measurement of the plasma sheet, enabling mapping of its location and variation with time.

Long-Range Weather Prediction

99054

Gregory Canavan

Edward Teller and others have proposed an ambitious scheme to enhance our ability to predict weather. This scheme calls for a constellation of lidars (laser infrared radars) in orbit and small retroreflecting balloons distributed throughout the atmosphere. These instruments would continuously monitor worldwide vector wind fields and variables such as temperature and would use these data to constrain advanced weather models on supercomputers. Such a system would extend our ability to predict weather from the present few days to two weeks or longer. The number of satellites required is estimated between 10 and 100, and a rough estimate of the number of transponders required is ten million. The cost of such a system would be hundreds of millions of dollars, and the balloons would have considerable environmental impact. Estimates of the economic benefit, on the other hand, range between tens and hundreds of billions of dollars per year.

This study has shown that constellations of small transponders could measure vector wind fields with sufficient accuracy for roughly two-week forecasts and that the benefits of such forecasts are much greater than the cost of the sensors and computations. Long-range weather predictions have great scientific and economic potential but require precise global observations. Small "transponder" balloons could serve as Lagrangian trace particles to measure the vector wind, the primary input to long-range numerical forecasts.

The vector wind is difficult to measure and is poorly sampled globally at present. Distance-measuring equipment (DME) or time-of-arrival triangulation of signals from about a million transponders could sample the wind fields with sufficient accuracy to support ~two-week forecasts. DME uses small, low-power transmitters on each transponder to broadcast short, low-power messages. These messages are detected by several small receivers and forwarded to the ground for processing of position, velocity, and state information. Thus, the transponder is little more than a balloon with a small radio, which should weigh a few grams and cost a few dollars. Message storage and forwarding could be performed with high-altitude balloons weighing a few kilograms and costing about $1,000. Although satellite read out would be faster, it could cost several orders of magnitude more.

Scaling estimates indicate that an average of 50-km spacing between transponders should support two-week weather forecasts. Those estimates, however, are based on turbulence theories that could significantly underestimate the predictability of the atmosphere. Measuring winds with the 1-m/s accuracy required for two-week forecasts within the time cycle for their reinitialization requires balancing the transponder and readout constellations. Our imperfect knowledge of small-flow features represents a source of errors, which corrupt the larger scales of interest. Global scales are largely two-dimensional, so errors propagate to scales twice as large in about a day. Thus, better resolution and more finely zoned numerical forecasts can forestall this corruption. The value of longer-range forecasts first increases rapidly and then asymptotically. Equating marginal costs and benefits of long-term forecasts determines the optimal forecast duration and resolution, which increase as resolution improves and economic value increases until they reach a limit set by increasing computational costs and three-dimensional flow effects.

Publications

Teller, E., et al., "Long-Range Weather Prediction and Prevention of Climate Catastrophes: A Status Report," in *International Seminar on Nuclear War and Planetary Emergencies—24th Session* (World Scientific, London, in press).

Galaxies and Large-Scale Structure in a Universe with a Cosmological Constant

99028

Wojciech H. Zurek

Understanding the large-scale structure of our universe is a key problem of cosmology. A popular assumption, which essentially states that the dynamics of the universe on the largest scales is currently dominated by the interplay between the kinetic energy of expansion and gravitational binding energy, has recently been challenged by observations of distant supernovae. It now appears that in addition to these two forces (expansion and gravity), there is another force—a cosmological constant that drives the continued expansion of the universe. The focus of this project is to understand the possible origins of these forces and to investigate their impact on the formation of large-scale structures in the universe.

This year we addressed this problem from two vantage points: (1) we studied the dynamics of phase transformations (which are most often invoked when attempting to explain the cosmological constant), and (2) we studied supernovae (which were used as a key "standard candle") to obtain nonzero estimates of the cosmological constant. The study of phase transformations allowed us to address another interesting and related issue: cosmic strings—topological defects that can form in the course of phase transformations—which have been invoked both to explain the cosmological constant and to act as "seeds" of large-scale structures. We made major progress in establishing a theory of the dynamics of phase transformations.

Publications

Antunes, N., et al., "Vortex String Formation in a 3D U(1) Temperature Quench," *Phys. Rev. Lett* **82**, 2824 (1999).

Frenk, C.S., et al., "The Santa Barbara Cluster Comparison Project: A Comparison of Cosmological Hydrodynamics Solutions" (to be published in *Astrophys. J.*).

Supermassive Black Holes and the Strong Field

97012

Warner A. Miller

Massive black holes are generally believed to exist at the center of galaxies, but complete acceptance of this theory has been impeded by a lack of evidence for strong-field relativistic effects. A very broad iron x-ray line was discovered in MCG-6-30-15 several years ago indicating emission from an accretion disk near the surface of a black hole, but the interpretation of the result was weakened by oversimplified assumptions used to model the disk line profile. As part of our project, we made a model-independent analysis of the characteristics of this iron line. We found that the inner edge of the accretion disk giving rise to the x-ray line is within 2.6 Schwarzschild radii. This is direct, model-independent evidence for the presence of a supermassive black hole. Moreover, we found that the black hole is rotating at a rate that is at least 17%–23% of its maximum allowable rate ($J \leq M^2$), although this conclusion depends on the source geometry of the hard x-ray continuum.

The observed iron alpha fluorescence lines in Seyfert galaxies provide strong evidence for an accretion disk near a supermassive black hole being the source of the line emission. These lines serve as powerful probes for examining the structure of inner regions of accretion disks. Previous studies of line emission have considered geometrically thin disks only, where the gas moves along geodesics in the equatorial plane of a black hole. We extended this work to consider the effects on line profiles from finite disk thickness, radial accretion flow, and turbulence. We adopted the Novikov & Thorne disk model and found that within this framework, turbulent broadening is the dominant new effect. The most prominent change in the skewed, double-horned line profiles is a substantial reduction in the maximum flux at both red and blue peaks. The effect is most pronounced when the inclination angle is large and the accretion rate high. We then showed that at the present level of signal-to-noise ratios in x-ray spectra, proper treatment of the actual structure of the accretion disk can change estimates of the inclination angle of the disk. Therefore, the effects discussed here will be important for future detailed modeling of high-quality observational data.

Finally, we used our model of a turbulent accretion disk to interpret observational data from MCG-6-30-15 and from samples of Seyfert {I} and Seyfert {II} galaxies. We found that there is no systematic difference in inclination angles of the disks between the galaxies, a result that does not support the unified scheme of Seyfert galaxies.

High-Resolution Records of Global Climate Change

97014

Steven Goldstein

Our objective is to use thermal ionization mass spectrometric analyses for uranium-series nuclides to date the paleoenvironmental records stored in deep-sea corals and polar ice. By comparing uranium-series and carbon-14 ages for deep-sea corals, we can establish carbon dioxide ventilation times for the deep ocean, both recent and over the past 20,000 years. These ventilation times are useful for basic studies in paleoceanography and can also be used to understand the oceans' role in modifying natural and man-made variations in atmospheric carbon dioxide. The use of more sensitive and precise uranium-series dating techniques for polar ice could lead to improved information on paleoclimate chronology and the glaciology of polar regions. Improved chronology for both deep-sea corals and polar ice would improve models for man-made and natural global change.

For dating deep-sea corals, we applied an improved cleaning method that removes the significant secondary oxide coatings present on older samples. This method was applied to samples of deep-sea coral from the Southern Ocean with mixed results: some of the samples had sufficiently low thorium-232 content for successful dating, while others had significant thorium-232 content, indicating the presence of noncarbonate material. From a collaborator at McMaster University, we obtained additional deep sea coral samples that had been previously dated using carbon-14 and thorium-230 techniques. These samples from the North Atlantic Ocean will be dated using protactinium-231 methods to test their concordance with the thorium-230 dates and to obtain additional ventilation ages for the past 20,000 years. Efforts to model the available deep-sea coral ventilation data using the Parallel Ocean Program circulation model at Los Alamos have continued. Another collaborator has added an age tracer to the model code and has begun a 1,000-year run of the model under modern conditions.

For dating polar ice samples, we optimized and quantitatively tested an EDTA (ethylenediaminetetraacetic acid)-based method for complexing actinides in solution while minimizing dust dissolution during ice melting and filtration. Using an EDTA concentration of 0.002 M, the actinide recoveries we achieved were uranium = 99.3%, thorium = 101.1%, and protactinium = 99%, while dust dissolution was <0.03%. We analyzed two samples from Allan Hills, Antarctica, that had been previously dated at 325 ± 75 ka (ka = 1,000 years) using uranium-series measurements by alpha spectrometry. Based on this age, on dust concentrations, and on previously reported activities of uranium-234, we expected protactinium-231 concentrations of ~50 fg/kg (fg = femtograms) in these samples. Preliminary results for protactinium-231 indicate much lower concentrations, with <0.3 fg/kg for both samples. This absence of recoil-produced protactinium-231 is surprising, and measurements of the other uranium-series nuclides are in progress to verify this result.

Publications

Cheng, H., et al., "Uranium-Thorium-Protactinium Dating Systematics," *Geochim. Cosmochim. Acta*. **62** (21/22), 3437 (1998).

Antarctic Circumpolar Wave and El Niño

99026

Chung-Chieng A. Lai

Our objective is to study the interannual climate variations that might be attributed to El Niño and to Antarctic Circumpolar Wave (ACW) cycles. These studies will help us understand not only the complex processes at work that produce the El Niño events, but also the role of the ACW in global climate. The goals of this research are (1) to answer key questions related to the occurrence, triggering mechanism, and aperiodicity of El Niño, (2) to understand the origin of and the atmospheric and ocean processes in the ACW, and (3) to apply a coupled climate system model to reproduce the interactions between the Southern Ocean and the equatorial Pacific.

We analyzed the South Pacific Ocean in situ and remotely sensed sea surface temperatures (SSTs). We also reviewed observational and theoretical studies of the ACW and its relationship with El Niño–Southern Oscillation (ENSO), a widely studied phenomenon. Based on limited current studies, we find two hypotheses that try to explain the generation of ACWs. One hypothesis suggests that the major source of ACWs is in the western, subtropical South Pacific Ocean, where local SST anomalies are created by ENSO activity to the north (on the equator), through the influence of an intervening Hadley cell (a vertical, closed circulation between the equator and a subtropical region). The other hypothesis argues that a local, coupled instability of the Antarctic Circumpolar Current (ACC) and its overlying atmospheric motion are essential in generating ACWs. Neither hypothesis addresses the possible forcing from ACWs to ENSO, which is what we plan to explore. Nevertheless, these recent studies have helped us modify our original working hypothesis.

Our preliminary analysis of South Pacific SST found that a warm SST anomaly in the ACC propagates eastward for a 4–5 year period, encircling Antarctica. This anomalous band of SST also stretches northeastward across most of the subtropical South Pacific. Part of this anomaly turns north, branching off into the Peru Current, which happens to be El Niño's birth place. We speculate that this warm anomaly originating from the ACC might trigger an El Niño event.

Our information about ACWs was based on data taken over a relatively short period of time (13 years). We believe that a much longer data set will be needed to determine if the dominant ACW period of 4–5 years is stable and if there exists decadal variability of ACWs. Since ENSO appears to vary on decadal time scales, it will be necessary to examine different modes of frequency of ACWs to get a better picture of possible ACW–El Niño links.

We have identified several longer data sets to use in our study. These sets include 124 years of SST observational data and results from a 300-year simulation done with the Climate System Model of the National Center for Atmospheric Research.

Publications

Huang, Z., and C.-C.A. Lai, "Possible Links between El Niño and Antarctic Circumpolar Wave Revealed in NCAR CSM Simulation" (submitted to the 6th International Conference on Southern Hemisphere Meteorology and Oceanography, Santiago, Chile, April 3–7, 2000).

Balloon-Based, High-Time-Resolution Measurements of X-Ray Emissions from Lightning

97029

David Suszcynsky

The objective of this project is to study the validity of the runaway air-breakdown mechanism using balloon-borne instruments to collect high-time-resolution x-ray and electric-field-change measurements in thunderstorms. The runaway air-breakdown mechanism is currently the leading theory to account for unexplained x-ray enhancements associated with lightning that have been recently measured from aircraft and balloons. Runaway breakdown is also believed to be the basic process responsible for recently discovered above-cloud lightning events (sprites, blue jets, etc.), the source of satellite-based observations of gamma-ray bursts of atmospheric origin, and the source of transionospheric pulse pairs measured from the ALEXIS and FORTE satellites.

However, no measurements with adequate temporal resolution have been made to confirm the operation of runaway breakdown in thunderstorms. Our experimental results could have important implications for understanding fundamental issues associated with lightning initiation, above-cloud lightning, and the global electric circuit and for the design of sensors to measure the electromagnetic pulse from an atmospheric nuclear detonation.

This year we have analyzed the data from the engineering flight from last year. The payload was recovered with its data storage system intact. During the flight, the instrument discovered evidence of the runaway electron process occurring in the uppermost region (14 km above sea level) of a large thunderstorm. Although similar measurements have been made by other researchers at much lower altitudes, we believe our data show the first indication that runaway breakdown is present near the tops of thunderstorms.

In addition, these data have allowed us to determine and implement improvements to the balloon payload that are either desirable or necessary for future flights. The most important of these is the inclusion of onboard Global Positioning System (GPS) timing. GPS will provide accurate timing for the onboard data recorder so that all science objectives can be achieved if telemetry is lost but the instrument is recovered, as occurred last year. Onboard timing will also reduce the complexity of the ground station equipment.

Publications

Beasley, W.H., et al. "Electric-Field Changes of Lightning Observed with Balloon-Borne Slow Antennas," in *Proceedings 11th International Conference on Atmospheric Electricity, Guntersville, Alabama* (NASA, Huntsville, AL, 1999).

Beasley, W.H., et al., "Electric-Field Changes of Lightning Observed in Thunderstorms," *Geophys. Res. Lett*. **27**, 189 (2000).

Eack, K.B., et al., "Gamma-Ray Emissions Observed in a Thunderstorm Anvil," *Geophys. Res. Lett*. **27**, 185 (2000).

Sky Patrol Analysis with the Robotic Optical Transient Search Experiment

99023

Galen Gisler

The Robotic Optical Transient Search Experiment (ROTSE), a NASA-funded collaboration, is a system of optical telescopes designed to respond quickly and automatically to alerts from satellites that detect gamma-ray bursts to detect optical counterparts of the gamma-ray bursts. To ensure readiness, monitor data quality, and provide baselines for the funded mission, the ROTSE telescopes additionally perform nightly automatic surveys (sky patrols) of the entire overhead sky. Data from these surveys are archived at Los Alamos and amount to 2 Tbytes per year. This project takes advantage of that archive of data to search for transient and variable objects outside the NASA-funded mission. These objects include flare stars (stars that have brief bursts of energy), ordinary variable stars (stars that have changes in intensity), active galactic nuclei, meteors, asteroids, and comets.

ROTSE presently consists of two telescope systems: ROTSE-I, a 2-by-2 array of Canon telephoto lenses on a custom, rapid-response mount; and ROTSE-II, a pair of 0.45-m reflecting telescopes. ROTSE-I has been operating automatically since March 1998 and achieved a major success in the first-ever detection of simultaneous optical emission from a gamma-ray burst that occurred January 23, 1999. The pair of ROTSE-II telescopes are still under development and have not yet produced usable data.

The sky patrol data from ROTSE-I passed the 2-Tbyte mark in March 1999, and our analysis of these data for variable and transient events is well under way. We have already mined selected sky patrol fields for new variable stars, and this work continues. The yield is extraordinarily high: roughly two-thirds of the variable stars detected in our data at 13th magnitude had not been reported before. These new variables will aid studies of galactic structure as well as the physics of variable stars themselves.

A campaign to observe the Leonid meteor shower in November of 1998 provided a highly useful and interesting observation of a fireball burst and led to plans to perform coordinated observations with the Starfire Optical Range near Albuquerque during the 1999 shower.

We also searched for x-ray transients from the Alexis satellite, and placed useful limits on these. We developed strategies to search for asteroids and comets in the data. These strategies led to the conclusion that ROTSE-I should see about six asteroids of 60-m diameter passing within six Moon distances of Earth every night.

A major goal of this project is to automate the analysis of the sky patrol data, using a pipeline for calibration, source extraction, and comparisons with a database of prior observations. The calibrations are now operating routinely, source extraction is well prototyped, and progress is good on the database construction.

Publications

Akerlof, C., et al., "Observation of Contemporaneous Optical Radiation from a Gamma-Ray Burst," *Nature* **398**, 400 (1999).

Amrose, S., et al., "All Sky Surveys for Variables Stars: Preliminary Results from ROTSE," *Bull. Amer. Astron. Soc.* ***31***, 82.03 (1999).

Zinn, J., et al., "Coordinated Observations of Two Large Leonid Meteor Fireballs over Northern New Mexico, and Computer Model Comparisons" (submitted to *Meteor. Planet. Sci.*).

Multiscale Physics of Multiphase Flow in Porous Media

99025

Dongxiao Zhang

The physical observations and theoretical treatments of multiphase flow in porous media are usually associated with three different length scales: pore (microscopic), local (lab or macroscopic), and field. Dominant processes and governing equations may vary with scales. Extending from one scale to another requires upscaling or downscaling, allowing the essence of physical processes at one level to be summarized at the coarser or finer level.

In this project we are using recently developed computational tools and a theoretical framework to systematically investigate fundamental issues of multiphase flow at the microscopic and macroscopic scales and to develop upscaling methods for predicting macroscopic quantities and characteristic relationships based on some statistical parameters of microscopic quantities. A successful upscaling approach would lead to greatly increased efficiency and accuracy in simulating multiphase flows in porous media at the lab and field scale.

This year we used an enhanced lattice Boltzman permeameter (LBP) to study single-phase flow through pore-scale geometries obtained through high-resolution computed microtomography of rock cores. The LBP allowed us to investigate some fundamental issues, such as the existence of representative elementary volume (REV), the scale dependence of porosity, specific surface area and permeability, and the relationship of these quantities (see the figure). We found that although REV may not be well defined in a deterministic sense, it does exist statistically. The concept of statistical REV is weaker than the deterministic REV but is more useful in applications. We also found that the size of REV may be different for different quantities.

Based on the computational results, we found that rock permeability may not be accurately predicted with existing relationships such as the Kozeny-Carman relation, which is based only on porosity and specific surface area—the lower moments of rock geometry. A more-accurate upscaling method would have to involve higher moments of pore geometry, and we will focus the remainder of the project on those. This year's results have positioned us to investigate multiphase flow in pore geometries.

Publications

Zhang, D., "Quantification of Uncertainty for Fluid Flow in Heterogeneous Petroleum Reservoirs," *Physica D* **133**, 488, 1999.

Zhang, D., and A.Y. Sun, "Stochastic Analysis of Transient Saturated Flow through Heterogeneous Fractured Porous Media: A Double-Permeability Approach," (to be published in *Water Resour. Res.*).

Zhang, D., et al., "Pore Scale Study of Flow in Porous Media: Scale Dependency, REV, and Statistical REV" (to be published in *Geophys. Res. Lett.*).

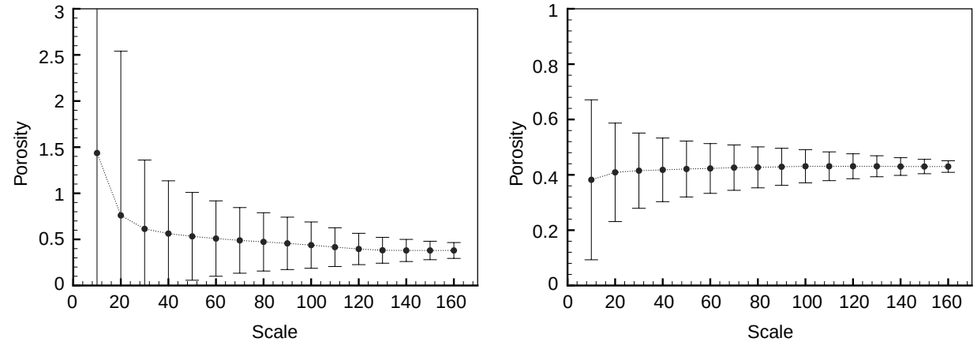

The expected value and confidence interval (obtained by adding and subtracting one standard deviation from the expected value) of permeability (left) and of porosity (right) as functions of the lattice scale. The results are obtained with simulations performed on computed microtomography (CMT) geometry of crushed glass beads divided into $180 \times 256 \times 256$ lattices. The resolution is 17.5 microns. At each scale, each quantity is computed by averaging over a window of this scale centered at a certain location. These values, obtained at different locations within the domain, are then analyzed to obtain the statistics. The expected values become constant and the standard deviations approach zero with scale. This indicates the existence of statistical REV. A similar observation is found for a CMT sample of Berea sandstone.

A Large-Aperture, Wide-Angle Air Cerenkov Telescope

98023

Constantine Sinnis

Earth is immersed in an isotropic flux of cosmic rays with energies up to and beyond 10^{20} eV. Although cosmic rays were discovered over 80 years ago, their origin is still unknown. Since charged cosmic rays do not point back to their sources, the best clue to the origins of cosmic rays is their composition. Energy-dependent changes in composition mark changes in either the sources of cosmic rays or their propagation throughout the galaxy. Direct measurements of cosmic-ray composition show that protons dominate the cosmic-ray flux below 50 TeV (10^{12} eV). At higher energies, the flux is too low for direct measurements and indirect, ground-based techniques must be used. We are building the first ground-based instrument capable of measuring cosmic-ray composition below 50 TeV and beyond 10^{15} eV. With this instrument, we hope to solve the long-standing puzzle of the origin of cosmic rays.

The WACT (wide-angle Cerenkov telescope) experiment will consist of six independent telescopes separated by approximately 100 m. Each telescope has four mirror segments, which form a 4-m^2 mirror. Twenty-five 5-cm photomultiplier tubes (PMTs) view each mirror. Located at the Lab's Milagro facility, the telescope will operate on clear, moonless nights to image the Cerenkov light generated in the atmosphere by the interactions of high-energy cosmic-ray nuclei.

An experiment of this scale requires extensive design and construction. The mirrors must be protected from the sun and the elements, yet be available for data collection. The camera must be designed to ensure a uniform response across the entire camera. The associated electronics of the PMTs must be optimized for high-light-level conditions. We completed most of this design and construction work during the past year. Concrete pads and removable buildings to house the telescopes were designed and built. The camera frame was designed and the first frame has been built and installed on the first telescope. We are using Winston cones to ensure a uniform response across each camera. These cones are currently being designed, and we expect delivery of four prototypes before the end of this fiscal year. We decided on a design for the PMT bases, set up a PMT test facility at the Laboratory, and have begun testing them.

Publications

Atkins, R., et al., "Atmospheric Cerenkov Detectors at Milagro to Measure Cosmic-Ray Composition Above 50 TeV," in *Proceedings of the 26th International Cosmic Ray Conference* (University of Utah, Salt Lake City, UT), Vol. 5, p. 295.

Nuclear and Particle Physics

Improved Matching of Lattice and Continuum QCD

99051

Tanmoy Bhattacharya

Quantum chromodynamics, discretized on a finite space-time lattice, provide a first principles, nonperturbative, method of determining the properties and interactions of hadrons by calculating the matrix elements of various operators between hadronic states. Earlier investigations have shown that at the finest lattice resolution currently accessible, ~0.05 fermi, discretization effects are quite large. In addition, the perturbative evaluation of matching constants needed to relate the lattice and continuum theories have large uncertainties, and calculations beyond leading order are prohibitive. The goal of this project is a systematic nonperturbative calculation of the quantities needed to remove the leading discretization errors and better match the lattice and continuum local fermion bilinear operators. To increase reliability of the calculation, we will use three methods: (1) application of chiral ward identities, (2) normalization of the operators using external quark states in a fixed gauge, and (3) study of the two point correlators at short physical distances.

This year we carried out the first pilot simulation for using the Ward identities to determine the renormalization constants and the coefficients of the terms that have to be added to improve the Wilson theory. Imposing Ward identities, we simulated $16 \times 16 \times 16 \times 48$ quenched lattices at $\beta = 6.0$ and found that we could determine all the leading improvement terms to reasonable accuracy.

The renormalization constants needed to match the scalar, pseudoscalar, and tensor currents are scale and scheme dependent and hence not amenable to determination by the Ward identity method. We are evaluating these constants using the method of external quark states in a fixed gauge.

To study the effect of the improved action on these constants, we did the calculation separately for the perturbatively and nonperturbatively improved actions. We found clear evidence that different evaluations of the same constant were more consistent when we used the nonperturbatively improved action. Furthermore, these constants differed from values obtained using perturbative methods—the most significant differences being in the coefficients of the improvement terms.

Our calculations highlight the importance of dealing with the $O(a^2)$ contributions consistently when comparing results from different methods of evaluating the $O(a)$ improvement terms at $\beta = 6.0$. Even though, formally, these $O(a^2)$ contributions are higher order in the continuum limit, at couplings where simulations are being done, their effects can be large. To study these effects, we are repeating the calculations at the weaker coupling, $\beta = 6.2$ on $24 \times 24 \times 24 \times 64$ lattices.

Publications

Bhattacharya, T., et al., "Nonperturbative Renormalization Constants Using Ward Identities" (to be published in *Phys. Lett. B*).

Bhattacharya, T., et al., "Order *a* Improved Renormalization Constants" (to be published in *Proceedings of the XVII International Symposium on Lattice Field Theory*, in *Nucl. Phys. B, Proceedings Supplements*).

A GaAs Detector for Dark Matter and Solar Neutrino Research

97037

Thomas J. Bowles

The ability to produce large gallium arsenide (GaAs) crystals with the requisite electronic properties to be fabricated into charged-particle and photon detectors would provide a detector medium that would find numerous applications in both applied and fundamental research. Applications would likely include x-ray detectors on satellites, environmental monitoring, medical imaging, borehole mining spectroscopy, searches for dark matter, and solar neutrino research. GaAs detectors have two primary advantages: (1) operation with high resolution (a few kiloelectronvolts) at room temperature and (2) specific nuclear properties that are of direct interest in fundamental physics research, such as in the areas of dark matter and solar neutrinos.

The objective of this project is to develop GaAs detectors for these various applications. Our emphasis has been on finding techniques for growing the large GaAs crystals that have the requisite electronic properties. We are collaborating with the Institute for Nuclear Research at the Russian Academy of Sciences in Moscow, Giredmet in Moscow, the Joffe Institute of Solid-State Physics in St. Petersburg, and Moscow State University on the work.

From our comprehensive study of the growth techniques, we chose the two most common means of producing bulk semi-insulating GaAs (liquid-encapsulated Czochralski and horizontal Bridgeman). We have been able to grow GaAs crystals very cost-effectively at Giredmet under carefully controlled conditions, characterize their electrical properties, and make them into detectors.

This year, in order to understand the limitations on possible detector thickness, we have continued studying the GaAs crystals and the detectors made from them in detail using a variety of measurements. We have found that there are intrinsic factors limiting the reduction of electrically active defects to the level required to produce large GaAs detectors. Although we have substantially improved on previous work by others, it seems that our chosen growing techniques for GaAs crystals limit the usable thickness of the detectors made from them to less than 1 mm. However, now that we understand the limiting factors for growing suitable GaAs, we plan to pursue the growth of GaAs with a novel technique at lower temperatures that should not be limited by the same factors that we discovered with growing techniques at higher temperatures.

Publications

Bowles, T.J., et al., "A GaAs Solar Neutrino Detector" (Xth International School "Particles and Cosmology," Baksan Valley, Kabardino-Balkaria, Russia, April 19–25, 1999).

Testing the Standard Model Using Bottom Quarks

97038

Rajan Gupta

Both experimental and theoretical particle physicists worldwide are extensively probing bound states involving heavy quarks. Interpretation of these data requires theoretical input. Our lattice calculations provide fully nonperturbative estimates that take into account the small momentum transfers in decay of hadrons containing charm or bottom quarks. Since bottom quarks are heavy, we use a nonrelativistic formulation to describe them. This approach has allowed us to calculate properties of hadrons, like the decay constants of B mesons and the fine and hyperfine splittings, that were previously inaccessible.

The objective of this project is to perform a comprehensive study of hadrons composed of one or more bottom quarks using lattice quantum chromodynamics (QCD). Our goals are to develop the necessary codes and to calculate the decay constants f_B and f_{B_s} and the spectrum of mesons and baryons with one or more bottom quarks.

We previously developed the codes and started the production runs for the comprehensive study. We also analyzed and published our results on decay. These estimates represent the most complete analyses of systematic errors from lattice simulations.

This year we completed the simulations required to calculate the spectrum of mesons and baryons and completed the analysis of data for heavy-light mesons and baryons. We are currently analyzing data to resolve the structure of P-wave states and are contributing to greater understanding of the various splittings in terms of a phenomenological model.

We also calculated parameters of the heavy quark effective theory and presented a detailed study of renormalon ambiguities that affect such calculations. We have made a first pass at the analyses of the meson spectrum made up of two bottom quarks (upsilon states). We are now analyzing data describing mesons with one bottom and one charm quark.

Publications

Bhattacharya, T., "f_B and f_{B_s}s Using NRQCD," *Nucl. Phys. B* (*Proc. Suppl.*) **73**, 369 (1999).

Bhattacharya, T., and R. Gupta, "B Physics Using NRQCD," in *Proceedings of LATTICE 99* (North Holland, Amsterdam, in press).

Gupta, R., "General Physics Motivations for Numerical Simulations of Quantum Field Theory," *Parallel Computing* **25**, 1199 (1999).

Gupta, R., "Lattice QCD," *AIP Conf. Proc.* **490**, 3 (1999).

Khan, A.A., et al., "Heavy-light Mesons and Baryons with b Quarks" (submitted to *Phys. Rev. D*).

The QCD Phase Transition in Relativistic Heavy-Ion Collisions

97040

Frederick Cooper

We are developing practical numerical methods from first principles of quantum chromodynamics (QCD) to describe the nonequilibrium phase transition of nuclear matter following ultrarelativistic heavy-ion collisions at the Relativistic Heavy Ion Collider (RHIC) at Brookhaven National Laboratory.

Based on a systematic $1/N$ expansion, our approach will allow us to make specific predictions for thermalization time scales, energy-momentum flow, lepton pair production, and correlations in the nonequilibrium evolution of the quark-gluon plasma produced in the collisions.

During the course of this project, we succeeded in understanding several aspects of nonequilibrium phase transitions associated with the phase structure of QCD. We first studied the O(4) sigma model, which is the effective field theory of the chiral phase transition, and did numerical simulations of the chiral phase transition for both a longitudinal and a radial expansion into the vacuum. Because the PHENIX detector at RHIC was designed to detect dileptons, we have invented a formalism for directly calculating the dileptons produced during a chiral phase transition. We have also succeeded in showing that the dilepton spectrum is altered from a thermal distribution when the effects of the chiral phase transition are included.

To include the effects of hard scattering, we studied some simple quantum mechanical models in a $1/N$ expansion to develop algorithms for including these effects. One unfortunate conclusion of our simulations was that the scattering correction terms are secular in time in that they become invalid on a time scale $t \sim N$. This led us to investigate various resummation methods which were found to overcome this problem. During the course of this project, we also discovered that QCD could undergo a new phase transition into a superconducting phase. Since this phase might be discovered at RHIC, we switched our attention to studying the phase structure of models undergoing such first-order phase transitions and are currently starting dynamic simulations in these models.

Another important issue we have begun to address is how to treat inhomogeneous time-evolution problems. Our early simulations assumed we were in scaling regimes for which the spatial dependence depended only on the ratio x/t. We have made some progress in removing this restriction and hope to begin numerical simulations in 1+1 dimensions shortly.

Publications

Bonini, G.F., et al, "Periodic Instantons in SU(2) Yang-Mills-Higgs Theory" (available online, *http://eprints.lanl.gov/lanl*, E-print No. hep-ph/9905243, May 1999).

Chodos, A., et al., "Competing Condensates in Two Dimensions" (available online, *http://eprints.lanl.gov/lan*, E-print No. hep-ph/9905521, May 1999).

Chodos, A., et al., "Cooper Pairing at Large N in a Two-Dimensional Model," *Phys. Lett. B* **449**, 260 (1999).

Cooper F., "From Landau's Hydrodynamical Model to Field Theory Models of Multiparticle Production," in *The State of Physics at the End of the 20th Century*, F. Cooper et al., Eds. (World Scientific, River Edge, NJ, 1999).

Search for Cosmic Antimatter with Milagrito

97004

Cyrus M. Hoffman

It is important in both cosmology and particle physics to understand whether the universe is composed entirely of matter or whether it consists of equal amounts of matter and antimatter. We are searching for extragalactic antimatter by observing the deflection of energetic cosmic rays in the geomagnetic field. Using data collected with the Laboratory's Milagrito detector, we are searching for cosmic antiprotons by studying their deflection in Earth's magnetic field.

The Moon casts a shadow in cosmic rays; the shadow due to 1-TeV cosmic protons is deflected west of the position of the Moon, while cosmic antiprotons would produce a shadow deflected in the opposite direction. The shadow of the Moon observed in the isotropic cosmic-ray flux can be used to determine the angular resolution of a detector and to search for systematic pointing errors. Teraelectron-volt cosmic rays are bent by Earth's magnetic field, so the shadow will be offset from its nominal position. The amount of the magnetic deflection varies with the rigidity of the primary particle, as well as with the magnitude and direction of the magnetic field, which changes with incoming direction. We can use the bending of the magnetic field to search for cosmic antiprotons, which are bent in the opposite direction from protons.

This study used data from 9 billion events obtained with the Milagrito water Cherenkov detector at Fenton Hill. We analyzed the shape of the deficit of events near the Moon (see accompanying figure) using the maximum likelihood method, which includes the finite resolution of the event reconstruction angle. This analysis yields both the width of the resolution function and the deficit centroid. We subjected events from a detailed Monte Carlo simulation of air showers and the Milagrito detector to the same analysis.

We identified a systematic pointing error in the Milagrito data: events are reconstructed with larger zenith angles than the true incident direction. We believe that this error is due to Cherenkov light traveling laterally across the pond. This effect displaces the Moon shadow by ~0.5° in declination, in qualitative agreement with our expectations from the simulations. The Moon shadow is also displaced ~0.8° to the west because of the magnetic deflection, in good agreement with our expectations from the simulations.

No obvious shadow is apparent east of the true Moon position. While the analysis is not yet complete, this implies that the flux of teraelectron-volt antiprotons is less than ~25% of the cosmic proton flux. When complete, this information will be the first limit placed on high-energy cosmic antiprotons.

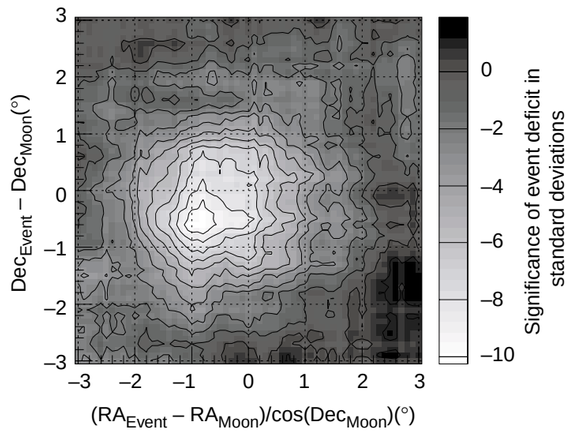

A two-dimensional plot of the Moon shadow expressed as the significance of the event deficit compared with the background. A deficit of cosmic ray events occurs to the west (right) of the Moon, indicating the presence of cosmic protons, rather than cosmic antiprotons. The axes are the differences between the declination and right ascension of the events and the Moon position. The origin is centered at the nominal position of the Moon.

Publications

Wascko, M.O., et al., "Study of the Shadows of the Moon and the Sun with VHE Cosmic Rays," in *Proceedings of the XXVI International Cosmic Ray Conference* (Salt Lake City, July 1999).

Instantons and Duality in Strongly Coupled Quantum Field Theories

97039

Michael Mattis

A long-standing goal of quantum field theory has been to understand the important properties of strongly coupled gauge theories analytically (as opposed to on the lattice). Recent theoretical advances rely on the interplay of two important assumptions: (1) supersymmetry, which relates fermions and bosons as components of a common underlying "superfield," and (2) duality, which exchanges the strong- and weak-coupling regimes of the theory and, at the same time, swaps the roles of the electric and magnetic fields.

This project, instead, accesses the very same physics in a complementary way: by a direct dynamical nonperturbative calculation of the instanton series. Using these techniques, we hoped to develop a compelling physical picture of the vacuum in strongly coupled gauge theories. We hoped, in particular, to be able to shed light on the long-unsolved problem of confinement in quantum chromodynamics (QCD).

This year we examined the possibility that the supersymmetric version of QCD contains an extra vacuum state, hitherto unsuspected, in which the gluino condensate vanishes. This hypothesized state, known as the Kovner-Shifman (KS) vacuum, has as its impetus a famous mismatch (recognized for over 15 years) between so-called strong-coupling and weak-coupling instanton calculations of the gluino condensate. By carefully reexamining the issue of cluster decomposition, we were able to show that this mismatch—and with it, the impetus for the KS vacuum—is an artifact of a mistaken calculation. The conclusion is that the entire strong-coupling approach pioneered by a CERN group is incorrect.

Publications

Davies, N.M., et al., "Gluino Condensate and Magnetic Monopoles in Supersymmetric Gluodynamics," *Nucl. Phys. B* **559**, 123 (1999).

Hollowood, T.J., et al., "Breakdown of Cluster Decomposition in Instanton Calculations of the Gluino Condensate" (submitted to *Nucl. Phys. B*).

Helium-3 Magnetometry for a Neutron EDM Measurement

97041

Martin Cooper

Our current research is aimed at developing an experiment that will help us understand how the fundamental particles of matter in the universe interact with each other. We plan to use a beam of neutrons to evaluate the feasibility of this experiment. The results are intended to enhance our understanding of the manner in which the universe cooled after the Big Bang and became the way it is today.

We have proposed an innovative experiment for the Los Alamos Neutron Science Center (LANSCE) to improve sensitivity to the electric dipole moment (EDM) of the neutron by three orders of magnitude. The neutron EDM is a quantity related to the amount of antimatter in the universe. A central feature of our experiment is the use of a dilute mixture of helium-3 atoms, used as a co-magnetometer, in a bath of superfluid helium-4. Our goal is to determine if the helium-3 atoms are uniformly distributed in the helium-4 bath.

We will measure the distribution for concentrations from 10^{-3} to 10^{-7} and for temperatures in the range 0.3 to 0.7 K using neutron tomography that we developed for gases during the first phase of this project. The accelerator at LANSCE will produce the neutrons necessary for this experiment.

This year we established the EDM laboratory and prepared the beam line in preparation for the delivery of a LANSCE beam. We have also developed a new target cell for a dilution refrigerator where we intend to make our measurements. The dilution refrigerator is required in order to produce the bath of superfluid helium-4 at temperatures close to absolute zero. We have built all of the components, and their final assembly is now under way.

Publications

Bangert, P.D., et al., "Enhancement of Superthermal Ultracold Neutron Production by Trapping Cold Neutrons," *Nucl. Instrum. Methods* **A410**, 264 (1998).

Exploring and Testing the Standard Model and Beyond

98038

Geoffrey West

We are working to extend and develop predictions and consequences of the standard model of elementary particle physics. Specifically, we are focusing on various aspects of the strong nuclear force as described by quantum chromodynamics (QCD), the unified electroweak theory, and the gravitational interaction.

This year we developed an improved way of relating the lattice QCD output for light quark masses to those used in phenomenology and used the results to improve current estimates for these fundamental quantities, an important step in predicting the ratio epsilon´/epsilon. We also evaluated the correlation functions needed to estimate semileptonic form factors for decays of D mesons. We developed an improved action based on a new method to determine the renormalization constants using Ward identities. This fixed-point action has a number of advantages over the conventional method of determination. It will reduce the amount of computational time in lattice QCD simulations significantly.

Building upon our earlier work on periodic instanton solutions of the SU(2) Yang-Mills-Higgs system (the standard electroweak model with no fermions), we discovered, and studied, a new class of complex instanton solutions whose consequences for baryon and lepton violating processes at high temperatures (appropriate in the evolution of the universe) and energies (conceivably accessible at accelerators) are currently under study.

We introduced a physical adiabatic particle number basis in Friedman-Robertson-Walker cosmological space-times that enables meaningful study of particle creation rates. This provided contact with a Boltzmann distribution function for quantum particles in the early universe. We also determined the scaling behavior of the theory in the far infrared, showing how it leads to a generalized notion of anomaly in field theory. In addition, we demonstrated that the distribution of conformal factor modes in two-dimensional lattice quantum gravity is exactly as predicted by the continuum Polyakov theory.

Publications

Alikhan, et al., “Heavy-Light Mesons and Baryons with B Quarks” (submitted to *Phys. Rev.*).

Anderson, J.D., et al., “Anderson et al. Reply (to the Comment of Katz on Pioneer 10/11),” *Phys. Rev. Lett.* **83** (1999).

Anderson, J.D., et al., “Anderson et al. Reply (to the Comment of Murphy on Pioneer 10/11),” *Phys. Rev. Lett.* **83** (1999).

Anderson, J.D., et al., “Indication, from Pioneer 10/11, Galileo, and Ulysses Data, of an Apparent Anomalous, Weak, Long-Range Acceleration,” *Phys. Rev. Lett.* **81**, 2858 (1998).

Bhattacharya, T., et al., “Continuous Quantum Measurement and the Emergence of Classical Chaos” (submitted to *Phys. Rev. Lett.*).

Bhattacharya, T., et al., “Non-Perturbative Renormalization Constants Using Ward Identities” (submitted to *Phys. Rev. B*).

Gupta, R., “General Physics Motivations for Numerical Simulations of Quantum Field Theory” (submitted to *Phys. Rev. Lett.*).

Gupta, R., “Lattice QCD” (IIIV Mexican School of Particles and Fields, Oaxaca de Juarez, November 20–28, 1999).

Habib, S., et al., “Energy-Momentum of Particles Created in an Expanding Universe” (submitted to *Phys. Rev. Lett.*).

Habib, S., et al., “Energy Momentum Tensor in an Expanding Universe,” *Phys. Rev. D.* **61,** 024010 (1999).

Lee, W., and S. Sharpe, “Partial Flavor Symmetry Restoration for Chiral Scattered Fermions,” *Phys. Rev. D.* **60**, 114503 (1999).

Molina-Paris, B., “Adiabatic Interpretation of Particle Creation in a de Sitter Universe” (submitted to *Int. J. Theo. Phys.*).

Nieto, M.M., “Analytic Description of the Motion of a Trapped Ion in an Even or Odd Coherent State,” in *The State of Physics at the End of the 20th Century*, F. Cooper et al., Eds. (World Scientific, Singapore, 1999), p. 75.

Nieto, M.M., “Electrons above a Helium Surface and the One-Dimensional Rydberg Atom,” *Phys. Rev. A.* 61, 034901 (2000).

Nieto, M.M., and D.R. Truax, “Higher-Power Coherent and Squeezed States” (to be published in *Opt. Commun.*).

Nieto, M.M., and D.R. Truax, “Schrödinger Equations with Time-Dependent P^2 and X^2 Terms” (submitted to *J. Phys. A.*).

Nieto, M.M., and D.R. Truax, “The Schrödinger System ” (submitted to *J. Phys. A.*).

Nieto, M.M., and D.R. Truax, “Time-Dependent Schrödinger Equations Having Isomorphic Symmetry Algebras. I. Classes of Interrelated Equations” (to be published in *J. Math. Phys.*).

Nieto, M.M., and D.R. Truax, “Time-Dependent Schrödinger Equations Having Isomorphic Symmetry Algebras. II. Symmetry Algebras, Coherent and Squeezed States” (to be published in *J. Math. Phys.*).

Turyshev, S.G., et al., “The Apparent Anomalous, Weak, Long-Range Acceleration of Pioneer 10 and 11” (in *Gravitational Waves and Experimental Gravity, Proceedings of the XVIIIth Moriond Workshop of the Rencontres de Moriond*, J. Dumarchez and J. Tran Thanh Van, Eds. (Editions Frontieres, Paris, in press).

Study of Parity Nonconservation in the Reaction $n + p \rightarrow d + \gamma$

98040

J. David Bowman

Our objective is to develop an experiment (known as the $n + p \rightarrow d + \gamma$ experiment) at the Los Alamos Neutron Science Center (LANSCE) to study parity violation in the capture of polarized neutrons on hydrogen. This experiment uses the intense flux of cold, polarized neutrons available at LANSCE. In addition to the strong force between nucleons, which is responsible for binding nuclei, there exists a much smaller, weak force between nucleons. This small, weak force can be distinguished from the dominant, strong force because the weak force violates parity (mirror symmetry), while the strong force is invariant under parity. We will observe an asymmetry, A, in the direction of emission of the gamma ray with respect to the direction of the neutron spin. The quantity A is zero if parity is conserved in the nucleon-nucleon interaction. Furthermore, A can be unambiguously related to that component of the weak force between nucleons that is carried by the π meson. We will use the pulse structure of the LANSCE neutron beam to control sources of systematic error and demonstrate that these errors are negligible.

We made considerable progress this year toward beginning our experiment. First, a technical review committee strongly recommended that the experiment proceed. Second, a safety review committee endorsed our conceptual design of the liquid hydrogen target.

The apparatus consists of a supermirror neutron guide that transports cold neutrons from the cold moderator to the apparatus, a frame overlap chopper, a helium-3 polarizer, a radio frequency (rf) neutron spin flipper, a liquid hydrogen target, a gamma detector, and a data-acquisition system. We built and tested an rf spin flipper, which reversed the neutron spin with 95% efficiency over the 9.5- by 9.5-cm^2 neutron-beam area.

In a cold-neutron beam, we also tested a scale model of the helium-3 polarizer, a spin transport, four CsI gamma detectors, a super-mirror analyzer, and a beam monitor. All components performed as designed. We then bench-tested a full-scale helium-3 polarizer, and tested this device in a cold-neutron beam.

We developed most of our data-acquisition system based on an array of VME-based transient digitizers in a UNIX platform. We demonstrated that the preamps we developed for the CsI detectors have noise levels far below the requirements of the experiment. We are making in situ measurements of electronic noise and are steadily reducing it. We will exercise the full data-acquisition system in a late 1999 test run.

We exhaustively studied possible sources of systematic errors and showed that they could be minimized. We refined our analysis of systematic errors and improved the design of the experiment to further reduce them. We also added several in situ auxiliary measurements to demonstrate that systematic errors are negligible.

Weak Interactions at Low Energies

99045

James L. Friar

Weak interactions are one of the four fundamental forces in nature (causing beta decays, for example). Present day weak-interaction theory has been very successful in accounting for the experimental data, but there are a number of small discrepancies, which may reflect imprecision in the experiments that have been performed, or may be the first glimmer that our basic understanding of the weak interactions is somehow flawed. The latter would be very exciting and important, implying that a new and better theory must be developed.

We have begun work on a number of these discrepancies, improving the theory to the point where strict judgments can be made on the validity of the "Standard Model," which embodies all of our current understanding. We calculated the first part of the electromagnetic corrections to the beta decays of special nuclei (called super-allowed decays) that form the basis for ultraprecise predictions of many of the weak interactions and examined new models for the beta decay of heavy hydrogen (tritium).

We have examined experimental constraints on the (special) weak interactions between electrons and nucleons that violate both parity (the difference between the world as we see it, and the world as seen in a mirror) and time-reversal invariance (invariance means that movies of certain processes run forward or backward are identical). In addition, we have developed new computer algorithms for treating the scattering of neutrons by alpha particles in order to analyze how the weak interactions change the spin of the neutrons during the scattering process.

Publications

Carlson, J.A., "Quantum Monte Carlo Methods and Few-Body Nuclei," in *Proceedings of the XVIth European Conference on Few-Body Problems in Physics*, Autrans, France, *Few-Body Systems Suppl.* **10**, 1 (1999).

Friar, J.L., and U. van Kolck, "Charge-Independence Breaking in the Two-Pion-Exchange Nucleon-Nucleon Force," *Phys. Rev. C* **60**, 34006 (1999).

Herczeg, P., "Lepton Family Number Violation," in *Proceedings of the Summer School on Hidden Symmetries and Higgs Phenomena*, D. Graudenz, Ed. (PSI Proceedings 98-02, 1998), p. 185.

Herczeg, P., "T-Violation in Semileptonic Decays and CP-Violation in Extensions of the Standard Model," in *Particles, Strings and Cosmology, Proceedings of the Sixth International Symposium on Particles, Strings and Cosmology (PASCOS 98)*, P. Nath, Ed. (World Scientific, 1999), p. 333.

A Search for Superradiant Emission in a Nuclear Isomer Crystal

98041

Robert S. Rundberg

We are examining the possibility that we can observe coherent emission states in crystals containing long-lived nuclear isomers. The release of stored energy from nuclear isomers (the long-lived excited state of a nucleus) would result in an explosive four times more powerful than conventional explosives. The theory that describes the emission of coherent gamma-rays from nuclear isomers in a Mössbauer crystal is based on Dicke's theory of supperradiance. The single excitation limit of Dicke's theory has been confirmed for iron-57; we intend to populate the high multiplicity state, i.e., the superradiant state, of niobium-93 in a lithium niobium crystal by starting from an almost fully excited state.

It is possible to produce nearly pure nuclear isomers by radiochemical methods. Our first goal is to assemble as much as 1 mg of niobium, with an isomer-to-ground-state ratio of 0.3, into an oriented crystalline film of lithium niobate. The energy contained in this sample would be on the order of 10 kJ. We intend to look for enhanced photon emission along Bragg angles as evidence of superradiant emission.

We developed a procedure for efficiently extracting niobium from highly radioactive molybdenum targets that were irradiated at the Los Alamos Neutron Science Center (LANSCE) for the DOE Isotope Production Program. We will also use this procedure to purify the molybdenum so that the molybdenum-93 can be used as a generator of 90% pure niobium-93m (the "m" refers to a metastable state, as opposed to a ground state, g). We expect to produce 100 μg of niobium-93m from the existing material per year. A nuclear isomer with this enrichment will potentially emit gamma rays at nearly the superradiant rate. According to Dicke's theory of superradiance, a 90% isomer will mostly populate a state with a cooperation number of $r = n/2 - 0.1\,n$. This state is preferred over higher-cooperation-number states because it has a high degeneracy. The emission rate increases with time as the number of available quantum states that cannot decay to the ground state increases, with the maximum emission rate occurring when the number of excited nuclei is one-half the total. At this point, the emission rate for the 90% isomer becomes $0.5\,n\,(0.5\,n - 0.1\,n)\,I_o = 0.2\,n{*}n\,I_o$, where n is the number of niobium-93 atoms within the volume defined by the coherence length (the distance a photon travels in a crystal without interacting with atomic electrons) of the crystal and I_o is the emission rate for an isolated nucleus.

The preliminary assay of spallation-produced niobium agrees with our previous estimates; we found the extraction of niobium from a mixture of hydrofluoric and hydrochloric acids to be an adequate means of purifying carrier-free niobium.

We developed a procedure for converting radioactive niobium into niobium ethoxide; we separated niobium from large quantities of molybdenum by the process of iron hydroxide coprecipitation, followed by extraction of the niobium from a mixture of hydrofluoric and hydrochloric acid. Using this procedure, we achieved a high yield from the synthesis of niobium ethoxide from milligram quantities of niobium, although we found the quality of niobium ethoxide thin films to be dependent on the stoichiometry. We then analyzed the reagents using direct-current plasma emission spectroscopy. We acquired a planar, hyperpure germanium (50 cm^2) gamma-ray detector with a thin beryllium window to detect the 30 keV niobium-93m gamma ray.

Determination of the Neutron Lifetime and Ultracold-Neutron Source Development

98039

Steve Lamoreaux

This project has two objectives: to study and understand the production of ultracold neutrons (UCNs) in cryogenic materials, and to develop a new technique to measure the neutron lifetime. In particular, an improved measurement of the neutron lifetime is crucial both to understanding the nature of the universe and to the parameterization and tests of fundamental particle interactions. It is also hoped that the study of UCN production in cryogenic materials will lead to a number of new experiments, possibly addressing neutron beta-decay asymmetry and the neutron electric dipole moment, both of which are of great interest.

The main accomplishment this year was detecting the first neutron decays in our magnetic trap; based on our technique, we have a preliminary result for the neutron lifetime with 20% accuracy, compared with the current accepted worldwide experimental average of about 0.1%. We hope to attain an accuracy of 0.01% using our technique, which in principle should be possible. We have identified the problems that will have to be solved before an accurate measurement can be made.

The principal problem is activation of the materials used to contain the superfluid helium, which serves as a moderator to produce UCNs and as a scintillation detector for neutron decay. In order to observe the neutron decay signal, we had to subtract a rather large background caused by activation scintillation light, increasing the system noise by roughly an order of magnitude. We verified that the decay signal was due to trapped UCNs by introducing helium-3 into the superfluid bath; the helium-3 completely absorbs the UCNs leaving the system sensitive only to an activation decay signal, which could in principle mimic the neutron decay signal. No such signal was observed.

The number of UCNs trapped agrees with calculations to 10% accuracy; this is an important result because there had been some question of the veracity of the theory of UCN production by inelastic scattering in superfluid helium. This result has important implications for the UCN electric-dipole-moment experiment being planned at the Laboratory.

Finally, we completed the study of the fundamentals of UCN production by scattering cold neutrons in solid deuterium. This work has led to an independent effort to develop an accelerator-driven spallation source of UCNs. We are still working on the theory of UCN production and trying to understand the finer details of the experimental results obtained in March 1998. So far, we have obtained agreement within a factor of 2, which can be considered quite good given the complexity of the apparatus and interactions.

Weak Interaction in Nuclei

99046

Anna C. Hayes

The main objective of this project is to investigate and improve models for (1) the role of nuclear structure and nuclear reactions in neutrino-nucleus scattering and (2) fundamental symmetry violation in the nucleus. Our goal is to couple our expertise in neutrino-nucleus scattering with our expertise in nuclear breakup reactions to develop a state-of-the-art neutrino nucleosynthesis code.

As the core of a massive star collapses to form a neutron star, neutrinos of all flavors are produced, with a significant flux up to energies of 100 MeV. Synthesis of the light elements—lithium, beryllium, and boron—in a supernova involves spallation of these neutrinos, primarily from carbon. Determining the key neutrino cross sections involved in neutrino spallation requires a detailed understanding of the underlying nuclear physics reactions; therefore, we examined the nuclear structure issues involved in all neutrino reactions measured to date.

The cross sections we analyzed include (a) those involved in solar neutrino detectors (the Soviet-American Gallium Experiment in Russia, the Gallium Experiment in Italy, and the Sudbury Neutrino Observatory experiments in Canada); (b) those involved in accelerator-based neutrino oscillation searches at the Liquid Scintillator Neutrino Detector (LSND) in Los Alamos and in the United Kingdom; and (c) those determining the interaction of atmospheric neutrinos with oxygen in the Kamiokande neutrino detector in Japan. The neutrino-carbon cross section from decay-in-flight neutrinos at LSND was found to be the most sensitive to the nuclear physics model used. The neutrino energies involved in supernova neutrino nucleosynthesis are similar to, though lower than, the neutrino energies at LSND. Neutrino nucleosynthesis involves the neutral-current as opposed to the charged-current reactions measured at LSND. Nonetheless, we find that the same isospin partner resonances in carbon-12 and nitrogen-12 dominate both processes.

If parity and time-reversal (PT) symmetry is violated in the nucleus, it would be manifested through a nuclear Schiff moment. A Schiff moment can occur when an opposite parity level is admixed into the nuclear ground state by a PT-violating nucleon-nucleon interaction. We investigated the nuclear structure required for enhancing the nuclear Schiff moment and have shown that, contrary to naive expectations, the giant dipole resonance (an oscillation of all the protons against all the neutrons in the nucleus) makes almost no contribution. We found strong correlation between states with large octupole strength and states with large Schiff strength. Thus, most of the strength determining Schiff moments in the nucleus lies at low excitation energy. The largest enhancement of Schiff moments is expected for octupole-deformed nuclei. However, we found that strong octupole vibrations also enhance Schiff moments. Thus, we expect plutonium-239, for example, to be enhanced to within a factor of 10 of the octupole-deformed nucleus of radium-225. However, our calculations suggest that the previous estimates for radium-225 overstated the enhancement of the Schiff moment by an order of magnitude.

Publications

Hayes, A.C., "Nuclear Structure Issues Determining Neutrino-Nucleus Cross Sections," *Phys. Rep.* **215**, 257 (1999).

Lewis, R., and A.C. Hayes, "Deuteron Stripping as a Probe of the Proton Halo in ^{17}F," *Phys. Rev.* **59**, 1211 (1999).

High-Energy Cosmic Transients

98042

Todd Haines

We are studying gamma-rays and other transients from throughout the cosmos with the Milagro/Milagrito gamma-ray observatory located at the Laboratory's Fenton Hill site. This observatory is the world's only air-shower array that is capable of operating at teraelectronvolt energies, providing critical capabilities to study these transients.

This year we phased out operation of the prototype Milagro gamma-ray observatory, known as Milagrito, as we completed construction of Milagro in November 1998 and began its operation February 1999. Most of our work this year was done on the prototype, Milagrito.

We analyzed data from Milagrito to search for several types of transients. We observed the first gamma-ray source ever detected by an air-shower array, an active galaxy known as Markarian 501, which shows transient variability in its output. We observed emission from a gamma-ray burst, and our study of this important observation continues. We also observed a burst of ~50-GeV particles from the sun during the Milagrito data gathering.

Exact Solutions of Quantum Gauge Theories from String Solitons

99047

Michael Mattis

This goals of this project have been to

(1) extract dynamical behavior of gauge field theories that lie beyond conventional perturbative methods using string theory. In particular we want to learn about strong coupling behavior of various supersymmetric generalizations of quantum chromodynamics using the AdS/CFT correspondence.

(2) investigate semiclassical effects in gauge theory at large N. Specifically, we want to find the role of instantons in this limit to correlation functions protected by nonrenormalization theorems from ordinary perturbative contributions.

(3) investigate the relation of gauge theory instanton effects and D-instanton effects in superstring theory using the AdS/CFT duality.

(4) use gauge theory instantons to probe the geometry of the dual supergravity theory, when it exists, or the singular superstring background.

Our results have provided the most compelling evidence for the existence of AdS/CFT duality, relating the strong coupling behavior of gauge theory to weakly coupled string theory, by relating various D-instanton induced terms in the Type IIB string effective action to the multi-instanton contributions to particular correlators in the gauge theory:

We showed how the interplay of the large N limit and supersymmetry greatly simplifies the ADHM multi-instanton formalism. In particular with a suitable change of variables, we showed how the nonlinear ADHM constraints, historically the biggest impediment to using the ADHM construction, can be explicitly resolved. We expect this technical advance to have important implications for other multi-instanton calculations in both physics and mathematics.

The second big technical advance was the discovery of the explicit volume form on the ADHM moduli space. We found this volume form for theories with arbitrary numbers of supersymmetries. We also rederived the multi-instanton measure by considering the dynamics of D-instantons in the background of D3-branes in Type IIB string theory. This result shows that there is a very close relation between string theory D-instantons and ordinary gauge theory instantons. In particular, this relation is convincing evidence for the "strong" form of the AdS/CFT Maldacena correspondence, namely the equivalence of the gauge and string theory for all g and N and not just large N.

We calculated, for the first time in any four-dimensional field theory, the leading order multi-instanton contributions exactly. The major conceptual advance that made the calculation possible was the realization that fermion zero-modes, as counted by the index theorem in an instanton background, can actually be lifted by tree-level scalar exchange via the Yukawa interactions in the Lagrangian.

We found compelling evidence of AdS/CFT duality: (1) large-N k-instanton collective coordinate space has the geometry of a single copy of $AdS_5 \times S^5$. The appearance directly of the S^5 factor is the most spectacular feature of our calculation—it arises as the saddle-point value of a set of auxiliary scalars introduced to bilinearize a four-fermion zero-mode interaction. (2) The integration measure on this space includes the partition function of 10-dimensional N=1 SU(k) gauge theory dimensionally reduced to 0 dimensions, matching the description of D-instantons in Type IIB string theory. This direct relation between D-instantons in string theory and ADHM instantons in gauge theory is a very appealing feature of the AdS/CFT correspondence, and as mentioned before is clear evidence for the strong form of the AdS/CFT correspondence. (3) In exact agreement with Type IIB string calculations, at the k-instanton level, we find that certain correlation functions match precisely nonperturbative terms in the supergravity effective action.

Publications

Dorey, N., et al., "Multi-Instanton Calculus and the AdS/CFT Correspondence in N=4 Superconformal Field Theory," *Nucl. Phys. B* **552**, 88 (1999).

Dorey, N., et al., "Multi-Instantons and Maldacena's Conjecture" (available online, http://eprints.lanl.gov/lanl, E-print No. hep-th/9810243, November 1998).

Hollowood, T.J., and V.V. Khoze, "ADHM and D Instantons in Orbifold AdS/CFT Duality" (available online, http://eprints.lanl.gov/lanl, E-print No. hep-th/9908035, August 1999).

Hollowood, T.J., et al., "Summing the Instanton Series in N=2 Superconformal Large N QCD" (available online, http://eprints.lanl.gov/lanl, E-print No. hep-th/9905209, May 1999).

Development of Detectors and Electronics for the Study of the Beta Decay of Polarized Neutrons at LANSCE

99048

W. Scott Wilburn

Precision measurements of the neutron beta-decay correlations *A*, *B*, *a*, and *b* provide important tests of the standard model of electroweak interactions. At the Los Alamos Neutron Science Center (LANSCE), we are designing an experiment to measure all four correlations to an accuracy that is better by an order of magnitude than existing measurements. The experimental design relies on the pulsed nature of the LANSCE beam.

One crucial feature of the experiment is the type of detector chosen for detecting both the proton and electron from the neutron decay: silicon strip detectors. With this project, we are proving the feasibility of using this type of detector to measure the neutron beta-decay correlations. Once feasibility is proved, we will be ready to design and construct the full experiment.

This experiment places severe demands on the detector. It must be capable of detecting low-energy (30-keV) protons as well as electrons with energies in the range of 50–800 keV. In addition, good timing resolution (few nanoseconds) is required over the full electron energy range. In the first year of this project, we have made substantial progress toward developing a detector and associated preamplifier that meet these requirements.

Commercial vendors can provide very thin dead-layer silicon detectors that are capable of detecting the low-energy protons. These detectors, however, have intrinsically high contact resistances, which cause the signal rise times to be long, making it impossible to achieve few-nanosecond timing resolution. We have worked with the manufacturer on a new design (with lower distributed resistance) that will solve this problem and have ordered samples for testing.

A second advance is the development of a design for a high-speed preamplifier that is able to achieve short rise times in spite of the large capacitances associated with silicon detectors. Our new preamplifier has a 4-ns rise time for a 50-pF detector capacitance, compared with 80 ns for a typical commercial device.

In addition, we have made significant advances in the design of the experiment. These advances include understanding the tradeoffs involved in selecting the thicknesses and number of detector layers, optimizing the transient digitizer speed, developing further the electric and magnetic field configuration, and understanding sources of systematic error.

Publications

Wilburn, W.S., et al., "A New Approach to Measuring the Neutron Decay Correlations with Cold Neutrons at LANSCE" (ILL Conference on Particle Physics with Slow Neutrons, Grenoble, France, October 22–24, 1998).

The Search for Dark Matter

99049

Salman Habib

We are exploring direct and indirect methods to detect dark matter particles in the universe. We will attempt the direct detection of weakly interacting massive particles (WIMPs) with cryogenic, low-background silicon(lithium) [Si(Li)] detectors. These detectors will be characterized in a special underground facility at the Waste Isolation Pilot Plant (WIPP).

With the Milagro Gamma-Ray Observatory at Los Alamos, we will search for high-energy gamma-rays from WIMP annihilation near the Sun. Theoretical issues we are addressing include (1) relevant cross-section calculations for direct detection, (2) sensitivity of Milagro to the WIMP annihilation signal, and (3) quantitative estimates of dark matter distribution, both in the galaxy and in the solar neighborhood, via high-resolution numerical simulations.

Construction of the Milagro Gamma-Ray Observatory was completed in winter 1998, and data gathering commenced in February 1999. Though the calibration of the instrument is not yet complete, we have observed a shadow in the signal from both the Moon and the Sun with the data taken so far. Once the calibration of the instrument is complete, we will operate Milagro at a trigger rate near 4 kHz (we are currently operating at 1.5 kHz). At this increased trigger rate, the energy threshold is estimated to be 250 GeV. This threshold is significantly lower than our first estimates of 400 GeV and will allow us to set limits (or obtain a positive detection signal) in a more physically plausible region of particle masses.

We constructed a specially designed low-background cryostat to house the three large Si(Li) detectors that we are using to assess backgrounds. We measured differential shielding using the Si(Li) detectors and a large, hyperpure germanium detector. This detector has allowed us to separate the gamma backgrounds emanating from the rock walls from the neutron and cosmic-ray backgrounds. We have already achieved a reduction factor of more than 100 in backgrounds compared with surface tests conducted at the Laboratory. We are now studying the effect of neutron backgrounds. We have started Monte Carlo simulations of backgrounds to compare the measured reductions in backgrounds that result from different amounts of shielding with those we would expect if the background were due to specific sources (such as uranium and thorium decay chains).

Our theoretical effort concentrated mainly on refining a code to compute elastic-scattering cross sections and developing a parallel *n*-body code for galactic dynamics to study dark matter distribution in the galaxy. This *n*-body code is based on a particle-mesh method with symplectic time-stepping and uses the Parallel Object-Oriented Methods and Applications (POOMA) framework developed at Los Alamos. We are testing the *n*-body code and plan to use it to investigate dark matter velocity distribution, as well as dark matter distribution near the galactic core and in the solar neighborhood. In addition, we are investigating the possibility of local dark matter density enhancements caused by a mechanism pointed out recently by other researchers.

Fundamental Symmetries with Trapped Atoms

99052

Andrew Hime

We are working to exploit magnetically trapped rubidium-82 in a new generation of fundamental symmetry experiments. Rubidium-82, a pure and allowed Gamov-Teller beta-decay nucleus, has the appropriate atomic structure and lifetime to be exploited in a magneto-optical trap (MOT). We have mounted a proof-of-principle experiment to measure the positron-spin correlation coefficient from polarized rubidium-82 in a magnetic, time-orbiting-potential (TOP) trap. In this case, an essentially massless source of polarized atoms is confined to a spatially localized cloud. We can exploit the pointlike geometry of such a source, together with a "rotating" nuclear polarization vector, to measure the positron-spin correlation as a continuous function of positron energy and emission angle in a single and fixed electron detector. This project exploits a number of unique opportunities at Los Alamos to study fundamental symmetries of the weak interaction at a new level of precision, which is required to understand the violation of parity symmetry.

This year we assembled and tested all of the hardware for the proof-of-principle experiment. Previous measurements obtained a record number of trapped radioactive rubidium-82 and showed the feasibility of obtaining sufficient numbers to accumulate the statistics for a precision measurement. The TOP trap hardware has been put into place and vacuum achieved at sufficiently low pressure to ensure a trapping lifetime that is long compared with the natural half-life of rubidium-82. In addition, we put into place a first-generation positron telescope, together with the associated electronics and data-acquisition equipment.

We focused on optimizing the rubidium-82 source and trapping efficiency. Our efforts have included fine-tuning/optimizing the ion source and mass separator and developing a more efficient catcher foil and primary trap. The strategy to transfer atoms from the MOT to the TOP trap has been exercised successfully. In addition, we have implemented a means for calibrating the magnetic field distribution as well as the detector response to positrons. We are prepared for our first dedicated data-taking sequence as a proof-of-principle exercise.

Proof-of-principle experiments are essential for assessing the feasibility of the symmetry experiment and for providing the data necessary to ascertain the ultimate precision and limitations of the existing apparatus. Eventually, we hope to perform a number of first-generation experiments that would lead to a first measurement of the positron-spin correlation using this technology.

Measurements of (n-gamma) Cross Sections for Unstable Nuclei

99050

John Ullmann

The objective of this project is to measure data on neutron capture reactions to aid in understanding the synthesis of heavy elements in the stars. In particular, neutron capture on radioactive elements with half-lives on the order of years is important in the understanding of the physical environment in a star where this synthesis takes place. Detailed measurements on radioactive elements, of the sort we will make, have not ever been made before. Los Alamos is unique because it has the facilities required to make these measurements in one place. These include facilities for radioisotope manufacture and handling, an intense source of neutrons, and a detector (under construction) optimized for studying these reactions.

This year we set up and conducted an experiment on Flight Path 2 at the Manuel J. Lujan Neutron Scattering Center. Considerable effort was devoted to understanding sources of experimental background. Unfortunately, before real astrophysical data could be gathered, problems with the neutron production facility resulted in a premature termination of the running period. Our full attention was then directed toward planning and designing a new dedicated neutron capture detector that will be built on Flight Path 14 at the Lujan Center. The preliminary studies provided important information to our understanding of the backgrounds, and we folded that information into the design of the new detector.

Publications

Wilhelmy, J.B., et al., "Neutron Capture on Radioactive Targets: Probing the s-Process," in *Proceedings of the Second International Conference on Fission and Neutron-rich Nuclei*, University of St. Andrews, Scotland, June 28–July 2, 1999 (in press).

New Paradigms in Simulating the Prediction, Intervention, and Control of Infectious Diseases

98009

James M. Hyman

Two of the most urgent public health challenges today are devising effective strategies to minimize the destruction caused by infectious diseases and predicting the spread of resistant strains. We are developing mathematical models based on the underlying transmission mechanisms of diseases to help the medical/scientific community understand and anticipate the spread of an infectious agent in different populations. These models will also allow us to evaluate the potential effectiveness of different approaches for bringing an epidemic under control. Our goal is to have the new models reduce the uncertainty in estimates of disease prevalence and increase scientific understanding of how infectious diseases spread.

We analyzed the sensitivity of two models for the spread of HIV in a homogenous population to (1) variations in the initial state of the population, (2) the migration rate in and out of the susceptible population, (3) the partner acquisition rate, and (4) the number of contacts per partner.

In the differential infectivity model, the infected population is divided into groups according to their infectiousness. For example, HIV is spread primarily by a small, highly infectious group of superspreaders. In the staged-progression model, every infected individual goes through a series of infection stages, and the virus is spread primarily by individuals in an initial, highly infectious stage or in the late stages of the disease.

We showed that the timing of the epidemic is sensitive to the initial distribution of the infected population, and we presented a robust initialization procedure that allows a comparison of the timing of the two models. We demonstrated that migration in and out of the population is an important, yet often neglected, factor in both models. We also illustrated the importance of distinguishing between the number of partners a person has and the number of contacts per partner. When we assumed that people with many partners have fewer contacts per partner than people with few partners, we found that the epidemic is only mildly sensitive to the partner acquisition rate. Rather, because the probability of transmission of HIV per contact is low, the epidemic is much more sensitive to the number of contacts per partner.

Publications

Hyman, J.M., and J. Li., "An Intuitive Formulation for the Reproductive Number for the Spread of Diseases in Heterogeneous Populations" (to be published in *Math. Biosci.*)

Hyman, J.M., and J. Li., "Modeling the Effectiveness of Isolation Strategies in Preventing STD Epidemics," *SIAM J. App. Math.* **58** (3), 912 (1998).

Hyman, J.M., et al., "The Differentiated Infectivity and Staged Progression Models for the Transmission of HIV," *Math. Biosci.* **155** (2), 77 (1999).

Development of a Human Artificial Chromosome

97019

Norman Doggett

Chromosomes contain specialized structures that serve to maintain chromosome integrity and functionality. These include telomeres, which protect the ends of chromosomes from shortening during DNA replication; centromeres, which are associated with the spindle attachment sites during mitosis and meiosis; origins of replication, where DNA replication initiates; and matrix attachment sites, where DNA attaches to the nuclear scaffold. Our goal was to develop a human (mammalian) artificial chromosome that contains the minimal essential chromosomal components for stable maintenance in the mammalian nucleus. A human artificial chromosome could serve as a vehicle for gene therapy as well as a tool for studying chromosome function and control of gene expression.

During this project we developed external collaborations with two groups and significantly advanced the strategy for developing an artificial chromosome. Research continues in these collaborating laboratories to develop a human artificial chromosome. We were successful in generating a library of very early replicating DNA which should be enriched in DNA replication origins necessary for a human artificial chromosome. Simultaneously with this work we pursued the cloning of a DNA mismatch repair gene that we intended to use in a human artificial chromosome for functional studies. We performed extensive studies with gene *hMSH5* and another MutS homologue, *hMSH4*, with emphases on the identification and functional characterization of human *hMSH5* and its mouse orthologue, as well as the identification of sequence polymorphisms that cosegregate with ovarian cancer.

The results of these studies demonstrated the existence of the fifth MutS homologue (*hMSH5*) in humans. We demonstrated that the *hMSH5* gene mapped to chromosome 6p21.3 within a region that has been implicated in the pathogenesis of ovarian carcinoma. The *hMSH5* gene is functionally related to the *hMSH4* gene as shown by yeast two-hybrid experiments. An *hMSH5* gene C85T polymorphism is highly associated with the occurrence of ovarian cancer, and somatic alterations of *hMSH5* gene are also observed in a significant fraction of ovarian tumors. We also learned that an *hMSH4* splicing variant (*hMSH4sv*) exists that is unable to interact with *hMSH5* at the protein level and is highly expressed in ovarian tumor cells. Mouse Msh5 shares conserved properties with those of human *hMSH5*. This observation is useful in identifying amino acid residues that are critical for function, and therefore, facilitates the functional characterization of sequence polymorphisms. In addition, recent studies have shown that Msh5 is critical in ovarian development in mice.

Publications

Brylawski, B.P., et al., "Construction and Characterization of Cosmid Libraries of DNA Replicated Very Early in the S Phase of Normal Human Fibroblasts" (submitted to *Nucleic Acids Res.*).

Cao, Y., et al., "A 12 Mbp Complete Coverage BAC Contig Map in Human Chromosome 16p13.1-11.2," *Genome Research* **9**, 763 (1999).

Her, C., and N.A. Doggett, "Cloning, Structural Characterization, and Chromosome Localization of the Human Ortholog of Saccharomyces Cerevisiae MSH5 Gene," *Genomics* **52**, 50 (1998).

Her, C., et al., "Identification and Characterization of the Mouse MutS Homologue 5: Msh5," *Mammalian Genome* **10**, 1054 (1999).

Kouprina, N., et al., "Construction of Human Chromosome 16- and 5-specific Circular YAC/BAC Libraries by In-vivo Recombination in Yeast (TAR cloning)," *Genomics* **53**, 21 (1998).

Predictive Models for Transcriptional Enhancers

97022

Goutam Gupta

Identification of gene control elements, such as transcriptional enhancers, requires knowledge of how these DNA elements interact with their corresponding proteins. The homeodomain is a small, conserved protein motif that binds specifically to DNA and plays a central role in gene regulation. The homeodomain/DNA complex provides an ideal system for studying the interactions between gene control elements and their binding proteins. To gain insight into such interactions, we developed an algorithm for predicting both protein and DNA structures using a homology modeling approach.

Working with a collaborator at Children's Hospital Research Foundation (Cincinnati, Ohio), we studied the recognition codes of Bicoid homeodomain for different DNA sites. Bicoid homeodomain binds to both a TAATCC consensus site (A1) and a TAAGCT nonconsensus site (X1). Mutation and methylation interference studies indicate the involvement of arginine-54 (ARG-54) of the homeodomain in an important base-specific recognition of DNA. Using our homology modeling method, we predicted structures of Bicoid homeodomain that bind to both A1 and X1 sites. In our modeled structures, ARG-54 makes one hydrogen bond (h-bond) with the N7 atom of the adenine in the third position of the A1 site (see top schematic in accompanying figure). If the residue of the ARG-54 is swung upward about 1.5 Å, it makes two h-bonds (one with the N7 atom of the adenine and the other with the O6 atom of the guanine 3' to the adenine) when the homeodomain binds to the X1 site (see bottom schematic in accompanying figure). Our results explain why the homeodomain mutant (arginine to alanine substitution at residue 54) binds to the A1 site with a reduced binding affinity, whereas this same mutation abolishes the binding of the homeodomain to the X1 site.

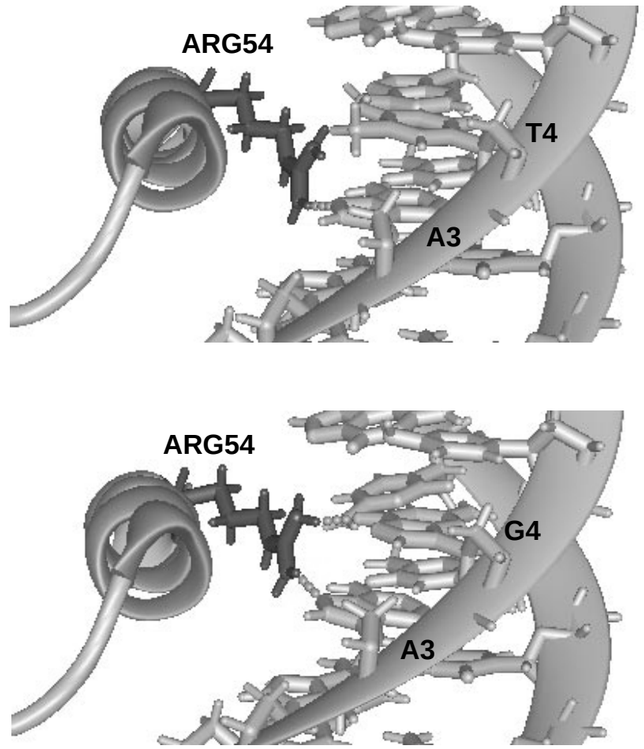

The specific interactions between ARG-54 and the targeted DNA when Bicoid homeodomain binds to a TAATCC consensus site, A1 (top), or a nonconsensus TAAGCT site, X1 (bottom). While ARG-54 forms one hydrogen bond with the third adenine in the consensus site (middle of top schematic), the same ARG-54 forms two hydrogen bonds with the third adenine and the fourth guanine in the nonconsensus site (middle of bottom schematic).

Publications

Dave, V., et al., "Reprogrammable Recognition Codes of Bicoid Homeodomain for Different DNA Sites" (submitted to *Genes and Development*).

Tung, C.-S., "Structural Study of Homeodomain Protein-DNA Complexes Using a Homology Modeling Approach," *J. Biomol. Struct. Dyn.* **17**, 347 (1999).

The Role of Low-Frequency Collective Modes in Biological Function: Ligand Binding and Cooperativity in Calcium-Binding Proteins

97020

Jill Trewhella

We studied the protein dynamics that are believed to be important for direct control of protein function. We combined nuclear magnetic resonance (NMR) relaxation and vibrational spectroscopy to probe the dynamic fluctuations and Ca^{2+}-binding properties of two proteins, calmodulin (CaM) and calcineurin (CnB). We also completed molecular dynamics (MD) simulations that predict specific motions in CaM and used scattering measurements to test predictions of the MD simulations. We seek a fundamental understanding of the relationship between the structural dynamics and function of proteins. This understanding is key to a broad range of biotechnology applications that depend upon engineering proteins for modified function, such as in bioremediation and in designer enzymes for industrial applications.

CaM and the regulatory component of CnB represent a large class of Ca^{2+}-binding proteins that are ubiquitous in eukaryotic systems and that regulate the functions of a large number of enzymes. These proteins are structurally homologous, having an unusual dumbbell shape with two globular Ca^{2+}-binding domains. Each globular domain has two Ca^{2+}-binding sites that share the same basic structural motif. The details of the protein scaffold and specific side-chain interactions are used to tune the Ca^{2+}-binding properties of each site for specific functions in the cell. We used Fourier transform infrared spectroscopy (FTIR) to study Ca^{2+} binding to CnB. Specific mutations were used to inactivate each Ca^{2+}-binding site. The FTIR and binding data show that there is communication between the Ca^{2+}-binding sites; we are completing x-ray scattering experiments to investigate possible mechanisms for this communication.

We completed MD simulations on the N-terminal globular domain of CaM. The Ca^{2+}-saturated crystal structure of CaM suggests that Ca^{2+}-binding to the globular domains induces a concerted movement of two pairs of helices within each domain, resulting in exposure of a hydrophobic cleft that is key to target enzyme recognition. Our simulations suggest that this motion may be an artifact induced by interprotein contacts in the crystal lattice. To test this idea, we completed x-ray scattering experiments to evaluate precisely the solution structural parameters for this domain in CaM. The scattering data confirm the predictions from the MD simulations. This result radically alters our understanding of the fundamental mechanism of enzyme regulation by Ca^{2+}-binding proteins.

Finally, we acquired NMR relaxation data on the N-terminal domain of CaM, both with and without Ca^{2+}. We performed an initial round of dynamical analysis with the Ca^{2+}-free data. We estimated the magnitude of the rotational motion for internal mobility in the picosecond-to-nanosecond time frame for the resolved carbon-13 and nitrogen-15 nuclei. We demonstrated the feasibility of extracting both fast-limit and generalized-order parameters. These parameters indicate that the magnitude of motion is faster than approximately 10 ps and faster than molecular tumbling (~4 ns). In marked contrast to earlier studies, this study provides relaxation data for multiple main- and side-chain atoms of a given amino acid residue. These more extensive data allow for dynamical interpretations in terms of correlated conformational fluctuations, thus yielding estimates for the conformational entropy of individual protein side chains. Full analysis of these data will continue beyond the duration of this project.

Publications

Gallagher, S.C., et al., "Ca^{2+} Binding to Calcineurin B Studies Using Site Specific Mutagenesis and Fourier Transform Infrared Spectroscopy" (submitted to *Biochemistry*).

Le Master, D.M., "NMR Relaxation Order Parameter Analysis of the Dynamics of Protein Sidechains," *J. Amer. Chem. Soc.* **131**, 1726 (1999).

Rapidly Photocleavable Caged Proteins

99011

Charlie E. M. Strauss

The mechanics of protein folding is one of the unsolved problems in structural biology. The central experimental limitation in this problem is the inadequacy of biophysical methods for probing protein molecules in the act of folding. A primary goal of this project is to develop a new, more versatile approach to initiating protein folding. A secondary goal is to develop new approaches to caging, denaturing, and deactivating proteins. A third goal is to apply these techniques to elucidate folding kinetics in protein.

The key distinction between our approach to protein unfolding and other denaturation techniques is that we do not disrupt the fundamental chemical process that drives protein folding and dynamics. We merely destabilize the native state (and the transition state) without appreciably affecting the unfolded state. To do this we attach a large chemical cage to a specific amino acid in the protein that blocks it from achieving its folded, native state. In contrast, conventional guanadine and thermal denaturation work by weakening the dominant interatomic forces between all of the protein residues. Our approach mechanically destabilizes the protein without changing the chemical forces and is therefore not plagued by questions of how the protein is perturbed by the unfolding technique. Because our technique disturbs the protein less, it is likely to reveal interactions masked by more globally disruptive approaches. In particular, we feel that our approach may more accurately reflect the character of the denatured state, such as the degree of collapse or secondary structure formation before folding.

We have shown that we can reversibly attach a single cage to a cystein in the interior of a protein and cause the protein to lose and regain its structure. We created point mutations of the single-domain protein known as "protein L." These mutations introduced a cystein amino acid into the hydrophobic core and a tryptophan amino acid near the cystein (as a quenchable fluorescent reporter). The degree of folding in the protein was monitored by tryptophan flourescence as well as by circular dicroism (CD). We chemically denatured the protein, reacted it with a cystein-binding cage molecule (BNPA), and then removed the chemical denaturant. Fluorescence measurement of the tryptophan was consistent with an unfolded (exposed) tryptophan residue, indicating that the protein was unfolded. Exposure to UV light removes the cage, and we observed the recovery of the folded (buried) tryptophan fluorescence.

This internal caging strategy differs from conventional random external caging. First, all of the caged proteins are identically and reproducibly prepared: a single cage is attached in a reproducible manner to the same residue on the protein in every case. Second, this single cage is strategically positioned in the interior of the protein to disrupt the protein's domain, thus unfolding the protein globally, not merely altering its local structure. Third, since a single cage is used, only a single photon is necessary to remove the cage. Thus, we are in a position to study the transient changes in an ensemble of identically prepared proteins after sudden laser photolysis of the cage. A secondary application of this single-cage inactivation technique is biomimetic amplification of a weak signal: reactivation of protein activity by a single photon (or possibly by ionizing radiation), which in turn can catalyze a macroscopic chemical response.

We also used a new technique for transient CD to examine a caged GCN4 mutant dimer. Our principal outcome of this technique so far is design requirements for the optical density and quantum efficiency of the cage for use in CD experiments. Unlike experiments in which transient protein dynamics are studied in a binary mixture of protein and photoactive molecules (e.g., Ph-jump or T-jump), experiments with the caged protein always have a one-to-one ratio of chromophore to protein. This caging strategy can create competing design goals when the optimal density of a protein for a probe technique is mismatched to the optimal density for photoinitiation.

We devised a transient CD system with collaborators at the University of California, Santa Cruz, and used this system to study a cage designed for the GCN4 peptide dimer developed at Caltech.

Substrate-Dependent Cell-Cycle Disturbances in Response to Ionizing Radiation

97021

Donna Gadbois

Ionizing radiation (IR) initiates a cellular stress response that causes a temporary delay in cell proliferation. Traditionally, it is thought that these delays allow time for DNA repair and that the length of delay is dictated by the extent of IR-induced DNA damage. However, our studies indicate that while the proliferation delay is initiated by DNA damage, the length of the delay is influenced by the cellular environment. For example, cells are surrounded by and interact with proteins in the extracellular matrix (ECM), and these cell–ECM interactions provide a signaling network to stress stimuli, such as IR.

We are studying the effect of cell–ECM interactions on cellular proliferation after exposure to IR. We have found that the length of proliferation delay after irradiation is determined by the identity of the proteins in the ECM. We also found that irradiated cells that arrest indefinitely on ECM containing predominately collagen will then express a protein called smooth muscle a-actin (SMA). The expression of SMA indicates that the cells are differentiating into a cell called myofibroblasts. This information is important because myofibroblasts are present in radiation-damaged tissue and are associated with fibrosis, a deadly side effect of radiation treatment. We discovered that we can halt the organized expression of SMA after irradiation by treating the cells with a neutralizing antibody to a protein called latent TGF-β1 binding protein (LTBP). This is significant because it indicates that the ECM effect on proliferation also involves the TGF-β1 pathway, a molecular pathway that is involved in radiation fibrosis.

We have observed the expression of SMA and differentiation to myofibroblasts even after very low doses of radiation. The presence of myofibroblasts in tissues is thought to be an indicator of susceptibility to radiation fibrosis. Our results may provide a marker for radiation susceptibility to low-dose radiation.

Publications

Dimitrijevic-Bussod, M., et al., "Extracellular Matrix and Radiation G_1 Cell Cycle Arrest in Human Fibroblasts," *Cancer Research* **59**, 4843 (1999).

Noninvasive Techniques for Genetic Analysis

98005

Jonathan L. Longmire

We are using molecular genetic approaches to study the Mexican spotted owl (*Strix occidentalis lucida*) population that resides in the Jemez Mountains of northern New Mexico. We are using a library of cloned DNA fragments to examine highly variable regions (known as microsatellites) within the spotted owl genome. These microsatellites then serve as markers that we apply to DNA samples isolated from molted feathers. We are using the resulting data to examine genetic variation within the owl population and to genetically compare the Jemez population with spotted owls from other geographic areas.

Because we are using molted feathers collected at nest sites as a DNA source, we do not have to trap and handle the owls. Thus, a unique aspect of this study is that it is noninvasive and of minimal disturbance to this threatened species.

Our study provides valuable insights into several aspects of spotted owl biology and ecology, such as turnover rates at nest sites, survival rates, possible multiple paternity, dispersal patterns, levels of genetic diversity, and genetic uniqueness of the Jemez population. This project contributes to our understanding of environmental issues related to threatened and endangered species that are of both local and national importance.

This year we screened a library of spotted owl DNA sequences for microsatellite repeats. This library consisted of all possible mono-, di-, and trinucleotide repeats, along with the tetranucleotide repeat (GATA)n and the pentanucleotide motif (GGAAT)n. In addition to identifying clones that contain microsatellites of interest, the results from this screening gave us new insights into the organization of repetitive DNA sequences in a genome that was previously unstudied.

We are currently subcloning these microsatellites to facilitate DNA sequencing. Oligonucleotide primers (developed from the sequence data) will allow us to amplify and analyze these highly poymorphic genomic regions in spotted owl DNA. We have also made progress in isolating DNA from feathers and in gender testing these DNA samples with a technique based on PCR (polymerase chain reaction).

Next Generation of Molecular Dynamics: Implicit-Solvent/Langevin Models for Folding of Peptides and Proteins

98008

Gerhard Hummer

How do proteins fold, and what are the mechanisms and forces underlying protein stability and complex formation? How can small changes in amino acid sequences result in disease-causing conformational variability and aggregation? What role do large-scale motions play in enzyme activity? These questions are central to structural biology. A unique theoretical method—molecular dynamics (MD) simulations—could, in principle, help to address them. However, typical simulations extend only into the nanosecond range, 2 to 4 orders of magnitude short of the time scales needed for folding and aggregation phenomena. To overcome the inherent time-scale limitations of MD, we develop implicit, solvent-averaged potentials to be used in combination with a stochastic Langevin dynamics for molecules with constrained bond lengths and angles. This implicit solvent/Langevin model provides a computationally efficient alternative to conventional Newtonian dynamics with vacuum interactions. Our goal is to use these tools to study the initial phases in peptide and protein folding, thus complementing unique experimental efforts at Los Alamos.

Our extensive MD simulations in explicit solvent of alanine- and glycine-based peptides helped us understand the molecular mechanisms involved in alpha-helix formation. The figure illustrates the folding and unfolding mechanisms of short helical peptides. We showed that the unfolding kinetics for these short peptides is a thermally activated process. We found, however, that folding is controlled by diffusion in conformation space for fast-folding peptides. For a peptide with sequence-induced folding traps (i.e., enthalpically stabilized conformations competing with the helical folded state), thermal activation controls escape from the intermediate states, followed by conformational diffusion.

We can also quantify the many-body effects in hydrophobic interactions; these effects form a major bottleneck in the development of accurate, solvent-averaged potentials. Hydrophobic interactions are a major stabilizing factor for folded proteins. Their strong, many-body character is frequently approximated by surface-area models. However, surface-area descriptions are ill suited to dynamics calculations and lack the molecular detail required for accurate energetics. We developed an alternative force-field description with a surprisingly simple quantification of many-body terms. This force field proved accurate for structural variations both at small- and intermediate-length scales, such as forming a model of a protein hydrophobic core. In addition, we obtained promising results using this force-field model for characterizing protein surfaces as targets in drug development.

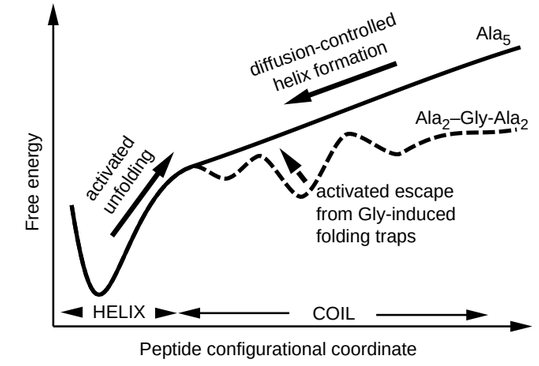

Schematic representation of the folding and unfolding mechanisms of short helical peptides. Folding (helix formation) is modeled as a diffusive process on a one-dimensional reaction coordinate. Unfolding requires thermally activated escape from the enthalpically stabilized folded state. Variations in the peptide sequence affect the roughness of the energy landscape in the unfolded state. Arrows near the free energy curves indicate "diffusional flow" along the reaction coordinate for folding and unfolding. The small arrow pointing upward left (between the dashed Ala_2–Gly-Ala_2 curve and the solid Ala_5 curve) indicates escape out of a high-lying minimum toward the folded state.

Publications

Hummer, G.S., "Hydrophobic Force Field as a Molecular Alternative to Surface-Area Models," *J. Am. Chem. Soc.* **121**, 6299 (1999).

Hummer, G.S., et al., "Hydrophobic Effects on a Molecular Scale," *J. Phys. Chem. B* **102**, 10469 (1998).

Role of New Cancer Gene in Environmental Carcinogenesis

98047

Min Sung Park

Greater than 50% of cancers (i.e., esophageal, colon, and lung cancer) appear to be caused by genetic defects in a newly discovered cancer gene, FHIT. The affected organs are heavily exposed to environmental carcinogens and can accumulate mutations that lead to cancer development. The amino acid sequence of the FHIT protein suggests that the gene product is probably an enzyme that, when induced by environmental stress and DNA damage, breaks down one form of dinucleotide (Ap4A). Owing to a paucity of information regarding the physiological role of intracellular Ap4A, the consequences of altered Ap4A metabolism cannot be predicted. Thus the study of FHIT and its substrate, Ap4A, may uncover novel biological phenomena with significant involvement in environmentally induced cancers. The results of this research will provide a foundation for understanding the molecular mechanisms of environmentally induced cancers and will have significant application in the areas of cancer risk assessment, diagnosis, and therapy.

We used a combination of biochemical and molecular biological approaches to understand the biochemical and cellular mechanisms that the FHIT protein uses to control the intracellular concentration of Ap4A under various environmental insults. These approaches included the production of recombinant FHIT, the characterization of its enzymatic activity, and the introduction of a new copy of the FHIT gene into a human cell that is deficient in the normal FHIT gene. This new cell system, with a copy of the introduced FHIT, will be useful in studying the dynamic changes of Ap4A level in vivo under various DNA-damaging conditions. This cell system will also be useful in determining the signaling pathways that control the intracellular concentration of Ap4A, considering the likelihood that there are other players that control Ap4A concentration as well.

We established five independent cell lines that express the exogenously introduced FHIT gene. The level of FHIT mRNA was comparable among all five clones except one that had about 60% mRNA compared with the other four clones. Those four clones were further tested for protein level to confirm the direct correlation between the mRNA and protein levels. We developed new FHIT antibodies by immunizing rabbits with purified recombinant FHIT proteins made in *E. coli*. This antibody recognizes the FHIT protein with high specificity and will be useful for future investigations of potential proteins that interact with FHIT. Protein-expression analysis using antibodies confirmed that all four clones express equivalent levels of FHIT. We used two of the four FHIT-positive cell lines to test Ap4A level changes under various physiological conditions: UV light, ionizing radiation, heavy metals (cadmium), and light metals (beryllium). We discovered that the Ap4A level dramatically changes under UV, ionizing radiation, and heavy-metal exposure, but not under light-metal exposure in cells that express the induced level of FHIT.

We purified a recombinant FHIT protein from *E. coli* and tested its biochemical activity. We tested its enzymatic activity for the hydrolysis of Ap4A in vitro by measuring the hydrolytic product AMP (adenosine nucleotide monophosphate). The recombinant FHIT exhibited full biochemical activity, demonstrated by expected K_m values and second-order enzyme kinetics that were enzyme- or substrate-concentration dependent. Our study represents the first production, purification, and characterization of the biochemical activity of recombinant FHIT. This material will be useful for studies of the detailed, structure-function relation of FHIT and other related hydrolases.

We also tested the effects of heavy metals on the enzymatic activity of FHIT in vitro, and found that cadmium has no direct affect, suggesting that the catalytic activity of FHIT in vivo might be regulated by other messengers within the cell. These messengers might be induced indirectly by heavy metals such as cadmium. Our results so far allow us to establish a relationship between environmentally induced cancer and FHIT.

Targeted In Vitro Evolution of Protein Ligands

98007

Bruce E. Lehnert

Our primary objective is to develop a new technique for peptide evolution, which will be used to select high-affinity peptide binders (ligands) to target molecules. The evolution of such peptides coupled with coding RNA is a fast-track approach to characterizing intermolecular interactions, which have potential downstream research, therapeutic, diagnostic, and biosensor applications.

We designed an in vitro process using a mutagenized coat-protein dimer from the MS2 bacteriophage, which binds a specific RNA stem-loop structure with subnanomolar affinity. By fusing this stem-loop structure upstream of the coat-protein dimer and following it with a randomized library sequence of RNA, we hope to optimize a system in which we can translate a pool of such constructs that will bind the nascent RNA encoding for a particular peptide and use this structure in a selection scheme against a target.

To assemble an in vitro library, we must first define the proper scaffolding for the components of the library. In addition, we must optimize parameters for each step of the selection scheme of in vitro translation, immunoprecipitation, RNA isolation, and RT-PCR (reverse transcription–polymerase chain reaction) for the particular construct. We assessed our various scaffold designs by subjecting them to conditions under which a very small amount of evolved ligand may be selected for and enriched when surrounded by similar ligands that can compete for the evolved ligand's operator region and produce false positives. After testing several constructs, adjusting the various scaffoldings for the library, varying selection and PCR protocols, and then translating with appropriate competitors, we were able to retrieve our original test RNA in preliminary experiments, when the experiments involved molar ratios of 1:100 (up from 1:10 in previous constructs). We believe this gain in retrieval is caused by a rational-designed linker placed between the two covalently fused monomers, allowing necessary flexibility for dimerization with the added attribute of reducing the predicted antigenicity of previous linkers.

Although this achievement is significant, further refinements are necessary if we are to realize our goal of 10^{13} diversity in ligands, predicted from a randomized library and emulated by our competition experiments. Another achievement was our development of a flow-cytometric technique to assess the ability of a generated ligand to compete with the binding of a protective antigen to its cell-surface receptor.

Publications

Cirino, N.M., et al., "Disruption of Anthrax Binding with the Use of Human Antibodies and Competitive Inhibitors," *Infection and Immunity* **67**, 2957 (1999).

Rapid Genotyping Assay for Beryllium Disease Susceptibility

98006

John P. Nolan

Our goal is to develop an accurate, high-throughput method to analyze genetic mutations associated with chronic beryllium disease (CBD). Susceptibility to this immunologic hypersensitivity appears to be associated with one or a few single-nucleotide polymorphisms (SNPs), single base changes in the genetic code. A rapid and cost-effective assay to screen past and future beryllium workers would greatly enhance efforts to reduce CBD. The genetic variant associated with CBD is only one of many examples where a genetic factor is associated with a susceptibility to disease. We expect our new method to have general use in screening for other diseases associated with SNPs.

We previously demonstrated the feasibility of a microsphere-based, flow-cytometric, oligonucleotide ligation assay for the glu69 variant of HLA DPB1 exonII that is associated with CBD. This year we optimized our microsphere-based assay in several respects. First, we determined the optimum concentration of reagents (primers, template, and enzyme) and reaction conditions (temperature, number and duration of thermal cycles) required for accurate determination of the SNP identity. These determinations allowed us to perform an assay that is both rapid and cost-effective. Second, we developed conditions for the multiplexed analysis of SNPs, allowing multiple genetic variants to be screened simultaneously and enhancing the predictive power of our screening assay. Finally, we developed methods for the covalent conjugation of synthetic oligonucleotides to microspheres, an essential step in providing assay kits that are robust and have extended shelf lives.

Computational Studies of the Role of Water Fluctuations in Protein Dynamics and Folding

99006

Angel Garcia

The purpose of this project is to elucidate the role of water dynamics in mediating large-scale fluctuations, ligand binding, and the unfolding/folding transitions of proteins. Proteins form the core of the biomolecular machinery of life. The functionality of proteins is related to their ability to fold and to their dynamical fluctuations. Water molecules interact strongly with proteins and determine protein dynamics and stability. We are using molecular dynamics (MD) simulations to study the stability, dynamic fluctuations, and early unfolding events in proteins. We are developing an atomic-level description of hydrogen exchange that describes hydrogen protection factors, taking into account protein dynamical fluctuations, hydration structure, and water relaxation. We are also studying the kinetics of water penetration into the hydrophobic core of proteins under various conditions to understand the mechanism for small-ligand binding to the protein interior. We are testing the recently postulated hypothesis that pressure-induced protein denaturation occurs via water penetration into the protein's hydrophobic core.

We studied the dynamical fluctuations of horse heart cytochrome c (cyt c) in an aqueous solution by MD simulations. These simulations took place at near the native state under native conditions (300 K), slightly above the experimental melting temperature (360 K), and above the melting temperature (430 K), at which the hydrophobic effect is large and mostly enthalpic. We studied the fluctuations of the cyt c in terms of collective motions that involve the whole protein and local motions that involve the forming and breaking of hydrogen bonds between the backbone amino groups and solvent water molecules. Our simulations show that structural changes associated with interbasin displacements are collective motions of the loops and coiled regions and relative motions of the alpha-helices as rigid bodies. Earlier observations suggested that similar motions, although covering a much larger range of time and conformational changes, may be involved in hydrogen exchange. However, some amino acids showing large, correlated motions do not expose the amino hydrogens to the solvent.

We also studied the kinetics of water penetration and escape in cyt c. Some of the interior water molecules occupy transient cavities and diffuse extensively within the protein. The motions of protein-bound water molecules are rotationally hindered but show large librations. An analysis of the kinetics of water escape in terms of a survival-time correlation function shows a power-law behavior in time that we can interpret in terms of a broad distribution of energy barriers, relative to kT (where k is the Boltzmann constant and T is temperature), for water exchange. At T = 300 K, estimates of the roughness of the activation energy distribution are 4–10 kJ/mol (2–4 kT). Activation enthalpies for water escape are 6–23 kJ/mol. Differences in activation entropies between fast-exchanging (0.01 ns) and slow-exchanging (0.1–1.0 ns) water molecules is –27 J/K/mol. Earlier work has estimated the maximum entropy loss of a water molecule because of binding to be 28 J/K/mol. Therefore, our results suggest that the entropy of interior water molecules is similar to the entropy of bulk water.

Publications

Garcia, A.E., and G. Hummer, "Conformational Dynamics of cytochrome c: Correlation to Hydrogen Exchange," *Proteins: Struct. Funct. Genet*. **36**, 175 (1999).

Garcia, A.E, and G. Hummer, "Water Penetration and Escape in Proteins," P*roteins: Struct. Funct. Genet.* **38,** 261 (2000).

Hillson, N., et al., "Pressure-Induced Protein Folding/Unfolding Kinetics," *Proc. Natl. Acad. Sci. U.S.A.* **96**, 14848 (1999).

The Molecular Aging Clock

99007

Tracy Ruscetti

The informational integrity of the genome is maintained, in large part, by DNA repair systems. DNA can be damaged by both external and internal stimuli resulting in a variety of DNA lesions. A lesion that damages both strands of the DNA (termed double strand breaks, or DSBs) poses a significant threat to the integrity of the genome. DSBs left unrepaired can lead to chromosome loss, genetic mutation, or cell death.

Double strand breaks can be repaired by either of two mechanisms: end-to-end joining (nonhomologous end joining, or NHEJ) or homologous recombination. It has been shown that the misrepair of DSBs in a particular part of the genome (ribosomal DNA, or rDNA) may be an important first step in the aging process. Here we seek to understand the choice between end-to-end joining and homologous recombination in repairing a DSB in rDNA. This project contributes to our understanding of the cellular response to DNA damage and the mechanisms of cellular aging.

We have constructed a segment of recombinant DNA that contains two genes with very similar sequences—green fluorescent protein and yellow fluorescent protein (see figure). By initiating a double strand break in one of the genes, we can measure whether the DSB was repaired by end-to-end joining (NHEJ) or by homologous recombination with flow cytometry. Our ability to measure and relate these two repair pathways will help us understand the mechanism of aging at the biochemical level.

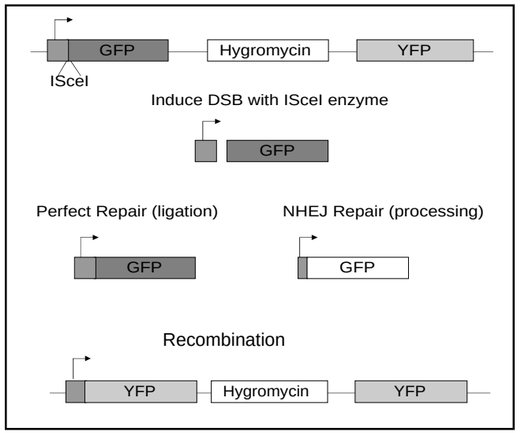

The green fluorescent protein (GFP) is disrupted with sequences encoding an endonuclease site. The endonuclease will cut the DNA and force the cell to repair the site by one of two mechanisms: (1) end-to-end joining (NHEJ), resulting in loss of green fluorescence, or (2) recombining GFP with yellow fluorescent protein (YFP), resulting in yellow fluorescence.

Publications

Ruscetti, T., et al., "Nucleolar Dynamics Associated with DNA Repair," *Molecular Biology of the Cell* **10**, 288a (1999).

Hyperthermophile Biocatalysis: The Molecular Basis of Enzyme Stability and Activity

99008

R. Brian Dyer

Hyperthermophile enzymes, which thrive at elevated temperatures, are potential biocatalysts for industrial synthesis, biomass conversion, and bioremediation. To realize this potential, we need a more-complete understanding of the molecular basis of the enzymes' thermal stability and activity.

The complex interplay between thermal stability and activity has led to contradictory hypotheses with important implications for the design of enhanced catalysts. Recent advances in the structural determination and genetic manipulation of hyperthermophile enzymes, combined with new laser spectroscopic methods for probing functional dynamics, offer the opportunity to resolve these issues. This project studies the structure and dynamics that determine stability and catalytic activity for the enzyme lactate dehydrogenase (LDH) from thermophilic and hyperthermophilic organisms and their mesophilic homologues—related forms existing at more-moderate temperatures.

We are characterizing the functional dynamics of the mesophilic forms of LDH while we work out the expression of a hyperthermophilic homologue. There are several tryptophan (Trp) residues in the enzyme, and two are within the nicotinamide adenine dinucleotide (NADH) binding domain. The strong distance dependence of fluorescence resonance energy transfer (FRET) from the Trp to the NADH provides a sensitive indicator of their proximity and hence of NADH binding and loop closure to form the activated complex.

Temperature-jump experiments, using either Trp fluorescence or NADH FRET probes, reveal complex, multiexponential relaxation kinetics (see figure, panel a). The observed transients contain contributions from the complex reaction dynamics (substrate binding, loop closure, hydride transfer), as well as from sample cooling. The 8.6-ms transient observed in the NADH FRET measurements (see figure, panel b) is likely associated with "loop" closure, although the time seems a bit too slow based on previous kinetics models. The origin of the 4.1-μs transient is unclear; our working hypothesis correlates the earliest process with the hydride transfer to pyruvate.

To assign the kinetic rates to specific processes, we performed a series of experiments as a function of both enzyme and NADH concentrations and in the presence of an LDH-bound inhibitor. The inhibitor is known to "stiffen" the loop structure considerably, thus changing loop-closure dynamics. Our calculations of the NADH binding rate, based on the concentration dependence, agree well with the diffusion constants we previously measured for the LDH enzyme. The presence of an inhibitor eliminates the slow (8.6 ms) transient, confirming that it is due to loop closure.

These experiments provide the first glimpse of the controlling dynamics for the reactivity LDH. The insight provided is critical for understanding how structure dynamics and function relate.

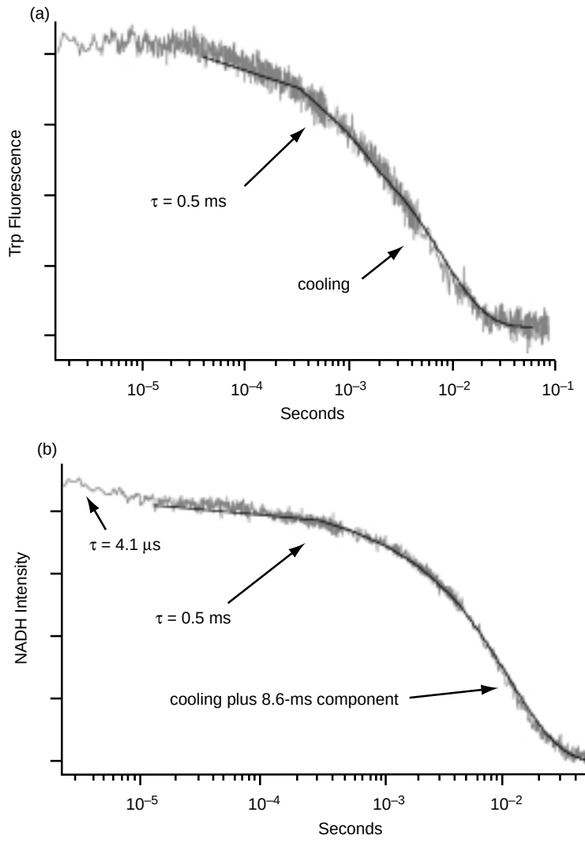

The emission of (a) the indole ring of Trp residues and (b) the nicotinamide ring of NADH in human LDH following a ca. 20°C T-jump. The initial temperature of the LDH and NADH solution was 20°C, concentration [LDH] = [NADH] = 0.2 mM. Exponential fits to the transient signals yielded the observed relaxation times shown in the figures with excellent accuracy. We observed no 4.1-μs transient in the Trp fluorescence.

New Approaches to High-Throughput DNA Sequence Validation

99009

P. Scott White

Genome sequencing generally requires measurements of quality, as determined by a variety of metrics. Base-identification accuracy is assessed indirectly from raw data, but resequencing methods are used either for randomly chosen sites or for sites for which a high probability of error is predicted. Resequencing suffers from the same artifacts as those found in the original data because it uses the same chemistry and base-identification methods as those used to generate the data. Therefore, strategies that use technologies different from those used to generate the data under scrutiny are valuable.

We have proposed using flow cytometry methods we developed to assess sequence quality at targeted sights (the Laboratory has filed two patents for these methods). To be cost-effective, these methods should be highly parallel, with a high rate of sample throughput and low reagent costs. Our goal is to develop the parallel aspects of the assays, with incremental improvements in cost and in sample throughput.

To perform highly parallel assays, it is necessary to have unique DNA "addresses" for each microsphere population. The design of the DNA sequences must yield a collection of these addresses and their complementary "capture tags" that will assemble correctly within complex mixtures. This capture step functions by having the reverse complement of the address as part of each oligonucleotide primer, with the remaining sequence targeting the site to be identified.

We have developed algorithms that design oligonucleotide sets that are optimized for low levels of interaction among capture tags with maximum affinity for the correct address tag. The address/capture tag design is a two-stage process that involves (1) generating lists of sequences of given lengths and then (2) evaluating the sequences with commercial software for their hybridization properties, such as homodimer formation, melting temperature, priming efficiency, hairpin formation, and so on. Our early algorithms produced sets of address/capture tag pairs by looking at only one of the two strands of DNA, and the complement was not considered when designing the set. The predicted success rate of the oligonucleotides from the first lists was approximately 1% when the hybridization properties were evaluated with the commercial software. Recent advances in our algorithms have improved the predicted success rate to approximately 50%, and we have the potential to generate multiple lists when larger final sets are needed. We synthesized and tested the 16 survivors from the first algorithm and found that their hybridization properties provide raw data within acceptable ranges, although signal variation among oligonucleotides was higher than desired. We will test the lists provided by the new algorithms in the coming months.

In addition to primer design, we have also examined different reaction components in order to optimize efficiency and sensitivity. We are at a level of sensitivity to perform the assay on purified clone DNA from large-insert clones called "bacterial artificial chromosomes," or BACs, but not on total DNA from clones.

Development of a SQUID Microscope for Imaging Cortical Neuronal Columns

99010

Robert H. Kraus, Jr.

Our objective is to develop a magnetic-field microscope with high spatial and temporal resolution to image cortical and brainstem activity. The microscope will use a superconducting quantum interference device (SQUID) sensor array and a superconducting image plane patented by the Laboratory. The superconducting image plane produces a gradiometric field at the sensor array for nearby sources and shields the array from ambient background fields. We will optimize this system to obtain spatial resolution better than 300 μm and temporal resolution better than 0.5 ms for in vivo measurements of neuronal columns. Imaging the activity of individual neuronal columns with high temporal resolution will provide a new level of understanding of the connectivity and communication between individual columns and the propagation of signals and information within the brain.

We have made exceptional progress during this past year—well over 50% of the original goals outlined in our proposal have been attained. Parallel efforts to develop a SQUID sensor array have been pursued at Los Alamos and with a collaborator/vendor in Jena, Germany. The SQUID development effort at the Los Alamos Superconducting Technology Center has not resulted in an operational device; however, we acquired significant information during the process to optimize design parameters for the array. Through our collaboration with the laboratory at Jena, we learned of a spin-off company capable of producing the needed high-critical-temperature (HTC) SQUID array. We received the first segment of the array in mid August. Our preliminary tests indicate that the sensor cross talk, one of the most critical parameters, was far better than expected. The measured cross talk for all channels was below –65 dB, with most channels below our measurement threshold (about –90 dB). This is an exciting and encouraging result. The noise performance of these SQUIDs is well within our requirements.

We have begun the design process for a new SQUID microscope based on technology developed for and lessons learned from the system built for the DOE Enhanced Surveillance Program. This effort continues with input from numerous Laboratory resources, including cryogenic vacuum experts, metallurgists, and mechanical engineers.

Publications

Espy, M.A., et al., "Design and Preliminary Results from a High-Temperature Superconducting SQUID 'Microscope' Used for Nondestructive Evaluation," *IEEE Trans. Appl. Superconductivity* **9**, 3692 (1999).

The Molecular Basis of Universal Scaling Laws in Biology

98056

William Woodruff

Virtually every aspect of an organism's biology is affected by its size. This effect is evident in the empirical "allometric scaling laws" that relate biological quantities to mass. One of the best known of these, governing metabolic rate (or power, $P = P_oM^{3/4}$), applies to organisms from bacteria to vertebrates and is related to others involving the scaling of drug doses, effects of exposure to toxic substances or radiation, and longevity ($L = L_oM^{1/4}$). The principles underlying these laws are fundamental to biology. We have made several advances.

We have developed a theoretical model that shows that the $M^{3/4}$ dependence of metabolic rate in metazoa can be understood from fundamental physical principles governing the transport of essential resources in biological distribution networks. We have shown that the relationship for metabolic rate spans more than 26 orders of magnitude of mass and that it not only applies to the largest and smallest animals but also to single cells, mitochondria, and the enzyme molecules of the respiratory complex. This model provides a molecular basis for understanding allometry. Finally, we have shown that the expressions for metabolic rate and longevity suggest that all aerobic organisms are allocated the same amount of metabolic energy (or O_2 turnovers) per unit mass per life span. The foregoing results suggest that we can generalize the theoretical model to understand cellular and subcellular processes. These results also suggest experimental approaches for examining the molecular and cellular basis of the variations in mass coefficients P_o and L_o among taxa, including the reasons for the correlation between the laws governing O_2 metabolism and longevity.

Developing the Groundwork for a Protein Structure Initiative

98547

Tom Terwilliger

Structural genomics is a new and rapidly developing field in biology. The goal of this field is to discover and analyze the structures of all natural protein molecules in order to provide a foundation for a fundamental understanding of biology. We have been leaders in the national and international effort to develop ideas for this field and to engage the worldwide biological community in discussing and advancing the field. We have written articles on structural genomics, cosponsored a workshop on the field, lectured on structural genomics at national and international meetings, developed critical technologies for the field, and are part of a multi-institution pilot project that is widely recognized as an important structural genomics effort. Structural genomics is closely tied to functional genomics, the identification of the functions of all proteins in nature, and to genomic sequencing, the determination of the genetic blueprints of all organisms. We believe that together these fields will revolutionize biology over the next two decades.

Our goal is to develop the groundwork for carrying out a large-scale structural genomics project. An important aspect of this project is demonstrating its feasibility. To do this, we carried out a small-scale project using the extreme thermophile *Pyrobaculum aerophilum*. We have cloned, expressed, purified, and crystallized proteins from this organism in a standard fashion to evaluate if this process can be readily made high-throughput.

Cloning the genes has turned out to be straightforward; it can be done in parallel with a high rate of success. Expression of a protein in a soluble form is much more difficult, however. Only about half the genes resulted in soluble protein when expressed in *E. coli*. Purification is also difficult. Only about half the proteins we expressed could be readily purified. Crystallization is not only difficult but also time-consuming; about half the purified proteins could be crystallized.

We were able to solve by x-ray diffraction measurements the structures of the two proteins from which high-quality crystals were obtained. Overall, our results indicate that we can determine the structures of about 10% of proteins using a one-pass procedure. Although this percentage is promising, many additional improvements in technology are necessary.

1999
LDRD

Table of Projects

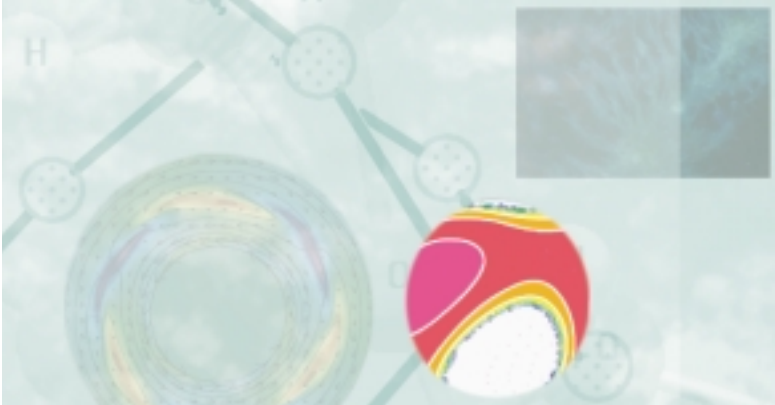

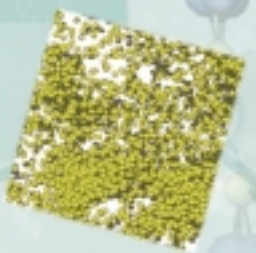

Relevancy of FY99 Projects to Major Laboratory Missions

Project Number	Page	Project Title	Defense Programs	Nonproliferation and International Security	Environmental and Waste Management	Department of Defense	All others
97001	94	Experimental Determination of Statistical Parameters for Improving a Micromechanical Model of Ductile Fracture	•			•	•
97002	143	Geometric Phase, Spatial Resonance, and Control in Spatially Extended Nonlinear Systems	•	•		•	•
97003	142	Strongly Coupled Dusty Plasmas	•			•	•
97004	204	Search for Cosmic Antimatter with Milagrito					•
97005	168	Soliton Optical Communications	•	•		•	•
97007	116	Recombination Kinetics: Correcting the Textbooks	•	•	•	•	•
97008	171	Imaging Time-of-Flight Ion Mass Spectrograph	•	•	•	•	•
97009	169	Subpicosecond Electron-Bunch Diagnostic	•	•	•	•	•
97010	153	Plasma-Wakefield Accelerator	•	•	•	•	•
97011	97	Experimental and Theoretical Investigation of Fracture and Deformation of a Revolutionary High-Temperature Gamma-TiAl Alloy	•			•	•
97012	195	Supermassive Black Holes and the Strong Field	•				•
97013	189	Determining the Mass of the Universe	•				•
97014	196	High-Resolution Records of Global Climate Change					•
97015	149	Laser Cooling of Solids	•	•		•	•
97016	98	Intrinsic Fine-Scale Structure in Complex Materials: Beyond Global Crystallographic Analysis	•	•		•	•
97017	157	The Compliance Method for Measuring Residual Stress	•		•	•	•
97018	127	A Theoretical Description of Inhomogeneous Turbulence	•	•		•	•
97019	216	Development of a Human Artificial Chromosome					•
97020	218	The Role of Low-Frequency Collective Modes in Biological Function: Ligand Binding and Cooperativity in Calcium-Binding Proteins			•		•

Relevancy of FY99 Projects to Major Laboratory Missions

Project Number	Page	Project Title	Defense Programs	Nonproliferation and International Security	Environmental and Waste Management	Department of Defense	All others
97021	220	Substrate-Dependent Cell-Cycle Disturbances in Response to Ionizing Radiation					•
97022	217	Predictive Models for Transciptional Enhancers					•
97023	112	Classical Kinetic Mechanisms Describing Heterogeneous Ozone Depletion					•
97024	116	Characterization of Propane Monooxygenase			•	•	•
97025	118	Ultrafast, Solid-State Electron Transfer in Donor-Acceptor Conducting Polymers	•	•	•	•	•
97026	156	The Plasma Fluidized Bed	•		•	•	•
97027	160	Tritium Recovery and Isotope Separation Using Electrochemical Methods	•	•	•	•	
97028	159	Virtual Bandwidth via Stochastic Polyspectra	•	•		•	•
97029	197	Balloon-Based, High-Time-Resolution Measurements of X-Ray Emissions from Lightning		•		•	•
97030	184	Ices on Titan: Laboratory Measurements That Complement the Huygens Probe					•
97031	172	Novel Signal Processing with Nonlinear Transmission Lines	•	•		•	•
97032	173	Thermal Detection of DNA and Proteins during Gel Electrophoresis				•	•
97033	126	Diffusion in Porous Media and Stochastic Advection		•	•	•	•
97034	132	New Ways of Representing Functions	•	•	•	•	•
97035	132	3-D, Unstructured, Hexahedral-Mesh S_n Transport Methods	•	•		•	•
97036	133	Completely Parallel ILU Preconditioning for Solution of Linear Equations	•	•		•	•
97037	202	A GaAs Detector for Dark Matter and Solar Neutrino Research					•
97038	202	Testing the Standard Model Using Bottom Quarks	•				•
97039	205	Instantons and Duality in Strongly Coupled Quantum Field Theories	•				•
97040	203	The QCD Phase Transition in Relativistic Heavy-Ion Collisions	•				•

Relevancy of FY99 Projects to Major Laboratory Missions

Project Number	Page	Project Title	Defense Programs	Nonproliferation and International Security	Environmental and Waste Management	Department of Defense	All others
97041	205	Helium-3 Magnetometry for a Neutron EDM Measurement	•				•
97042	100	Optimum Design of Ultrahigh-Strength Nanolayered Composites	•			•	•
97513	130	Simulation of Thin-Film Formation	•	•		•	•
97517	103	Application of High-Temperature Superconductors to Underground Communications		•		•	•
97523	99	Targetry Development for the Production of Research Radioisotopes					•
97601	38	Multiscale Science for Science-Based Stockpile Stewardship	•	•	•	•	•
97603	28	Catalysis Science and Technology	•	•	•	•	•
97604	39	Advancing X-Ray Hydrodynamic Radiography	•	•		•	
97609	35	Actinide Molecular Science	•	•	•	•	
97610	84	Integrated Structural Biology Resource	•	•	•	•	•
97611	10	Electrons in High Magnetic Fields	•	•	•	•	•
97614	12	Science of Polymer-Based Materials Aging	•	•		•	•
97616	69	Urban Security		•	•	•	•
97618	63	Advanced Dynamic Radiography with Protons	•	•	•	•	•
97619	23	Materials with Complex Electronic/Atomic Structures	•		•	•	•
97621	41	Evolutionary Computation	•	•		•	•
97801	18	Fundamental Studies of Radiation Damage in Two-Phase Oxide Composites	•	•	•	•	•
97802	24	Multiscale Phenomena in Materials	•		•	•	•
97803	66	Solar Terrestrial Coupling through Space Plasma Processes		•		•	•
97807	27	Energy Transfer in Molecular Solids	•			•	•
97808	65	Algorithm Development for Ocean Models				•	•
97809	55	Manipulation of Residual Stresses to Control Material Properties	•			•	•
97811	74	Low-Luminosity Compact Stellar Objects and the Size of the Unverse	•				•

Relevancy of FY99 Projects to Major Laboratory Missions

Project Number	Page	Project Title	Defense Programs	Nonproliferation and International Security	Environmental and Waste Management	Department of Defense	All others
97812	68	Elements of Water Resources and Urban Pollution			•		•
97813	70	Theoretical and Observational Studies of the Earth's Mantle				•	•
97814	76	Earth Materials and Earth Dynamics		•	•	•	•
97815	67	Lithospheric Processes		•	•	•	•
98001	144	Artificial Atoms Probed by Femtosecond Pulses: Evolution of Optical Properties during the Bulk-Atomic Transformation	•	•	•	•	•
98002	153	Laser-Plasma Interactions in Diffraction-Limited Beams	•	•	•	•	•
98003	152	Stochastic Resonance in Arrays with Tunable Nonlinearity and Coupling		•		•	•
98004	147	Quantum Computation and Nuclear Magnetic Resonance		•		•	•
98005	220	Noninvasive Techniques for Genetic Analysis					•
98006	223	Rapid Genotyping Assay for Beryllium Disease Susceptibility					•
98007	223	Targeted In Vitro Evolution of Protein Ligands					•
98008	221	Next Generation of Molecular Dynamics: Implicit-Solvent/Langevin Models for Folding of Peptides and Proteins					•
98009	215	New Paradigms in Simulating the Prediction, Intervention, and Control of Infectious Diseases		•			•
98010	124	Solvation Dynamics of Ion Pairs	•	•	•	•	•
98011	113	Fundamental Process in Polymer Light-Emitting Electrochemical Cells	•	•	•	•	•
98012	120	Unraveling Heterogeneous Surface Reaction Kinetics	•	•	•	•	•
98013	114	Soluble Polymers for Enhancing Biocatalysis			•	•	•
98014	166	Using Metallic Glasses in Ceramic-Metal Joining	•			•	•
98015	155	Development and Engineering of the Ion-Cut and Low-Temperature Direct-Bonding Process	•	•	•	•	•
98016	160	Pulse Shaping in Explosive-Pulsed Power	•			•	•

Relevancy of FY99 Projects to Major Laboratory Missions

Project Number	Page	Project Title	Defense Programs	Nonproliferation and International Security	Environmental and Waste Management	Department of Defense	All others
98017	158	Acoustic-Network Refrigerators				•	•
98018	191	Lightning in the Atmosphere and in the Solar Nebula		•			•
98019	186	High-Pressure Crystal Chemistry of Hydrous Minerals	•		•	•	•
98020	181	New Windows on Gamma-Ray Bursts	•	•			•
98021	192	Advanced Computational Analysis of Disordered Materials and Clay Minerals			•	•	•
98022	188	Tsunami from Asteroid and Comet Impacts		•		•	•
98023	200	A Large-Aperture, Wide-Angle Air Cerenkov Telescope					•
98024	182	A New Method for Modeling Wave Propagation in Strongly Heterogeneous Media: Applications to Seismic Wave Propagation in the Earth		•	•	•	•
98025	167	Stable Polymeric Light-Emitting Devices	•	•	•	•	•
98026	178	Development of Radial Probe Instrumentation for Use in DNA Sequencing					•
98027	174	An Integrated Solid-State Optical Device with High-Speed Scanning, Variable Focusing, and Frequency-Doubling Capabilities	•	•	•	•	•
98028	178	Cryptographic Key Generation Using Long-Base-Line Radio Interferometry	•	•		•	•
98029	128	Efficient Multilevel Iterative Methods for Nonlinear PDEs	•	•		•	•
98030	129	Extending the Theory of Resonant Perturbations to Partial Differential Equations, with Applications to Nonlinear Optics	•	•		•	•
98031	139	Invariant Discretizations for Computational Gas Dynamics	•	•		•	•
98032	131	Unitary Symmetry, Discrete Mathematics, and Combinatorics	•	•		•	•
98033	139	Multigrid Homogenization of Heterogeneous Porous Media			•		•
98034	105	Unusual Metal Behavior in Taylor Microwires	•	•		•	•
98035	104	Bulk Ferromagnetic Metallic Glasses	•	•		•	•

Relevancy of FY99 Projects to Major Laboratory Missions

Project Number	Page	Project Title	Defense Programs	Nonproliferation and International Security	Environmental and Waste Management	Department of Defense	All others
98036	108	Unconventional Superconductivity and Violation of Time-Reversal Invariance	•	•	•	•	•
98037	96	New Vortex Phases in Irradiated High-Temperature Superconductors	•	•	•	•	•
98038	206	Exploring and Testing the Standard Model and Beyond	•			•	•
98039	209	Determination of the Neutron Lifetime and Ultracold-Neutron Source Development	•	•		•	•
98040	207	Study of Parity Non-Conservation in the Reaction n + p→d + γ	•	•		•	•
98041	208	A Search for Superradiant Emission in a Nuclear Isomer Crystal				•	•
98042	210	High-Energy Cosmic Transients					•
98047	222	Role of New Cancer Gene in Environmental Carcinogenesis			•		•
98054	148	High-Gain Self-Amplified Spontaneous-Emission Experiments in the Infrared				•	•
98056	228	The Molecular Basis of Universal Scaling Laws in Biology					•
98535	101	Plutonium Aging: Investigation of Changes in Weapon Alloys as a Function of Time	•	•	•		
98547	229	Developing the Groundwork for a Protein Structure Initiative					•
98555	140	Signal Integrity Verification	•	•		•	•
98556	136	National Transportation System Analysis Capability		•	•	•	•
98566	133	Design of an Indexing Scheme for Knowledge Management at Los Alamos National Laboratory	•	•			•
98601	61	Advanced Nuclear Measurement Science		•	•	•	•
98602	32	A New Paradigm in Separations: Molecular Recognition Membranes			•		•
98603	30	Condensed Phase Kinetics and Reduced Reaction Mechanisms of Energetic Materials	•			•	•
98604	73	Coupled Environmental Modeling		•	•	•	•
98605	79	Nonequilibrium Science: Assessment, Control, and Prediction	•		•	•	•

Relevancy of FY99 Projects to Major Laboratory Missions

Project Number	Page	Project Title	Defense Programs	Nonproliferation and International Security	Environmental and Waste Management	Department of Defense	All others
98606	80	Ultracold Neutron Science	•				•
98610	17	Advanced Research Capabilitites for Neutron Scattering	•	•	•	•	•
98801	22	Atomic Resolution Probes of Materials	•	•	•	•	•
98805	37	Discrete Simulation of Nonlinear Systems	•	•	•	•	•
98806	46	Probabilistic Combinatorial Analysis for Biological Systems					•
98817	20	Comparative Investigation of Spin, Charge, and Lattice Degrees of Freedom in Colossal Magnetoresistive Materials	•	•	•	•	•
99001	150	Create and Study Quantum Degenerate Systems		•		•	•
99002	146	Dynamical Stability and Quantum Chaos of Ions in a Linear Trap		•		•	•
99003	151	Quantum Coherence and Decoherence: Trapping a Schrödinger Cat		•		•	•
99004	141	Quantum Feedback Control: Methods and Applications		•		•	•
99005	145	Direct Observation of Individual, Optical Energy-Transfer Events		•		•	•
99006	224	Computational Studies of the Role of Water Fluctuations in Protein Dynamics and Folding					•
99007	225	The Molecular Aging Clock					•
99008	226	Hyperthermophile Biocatalysis: The Molecular Basis of Enzyme Stability and Activity					•
99009	227	New Approaches to High-Throughput DNA Sequence Validation					•
99010	228	Development of a SQUID Microscope for Imaging Cortical Neuronal Columns	•				•
99011	219	Rapidly Photocleavable Caged Proteins					•
99012	111	Alkane Chemistry of Ligated (Allyl)Iridium Moieties on Metal Oxide Supports and Multilayer Hydrogen Transport Membranes			•		•
99013	119	Novel Surfactants and Micellar Chemistry for Enhanced Reactivity and Separations			•		•

Relevancy of FY99 Projects to Major Laboratory Missions

Project Number	Page	Project Title	Defense Programs	Nonproliferation and International Security	Environmental and Waste Management	Department of Defense	All others
99014	115	Supported Technetium Chemistry	•		•		•
99015	120	Nonadiabatic Processes in Chemical Reactions			•		•
99016	122	Description of Complex Adsorption from a Simple Equation of State			•		•
99017	162	Use of Directed Light Fabrication for Fabricating Functionally Gradient Materials	•			•	•
99018	165	Composite Films Made with Metallic Carbon Nanotubes				•	•
99019	158	Highly Constrained Bandwidth Combinational Algorithm for Transmission of Speech (HC-BATS)		•		•	•
99020	164	Hydrogen Storage in Intermetallic Alloys	•			•	•
99021	161	Next-Generation High-Power Microwave Source				•	•
99022	183	The Genesis and Evolution of Basalt on the Moon					•
99023	198	Sky Patrol Analysis with the Robotic Optical Transient Search Experiment		•			•
99024	190	Galactic and Extragalactic Magnetic Fields: Their Origin and Manifestation in Accretion Disks around Supermassive Black Holes					•
99025	199	Multiscale Physics of Multiphase Flow in Porous Media			•		•
99026	196	Antarctic Circumpolar Wave and El Niño					•
99027	193	Low-Energy Neutral-Atom Imaging: Watching Magnetospheric Dynamics					•
99028	195	Galaxies and Large-Scale Structure in a Universe with a Cosmological Constant					•
99029	175	X-Ray Refractive Optics for Astrophysics and Nonproliferation		•		•	•
99030	177	Time-Resolved Photon Migration Tomography and Spectroscopy				•	•
99031	176	An Integrated Optical Biosensor		•		•	•
99032	179	High-Quantum-Efficiency, Silicon-Integrated, Tunable-Band-Gap Infrared-Detection Devices Based on Rhenium Molybdenum Disilicide		•	•	•	•

Relevancy of FY99 Projects to Major Laboratory Missions

Project Number	Page	Project Title	Defense Programs	Nonproliferation and International Security	Environmental and Waste Management	Department of Defense	All others
99033	170	Electron Tunneling Spectroscopy of Buried Interfaces	•	•		•	•
99034	134	Statics and Dynamics of Granular Media	•		•	•	•
99035	138	Quantum Physics Algorithms	•	•		•	•
99037	137	New Dispersive Models of Fluid Turbulence	•			•	•
99038	137	New Perspectives in Mathematical Modeling of High-Bit-Rate Fiber-Optical Telecommunications	•			•	•
99039	125	Scalable Algebraic Multilevel Preconditioning for General Sparse Systems Using Sparse Approximate Inverses	•	•		•	•
99040	93	Novel Approaches to Low-Temperature Thin Film Materials Chemistry: Kinetic Energy Activated Molecular Beam Epitaxy	•	•	•	•	•
99041	107	Bulk Rapid Solidification	•	•	•	•	•
99042	109	Intrinsic Nonlinear Local Modes in Low-Dimensional Materials					•
99043	102	Organic Electronic Materials under Intense Electrical Injection	•	•		•	•
99044	106	Investigation of Experimental Defect Interactions in Materials by Integrating Experimental Techniques with Large-Scale Simulations	•			•	•
99045	208	Weak Interactions at Low Energies	•				•
99046	210	Weak Interactions in Nuclei	•				•
99047	211	Exact Solutions of Quantum Gauge Theories from String Solitons	•				
99048	212	Development of Detectors and Electronics for the Study of the Beta Decay of Polarized Neutrons at LANSCE	•				•
99049	212	The Search for Dark Matter	•				
99050	214	Measurements of (n-gamma) Cross Sections for Unstable Nuclei	•				
99051	201	Improved Matching of Lattice and Continuum QCD	•				•
99052	213	Fundamental Symmetries with Trapped Atoms		•		•	•

Relevancy of FY99 Projects to Major Laboratory Missions

Project Number	Page	Project Title	Defense Programs	Nonproliferation and International Security	Environmental and Waste Management	Department of Defense	All others
99053	117	Utilization of High-Nitrogen Compounds	•	•		•	
99054	194	Long-Range Weather Prediction				•	•
99055	182	Astrophysics with the Sloan Digital Sky Survey					•
99500	85	Bioremediation Science to Meet National Challenges			•	•	•
99501	77	Integrated Remote Sensing Science		•		•	
99502	40	Taking the Next Step with Intelligent Monte Carlo	•	•	•	•	•
99503	13	Self-Assembling Organic Electronic Materials	•			•	•
99504	56	Characterization of Liquid Lead-Bismuth Eutectic for High-Power Neutron Spallation Applications	•		•	•	•
99505	53	Applications of Quantum Technologies		•		•	•
99506	88	Optical Biosensor		•		•	•
99507	14	Coordinated Synthesis, Characterization, and Modeling of Materials	•		•	•	•
99508	42	Nonlinear Complex Phenomena	•			•	•
99509	18	Development of Semiconducting Polymeric Films with High Concentrations of Boron	•	•		•	•
99510	59	Hard and Deeply Buried Target Defeat				•	
99511	72	Space Science and Exploration		•			
99512	44	Quantifying and Reducing Uncertainty in Predictions of Complex Phenomena	•				•
99513	43	Management of Nuclear Warhead and Infrastructure Reduction	•	•		•	
99514	81	Neutrino Physics Experiments	•				•
99515	45	Strategic Computing Applications	•	•			•
99516	83	Pathogen Detection in the Real World		•		•	•
99517	47	Novel Fundamentals in Strategic Computing	•			•	•
99518	86	Functional Genomics		•			•
99519	9	Neutron and Accelerator-Based Science	•		•		•

Relevancy of FY99 Projects to Major Laboratory Missions

Project Number	Page	Project Title	Defense Programs	Nonproliferation and International Security	Environmental and Waste Management	Department of Defense	All others
99520	82	Enabling R&D for Future Proton Applications	•				•
99521	58	Nuclear Materials Management Systems for Proliferation Resistance, Environmental Protection, and Sustainability	•	•	•		•
99522	52	High-Power Microwave Science and Technology				•	
99523	34	Cradle-to-Grave Carbon Management					•
99524	50	Next-Generation Sophistication in Defense and High-Energy-Density Physics Exploratory Research	•				•
99525	49	Strongly and Moderately Coupled Plasma Physics in Inhomogeneous Matter	•				•
99526	16	Competing Interactions in Complex Materials—Bridging Hard, Soft, and Biological Matter	•	•			•
99527	52	Numerical Modeling and Diagnostic Methods for Magnetized Target Fusion	•				•
99528	11	Organizing Principles of Materials near a Quantum-Critical Point	•				•
99529	89	The Identification of Proteins That Bind to Novel DNA Sequences/Structures		•			•
99530	19	Critical Current Mechanisms in High-Temperature Superconducting Films					•
99531	15	A Scalable Silicon-Based Nuclear Spin Quantum Computer	•	•			•

1999
LDRD

Index of Principal Investigators

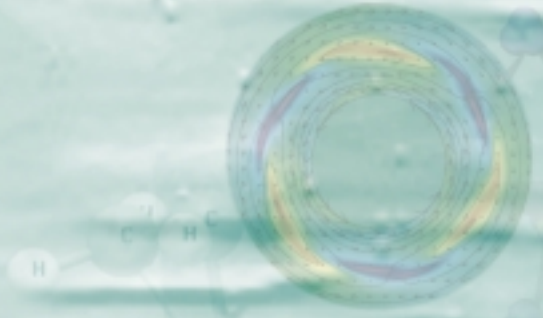

Index of Principal Investigators

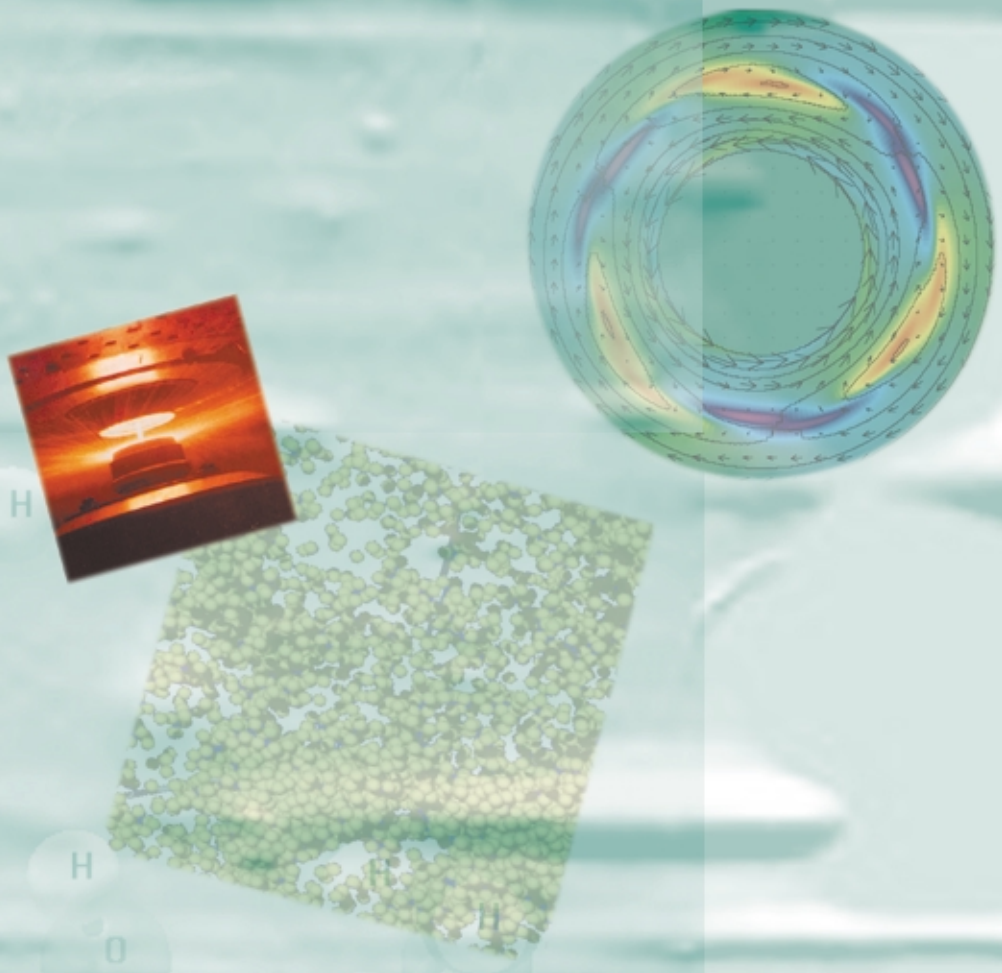

Los Alamos
NATIONAL LABORATORY
Los Alamos, New Mexico 87545

A US Department of Energy Laboratory